Molecular mechanisms of coccoid form formation in *Campylobacter jejuni*

Naomi Ikeda

This thesis is being submitted in partial fulfilment of the requirements of Kingston University for the award of Doctor of Philosophy.

May 2014

Declaration

I declare that the work within this thesis is entirely my own and has been carried out at Kingston University, UK

This Thesis has not been submitted, in whole or in part, for any other degree at this or any other university.

Naomi Ikeda May 2014

Abstract

It is known that under stress conditions *Campylobacter jejuni* can change morphology from a characteristic spiral to coccoid form (CF). Genetic and biochemical mechanisms of CF formation (CFF) in *C. jejuni* remain unclear, however cell shape maintenance in other microorganisms is known to be genetically determined.

The focus of this study is the functional analysis of *spoT* and *amiA* genes in *C. jejuni*. Inactivation of the *spoT* gene stimulated CFF in strain 11168H and 81116, but the direct role of this gene in CFF is unclear due to the pleiotropic effects of *spoT* mutation. The *amiA* gene, encoding a putative peptidoglycan amidase, is involved in CFF in the closely related bacterium *H. pylori*. Comparative genomics studies revealed conservation of the *amiA* gene clusters among diverse bacteria. Amino acid sequence analysis of AmiA orthologs suggests a possible dual function of these proteins due to high variability in their N-terminal domains, as opposed to high conservation of the C-terminal domains responsible for amidase activity.

The inactivation of this gene in *H. pylori* affected the accumulation of a dipeptide motif peptidoglycan unit suggesting additional (peptidase) activity of this enzyme. In contrast to *H. pylori*, attempts to inactivate *amiA* in *C. jejuni* strains 11168H and 81116 proved unsuccessful suggesting the gene is essential for bacterial viability. Over expression of *C. jejuni* AmiA in *E. coli* resulted in decreased viability due to loss of membrane integrity as revealed by BacLight LIVE/DEAD staining. *C. jejuni* AmiA overexpression also lead to a change in the *E. coli* muropeptide profile compared to native levels.

Results suggest that, similar to AmiA proteins in other bacteria, AmiA of *C. jejuni* may also be involved in peptidoglycan maintenance and in CFF.

Acknowledgements

I would like to thank my Director of studies, Professor Andrey Karlyshev for the opportunity to work on this project and his assistance with my research in regards to helping with my experiments and troubleshooting problems.

I want to also thank my secondary supervisor, Dr Lori Snyder for her continued support and providing invaluable advice in my experiments and throughout my PhD.

I would like to acknowledge the support and financial funding from Kingston University and the Biomedical and Pharmaceutical Sciences Research Group. I am grateful to the department of Life Sciences and would like to thank my colleagues and friends, Dr Lauren Mulcahy, Dr Simon Gould and especially Dr Suzanne Gould for their individual contributions. I would also like to express my gratitude to the technicians of the School of Life Sciences at Kingston University; Jayne, Gurm, Michael and Lindsey for all their help.

I want to express my gratitude to my examiners Professor Edith Sim and Dr Andrew Grant for the advice they gave me with my corrections.

Many thanks to my fellow students in EM131, I have been blessed by their kindness and support over the years. A special thanks to Sona Rubinchik, my fellow PhD student and lab mate in lab S11 for her constant and generous support. I would also like to offer my sincerest gratitude to Carl Jenkinson for his guidance with HPLC.

I would like to thank Michael Amdi Madsen for his constant encouragement and motivation, pushing me to be the best I can and believing in me. You make me a better person.

I also want to express my gratitude for the support from my friends and family, for each being there for me in their own way. A special thanks to my friends Mark Bradley, Liz Archer, Delphine Thenet, Abim Aniyam, Max Pearson and Mat Smith for their kindness and patience whilst reading my work.

Finally I would like to thank my father, Haruyoshi Ikeda for everything he did for me.

I dedicate all my work to those that have helped me to where I am today but are unfortunately no longer with us. May you rest in peace.

Contents

List of figures

List of tables

Abbreviations

ATP	Adenosine triphosphate
BSA	Bovine serum albumin
CBA	Columbia Blood Agar
CF	Coccoid form
CFF	Coccoid form formation
CFU	Colony forming unit
DNA	Deoxyribonucleic acid
HPLC	High performance liquid chromatography
GBS	Guillian-Barré syndrome
LB	Luria Bertani
OD	Optical density
PBS	Phosphate buffered saline
PCD	Programmed cell death
PCR	Polymerase chain reaction
PVDF	Polyvinylidene fluoride
qPCR	Quantitative polymerase chain reaction
RNA	Ribonucleic acid

ROS	Reactivee oxygen species
rRNA	Ribosomal ribonucleic acid
SD	Standard deviation
SDM	Site directed mutagenesis
SDS PAGE	Sodium dodecyl sulphate polyacrylamide gel electrophoresis
SEM	Standard error of mean
TLC	Thin layer chromatography
TTBS	Tris buffered saline with tween
VBNC	Viable but non culturable
WT	Wild type

1.0. Introduction

Some bacteria have a classical rod shaped morphology, yet there have been descriptions of these organisms altering their morphology, varying in size and membrane structure. Despite many bacterial genera and species being named after their shape, bacterial morphology is not static in all organisms. In some cases, the morphology of many bacteria like *Escherichia coli* or *Bacillus subtilis* is in a changing state dependent on the environmental conditions, such as external physical pressures or growth of the organism. These changes may be in response to temperature variations, nutrient availability, presence of antibiotics, toxins, chemicals and other stress factors. This project looks further into morphology transition of the persistent albeit fastidious paradoxical organism, *Campylobacter jejuni*.

1.1. Campylobacteraceae

Campylobacter are described as mostly spiral rods that can vary in size between 0.5 μm and 5 μm long and 0.2 μm and 0.8 μm wide (Debruyne *et al.*, 2008). *E. coli* size ranges between 2.0 to 6.0 μm long and 1.1 to 1.5 μm wide, showing *Campylobacter* to be a generally smaller organism and to have similar size variations to *E. coli* (Prescott *et al.*, 1996).

Campylobacter cells vary in size, appearance and other features. Most species of *Campylobacter* are motile and possess flagella; some are either uni- or bi- flagellated like *C. jejuni*, although there are some subspecies that are multiflagellated like *C. showae*. *C. gracilis* and *C. hominis* have been described as non-motile (Debruyne *et al.*, 2008; Vandamme & de Ley, 1991).

1.2. *Campylobacter jejuni (C. jejuni)*

The first descriptions of *Campylobacter* were in 1886 by Heinrich Escherich and originally was called *Vibrio fetus.* The bacterial species was reclassified in 1994 as a subspecies of *Campylobacteraceae.*

C. jejuni is a Gram-negative, flagellated, spiral member of the delta-epsilon proteobacteria group. This species is microaerophilic, capnophilic, and thermophilic with optimal growth temperature ranging from 37°C to 42°C and it has been documented previously that *C. jejuni* is unable to grow at temperatures below 30°C (Kelly *et al.*, 2001).

C. jejuni is well known for its fastidious growth requirements within a laboratory setting, requiring specific growth temperatures and complex media. The medium to support *Campylobacter* cultures requires reactive oxygen species (ROS) quenchers such as blood and pyruvate due to the microaerophilic nature of the organism (Chou *et al.,* 1983; Chynoweth *et al.*, 1998; Verhoeff-Bakkenes *et al.*, 2007; Verhoeff-Bakkenes *et al.,* 2008).

Despite the fastidious growth requirements in the laboratory environment, *C. jejuni* is the greatest cause of bacterial food borne illness to humans in the world, more so than *Shigella* and *Salmonella* combined (Murphy *et al.*, 2006; Verhoeff-Bakkenes, 2008).

1.3. *C. jejuni* genome

The first *C. jejuni* genome that was sequenced was *C. jejuni* NCTC 11168 by Parkhill *et al.* (2000); this was subsequently reannotated by Gundogdu *et al.* in 2007. According to the sequencing of *C. jejuni* NCTC 11168, it has a low GC content of approximately 30% and has been predicted to encode for 1,643 proteins (Gundogdu *et al.*, 2007). The reannotation

of *C. jejuni* NCTC 11168 led to a reduced total number of coding sequences, from 1654 to 1643 and 18.2% of coding sequence product functions to be revised. Along with the lack of repeat sequences, insertion sequences and phage associated sequences, it was shown that *C. jejuni* has hypervariable sequences, which are short homopolymeric nucleotide sequences. *C. jejuni* NCTC 11168 has a low level of redundancy and non-coding sequences as it was determined that 94.3% of the genome coded for proteins. According to NCBI, there are 17 complete whole genome sequences for *C. jejuni* strains as of February 2014; the most recently fully sequenced strain is *C. jejuni* PT14 (Brathwaite *et al.*, 2013). Currently there are 77 *C. jejuni* strain chromosome sequences in draft or incomplete form.

1.4. Clinical manifestations and the diseases caused by *C. jejuni*

C. jejuni is the aetiological agent of campylobacteriosis, an acute infection recognised by the symptoms of watery to bloody diarrhoea, general malaise, fever, nausea and vomiting (Butzler & Skirrow, 1979). Reports of an infectious dose have been shown to be a result of as few as 500 organisms (Robinson, 1981). Due to its self-limiting nature, it can be fatal to the immunocompromised, the very young, or the elderly. *C. jejuni* infection can also lead to such-complications as reactive arthritis, inflammatory bowel syndrome and Guillian-Barré syndrome (GBS), an autoimmune disease which causes temporary paralysis due to oligosaccharide mimicry (Rhodes & Tattersfield, 1982).

1.5. Epidemiology

Despite the fastidious nature of *Campylobacter*, the rates of *Campylobacter* cases have been continually increasing, becoming an emerging problem over the past decade. The

prevalent nature of *C. jejuni* as bacterial gastrointestinal pathogen causing 72,571 reported cases in the UK in 2012 according to Food Standards Agency (FSA) is paradoxical to the fastidious growth requirements within the laboratory, unlike other food-borne pathogens. According to Public Health England the rates of reported cases of *Campylobacter* infection increased every year between 1989 and 2000, and from 2004 onwards, with the most common agent, *C. jejuni,* becoming a public health and economic concern (Figure 1.1). However, due to the lack of reporting, the self limiting nature, short disease periods, and the lack of testing, the true number of cases is unknown but is estimated to be much greater than those reported. The economic impact of *Campylobacter* infections can be great. In 1995, the annual total cost from *Campylobacter*, including GBS and campylobacteriosis, in medical care and lack of productivity due to inability to work was estimated to cost the US economy $1.5-8 billion; this does not include long-term care for GBS patients (Buzby *et al.,* 1997; Akobundu *et al.,* 2006). In 2013, the estimated costs of campylobacteriosis in the UK were £900 million out of the total £1.5 billion costs of all foodborne infections according to a recent FSA Open Board report (2013). The average medical cost for long term sequelae (not including secondary complications such as GBS) is £314 per case, in accordance with 1995 costs and the FSA report of Infectious Intestinal Disease (IID) (2000) whilst more recent estimated costs of *Campylobacter* infections in the US including long term sequelae to be $8,901 per case (Scharff, 2010).

However, this may not be a true reflection of the costs of *Campylobacter* infection as Tam *et al.,* (2003) stated, *Campylobacter*-associated GBS can be up to 10 times greater than predicted. The increasing rates of infections from 2004 to the present time and the underreporting of cases may suggest that the economic implications are much higher than originally assumed.

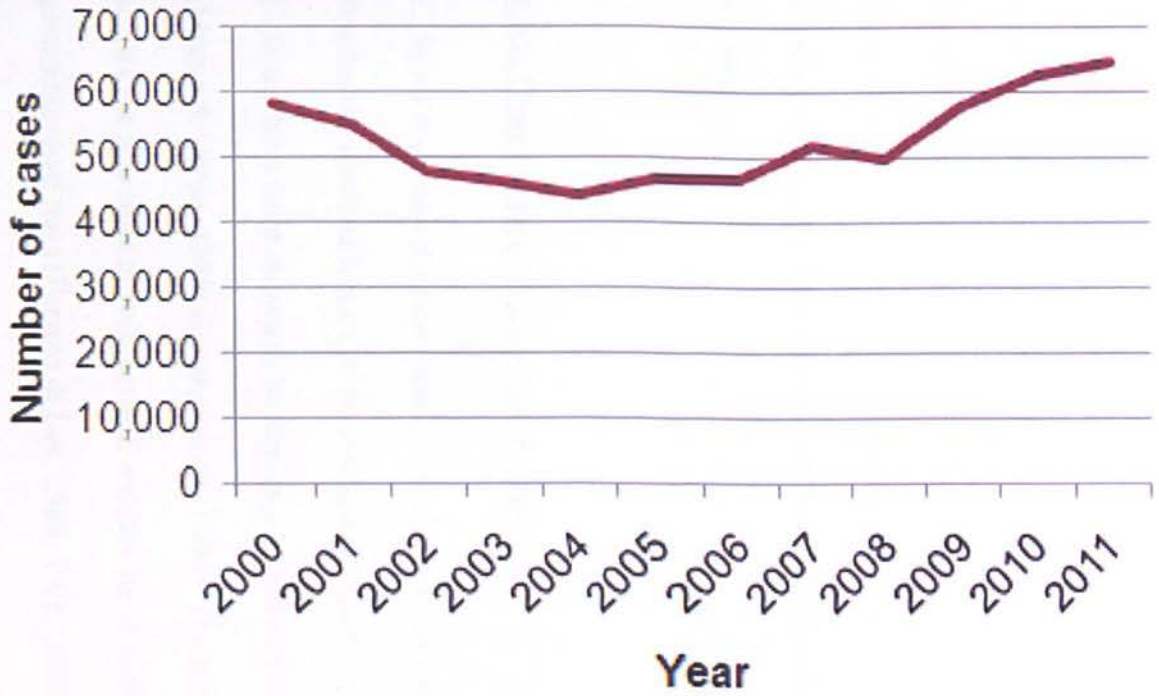

Figure 1.1. Reported cases of *Campylobacter* infections per year from 2000-2010 in England and Wales according to the Health Protection Agency Centre for Infections.

Over the decade the reported cases have increased dramatically from 50,000 in 2009 to 65,000 in 2011. Image was taken from the HPA *Campylobacter* Epidemiology website page (http://www.hpa.org.uk/Topics/InfectiousDiseases/InfectionsAZ/Campylobacter/EpidemiologicalData/campyDataEw/)

1.6. *Campylobacter* morphology

Ng *et al.*, (1985) described many morphologies of *C. jejuni* ranging from 'seagull like shape, s shaped, curved.' This was relating to the varying curvature of the cells. Campylobacter cells have also been described as filaments, doughnuts and straight rods, which are not considered classical *Campylobacter* morphologies (Ng *et al.*, 1985). Early classification and taxonomic naming of microorganisms was based on morphology. The name *Campylobacter* is derived from the Greek meaning curved rod, however it has been noted that the organism can convert to a round, spherical shape or a coccoid form (CF). The CF morphology was first described for *C. jejuni* in 1962 (Ogg, 1962) and despite decades of research there still has not been full elucidation of the biological role of this morphology.

1.6.1. Characteristics of coccoid morphology

C. jejuni coccoid cells have been shown by previous studies to have various characteristics besides the obvious feature of their shape. Despite the presence of flagella, coccoid cells of *C. jejuni* have been shown to be non-motile and exhibit no movement of the flagella (Moran & Upton, 1986; Boucher *et al.*, 1994). The typical corkscrew rod morphology allows for smoother movement and motility itself within the mucous membrane of the gastrointestinal tract (Ferrero & Lee, 1988; Park, 2002), therefore the spherical coccoid morphology could be the cause of lack of motility. An alternative theory is that the CF non-motility is due to the inability of the cells to produce or maintain energy required for flagella movement despite retaining flagella (Moore, 2001).

Electron microscopy (EM) images have revealed that the size range and the shape of the CF cells can also vary to a great extent with the diameter ranging from 0.1 to1μm (Ng *et al.*, 1985; Rollins & Colwell, 1986). Whilst the rod spiral cells are stained typically as Gram-negative bacteria, coccoid cells are unable to retain the same amount of counter stain, such as safrarin or carbol fuchsin, due to differences within the cell wall structure (Moran & Upton, 1986; Svensson *et al.*, 2008). This could be linked with other studies where it was observed that CF membranes lacked structural integrity, and were thus described as having 'leaky' walls, leading to reduced levels of nucleic acids, peptides and superoxide dismutase found within the cells (Moran & Upton, 1986; Boucher *et al.*, 1994). These findings suggested that CF cells are undergoing autolysis (Buck *et al.*, 1983) and the morphology was representative of a degenerative form of the bacteria. However this was found to be conflicting with EM images that show no signs of autolysis in any CF (Merrell *et al.*, 1981). The conflicting results with the same morphology may be due to different types of stress conditions which have caused induction of CF formation. Characteristics like changes in cell wall integrity have a greater relationship to the conditions of CF induction (described in further detail in section 1.7).

1.6.2. Reporting the coccoid morphology

After the original study in 1962 (Ogg, 1962) showing the presence of *C. jejuni* CF structures, there were no publications on the subject again until the 1980s. Due to potential findings of morphological induction of viable but non culturable states in 1994, the phenomenon of CF formation generated increasing interest in the latter half of the 1990's and the 2000's (Figure 1.2) (Ikeda & Karlyshev, 2012). However, more recently the interest in CF *C. jejuni* has declined, mostly due to speculation that these and similar forms

in *Helicobacter pylori* are degenerative forms of the bacteria (Kusters *et al.*, 1997). Even the sequencing of the first *C. jejuni* genome in 2000 (Parkhill *et al.*, 2000) did not increase research publications in the field of CF research.

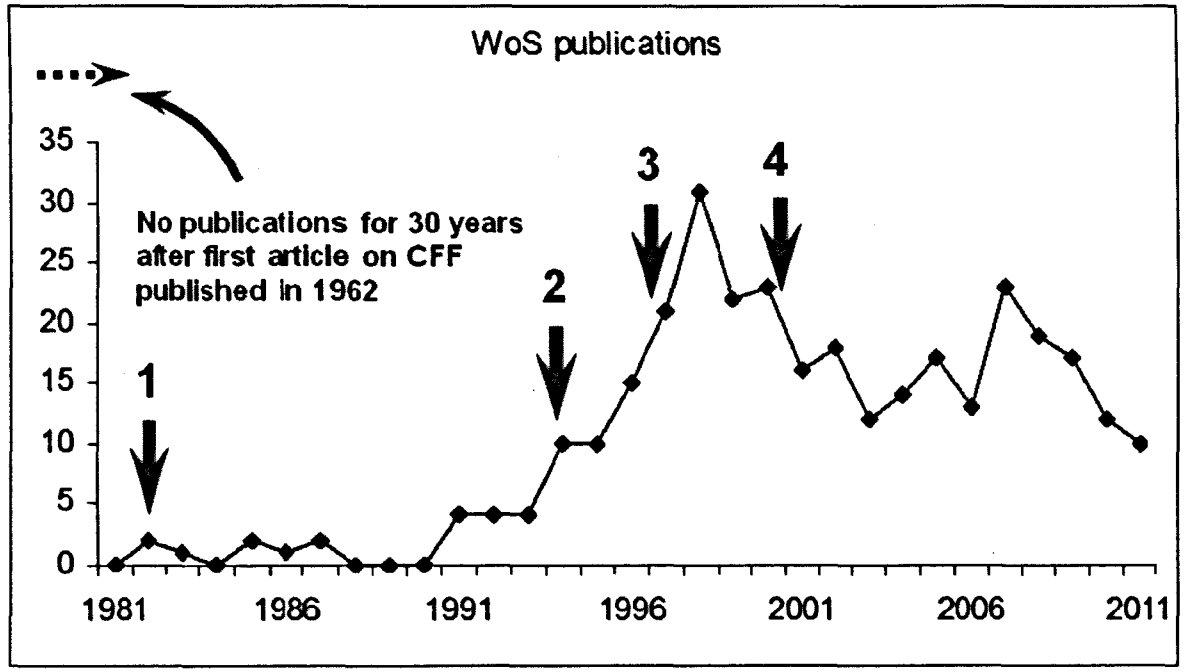

Figure 1.2. The annual rate of publications according to the Web of Science (WoS) regarding CF within *Campylobacter* and *Helicobacter*. Keyword combination "coccoid AND (*Campylobacter* OR *Helicobacter*)" was used for search using WoS website. Image was taken from Ikeda & Karlyshev (2012). The following time points are marked by arrows: 1) the first mentioning of CF of *Campylobacter spp.* (Koike, 1982) 2) The interest to these forms received a burst after a publication suggesting that CF are dormant but viable cells (Ursing, 1994) 3) Publication of an article suggesting that CF of *Helicobacter* is a "morphologic manifestation of cell death" (Kusters, 1997) 4) Publication of the first *Campylobacter* genome sequence (Parkhill *et al.*, 2000). The first article on CFF was published by Ogg, 1962.

1.7. Stimuli of CF induction

1.7.1. Temperature

Temperature has been shown to have a dramatic effect on the rate of CF formation (CFF) and also the 'type' of coccoid cells that are formed (Hazeleger *et al.*, 1995; Hazeleger *et al.*, 1998). The transition to CF of *C. jejuni* and *C. coli* was found to be increased at 37°C compared to lower temperatures of 10°C and 20°C. There was a decrease in the amount of CF present as the temperature decreased, with almost all cells being in the CF at 37°C whilst at 4°C there was lower than 10% accumulation of CF after extended periods of incubation (Chou *et al.*, 1983; Höller *et al.*, 1998; Hudock *et al.*, 2004). Temperatures above 55°C also stimulate CFF, with resultant increased cell degradation and cell death than CFF induction at lower temperatures (Klacnik *et al.*, 2009).

C. jejuni is incapable of growth at temperatures below 30°C, with notable decrease in the intracellular biochemical activity (Hazeleger *et al.*, 1998; Tangwatcharin *et al.*, 2006). The effects of temperatures below 30°C on the level of biochemical activity and cellular degradation on CF are well documented (Hazeleger *et al.*, 1995). In particular, CF formed at 25°C with pre-grown cultures exposed to lower temperatures have been shown to have higher levels of degradation in comparison with those formed at 4°C that had comparable fatty acid composition and a similar intracellular/extracellular ATP ratio to those of spiral/rod cells. It was suggested that CF formed at lower temperatures (4°C & 25°C) are in viable but non-culturable (VBNC) or VBNC-like state, allowing bacterial survival for extended periods of time without observable growth (Hazeleger *et al.*, 1995).

The decrease in temperature reduced the formation of CF, which could be beneficial for survival according to Hudock *et al.* (2004). It was also shown that similar to

Campylobacter, *Helicobacter* cells maintain as rod forms at 4°C for a longer period than at 25°C and 37°C. Despite *C. jejuni* being capable of surviving in low temperatures, this is still a stressful environment for the bacteria and it is incapable of growth (Tangwatcharin *et al.*, 2006). Other studies have shown that the variations in the effect of low temperatures, the rate of CFU decline and the transition to CF could be strain dependent (Lazaro *et al.*, 1999; Chan *et al.*, 2001).

1.7.2. Oxidative stress

C. jejuni is a microaerophilic organism, with atmospheric growth conditions usually consisting of approximately 10% O_2. Oxidative stress results from the effect of ROS like superoxides and hydrogen peroxide. As a stress factor, oxygen has been shown to induce CFF in *C. jejuni* (Boucher *et al.*,1994; Lee *et al.*, 2005; Klancnik *et al.*, 2006). Oxidative stress advances the rate of conversion, which is also known by the comparative rates of conversion of morphologies in broth and on agar (Boucher *et al.*, 1994). Broth enables greater circulation of oxygen, rapidly affecting cell morphology (Moran & Upton, 1986). However, recent studies on the effects of aerobiosis of oxygen on *C. jejuni* have been shown to be either neutral, detrimental, or potentially beneficial to viability and morphology (Svensson *et al.*, 2008). It has been demonstrated that there is increased formation of CFs after exposure to oxygen within a 24 hour period (Ogg, 1962; Karmali *et al.*, 1981). *C. jejuni* cells exposed to prolonged periods of atmospheric oxygen levels almost completely transitioned to CF, yet the membrane was intact, suggesting it could be potentially viable (He & Chen, 2010). Conversely, previous studies had shown cells with high levels of degradation when placed under high levels of oxygen (Harvey & Leach, 1998).

C. jejuni has been shown to have the capability to grow in ambient atmosphere oxygen levels. This is possibly due to either an adaptation of the bacterium to the aerobic environment or due to the growth media containing oxygen scavengers, such as blood and pyruvate (Chou *et al.,* 1983; Chynoweth *et al.*, 1998; Verhoeff-Bakkenes *et al.*, 2007; Verhoeff-Bakkenes *et al.,* 2008). The presence of these oxygen scavengers can also have an effect on the rate of transformation to CF (Chou *et al.*, 1983). CF induced at 37°C under anaerobic conditions appeared uniformly spherical, unlike the irregular shaped coccoid cells formed under microaerophilic and aerobic conditions (Shimomura *et al.*, 2004).

1.7.3. Stationary phase / age related stress

Stationary phase growth leads to decreases in available nutrients and space, and an increase in the amount of toxic materials present. Entry into the stationary phase for many bacteria is accompanied by biochemical and morphological changes to enable the cells to increase resistance to inhospitable environments (Kolter *et al.*, 1993). The transition from the classical morphology to CF is a standard occurrence in the stationary phase of growth for *C. jejuni* due to the reduction in nutrients and the increase in toxic products, similar to the effect of exposing exponentially grown cells to starvation conditions (Rollins & Colwell, 1986; Bovill & Mackey, 1997). There is, however, controversy regarding the shape change under starvation conditions with recent studies showing the maintenance of the rod morphology after exponentially grown cells were incubated for 72 hrs in saline solution (Ma *et al.*, 2009).

Stationary phase was shown to induce morphological changes in liquid cultures that are not always present in solid medium cultures. Filaments or elongated cells as described by

Griffiths (1993) may appear due to a differential gene expression in response to a change in the environment and the availability of nutrients affecting cell division. Filamentation occurs in cells undergoing growth without septation, creating elongated cells. Uropathogenic *E. coli* was also found to be capable of forming filamentous cells, which enable the bacteria to evade host immune responses and allow it to persist within the urinary tract (Justice *et al.*, 2003). It is also seen that *H. pylori* after 7 days within liquid cultures show undivided rods and became filamentous (Donelli *et al.*, 1998).

The *C. jejuni* bacterial cells taken from the stationary phase of growth were found to be more sensitive to heat and aerobic stress than cells from an exponential phase (Kelly *et al.*, 2001). A possible reason for this sensitivity is the lack of a 'traditional' RpoS-mediated stationary phase response. It appears that unlike most other Gram-negative bacteria *C. jejuni* does not have RpoS, which has led to the theory that an alternative mechanism for resistance is induced during stationary phase (Park, 2002; Parkhill *et al.*, 2000; Kelly *et al.*, 2001). However, starved cells of *C. jejuni* in a closely controlled environment showed increased heat resistance (Cappelier *et al.*, 2000). These conflicting reports could be explained by different methods to measure viability (*i.e.* metabolic activity and CFU). Alternatively, these differing reports may be a result of strain-to-strain variation, which would help to further explain the potential for strain and species variations in resistance to stress. Interestingly, *C. jejuni* cells that were taken from exponential growth phase, then put under starvation conditions were found to have increased heat sensitivity and increased bacterial tolerance, which declines through the stationary phase (Klancnik *et al.*, 2009). This shows that the stationary phase and the starvation conditions induce similar responses, including the decline in sensitivity to stress conditions over time. Although the cultures demonstrate an obvious decline in viability and resistance to heat and aerobic stress in the stationary phase, these disadvantages become less obvious over time. The stationary phase

is a potentially dynamic environment, in which new subpopulations could lead to greater fluctuations in heat resistance and viability over extended aged cultures (Kelly *et al.*, 2001).

1.8. Role of CF

1.8.1. Viable But Non Culturable (VBNC)

Morphological changes to CF are coincident with the decrease in CFU counts and were initially associated with the VBNC state (Beumer *et al.,* 1992; Hudock *et al.*, 2005). The VBNC state is defined as "a state of dormancy where growth ceases on bacteriological media normally used for culture of the organism yet the bacteria retain vitality with minimal activity" (Svensson *et al.,* 2008). The VBNC state has been suggested to be a state of great importance for many different bacteria due to its capacity to allow survival until conditions are favourable (Oliver, 2005). However, the relationship between CF and VBNC states is ambiguous due to findings showing non-coccoid *C. jejuni* that were in a VBNC-like state (Federighi *et al.*, 1998; He & Chen, 2010). Beumer *et al.* (1992) measured the levels of ATP present in CF concurrently with culturability. However, the amount of ATP within the cells remained constant for 3 weeks, potentially indicative of viability. He & Chen (2010) showed that morphology was not indicative of degeneration of the membrane, with isopropanol killed cells retaining spiral morphology. In contrast, cells that were stressed by ambient oxygen levels adopted CF and were unculturable, but maintained membrane integrity.

There have been reports of *C. jejuni* VBNC forms reverting to culturable forms within aquatic systems (Thomas *et al.*, 1999) and after acid treatment (Chaveerach *et al.*, 2003). In addition, in studies using animal models of infection, the VBNC CF of *C. jejuni* reverted into fully infectious classical morphology forms (Jones *et al.,* 1991; Saha *et al.,* 1991; Pearson *et al.,* 1993), however, the results of these studies are controversial due to irreproducibility (Medeema *et al.*, 1992).

It has been demonstrated within *Vibrio parahaemolyticus* that the VBNC state exhibits a cell shape change with a change in protein profile (Lai *et al.*, 2009). However, *C. jejuni* CF showed significant reduction in the level of protein synthesis, which supports the theory of degeneracy (Boucher *et al.*, 1994; Hazeleger *et al.*, 1995; Hudock *et al.*, 2005). In the related organism *H. pylori*, controversially, the coccoid morphology has been considered related to the life cycle of the bacteria as a sign of programmed cell death (Kusters *et al.*, 1997; Cellini *et al.*, 2001).

The VBNC state and CFF are distinct though related phenomena in *C. jejuni* life cycles. It is possible that the VBNC state may induce CF formation although CF may not be indicative of a VBNC state. The most likely VBNC state appears to be the spiral rod forms at lower temperatures (Lazaro *et al.*, 1999; Hudock *et al.*, 2005). It has been theorised that there are several states of viability in both the morphologies of *C. jejuni* and the existence of different types of CF may depend on the conditions under which they are formed (Hazeleger *et al.*, 1995). The current methods used to determine the VBNC state in connection with the CF may not be adequate and more advanced methods are required to fully determine the relationship.

1.8.2. Stringent response

The stringent response is defined as 'a global stress response that alters gene expression pathways to allow bacterial survival under a multitude of unfavourable conditions and is typically activated by environmental stresses such as nutrient deprivation' (Gaynor *et al.*, 2005). The gene *spoT* is known for controlling this stringent response within *C. jejuni* (Gaynor *et al.*, 2005). Within other bacteria the stringent response is controlled by two

genes, *spoT* and *relA*. However, no *relA* homologues have been found in *Campylobacter* and *Helicobacter* (Gaynor *et al.*, 2005; Mourey *et al.*, 2006). The *spoT* gene was found to be important for bacterial survival inside epithelial cells, and knocking out *spoT* in *C. jejuni* had a pleiotropic effect (Gaynor *et al.*, 2005). In *C. jejuni, spoT* encodes a bifunctional synthetase-hydrolase that is involved in the maintenance of guanosine tetra- and pentaphosphate [(p)ppGpp], which are molecular signals altering promoter specificity (Gaynor *et al.*, 2005). It was demonstrated within *C. jejuni*, that the mutation of *spoT* resulted in an accelerated rate of CFF (Gaynor *et al.*, 2005). In the closely related bacterium *H. pylori*, a *spoT* mutation also caused an increase in CFF and a decreased resistance to aerobic shock and acid stress (Mouery *et al.*, 2006).

1.8.2.1. Comparison of guanosine-3',5'-bis(diphosphate) 3'-pyrophosphohydrolase/synthase (*spoT*) in *C. jejuni* and *H. pylori*

The *C. jejuni spoT* homologue was annotated during genome re-annotation (Gundogdu *et al.*, 2007), due to a slightly higher similarity to *E. coli spoT* compared to *E. coli relA* (Gaynor *et al.*, 2005). It was found with *C. jejuni* and *H. pylori* strains that the bifunctional homologue had a higher similarity with *E. coli spoT* than *relA* (Table 1.1 & 1.2).

The *spoT* and *relA* genes from *C. jejuni*, *H. pylori* and *E. coli* were of a similar approximate size of 2.2 kb. A comparison of *spoT* DNA sequence from *C. jejuni* NCTC 11168 with other genomes showed high similarity with other annotated and/or putative *relA*/spoT genes, with the highest similarity found with *spoT* amongst other *C. jejuni* strains (99-100% identity) and with related species, like *C. doylei* (95% identity), *C. lari* (72% identity) and *C. fetus* (68% identity). Similarly high levels were found in other organisms; multiple strains of *H. pylori* (83-71% identity), *Arcobacter* (77-67% identity)

and *Wollinella* (68%). Comparisons using the deduced protein sequence of *C. jejuni* NCTC 11168 SpoT compared with other sequenced genomes in BLASTp gave similar results as with the nucleotide sequence. The pairwise scores were the number of identities between the two sequences, divided by the length of the alignment as a percentage. Pairwise scores between the sequences showed high similarity between the *C. jejuni spoT* genes with a score of 98. Relatively high similarity was found between *C. jejuni* strains 11168H and 81116 with *C. fetus* and *H. pylori spoT* genes, both strains with the scores of 69 and 63 respectively.

Table 1.1. A key of gene sequence reference number for *C. jejuni, C. fetus, H. pylori* and *E. coli spoT* and *relA* DNA sequences.

Sequence name and reference number	Gene size
Sequence 1: Campylobacter_jejuni_NCTC11168_spoT	2196 bp
Sequence 2: Campylobacter_jejuni_81116_spoT	2196 bp
Sequence 3: Campylobacter_fetus_82-40_spoT	2199 bp
Sequence 4: Helicobacter_pylori_26695_spoT	2328 bp
Sequence 5: Escherichia_coli_K-12_spoT	2109 bp
Sequence 6: Escherichia_coli_K-12_relA	2235 bp

Table 1.2. A comparison of the *C. jejuni, C. fetus, H. pylori* and *E. coli spoT* and/or *relA* nucleotide sequences showing pairwise score percentages.

Sequences compared (A:B)	Score (%)
Sequences (1:2)	98
Sequences (1:3)	69
Sequences (1:4)	63
Sequences (1:5)	51
Sequences (1:6)	50
Sequences (2:3)	69
Sequences (2:4)	63
Sequences (2:5)	50
Sequences (2:6)	49
Sequences (3:4)	62
Sequences (3:5)	49
Sequences (3:6)	51
Sequences (4:5)	53
Sequences (4:6)	51
Sequences (5:6)	57

1.8.3. Programmed cell death (PCD) and Biofilm formation

An alternative theory of the coccoid morphology is a stage of cell death, necessary for survival as a population (Cellini *et al.*, 2001). The theory of bacterial PCD is still a relatively new concept in relation to microorganisms and single cell organisms as our understanding of PCD is based on metazoans (Engelberg-Kulka, 2006). CF has been linked to PCD in *H. pylori* where morphology change is associated with viability decline and loss of membrane integrity (Cellini *et al.*, 2001). A method of induction of bacterial PCD is *via* toxin-antitoxin system modules, also known as 'addiction modules'. An example of this is the *mazEF* gene pair in *E. coli* (Aizenman *et al.*, 1996). The toxin-antitoxin system consists of the stable toxin and the unstable antitoxin, which prevents the action of the toxin's lethality. The MazEF module or similar have been described in other organisms besides *E. coli*, such as *B. subtilis* despite the lack of genetic similarity (Pellgrini *et al.*, 2005). It has been noted that this module system has been linked with the products of RelA/SpoT, ppGpp; the global control alarmone for the stringent response. Within *E. coli*, *mazE* and *mazF* are located downstream from the *relA* gene (Metzger *et al.*, 1988; Aizenman *et el.*, 1996). This module furthers the potential for the role of PCD for the greater population as opposed to individual cells. This could also lead to speculation of the potential of PCD within *C. jejuni* biofilms.

Biofilm formation is a crucial aspect of survival of many microorganisms, including *Campylobacter* spp. (Joshua *et al.*, 2005). The monospecies biofilms of *C. jejuni* have been shown to increase resistance to environmental stresses (Joshua *et al.*, 2005). It was suggested that CF in biofilms of *C. jejuni* may have a supportive role by forming a layer of coccoid cells, protecting the viable spiral rods from the hostile environment (Karlyshev & Wren, 2005). It seems that CF is potentially involved in bacterial survival and persistence,

which is particularly important for a fastidious organism like *Campylobacter*. *Campylobacter* biofilms are also an area of particular interest due to the composition of the matrix. A bacterial matrix is comprised of a wide assortment of macromolecules including nucleic acids, proteins and sugars, secreted out of live cells and the remnants of dead lysed cells (Sutherland, 2001; Branda *et al.*, 2005). *Pseudomonas aeruginosa* was also found to form biofilms with the primary constituent being DNA, crucial for the initial establishment of the biofilm (Whitchurch *et al.*, 2002). This has also been found within *C. jejuni* biofilms (Svensson *et al.*, 2009). However, how the DNA becomes a part of the biofilm is still questioned, with two main theories being either the aggregation of DNA from lysed cells or secreted by surrounding live cells. In *C. jejuni*, it is possible that the exogenous DNA for the biofilm matrix could be contributed by CF as opposed to vesicles from live cells. The presence of DNA in biofilms along with CF with various states of membrane permeability could provide great insight into the lifestyle of *C. jejuni* and reveal the potential biological role of the CFF.

If the CF biological role is within biofilms, to maintain and create a microenvironment with the release of nutrients and providing protection from external stresses enabling the survival of a subpopulation of viable cells, PCD would likely be necessary. The role the suicide module plays within CF transitions and role within biofilms could be an area of interest.

1.9. Factors involved in bacterial cell shape

1.9.1. Cell shape maintenance

MreB proteins are actin-related homologues required for maintenance of bacterial cell shape by forming helical filaments underneath the cell membrane and mostly found in rod shaped organisms and in non-spherical bacteria (Jones *et al.,* 2001; Graumann, 2007). However, there has been recent evidence suggesting MreB protein does not form helical structures and the structure is artefactual (Swulius & Jensen, 2012). Cytoskeletal elements like MreB protein are important for cell shape maintenance and are connected to other membrane proteins such as penicillin-binding protein (PBP) 2 in *E. coli* (Young, 2001; Popham & Young, 2003). In *B. subtilis*, there are multiple functional copies of MreB, which are not present within other rod shaped organisms. It has been shown that the homologues of MreB can induce the rod morphology as well (Daniel & Errington, 2003). Mbl, a MreB-like protein that encoded independently of MreB, can create the rod-like morphology using polar growth. Polar growth has been postulated to cause elongated rod morphologies, despite not having MreB or MreB-like machinery (Daniel & Errington, 2003). Another well known cytoskeletal element is the intermediate filament-like protein called crescentin, which is an essential factor for the curved rod shape of *Caulobacter crescentus* (Ausmees *et al.*, 2003). However, how crescentin leads to cell curvature is still unclear (Cabeen *et al.*, 2009).

PBPs are necessary for the maintenance and composition of the peptidoglycan, involved in the synthesis and crosslinking of strands (Popham & Young, 2003). The deletion of PBP2 in *E. coli* has been shown to induce a spherical morphology due to the lack of cell division and cell elongation, leading ultimately to cell death (Vinella *et al.,* 1993). Ishino *et al.* (1986) found that RodA with PBP2 were essential for the synthesis of peptidoglycan in *E.*

coli, and for elongation of the cell. It has been documented in several rod organisms that without functioning RodA, the cells become spherical (Matsuzawa *et al.*, 1973; Henriques *et al.*, 1998). A number of other genes constituting the *dcw* gene cluster (for division/cell wall) are involved in defining bacterial cell shape and a correlation between bacterial cell morphology and organisation of this cluster has been found (Tamames *et al.*, 2001).

1.9.2. Cell shape structure: peptidoglycan

The main constituent involved in maintenance of cell shape is peptidoglycan. Peptidoglycan (also known as sacculus or murein) is comprised of disaccharide-pentapeptide precursors that are made of two aminosugars, *N*-acetylglucosamine and *N*-acetylmuramic acid, connected by a ß- 1,4 glycosidic bond (Figure 1.3). It is found outside the plasma membrane making up the cell wall, maintaining structure and countering osmotic pressure. The standard model of peptidoglycan is based on *E. coli* and though the constituents may be the same in *H. pylori*, it was found to have a very different composition of muropeptides. Costa *et al.* (1999) found that peptidoglycan from *H. pylori* had a dramatically higher proportion of 1, 6 anhydro-N-aceytlmuramic acid and muropeptides with pentapeptide side chains, without trimeric muropeptides, lipoproteins and L-D crosslinked muropeptides, in comparison to *E. coli*. Two possible models of peptidoglycan arrangement in *H. pylori* were derived, given the different levels of specific constituents. The first model has long glycan strands crosslinked with single anhydro-disaccharide units, whilst the second model has short strands crosslinked together 'head to tail', which are then linked to longer glycan strands. These two models described by Costa *et al.* (1999) could coexist but contribute differently to the strength of the entire macromolecule (Figure 1.4).

The amount of peptidoglycan isolated can be indicative of spiral bacteria present. Amano and Shibata (1992) compared the peptidoglycan content in rod shaped cells and CF in three different species of *Campylobacter*: *C. coli*; *C. jejuni*; and *C. fetus.* They found that very little peptidoglycan could be removed from the bacterial cells whilst in their CF. Remarkably, peptidoglycan was always obtainable from *C. fetus,* coincident with an inability of this subspecies to form CF. It was therefore suggested that transformation of *C. jejuni* and *C. coli* into CF may be induced by partial degradation of the peptidoglycan.

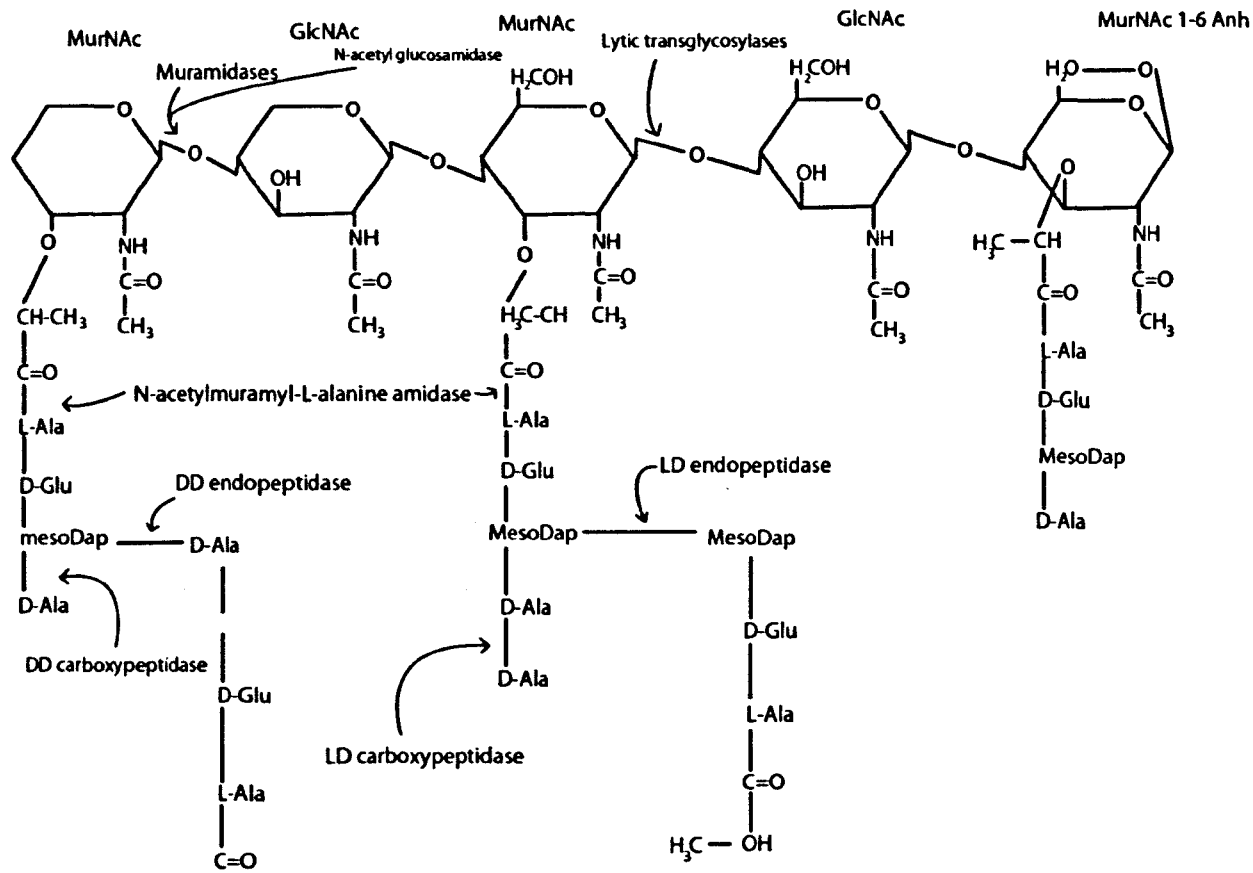

Figure 1.3. The classical structure of peptidoglycan derived from the model organism *E. coli* showing the action of various peptidoglycan specific enzymes.

MurNAc - *N*-acetylmuramic acid, GlcNAc - *N*-acetylglucosamine, MesoDap - meso-diaminopimelic acid. Figure drawn by Ikeda based on Vollmer *et al.*, 2008.

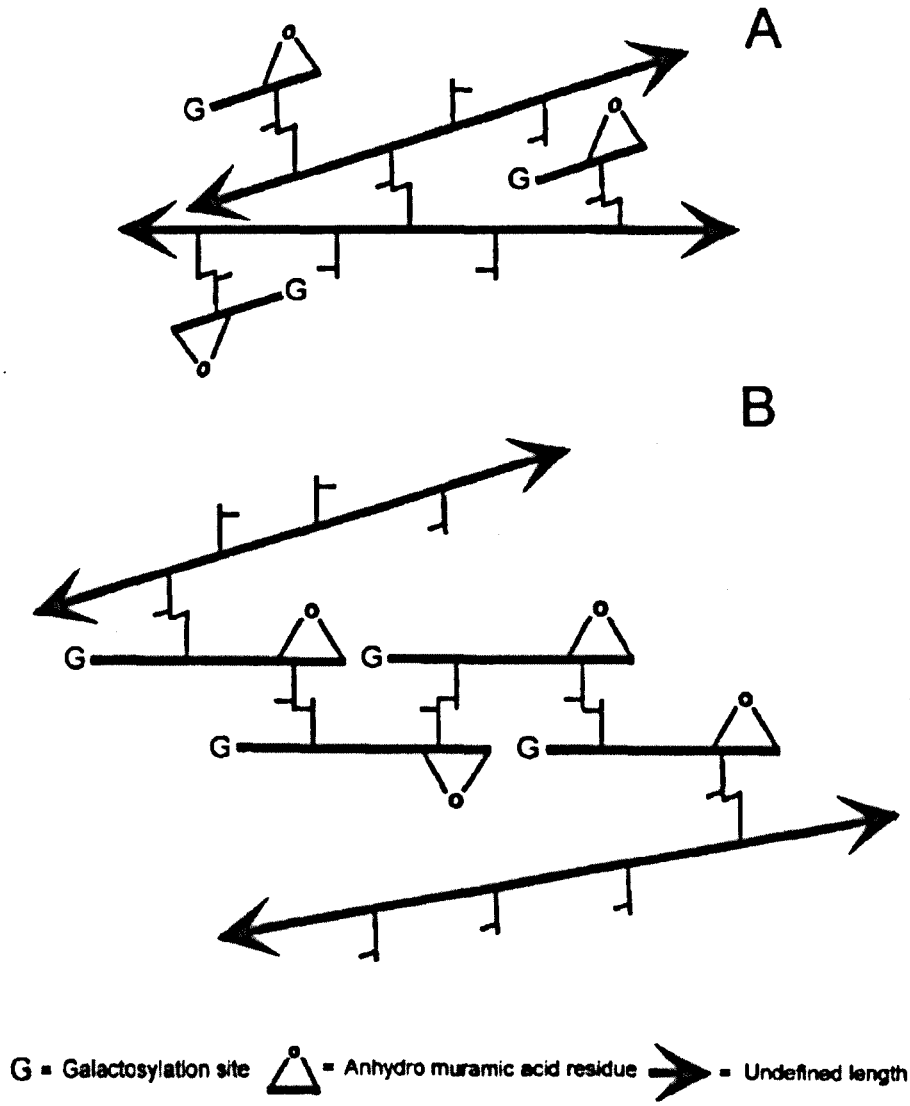

Figure 1.4. Skeletal diagrams of 2 hypothetical structures of peptidoglycan within *H. pylori*. HPLC studies showed two possible models A - long glycan strands crosslinked with single anhydro-disaccharide units and B - short strands crosslinked together 'head to tail', which are then linked to longer glycan strands. Key for structures located on the bottom of the diagrams. Image borrowed from Costa *et al.*, (1999).

1.9.3. Peptidoglycan maintenance enzymes related to cell morphology

The action of other peptidoglycan hydrolases have been shown to influence bacterial cell morphology and whilst the mechanisms for the morphological conversion are still unresolved, the understanding of the maintenance of the helical/spiral shape has progressed. Sycuro *et al.* (2010) identified 4 genes (*csd* 1-3 and *ccmA*) that have been shown through knockout studies to induce straight rod morphology in *Helicobacter*. These genes were involved in the modification of peptidoglycan crosslinks, which when hydrolysed at specific parts along the cell, allowed relaxation of curvature and twist. Despite initial theories of the spiral morphology being necessary for motility in a mucosal environment, it was shown that the deletion of the genes necessary for curvature did not decrease motility. However, it did decrease stomach colonization in mice (Sycuro *et al.*, 2010). The helical morphology within *C. jejuni* was found also to be connected to peptidoglycan. Knockout of *pgp*1, encoding a DL-carboxypeptidase, and overexpression of the protein both lead to straight rod morphology (Frirdich *et al.*, 2012). HPLC studies of the knockout mutant showed an increase in tripeptides and a reduction in dipeptides and tetrapeptides whilst the overexpression showed the inverse in abundances. Recent knockout studies of *pgp*2 also lead to a straight rod morphology in *C. jejuni.* HPLC studies showed an increase in tetrapeptides and an absence of tripeptides, which are consistent with the activity of an LD-carboxypeptidase (Frirdich *et al.*, 2014). Similarly to the straight morphology mutants in *H. pylori,* the *pgp*1 and *pgp2* mutants in *C. jejuni* showed a decrease in chick colonization and also showed a decrease in motility and biofilm formation (Frirdich *et al.*, 2012, Frirdich *et al.*, 2014).

AmiA encodes for N muramoyl-L-alanine amidase, another peptidoglycan hydrolase influencing morphology through cleavage of the bond between the sugar backbone and the

peptide chain. In *H. pylori,* an *amiA* knockout leads to a dramatic decrease in the accumulation of CF and was considered the first genetic determinant of CF (Costa *et al.*, 1999). Interestingly, it was found that the peptidoglycan underwent substantial modifications as bacteria transitioned to the CF, leading to the accumulation of *N*-acetyl-D-glucosaminyl-β(1,4)-*N*-acetylmuramyl-L-Ala-D-Glu (GM-dipeptide). Chaput *et al.* (2006) have stated possible reasons for the increase in GM-dipeptides despite the fact that the action of the amidase is inconsistent with the accumulation due to a potential bifunctional nature of AmiA. Another possible explanation for the accumulation of GM-dipeptides was derived from the human serum amidase, which is unable to cleave peptide chains with less than 3 amino acids (Wang *et al.*, 2003). AmiA present within *Campylobacter* or other bacteria has not yet been shown to be selective on the basis of peptide chain length and the specificity requires further investigation. However, this specificity would be crucial for maintaining the rigidity of the peptidoglycan if only peptide chains with 3 to 5 amino acids could be cleaved. These peptide chains could increase the stability of the peptidoglycan by increasing the number of bonds formed between meso-D and D-Ala, thus creating a looser macromolecule. The role of *amiA* within *Campylobacter* has not been researched previously.

1.10. *N*-acetylmuramoyl-L-alanine amidases in *E. coli* and *C. jejuni*

AmiA (Cj1269c) in *C. jejuni* is annotated as a probable *N*-acetylmuramoyl-L-alanine amidase (Gene ID: 905560). Within the model organism *E. coli*, there are currently five known *N*-acetylmuramoyl-L-alanine amidases: AmiA; AmiB; AmiC; AmiD and AmpD (Vollmer *et al.*, 2008; Kerff *et al.*, 2010). These amidases can be subdivided into protein families; the amidase_2 family (PF01510), including AmiD and AmpD, and the amidase_3 family (PF01520), including AmiA, AmiB, and AmiC, according to the Pfam database (Kerff *et al.*, 2010). The amidase_3 family have specificity for the amide bond between the sugar backbone of the peptidoglycan monomer and the L-alanine of the peptide chain. However, these enzymes have no specificity for the peptidoglycan units with an anhydro-MurNAc group (Uehara & Park, 2007). All of the enzymes in this family play an important role within peptidoglycan cleavage and cell division (Heidrich *et al.*, 2001). In *E. coli*, the deletion of AmiA and AmiC individually prevent division, producing long chains of un-separated cells. This was interestingly not the case with the AmiB mutant (Heidrich *et al.*, 2001). The amidase_2 family does not share the same specificity as the amidase_3 family. AmpD specificity is for peptidoglycan units with anhydro-MurNAc and is necessary for bacterial peptidoglycan recycling and turnover. It is the only *N*-acetylmuramoyl-L-alanine amidase present in the cytoplasm, whilst the others are periplasmic (Jacobs *et al.*, 1994). AmiD, in contrast, has no specificity for either form of MurNAc (Uehara & Park, 2007; Pennartz *et al.*, 2009). Its full role has not been elucidated as of yet. However, it has become apparent that AmiD does not play a role in bacterial division, and unlike other members of the amidase_3 family it is an insoluble lipoprotein-anchored enzyme in the outer membrane (Uehara & Park, 2007).

E. coli has a high level of redundancy for *N*-acetylmuramoyl-L-alanine amidases necessary for both bacterial growth and peptidoglycan cleavage, specific for MurNAc and anhydro-MurNAc. It was shown by Heidrich *et al.* (2001) that despite combined deletions of AmiA, AmiB and AmiC, as long as there was at least one amidase that remained active, cell division and separation would still happen. It has become apparent that each of these enzymes may have a partially different role; through protein fusion studies with green fluorescent protein in *E. coli* it was found that AmiC localized around the septal ring whilst AmiA appeared to be distributed throughout the periplasm (Bernhardt & de Boer, 2003). AmiC is now distinguished as an entirely periplasmic septal ring component. However it is not known how the specification for the area occurs or what other factor it may be connected to associated with the septal ring (Bernhardt & de Boer, 2003).

Unlike *E. coli*, *C. jejuni* and *H. pylori* do not have the same level of redundancy, with only one *N*-acetylmuramoyl-L-alanine amidase annotated (Chaput *et al.*, 2005, Costa *et al.*, 1999). Despite *amiA* having been described as the first genetic determinant for CFF in *H. pylori*, this gene has not been shown to be the same determinant in *C. jejuni* (Chaput *et al.*, 2005).

1.10.1. Analysis and comparison of *amiA* and other *N*-acetylmuramoyl-L-alanine amidases genes and gene products

The presence of other *N*-acetylmuramoyl-L-alanine amidase sequences located within the *C. jejuni* NCTC 11168 genome were verified using BLASTn search using nucleotide sequences, searching for genes and DNA sequences with high similarity to *C. jejuni* NCTC 11168 *amiA, C. jejuni* 81116 *amiA, E. coli* K12 *amiA, amiB, amiC, amiD* and *ampD*. No similarity between other sequences within *C. jejuni* NCTC 11168 and 81116 genomes were found. Therefore the only predicted *N*-acetylmuramoyl-L-alanine amidase within *C. jejuni* NCTC 11168 was annotated as *amiA*/Cj1269c. *N*-acetylmuramoyl-L-alanine amidase nucleotide sequences from *H. pylori* 26695 and *E.coli* K12 were compared with *N*-acetylmuramoyl-L-alanine amidase nucleotide sequences from *C. jejuni* to elucidate potential similarity. The *N*-acetylmuramoyl-L-alanine amidases from *H. pylori* and *E. coli* used for comparison as the enzymatic function of all the enzymes have been previously experimentally proven (Heidrich *et al.*, 2001; Chaput *et al.*, 2006; Vollmer *et al.*, 2008; Kerff *et al.*, 2010). Though it was not experimentally tested, the annotated *amiA* of the related species *C. fetus* 82-40 was also compared, although this species is unable to form CFs under stress according to a study by Amano & Shibata (1992).

Using BLASTn with the *amiA* gene from *C. jejuni* NCTC 11168 showed the highest identity similarity was the other *C. jejuni* strains, with percentage scores ranging from 97-100% across the whole length of the gene and *C. jejuni* 81116 showing percentage similarity score of 99% across the entire gene. The next highest similarity was with the other *Campylobacter* species *C. doylei* (97%), *C. hominis* (88%), *C. fetus* 82-40 (87%) and *C. lari* (79%). The highest similarity to *C. jejuni* NCTC 11168 annotated or putative *N*-acetylmuramoyl-L-alanine amidases were found in *H. pylori* strains (present within all at

an identity percentage of 72-65%), *Sulfurimonas denitrificans* (71% identity) *Sulfurospirillum* (68%) and *Arcobacter* (88%).

In accordance to ClustalW2 multigene alignment, annotated *amiA* genes from *C. jejuni* strains NCTC 11168 and 81116 showed very high similarity, with 98 pairwise identity score. Annotated *amiA* from *H. pylori* compared with *C. jejuni* NCTC 11168 *amiA* gene showed 68 pairwise score whilst *C. fetus amiA* and the *E. coli amiA, amiB, amiC, amiD* and *ampD* gave 71, 64, 49, 52, 62 and 70 pairwise scores respectively. *C. jejuni* 81116 showed higher pairwise scores to *H. pylori* and *E. coli amiB* and *amiC* compared to *C. jejuni* NCTC 11168, which showed some strain variation was present between *C. jejuni* strains. Interestingly, *H. pylori amiA* showed a higher pairwise score with *E. coli ampD* than *E. coli amiA.* (Table 1.3 & 1.4).

The DNA sequences of all the *N*-acetylmuramoyl-L-alanine amidase showed large variation in size. *C. jejuni* genes have the largest sequence (1980 bp) compared to the genes within other organisms with *E. coli ampD* (552 bp), *E. coli amiA* (870 bp) and *H. pylori amiA* (1323 bp) (Table 1.3).

Using BLASTp with the AmiA sequence from *C. jejuni* NCTC 11168 showed similar results as comparisons using the DNA sequence. The most similar annotated and/or putative *N*-acetylmuramoyl-L-alanine amidases were from other *C. jejuni* strains with 100-93% max identity score. Other *Campylobacter* species showed high percentage similarity, like *C. coli* (72% identity score) and *C. hominus* (63%). Other similar gene sequences found were in *H. pylori* (56% identity score), *W. succinogens* (49%) and *H. canadensis* (48%).

Alignment of the *N*-acetylmuramoyl-L-alanine amidase sequences in BLASTp showed high similarity across all sequences within the C-terminus of the putative protein (Figure 1.4). This ~650 bp region across the *N*-acetylmuramoyl-L-alanine amidases is highly conserved C-terminal whilst the N-terminal region showed little similarity and was more evident in the derived amino acid sequence comparison. It became apparent across all the *N*-acetylmuramoyl-L-alanine amidase sequences of the three organisms there are two distinct domains, the highly variable N-terminal domain with little to no conservation and the highly conserved 'amidase' C-terminal domain (Figure 1.5 & 1.6). The highly variable N-terminal region across all the sequences showed no functional enzymatic motifs which would cause bifunctionality in *C. jejuni* and *H. pylori*.

The motifs of *N*-acetylmuramoyl-L-alanine amidase genes from *C. jejuni*, *H. pylori* and *E. coli* were compared to find common structures in the derived protein sequence (Appendix 1.0). The motifs present in *C. jejuni* NCTC 11168 and 81116 *amiA* sequences were identical. Despite *H. pylori amiA* having only a 68% identity score compared to *C. jejuni amiA* DNA sequence, all motifs except for two were present in *H. pylori amiA*. Unexpectedly, certain motifs that were expected to be present in all sequences, like peptidoglycan binding domains, were only present in the *E. coli amiD* sequence.

Three phylograms were created from the whole amino acid sequence and the amino acid sequences of the two main domains of the *N*-acetylmuramoyl-L-alanine amidase, the N-terminal and the 'amidase' C-terminal (Figure 1.7). Comparing the differences and similarities between the domain amino acid sequences with one another could help determine the closest *E. coli N*-acetylmuramoyl-L-alanine amidase, functionally to *C. jejuni* AmiA. From both phylograms it can be seen that regardless of the terminus, N or C terminal used for comparison, the epsilonproteobacteria *N*-acetylmuramoyl-L-alanine

amidases cluster together, showing the closest in similarity. The phylogram derived from the N-terminus shows *C. jejuni* and *H. pylori* AmiA has a closer relationship to *E. coli* AmiA, AmiB and AmiD, however it does not differentiate the *N*-acetylmuramoyl-L-alanine amidases in *E. coli* according to specificity, location or functionality.

The phylogram using the *C*-terminus shows a closer relationship between *C. jejuni* and *H. pylori* AmiA with *E. coli* AmiD and AmpD. *E. coli* AmiD and AmpD were shown within this phylogram to be different to the other *E. coli N*-acetylmuramoyl-L-alanine amidases. This is related to previous literature showing they are unlike AmiA, AmiB and AmiC. *E. coli* AmiD and AmpD belonging to the amidase_2 protein family have specificity for peptidoglycan units with the anhydro-MurNAc. *E. coli N*-acetylmuramoyl-L-alanine amidases AmiA, AmiB and AmiC have no specificity for anhydro-MurNAc and have shown differential locations of action in the cell. *C. jejuni* AmiA closer relation to amdiase_2 protein family *N*-acetylmuramoyl-L-alanine amidases could show the function and potential specificity for anhydro-MurNAc units as well.

Table 1.3. A key showing the gene size and gene sequence of *C. jejuni, C. fetus, H. pylori* and *E. coli N*-acetylmuramoyl-L-alanine amidase DNA sequences.

Sequence name and reference number	Gene size
Sequence 1: Campylobacter_fetus_82-40_CFF8240_1209	1410 bp
Sequence 2: Campylobacter_jejuni_NCTC11168_AmiA	1980 bp
Sequence 3: Campylobacter_jejuni_81116_AmiA	1980 bp
Sequence 4: Helicobacter_pylori_26695_AmiA	1323 bp
Sequence 5: Escherichia_coli_K-12_AmiA	870 bp
Sequence 6: Escherichia_coli_K-12_AmiB	1338 bp
Sequence 7: Escherichia_coli_K-12_AmiC	1254 bp
Sequence 8: Escherichia_coli_K-12_AmiD	831 bp
Sequence 9: Escherichia_coli_K-12_AmpD	552 bp

Table 1.4. Multigene alignment showing the similarity via pairwise percentages, of *C. jejuni, C. fetus, H. pylori* and *E. coli N*-acetylmuramoyl-L-alanine amidase nucleotide sequences.

Sequences compared (A:B)	Score (%)
Sequences (1:2)	71
Sequences (1:3)	71
Sequences (1:4)	58
Sequences (1:5)	55
Sequences (1:6)	47
Sequences (1:7)	50
Sequences (1:8)	56
Sequences (1:9)	64
Sequences (2:3)	98
Sequences (2:4)	66
Sequences (2:5)	64
Sequences (2:6)	49
Sequences (2:7)	52
Sequences (2:8)	62
Sequences (2:9)	70
Sequences (3:4)	68
Sequences (3:5)	64
Sequences (3:6)	52
Sequences (3:7)	56
Sequences (3:8)	61
Sequences (3:9)	69
Sequences (4:5)	59
Sequences (4:6)	48
Sequences (4:7)	48
Sequences (4:8)	60
Sequences (4:9)	67
Sequences (5:6)	63
Sequences (5:7)	67
Sequences (5:8)	50
Sequences (5:9)	64
Sequences (6:7)	57
Sequences (6:8)	64
Sequences (6:9)	71
Sequences (7:8)	62
Sequences (7:9)	73
Sequences (8:9)	62

```
Campylobacter_jejuni_NCTC11168      LDNNNLTLGFYIQTTNQNANKKATQSSSKTLNTNYKSGKLVVIDAGHGGK 445
Campylobacter_jejuni_81116_Ami      LDNKNLTLGFYAQTTNQNVNKKATQSSSKTLNTNYKSGKLVVIDAGHGGK 445
Campylobacter_fetus_82-40_CFF8      ----------VAAKTAKKEDDKKSQTQNKNTIKNIPRNKTIVLDAGHGGK 257
Helicobacter_pylori_26695_AmiA      ----------------SKNQVFIAEKNDTFIKTKRKKHKKIVLDAGHGGK 228
Escherichia_coli_K-12_AmiA          -----------------------GHSKPKAKKSGGKR--VVVLDPGHGGI 68
Escherichia_coli_K-12_AmiC          --------------GDLEKQVPPAQSGPQPGKAGRDRPIVIMLDPGHGGE 199
Escherichia_coli_K-12_AmiB          --------------TTGVISSNTVTRPAARATANTGDKIIIAIDAGHGGQ 203
Escherichia_coli_K-12_AmiD          ------------------------------QAQAAYPRIKVLVIHYTADDF 56
Escherichia_coli_K-12_AmpD          -------------------------ISLPPGEFGGPWIDALFTGTIDPQA 60
                                                                          :

Campylobacter_jejuni_NCTC11168      DSGALSDKKGSLKEKDIVLSTALKLGNELKKRG-YKVLYTRSSDKFINLR 494
Campylobacter_jejuni_81116_Ami      DSGALSDKKGSLKEKDIVLSTALKLGNELKKRG-YKVLYTRSSDKFINLR 494
Campylobacter_fetus_82-40_CFF8      DAGAVGSR--TLYEKNVVLKVALKAGKILKNRG-YKVYYTRDKDKFIGLR 304
Helicobacter_pylori_26695_AmiA      DCGAMSAN--LVCEKDIVLEVVKFLHKELKKRD-YSVLLTRDKDIYIDLV 275
Escherichia_coli_K-12_AmiA          DTGAIGRN--GSKEKHVVLAIAKNVRSILRNHG-IDARLTRSGDTFIPLY 115
Escherichia_coli_K-12_AmiC          DSGAVGKY--KTREKDVVLQIARRLRSLIEKEGNMKVYMTRNEDIFIPLQ 247
Escherichia_coli_K-12_AmiB          DPGAIGPG--GTREKNVTIAIARKLRTLLNDDPMFKGVLTRDGDYFISVM 251
Escherichia_coli_K-12_AmiD          DSSLATLTDKQVSSHYLVPAVPPRYN---GKPRIWQLVPEQELAWHAGIS 103
Escherichia_coli_K-12_AmpD          HPFFAEIAHLRVSAHCLIR----------RDGEIVQYVPFDKRAWHAGVS 100
                                    .            : :            .   .    .   .  :

Campylobacter_jejuni_NCTC11168      DRTKYANDKRADLFISIHANAAPNATKAKSSEGVETFFLSPARSERSKKA 544
Campylobacter_jejuni_81116_Ami      DRTKYANDKRADLFISIHANAAPNATKAKSSEGVETFFLSPARSERSKKA 544
Campylobacter_fetus_82-40_CFF8      NRTSFANDKMADLFISIHANAAPNSKKAPEMQGIETFFLSPTRSERSMRA 354
Helicobacter_pylori_26695_AmiA      ARTELANKKSADLFISVHANSIPKHSTSN-AHGIETYFLSTARSERARKV 324
Escherichia_coli_K-12_AmiA          DRVEIAHKHGADLFMSIHADGFTNPKAAGASVFALSNRGASSAMAKYLSE 165
Escherichia_coli_K-12_AmiC          VRVAKAQKQRADLFVSIHADAFTSRQPSGSSVFALSTKGAISTAAKYLAQ 297
Escherichia_coli_K-12_AmiB          GRSDVARKQNANFLVSIHADAAPNRSAIGASVWVLSNRRANSEMASWLEQ 301
Escherichia_coli_K-12_AmiD          AWRGATRLN--DTSIGIELENRGWQKSAGVKYFAPFEPAQIQALIPLAKD 151
Escherichia_coli_K-12_AmpD          QYQGRERCN--DFSIGIELEG---------TDTLAYTDAQYQQLAAVTRA 139
                                          . :  :  :.:. :

Campylobacter_jejuni_NCTC11168      AEKENQGDFEE----INYFSKQSILNFLNREKIVASNKLAIDVQKNILTQ 590
Campylobacter_jejuni_81116_Ami      AEKENQGDFEE----INYFSKQSILNFLNREKIVASNKLAIDVQKNILTQ 590
Campylobacter_fetus_82-40_CFF8      ANLENKSDTDE----MNYFTKISFLNFLNREKIIASNKLAIDIQTNLLSS 400
Helicobacter_pylori_26695_AmiA      AEQENKDDVNL----MDYFSKSLFLNSLNTQRLIVSNKLAIDVQYGMLQS 370
Escherichia_coli_K-12_AmiA          RENRADEVAGK----KATDKDHLLQQVLFDLVQTDTIKNSLTLGSHILKK 211
Escherichia_coli_K-12_AmiC          TQN-ASDLIGG----VSKSGDRYVDHTMFDMVQSLTIADSLKFGKAVLNK 342
Escherichia_coli_K-12_AmiB          HEKQSELLGGAGDVLANSQSDPYLSQAVLDLQFGHSQRVGYDVATSMISQ 351
Escherichia_coli_K-12_AmiD          IIARYHIKPEN-----VVAHADIAPQRKDDPGPLFPWQQLAQQGIGAWPD 196
Escherichia_coli_K-12_AmpD          LIDCYPDIAKN-----MTGHCDIAPDRKTDPGPAFDWARFRVLVSKETT- 183
                                                                  .
```

Figure 1.5. Alignment of nine *N*-acetylmuramoyl-L-alanine amidases protein sequences in *C. jejuni, C. fetus, H. pylori* and *E. coli* showing part of the C-terminal region within the amidase region with the highest level of conservation across all the sequences.

The other regions of the alignment show little to no similarity.

A : (Double dot/colon) indicates conservation between groups of strongly similar properties - scoring > 0.5 in the Gonnet PAM 250 matrix.

A . (single dot) indicates conservation between groups of weakly similar properties - scoring =< 0.5 in the Gonnet PAM 250 matrix.

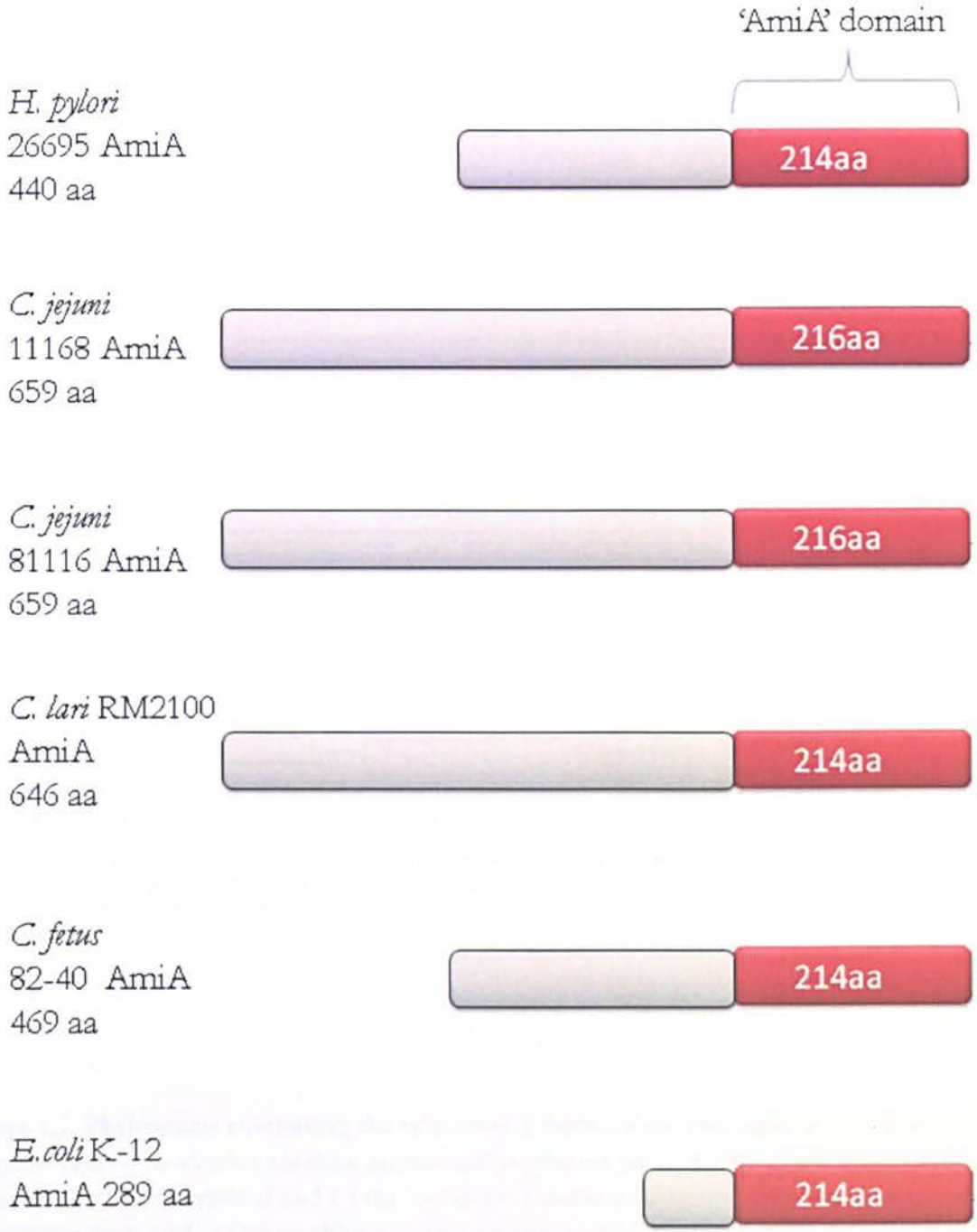

Figure 1.6. A representative illustration showing the conserved amidase regions of AmiA amino acid sequences from *C. jejuni, C. fetus, C. lari, H. pylori* and *E. coli.*
The amidase region is present within all experimentally *E. coli* and *Campylobacter N*-acetylmuramoyl-L-alanine amidases, regardless of size. The regions were defined using InterProScan.

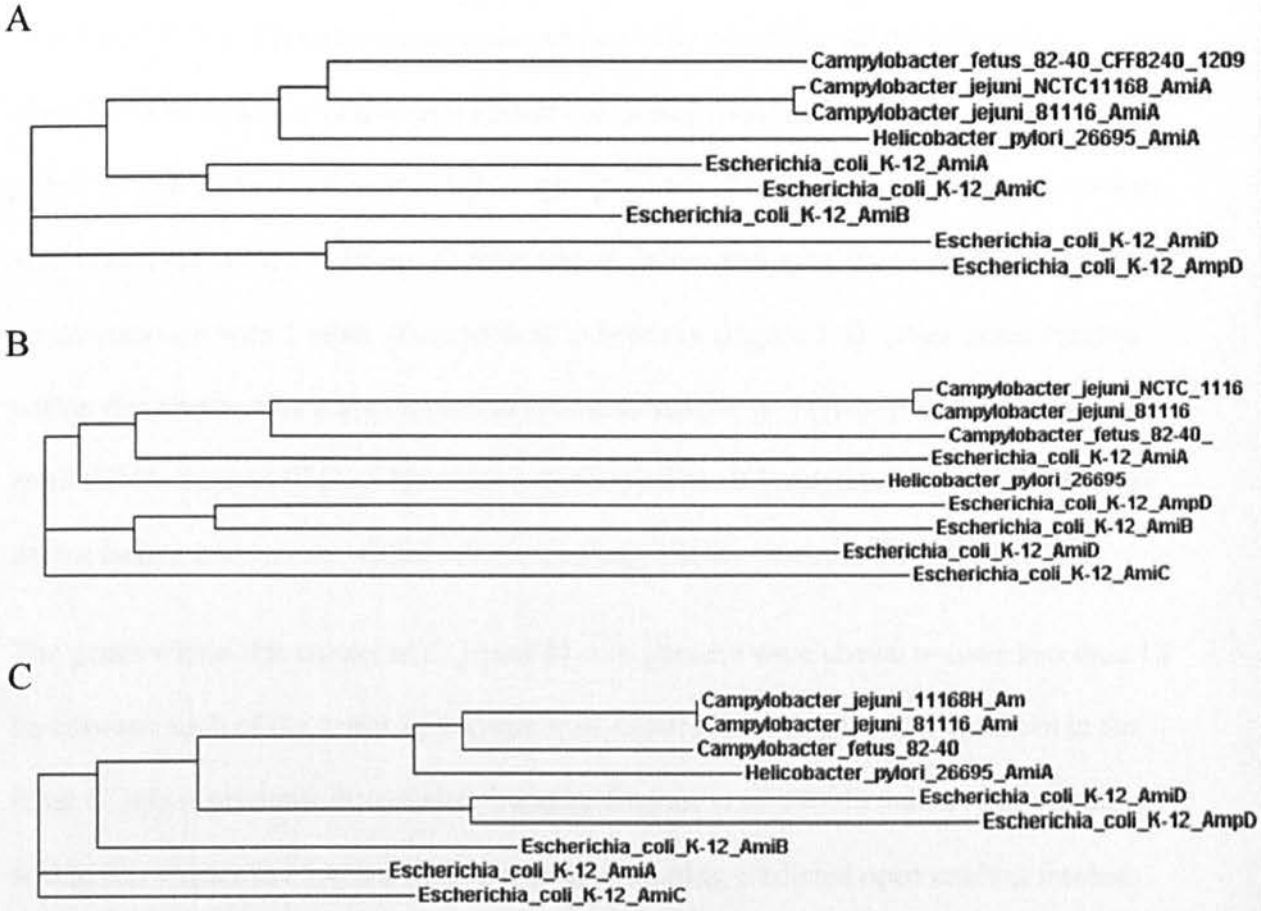

Figure 1.7. Phylograms comparing the relationship between the two main domains of the *N*-acetylmuramoyl-L-alanine amidase amino acid sequences using A) the whole amino acid sequence, B) the N-terminal and C) the 'amidase' C-terminal.
Phylograms were made using neighbour joining algorithm and ClustalW2.

1.10.2. Cluster arrangement of *amiA* and *spoT* region between organisms

Both *amiA* and *spoT* are located within the same region of the genome in *C. jejuni* NCTC 11168 and 81116. This arrangement was shown to be present in all the sequenced *C. jejuni* genomes. The structure of the gene cluster containing *amiA* and *spoT* was compared in *H. pylori, E. coli* and other *Campylobacter* spp. genomes. The position of *spoT* to *amiA* was well conserved within *C. jejuni, C. fetus* and *H. pylori* genomes, being approximately 2500 bp downstream with 2 other genes present in between (Figure 1.8). Other genes located within this cluster which also appear to be conserved are *tyrS* (tyrosyl tRNA synthestase), *rpoZ* (DNA directed RNA polymerase subunit) and *pyrH* (uridylate kinase). These genes do not have a known role within cell morphology but are essential for cell life cycle.

The genes within this cluster in *C. jejuni* 81-176 genome were shown to have less than 12 bp between each of the genes by Gaynor *et al.* (2005) and this pattern was shown in the other *C. jejuni* genomes. It was also found by Gaynor *et al.* (2005) that several genes within this cluster in *C. jejuni* 81-176 have overlapping predicted open reading frames. Functional database searches suggested that one or more genes downstream of *spoT* in *C. jejuni* 81-176 are essential and possibly co-regulated. The proximity of the genes within this cluster were analysed within other *C. jejuni* strains, NCTC 11168 and 81116, exhibiting a similar distance and the same orientation.

Unlike *C. jejuni* and *H. pylori, E. coli* K12 *spoT* (b3650) and *relA* (b2784) are not located within the same genomic region as any of the annotated *N*-acetylmuramoyl-L-alanine amidases *amiA*(b2435), *amiB*(b4169), *amiC*(b2817), *amiD*(b0867) and *ampD*(b0110).

SpoT in *E. coli* K12 is located next to the *rpoZ* gene and this is also found within *C. jejuni.* The other genes such as *gmk* (guanylate kinase) and *recG* (ATP-dependent DNA helicase) are also located nearby which could also have an essential function.

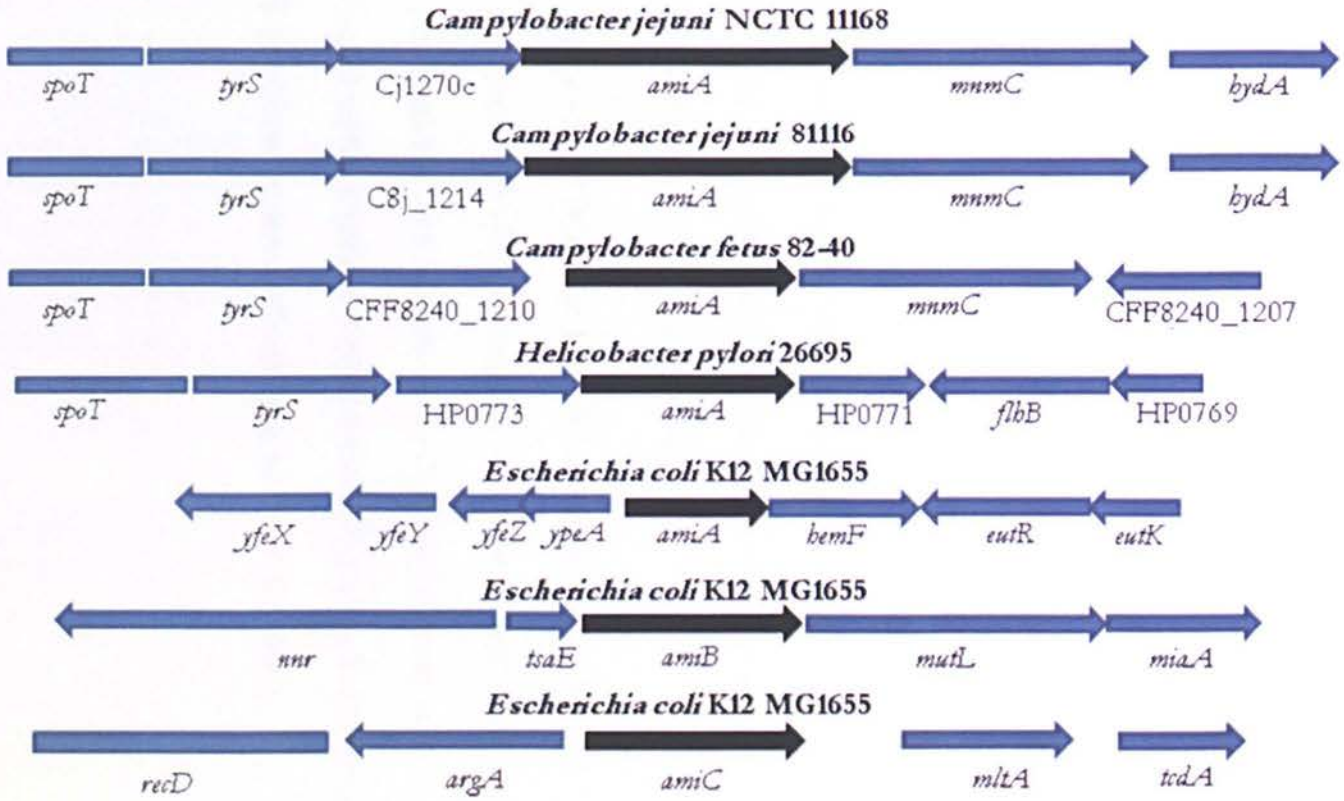

Figure 1.8 A genomic region comparison of *N*-acetylmuramoyl-L-alanine amidase genes from *C. jejuni, H. pylori* and *E. coli.*
N-acetylmuramoyl-L-alanine amidase genes are in black. Genome region comparison function settings were for >=40% similarity, >=10% identity and <=1.0 P-Value. *RelA/spoT* is present on the *C. jejuni* and *H. pylori* regions two genes upstream. Image was created using information from Comprehensive Microbial Resource from JCVI and NCBI.

The searches have shown that there is not a redundancy of *N*-acetylmuramoyl-L-alanine amidases within *Campylobacter* and *Helicobacter* strains like within *E. coli*. Within *E. coli*, the various *N*-acetylmuramoyl-L-alanine amidases have been shown to have differential specificity for muropeptide units and localisation within the cell. The localisation of *C. jejuni* and *H. pylori* AmiA have not yet been elucidated to determine whether these proteins are able to fulfil all the same requirements as five *N*-acetylmuramoyl-L-alanine amidases within *E. coli*.

The gene cluster containing *amiA* and *spoT* in *C. jejuni* and *H. pylori* has several genes that are related to viability, which could suggest that *amiA* may have an essential role within the *C. jejuni* life cycle, unlike *E. coli* where none of the *N*-acetylmuramoyl-L-alanine amidases are co-located with similar genes. The lack of redundancy within *C. jejuni* and *H. pylori* for *N*-acetylmuramoyl-L-alanine amidases could also be further evidence supporting the essential role these enzymes play.

The concept of PCD with bacterial cells is still controversial. The *mazEF* module is influenced by the levels of ppGpp, which are altered by *relA/spoT*. Although a similar system has not been located within *C. jejuni* genomes, several homologous genes are located within a variety of other bacteria including *S. Typhimurium, P. aeruginosa* and *Staphylococcus aureus* (Engelberg-Kulka *et al.*, 2006).

1.11. Aims of the study

The coccoid morphology has been well documented within *C. jejuni* and other bacillary organisms for decades. However, the mechanism and biological role of this morphology within *C. jejuni* has not yet been elucidated. Research into this area showed a noticeable decline after 1998 due to the suggestion that the coccoid form in *H. pylori* was in a degenerative state (Kusters, 1997). Coccoid morphology has been proposed to play a role within biofilm survival (Karlyshev & Wren, 1995). There are currently no genes within *C. jejuni* that are considered as genetic determinants for CFF. However, *amiA* in *H. pylori* has been defined as the first genetic determinant for the CFF (Costa *et al.*, 1999). The function of the enzyme encoded by this gene has not been elucidated within *C. jejuni* nor has it been linked to CFF. Downstream of *amiA* is the gene *spoT*, which has been linked to CFF in *C. jejuni* 81-176 (Gaynor *et al.*, 2005), leading to further consideration that the gene cluster may have a role in CFF. Understanding the role and mechanism of CFF in *C. jejuni* could provide further information into the persistence of this seemingly fastidious and sensitive organism.

The aim of this study is to investigate the potential role of *amiA* and *spoT* in CFF in *C. jejuni* 11168H and 81116. The objectives are to:

1. Determine the effect of deleting *spoT* and *amiA* in *C. jejuni* on CFF accumulation, as well as cell viability and growth.
2. Measure the levels of *amiA* mRNA expression concurrent with the accumulation of CF over time in *C. jejuni.*

3. Create a *Campylobacter* specific expression system for determination of the effects of *amiA* overexpression on growth (colony forming units), membrane integrity and morphology in *C. jejuni* and *E. coli.*
4. Assess the functional activity of purified *C. jejuni* AmiA on peptidoglycan isolated from *E. coli* and *C. jejuni* using TLC and HPLC.

2.0. Materials and Methods

2.1. General methods

2.1.1. Bacterial strains, media and culturing methods

Laboratory stocks were stored at -80°C in Brucella broth (Oxoid) supplemented with 15% glycerol, prepared originally from fresh 2 day culture. *C. jejuni* strains 81116 (NCTC 11828) and hyper motile derivative of NCTC 11168, 11168H (Karlyshev *et al.*, 2002) were recovered from -80°C by incubation in microaerobic conditions (5% O_2, 10% CO_2 in N_2) within the controlled atmosphere incubator (Don Whitley); or by incubating in jars containing Campygen Gas generating Kit (Oxoid) on Columbia Blood Agar (CBA, Oxoid) supplemented with 5% defibrinated horse blood at 37°C for 48 hrs.

For liquid cultures, cells were transferred from the solid media in Brain Heart Infusion (BHI, Oxoid) Broth, incubated with shaking (90 rpm) at the starting OD_{600} 0.02. These cultures were monitored at the time points of 0, 6, 24, 30 and 48 hrs.

E. coli cultures were grown at 37°C on Luria Bertani (LB) media. When necessary, the media was supplemented with appropriate antibiotics, ampicillin (100mg/ml), kanamycin (50mg/ml) or chloramphenicol (10mg/ml).

2.1.2. Cell morphology determination and counting

Cells were visualised using light microscopy after Gram staining. Samples from solid media were heat fixated onto glass slides and stained using crystal violet, Grams Iodine, 90% ethanol and carbol fuchsin. For liquid cultures, a 1ml sample was added to 100µl of 10% neutral buffer formalin solution for 20 mins. A 10µl sample of the suspension was left to air dry on glass slides. Once dry, the samples were methanol fixed and stained with

crystal violet for 15 sec. Slides were visualised at x100 oil immersion objective lens and were captured in triplicates with a Nikon 80i (Nikon, Telford). For each time point or sample, a minimum of 100 cells were counted for the different morphologies using the ImageJ computer program.

For scanning electron microscopy, samples were prepared on methanol cleaned poly-L-lysine coated cover slips in PBS by a dehydration protocol as follows: The primary fixation was performed in 2.5% glutaraldehyde in 0.1M phosphate buffer. Cover slips were washed in 0.1M phosphate buffer (pH 7.5) 4 times for 15 mins. The secondary fixation was performed with 1% osmium tetroxide in 0.1M phosphate buffer (pH 7.5). The sample was put through an ethanol graded series (50, 70, 80, 90 and 95%) for 20 mins each then 100% three times for 20 mins. The sample was then immersed in hexamethyledisilizane and allowed to air dry for 24 hrs. The samples were mounted onto stubs and sputter gold coated and visualised on a Zeiss EVO 50 Scanning electron microscope.

2.2. Gene comparison, protein function programs and sequencing data analysis

2.2.1 Gene, genome and cluster comparison

Sequences of genes and genomes were obtained from National Centre for Biotechnology (NCBI) Entrez Genome database (www.ncbi.nlm.nih.gov). Gene and genome region analysis was conducted using BLAST (blast.ncbi.nlm.nih.gov), xBase (www.xbase.ac.uk), JCV Comprehensive Microbial Resource (cmr.jcvi.org) and ClustalW (www.ebi.ac.uk/Tools/msa/clustalw2).

2.2.2 Protein and structure analysis

Amino acid sequences were obtained from the NCBI database. Protein alignments and phylograms were produced using ClustalW. Prediction of tertiary protein structures from amino acid sequences were derived using LOMETS (Local Meta-Threading-Server) (zhanglab.ccmb.med.umich.edu/LOMETS).

2.2.3. Sequencing data analysis

Nucleotide sequencing results from Cogenics (Beckman Coulter) were analysed as chromatograms and in FASTA format using Chromas Lite program.

2.3. General molecular and cloning techniques

2.3.1. DNA isolation

2.3.1.1. Chromosomal and plasmid isolation

Plasmid DNA was isolated using the Qiagen plasmid purification kit (Qiagen). Chromosomal DNA was isolated by Gentra® Puregene® Yeast/Bacteria Kit (Qiagen). The kits were used according to manufacturers' specifications and protocol.

2.3.1.2. Agarose gel DNA extraction and purification methods

DNA samples were purified using two methods and kits; NucleoSpin Extract II using protocol for DNA extraction from Agarose gel, and the QIAquick PCR purification kit (Qiagen).

For the isolation of specific fragments of DNA that were derived from restriction digested DNA, NucleoSpin Extract II agarose gel purification was used. The DNA samples were run on an agarose gel and the DNA fragment of interest was extracted from the agarose gel using a clean scalpel. The sample was placed into a clean 1.5ml Eppendorf tube and was purified according to manufacturers' protocol. The QIAquick PCR purification Kit was used to purify DNA samples after restriction digestion and PCR products for downstream reactions. The kit was used according to manufacturers' specifications.

2.3.2. Polymerase Chain Reaction (PCR)

Within each of the PCRs, along with the DNA polymerase and the appropriate buffer (except for the ReadyMixTaq^{tm} PCR Mix), the following constituents were added: PCR Nucleotide Mix (Promega), appropriate reverse and forward primers and nuclease free water. The cycler conditions and the concentration of the primers and dNTPs were performed and used in accordance to the manufacturers' protocol. All the thermal cycler conditions for each of the DNA polymerases used are listed in Tables 2.1, 2.2, 2.3 and 2.4.

Table 2.1. The thermal cycler conditions for Phusion® High-Fidelity DNA Polymerase (NEB) used with Standard Phusion HF Buffer containing 1.5mM $MgCl_2$ at 1x reaction concentration.

PCR step	Temperature (°C)	Duration of step	Number of cycles
Initial denaturation	98	30 sec	1
Denaturation	98	10 sec	
Annealing	45	30 sec	30
Extension	72	30 sec per kb	
Final extension	72	10 mins	1

Table 2.2. The thermal cycler conditions for One*Taq*® DNA Polymerase (NEB) used with One*Taq*® Standard Reaction Buffer containing 1.8mM $MgCl_2$ at 1x reaction concentration.

PCR step	Temperature (°C)	Duration of step	Number of cycles
Initial denaturation	94	30 sec	1
Denaturation	94	30 sec	
Annealing	45	30 sec	30
Extension	68	1 min per kb	
Final extension	68	5 mins	1

Table 2.3. The thermal cycler conditions for GoTaq® DNA Polymerase (Sigma Aldrich) used with GoTaq® Buffer containing 1.5mM $MgCl_2$ at 1x reaction concentration.

PCR step	Temperature (°C)	Duration of step	Number of cycles
Initial denaturation	95	2 mins	1
Denaturation	95	30 sec	
Annealing	50	30 sec	30
Extension	72	1 min per kb	
Final extension	72	5 mins	1

Table 2.4. The thermal cycler conditions for ReadyMixTaq™ PCR Mix (Sigma Aldrich) with 1.5mM $MgCl_2$ and 0.2mM dNTP at 1x reaction concentration.

PCR step	Temperature (°C)	Duration of step	Number of cycles
Initial denaturation	94	1 min	1
Denaturation	94	30 sec	
Annealing	55	30 sec	25
Extension	72	1 min per kb	
Final extension	72	5 mins	1

2.3.3. Agarose gel electrophoresis

To visualise PCR products, plasmids and DNA fragments from restriction digests, the samples were run on agarose gels. All DNA gels were 1% agarose gel (Sigma) containing 0.1μg/μl ethidium bromide (Fisher) for visualisation and 1x Tris-Borate EDTA Buffer (TBE) (pH 8.3) (Fisher). Samples were loaded into the gel with bromophenol blue based loading buffer (NEB). 1 kb molecular weight ladder (NEB) was used as a standard to estimate the DNA fragment sizes. Gel electrophoresis was conducted in a horizontal gel tank (Fisher) containing 1x TBE buffer. The gel was run at 150V for 40 mins. The gel was visualised with the transilluminator setting in the G:Box (Syngene) using GeneSnap software (Syngene).

2.3.4. *E. coli* transformation

E. coli XL1 Blue Supercompetent, Xl2 Blue Ultracompetent and BL21 -CodonPlus® (DE3) RIL competent cells were used according to manufacturers' protocol.

For cloning experiments *E. coli* XL1 Blue Supercompetent or *E. coli* XL2 Blue Ultracompetent competent cells (Stratagene) were grown overnight on Luria Bertani (LB, Oxoid) agar plates at 37°C, supplemented with appropriate antibiotic. XL1 Blue Supercompetent cells give an average transformation efficiency of $\geq 5 \times 10^9$ transformants/μg of supercoiled DNA and are resistant to tetracycline. XL2 Blue Ultracompetent cells give an average transformation efficiency of $\geq 5 \times 10^9$ transformants/μg of supercoiled DNA and are resistant to tetracycline and chloramphenicol.

2.3.5. *C. jejuni* competent cell preparation, electroporation and sepiolite transformation method

C. jejuni was grown as a lawn on Columbia Blood Agar overnight at 37°C under microaerobic conditions. The cells were harvested into 2ml of wash solution (272mM sucrose, 15% glycerol). The bacteria were spun down via centrifugation for 20 mins at 3000 x g at 4°C. The pellet was resuspended in fresh ice cold wash buffer. The process was repeated 3 times before cells were finally resuspended in 1ml of ice cold wash buffer. The competent cells were made into 50µl aliquots and used either immediately or stored at -80°C. DNA was introduced into competent *C. jejuni* cells by electroporation using 2.5 kV, 200 Ω and 25µF with the time constant >4 ms in a 0.2cm electroporation cuvette (Biorad) (Wassenaar *et al.*, 1993). After electroporation, the cuvettes were flushed with 100µl Super Optimal Broth with Catabolite repression (SOC) media (Fisher) and the cells were spread onto a non selective CBA plate. The plates were incubated for a minimum of 5 hrs or the maximum of overnight under optimal atmospheric conditions (37°C) before replating onto media containing selective antibiotic.

The sepiolite method for bacterial transformation was previously described by Wilharm *et al.* (2010). *C. jejuni* cells were grown on CBA under optimal conditions for 48 hrs and cells were harvested and suspended in BHI broth suspension with OD_{600} to the optical density of 0.5 – 1.0 to an absorbance of 600nm. Cells were centrifuged at 6708 x g (10,000 rpm) for 3 mins (at room temperature) to form a pellet. The supernatant was removed and pellet was resuspended with 100µl of sterile sepiolite suspension (0.01% sepiolite in deionised H_20 supplemented with 5mM Hepes and 200mL KCl). 50ng of transforming DNA was added and the mixture was spread across a CBA plate for 30

seconds after the agar was dry. After 24 hrs incubation at 37°C, the cells were harvested and re-plated onto a CBA plate with selective antibiotic.

2.3.6. Restriction digestion and other cloning enzymatic reactions

Restriction enzymes (NEB) were used to digest plasmids and fragments of DNA. According to the enzyme, the appropriate NEB buffer was used at 1x concentration, when necessary supplemented with 100μg/ml Bovine Serum Albumin (BSA).

Antarctic Phosphatase (NEB) was used for dephosphorylation of vectors after restriction digestion by the removal of the 5′ phosphate from DNA to prevent recircularisation, which creates background during cloning. Antarctic Phosphatase buffer was used at 1x working concentration within each reaction.

T4 Polynucleotide Kinase (NEB) was used to catalyse the phosphorylation of PCR products for cloning by the transfer of phosphate from ATP to the 5′ -hydroxyl terminus of polynucleotides. This was used either with T4 ligase reaction buffer (50mM Tris-HCl, 10mM $MgCl_2$, 1mM ATP, 10mM DTT, pH 7.5) or T4 Polynucleotide Kinase buffer (70mM Tris-HCl, 10mM $MgCl_2$, 5mM DTT, pH 7.6). Both are acceptable as they both contain ATP, which is necessary for the reaction to take place.

T4 DNA ligase (NEB) was used for the ligation of DNA to form a new construct by catalyzing the formation of a phosphodiester bond between two termini. This was used with the T4 ligase reaction buffer at 1x working concentration within each reaction.

T4 DNA polymerase (NEB) catalyzes the synthesis of DNA in the 5′→ 3′ direction and so removes 3' overhangs and fills in 5' overhangs to form blunt ends with dNTPs. The

enzyme was used with either T4 DNA polymerase buffer or restriction enzyme buffer as both were appropriate for the reaction.

CloneChecker (Invitrogen) was used to rapidly screen recombinant bacterial cultures for target plasmids. 4µl of the green solution was used, mixed with the bacterial culture scraped from the agar plate. This was heated to 100°C for 1 min. The resulting lysates were then mixed with 10µl 1x TE Buffer. The lysates were later used for PCR or restriction digestion for verification. The Supercoiled Plasmid protocol was used for checking plasmids for the presence of an insert after ligation and transformation. The Supercoiled Plasmid protocol was conducted according to manufactures' specifications.

2.4. Quantitative polymerase chain reaction (qPCR)

2.4.1. Total RNA isolation

To isolate total RNA, Bacteria Protect Reagent (Qiagen) was applied directly onto plate culture or double volume to liquid culture. The culture and Bacteria Protect Reagent were mixed and spun down 4000 x g for 20 mins (4°C). The supernatant was removed and the pellet was either processed immediately or stored at -80°C. The RNA was isolated using the RNeasy Mini Prep kit (Qiagen) with the protocol as described by manufacturers with the Bacteria Protect Reagent. The cells were lysed using lysozyme (15mg/ml) and proteinase K (120 mAU). The RNA samples are treated with RNase free DNase kit (Qiagen) to prevent DNA contamination. The RNA isolated was aliquoted and stored at -80°C or used immediately for quantitative real time PCR (qPCR).

2.4.2. Quantification of total RNA

RNA samples were measured on the NanoVue system. The NanoVue system used two measurements of sterile nuclease free water twice for calibration. The samples were considered pure if the A260/280 ratio was between 1.7 and 2.0 and the A260/230 ratio was above 2.0. Despite the RNeasy RNA isolation method using no phenol, the A260/230 value could be altered by the presence of other solvents and chaotropic salts, which are present within the buffers of the RNeasy Mini Prep Kit. In accordance to the manufacturers, a decrease in this value would not necessary alter downstream reactions.

2.4.3. qPCR Primers

Primers were designed from *C. jejuni* DNA sequences from NCBI. The sequences of the genes of interest were analysed by Primer BLAST (NCBI) to design primers specific to the template. The primers were designed to provide an amplicon length of between 85 and 250 bp and the primers were between 18 and 21 bp. Potential primers were verified for secondary structures and primer dimers using the Sigma Genosys DNA calculator (Sigma). The size of the amplicon was verified using the program Sequence Manipulation Suite: PCR products. Once the primers were verified with the previous programs, the primers were checked through NCBI BLAST nucleotide tool to ensure specificity with *C. jejuni*, with no additional gene hybridisation. Initial set of primers created were not optimal due to variation between amplicon lengths (Table 2.5.) and so a second set were created and were used in all experiments (Table 2.6.)

2.4.4. qPCR

Two step quantitative real time PCR was performed using 2x QuantiFast SYBR Green RT-PCR Kit (Qiagen), which contains QuantiFast SYBR Green RT-PCR Master Mix (containing QuantiFast SYBR Green RT-PCR Buffer with $MgCl_2$, dNTP mix and ROX™ passive reference dye) and QuantiFast RT Mix (containing Omniscript® Reverse Transcriptase and Sensiscript® Reverse Transcriptase). For each experiment, the master mix for each primer set was made freshly including 2x QuantiFast SYBR Green RT-PCR Master Mix, QuantiFast RT Mix, forward primer (100μM) and reverse primer (100μM). Each reaction well of a 96 well plate contained RNA at a concentration ≤100ng, master mix and RNase free water to the total volume of 12.5μl. Each sample was performed in technical duplicates and biological triplicates. Every run contained no template (RNase free water added instead of RNA), no primer (RNase free water added instead of primers) and water controls and was performed in duplicates. The PCR plate was then placed into CFX96 Real time System C1000 Thermocycler (Bio-Rad). The cycler conditions were programmed in accordance to the manufacturers' protocol, as listed in Table 2.7.

2.4.5. Analysis using $2^{-\Delta\Delta}$CT method

The relative change in gene expression was calculated using the Livak and Schmittgen (2001) $2^{-\Delta\Delta Ct}$ method.

Table 2.5. The primers used in gene expression studies, with primer sequence and amplicon length listed.

Primer name	Primer sequence (5'-3')	Amplicon length (bp)
16srna for	ACAGGTGCTGCACGGCTGTC	125
16srna rev	TGCTCGGCCGAACCGTTAGC	
RpoA forward	CCCTAGCCCATCCTTTACGCCG	103
RpoA reverse	TGCTACATCTTCAAGCATACCACGCA	
AmiA forward	TGTGGCATTTGGTGCTGCGT	244
AmiA reverse	TGCGGGGCATGGTGGAAAAAGA	

Table 2.6. The revised primers that were used in gene expression studies, with primer sequence and amplicon length listed.

Primer name	Primer sequence (5'-3')	Amplicon length (bp)
q-16S for	ACAGGTGCTGCACGGCTGTC	103
q-16s-rev	TGCTCGGCCGAACCGTTAGC	
q-rpoA-for	CCCTAGCCCATCCTTTACGCCG	125
q-rpoA-rev	TGCTACATCTTCAAGCATACCACGCA	
q-amiA-for	TGGGGTTTTAGAAGGGGGTA	92
q-amiA-rev	CCACTATGCGTATGGTTTTGG	

Table 2.7. The thermal cycler protocol and conditions for qPCR using QuantiFast SYBR Green.

PCR step	Temperature (°C)	Duration of step	Number of cycles
Reverse transcription	50	10 mins	1
Enzyme activation	95	5 mins	1
Denaturation	95	10 sec	35 (The SYBR fluorescence data is measured after each cycle)
Annealing/Extension	60	30 sec	
Melt curve	90	1 min	1
	55-95	10 sec for each 0.5°C increment	

2.5. Site Directed Mutagenesis (SDM)

The genes of interest were disrupted by a kanamycin resistance (*kan*^{r}) cassette method as previously described (Karlyshev, 2005). Primers AmiA_for and AmiA_rev (Table 2.8) were used to amplify the 2 kb fragment containing *amiA* gene from *C. jejuni*11168H chromosomal DNA. For the amplification of the 2.2 kb *spoT gene*, primers SpoT_for and SpoT_rev were used (Table 2.8). The PCR products were subsequently cloned into pGEM®-T Easy (Promega). The recombinant plasmids were confirmed by restriction digest. The kanamycin cassette (*kan*^{r}) was obtained from vector pJMK30 by digestion with *Bam*HI (Trieu-Cuot *et al.*, 1985). The *kan*^{r} was blunt ended for insertion into pGEM®-T Easy-*amiA*. pGEM®-T Easy-*amiA* was digested by restriction enzymes for the insertion of *kan*^{r} into the N-terminal region and C-terminal region. pGEM®-T Easy-*spoT* was also digested at 1 restriction site for *kan*^{r} to be inserted for the construction of *amiA-kan*^{r}N, *amiA-kan*^{r}C and *spoT- kan*^{r} plasmid. Orientation of *kan*^{r} in *amiA-kan*^{r}N, *amiA-kan*^{r}C and *spoT- kan*^{r} was determined using restriction digest. The plasmids containing the insert of interest in the correct orientation were used.

An additional construct with extended flanking regions for higher complementation were created for the *amiA* knockout mutant. This construct was made in the same method as *amiA-kan*^{r}N, *amiA-kan*^{r}C, however the *amiA* gene had an additional 0.5 kb extending region on each terminal. This fragment of 3 kb was amplified using primers AmiAXF_for and AmiAXF_rev (XF abbreviated from extended fragment). The *amiA* derivative plasmid with extended flanking regions and *kan*^{r} inserted were named *amiAXF-kan*^{r}N, *amiAXF-kan*^{r}C plasmids. All plasmids were cloned into *E. coli* XL2 Blue competent cells. Transformation into *C. jejuni* was conducted by electroporation. The efficacy of the transformation was verified using PCR on the *C. jejuni* transformants chromosomal DNA.

Table 2.8. The primer sequences used for the amplification of target genes *amiA* and *spoT* for SDM.

Gene name of selection	Primer Name	Primer sequence (5' to 3')
AmiA	AmiA_for	GCTAAAATTTTTGTATTTTTAGTATTTG
	AmiA_rev	TCATCGGTTGTTATAAAAATAACTCTC
	AmiAXF_for	ATGCTATTTCTTTAGGGGCTAGTGGTG
	AmiAXF_rev	AAAAGGTGCAAATTTGTGTATTTTT
SpoT	SpoT_for	TTGAAACCAATCGATGAAGAATTATTGC
	SpoT_rev	TTAACTTTCTTTATAAGCATCATTTAAAGATG

2.6. Construction of regulated *C. jejuni* specific expression system

2.6.1. Construction of pRRBC system

The pRRBC system was derived from the pRRC construct that has complementary flanking regions of several rRNA gene clusters in *Campylobacter*, which allows for the insertion of the construct into the chromosome by homologous recombination (Karylshev & Wren, 2005). pRR contains the parts of the 16S and 28S flanking regions cloned into pGEM®-T Easy vector (Promega). An arabinose inducible system was derived from pBAD33. The *Cla*I and *Sal*I blunt ended restriction digest fragment contains a pBAD promoter and regulatory region, *araC*. The pBAD33 fragment was ligated into pRR *Xba*I blunt ended site to form pRRB. *Cam*^{r} gene cassette was inserted in the unique *Xba*I in pRRB. *Cam*^{r} was derived from pAV35 *kpn*I blunt ended fragment. The insertion of *cam*^{r} into pRRB created pRRBC with a unique *kpn*I site for insertion of genes of interest.

2.6.2. Construction of pRRT-lacYA177C

LacY gene was amplified via PCR from *E. coli* K12 chromosomal DNA using primers lacYfor and lacYrev (Table 2.9). The 1.3 kb PCR product was then cloned into pGEM®-T Easy vector (Promega). The recombinant plasmids were confirmed by restriction digest. Using PCR and primers lacY-A177Cfor and lacY-A177Crev with the template pGEM®-T Easy-*lacY*, a linear pGEM®-T Easy-*lacY* with point mutation A177C was produced. The PCR product was phosphorylated and self-ligated to recreate the circular plasmid. The mutated gene was cut out of pGEM®-T Easy and inserted into the pRRT vector. The presence of the point mutation was verified using primer walking sequencing (Beckman Coulter Cogenics) and restriction digestion. The underlined regions in Table 2.9. show the *Sal*I site to allow for integration into the unique site in pRRBCD-*egfp*.

Table 2.9. List of primers used for the amplification of *E. coli lacY* and the insertion of a base mutation using PCR.

Primer name	Primer sequence (5' to 3')
lacYfor	GTCGACAAGGAAATCCATTATGTACTATTTAAAAAAC
lacYrev	GTCGACTTAAGCGACTTCATTCACCTGACGACGCAG
lacY-A177Cfor	TGTCTCATCCTCGCCGTTTTACTC
lacY-A177Crev	ACAGCCAGAGCCCAGCCAGAAAAC

2.6.3. Quantification of membrane integrity with fluorescence microscopy

LIVE/DEAD® *Bac*Light™ Bacterial Viability Kit (Invitrogen) was used in accordance to the manufacturers' protocol for microplate reading and for confocal microscopy. The protocol for preparation of *C. jejuni* culture was derived from the protocol provided for the

preparation of *E. coli* cells. The protocol for preparation of *E. coli* culture was used according to the manufacturers' protocol.

For *E. coli* cultures, the sample culture was pelleted by centrifugation at 4,000 rpm (rotor diameter 6 cm) for 10 mins (4°C). After removing the supernatant the bacterial pellet was resuspended in 20ml 0.85% NaCl. The suspension was centrifuged again at 4,000 rpm for 10 mins. The culture was resuspended in 20ml of 0.85% NaCl. The sample was then incubated at room temperature with mixing every 15 mins. The sample was pelleted with centrifugation as before. The sample was then resuspended in a final volume of 5-10ml in 0.85% NaCl. For *C. jejuni* cultures, the sample culture was pelleted by centrifugation at 4,000 rpm for 10 mins. The supernatant was discarded and the pellet was resuspended in 20ml 0.85% NaCl. The suspension was centrifuged again under the same conditions as previously stated. The sample was resuspended in a final volume of 5-10ml in 0.85% NaCl. The optical density of the culture after preparation was adjusted to 0.1 OD_{600nm} or 1.0 OD_{600nm}. For visualisation under the confocal microscope, 5µl of the stained solution was trapped between the slide and the glass cover slip. For measurement of fluorescence using the microplate reader, a 2x stain solution was made and added to 100µl of bacterial suspension, each sample in triplicates, in the 96 well flat bottom plate. The cultures were stained with the propidiumiodide (PI) (1.67mM) and SYTO 9 (1.67mM) solution and incubated in the dark for 15 mins before visualisation and analysis. The samples were visualised on a Leica TCS SP2 AOBS confocal laser scanning microscope. The slides were visualised using a 20x dry objective, and 40x and 63x with oil immersion objectives. Higher resolution and increased magnification was obtained using the Leica software with digital zoom. The images were obtained using Leica software.

2.7. Protein purification

2.7.1. Construction of recombinant plasmids

AmiA was placed into the *E. coli* expression vector pBAD33, which contains the arabinose promoter region from the arabinose operon along with the positive and negative regulator (*araC*) (Guzman *et al.*, 1995). The gene sequence suggested the translated protein to be non-secretory via Softberry and the only possible cleavage site found by SignalP at the C-terminal between position 20 and 21. Primers were designed to amplify *amiA* with a 6 Histidine (x6) tag onto the C- terminal along with specific restriction sites of *Xba*I and *Pst*I into the flanking regions of the gene for insertion into the pBAD33 or pTrc99A vector (Table 2.10). An additional set of primers were designed (AmiAHis_foralt and AmiAHis_revalt) for the different Shine Dalgarno (SD) region to provide increased specificity for expression within *E. coli*. The original set of primers used a SD region that was specific for *C. jejuni*. Insertion and orientation of *amiA*- x6His tag sequence into pBAD33 and pTrc99A was verified by restriction digest analysis using *Sty*I or *Xba*I & *Pst*I. Confirmation of the sequence was performed through primer walking sequencing (Cogenics, Beckman Coulter). The plasmids were cloned into *E. coli* XL2 competent cells first then transformed into *E. coli* BL21 competent cells (Agilent).

Table 2.10. List of primers for the construction of histidine tagged *amiA*.

Primer name	Primer sequence (5'-3')
AmiAHis_for	AATATCTAGAAAGGAAATACTATGGCTAAAATTTTTGTATTTTTAGTAT
AmiAHis_rev	GTTTTTCTGCAGTCAATGATGATGATGATGATGTCGGTTGTTATAAAAATAA
AmiAHis_foralt	AATATCTAGAAAGAAGGAGATATACCATGGCTAAAATTTTTGTATTTTTAGTAT
AmiAHis_revalt	CTTTTTCTGCAGTCAATGATGATGATGATGATGTCGGTTGTTATAAAAATAA

2.7.2. Production and purification of recombinant protein

The *E. coli* culture that contained pBad33-*amiA*-x6His tag or pTrc99a-*amiA*-x6His tag was grown in LB broth overnight shaking at 37°C. The overnight culture was used to inoculate 100ml LB broth to OD_{600} 0.05-0.1. The culture was grown at 37°C with shaking and measured until it reached OD_{600} 0.5-0.6. The culture was then inoculated with 0.1% l-arabinose and continued to grow for an additional 3 hrs before harvesting the cells by centrifugation at 4,000 rpm for 10 mins (room temperature). The supernatant was discarded and the pellet was processed immediately or stored at -80°C for future use.

For large scale protein purification (60-100ml culture volume), QIAexpress Ni-NTA Fast Star was used. Proteins were purified according to the protocol described in the manufacturers' kit (Qiagen) using the protocols 'Purification of 6xHis tagged proteins under native conditions' & 'Purification of 6xHis tagged proteins under denaturing conditions.'

For small scale protein purification (10-20ml culture volume), Ni-NTA Agarose Magnetic Beads were used. Proteins were purified according to the protocol described in manufacturers' kit (Qiagen) using the protocol 'Purification in single reaction tubes'. The volume of the final elutant was 10-20µl.

A 20µl aliquot from all samples were mixed with 7µl of 4x NuPAGE® LDS sample buffer (Life Technologies) for SDS-PAGE analysis.

S30 T7 High Yield Protein Expression System was used according to manufacturers' protocol (Promega). The amount of purified plasmid DNA used was 250-500ng/µl. Standard reaction volumes for the experiments were 50µl and 25µl. To run the purified protein on a SDS-PAGE gel, a 5µl aliquot was taken and mixed with 14µl 1x TBS and 1µl

RNase A. The sample was incubated at room temperature for 5 mins then 20µl of 2x NuPAGE® LDS sample buffer was added followed by denaturing by heating at 100°C for 2 mins. An 8µl aliquot of the sample was loaded onto the gel.

2.7.3. SDS-PAGE and Coomassie Blue staining

The purified protein samples and Colourplus protein molecular weight marker (NEB) were loaded into precast 4-12% Bis-Tris acrylamide gel (Invitrogen). The samples and the protein molecular weight marker were run at 120V for approximately 95 mins in 1x MOPS Buffer (pH 7.7) (Invitrogen). After the gel had been removed from the cassette, it was washed 3 times for 5 mins in deionised water. The gel was incubated in the SimplyBlue™ SafeStain Coomassie Blue (Life Technologies) for 1 hr with gentle shaking. Before visualisation, the gel was washed in deionised water for 1 hr with gentle shaking. The gel was visualised using G:Box(Syngene) imaging system with GeneSnap software.

2.7.4. Western Blotting

After the protein samples were run, the gels were removed from the cassette and equilibrated in transfer buffer (48mM Tris, 39mM glycine, 1.3mM SDS, 20% methanol). The proteins on the gel were transferred onto prepared 0.45µm polyvinylidenedifluoride (PVDF) membrane (SLS) using a semidry transfer unit at 15V for 90 mins with transfer buffer. Efficiency of transfer of proteins to the membrane was checked by incubating the membrane in Ponceau S stain for 2 mins. The stain was subsequently removed with 2 washes with x1 Tris buffered saline containing 0.1% Tween 20 (TTBS) (15mM Tris, 150 mM NaCl, 0.001% Tween 20, pH 8.0) for 2 mins. The membrane was incubated in 5%

non-fat skimmed milk in 1x TTBS for 1hr at room temperature with gentle shaking to prevent non-specific binding. The membrane was then incubated with primary antibody anti-Hisx6 Mouse (NEB) diluted 1/1000 in 1x TTBS at 4°C overnight with gentle shaking. The membrane was washed 4 times with x1 TTBS for 5 mins. The membrane was then incubated in secondary antibody IgG anti-Mouse horseradish peroxidase linked antibody (NEB) diluted 1/10000 in 1x TTBS for 2.5 hrs at room temperature with gentle shaking. Before visualisation, the membrane was washed 4 times for 5 mins in x1 TTBS. The proteins on the membrane were visualised using Supersignal West Pico chemiluminescent substrate (Pierce) and the GeneGnome imaging system (Syngene) with GeneSnap software.

2.8. Peptidoglycan cleavage analysis

2.8.1. Isolation of *E. coli* and *C. jejuni* sacculi

The sacculi or peptidoglycan was isolated as previously described by Glauner (1988) and Singh *et al.* (2012). *E. coli* and *C. jejuni* cells were harvested from exponentially growing cultures with the approximate OD_{600} 0.6 by centrifugation at 4 000 x g for 40 mins at 4°C. The bacterial pellet was resuspended in 3ml ice cold deionised water. To the bacterial pellet, 3ml of boiling 8% SDS was added drop-wise to the suspension with vigorous stirring within 10min. The suspension was boiled for a further 30min to solubilise the membrane and degrade genomic DNA. The suspension was incubated for approximately 16 hrs at room temperature. The sacculi are isolated by ultracentrifugation at 130 000 x g for 60min at 4°C and washed 4 times with 8 ml of sterile deionised water. Pellet was digested with α-amylase (100μg/ml in 1ml of 10mM Tris-HCl pH 7.0, for 2 hrs at 37°C)

and pre-digested pronase (200μg/ml for 90 mins at 60°C). The suspensions were boiled with equal volume of 8% SDS for 15 mins to deactivate the digestive enzymes. The suspension was further diluted with 6ml of sterile deionised water. The samples were ultracentrifuged and washed with 8ml of sterile deionised water as previously described to wash out excess SDS. The final pellet was resuspended in 25mM Tris-HCl (pH 8.0).

For TLC and HPLC analysis, 100μl isolated sacculis were treated with 20 U of mutanolysin (Sigma) at 37°C in 25mM Tris-HCl (pH 8.0) for 16 hrs. The insoluble material was removed by centrifugation at 10 000g, 15 mins at room temperature and the soluble fraction was then reduced with 1mg of sodium borohydride in 50mM sodium borate buffer (pH 9.0) for 30 mins at room temperature. The excess borohydride was destroyed by the addition of 20% phosphoric acid, and the pH was adjusted to 3-4.

2.8.2. Thin Layer Chromatography (TLC)

The method used was previously described by Barzilai *et al.* (1984) to study peptidoglycan using TLC. The silica gel plates were heated for 30 mins at 110°C to 'inactivate' the plate. 10μl samples were spotted onto the plates and left to air dry. The one dimensional TLC was conducted using the solvent system of isopropanol/acetic acid/water (75/10/15, vol/vol/vol). The plates were developed and then allowed to air dry. The plates were sprayed with 0.3% ninhyrdrin in 3% acetic acid in N-butanol. The plates were then heated at 110°C for 10 mins. The plates were visualised using the Camag TLC visualisation system (Camag).

2.8.3. High performance liquid chromatography (HPLC) analysis of peptidoglycan products

HPLC analysis was performed to observe the effects of amidase overexpression on peptidoglycan as previously described by Glauner (1988) with modifications. Samples were run in a linear gradient with 0 to 70% acetonitrile in 50mM sodium phosphate buffer (pH 4) with the run time of 25mins with the flow rate of 0.8ml per minute. The HPLC was performed using LC-2010A HT Liquid Chromatograph (Shimadzu). The column used was PhenomenexSphereclone C18 column (150 x 4.5mm, 5μm). The program used to analyse the chromatograms was LabSolutions (Shimadzu).

3.0. The effects and visualisation of environmental stresses on *C. jejuni* and *C. fetus* CFF

3.1. Introduction

CFF in *C. jejuni* and *H. pylori* has been documented for several decades. It was shown to be induced by various unfavourable environmental stresses and has been considered a degenerative state (Buck *et al.*, 1983). This led to a decline in research within the field however, a holistic overview of the CF morphology within *C. jejuni* and related organisms suggests an alternative role of the CF and the various CFs created under different stress conditions, strengthening the link between CF and potential VBNC states (Ikeda & Karlyshev, 2012). The relationship between CF and VBNC states have become more ambiguous after findings of *C. jejuni* coccoid and non-coccoid VBNC cells dependent upon the environmental stresses they are formed (Federighi *et al.*, 1998; Lazaro *et al.*, 1999; Hudock *et al.*, 2005; He & Chen, 2010).

As stated previously, transformation into CF in *C. jejuni* is stimulated by various stress-inducing factors (section 1.8.). The mechanisms of CFF under different stress factors can lead to differential properties of CF observed, which may partly explain the reason for varied results obtained with CF of *C. jejuni* in different labs. An example of this is temperature stress, which leads to CFs formed at temperatures of 37°C and 42°C to have the highest level of membrane permeability and DNA degradation when compared with CFs induced at 4°C (Hazeleger *et al.*, 1998).

Oxidative stress is a well known inducing factor of CFF in *C. jejuni,* with its effects well documented, and was also one of the first stressors known to generate the morphological transition (Ogg, 1962, Karmali *et al.*, 1981, Moran & Upton, 1986, Boucher *et al.*, 1994, Lee *et al.*, 2005, Klancnik *et al.*, 2006). Oxidative stress can also result from the effect of reactive oxygen species (ROS), like superoxides and hydrogen peroxide.

It was suggested that the morphological transition to the CF occurs via an intermediate shape that resembles a 'doughnut', which appears as though the cells curl to become spherical (Ng *et al.*, 1985). Another intermediate shape that has been seen is the 'club' shape, which is characterised by localised expansions of the cell (Moran & Upton, 1986; Thomas *et al.*, 1999). However, both of these structures are rarely seen in *C. jejuni* electron micrographs, suggesting that these forms exist transiently or are an artefact of fixation.

Though CFF in *C. jejuni* has been studied for several decades, the morphological transition with other *Campylobacter* spp. has not been explored as extensively. Amano and Shibata (1992) compared the peptidoglycan content in rod and coccoid morphology of three different species of *Campylobacter*: *C. coli*; *C. jejuni*; and *C. fetus*, and found that very little peptidoglycan could be removed from the bacterial cells of *C. coli* and *C. jejuni* whilst in their CF. Remarkably, peptidoglycan was always obtainable from *C. fetus* cells, coincident with an inability of this subspecies to form CF. Amano and Shibata (1992) showed *C. fetus* was unable to form CF under stationary stress, however the effects of extended periods of nutrient deprivation and temperature stress induced CFF in *C. fetus* has not been previously studied.

There are several aims of the work presented within this chapter; firstly, to determine the progression of the coccoid morphology of *C. jejuni* strains under stationary phase and aerobic stresses. Secondly, to compare the methods of visualisation of CF and the presence of possible intermediate structures. Thirdly, to determine the effect the different systems used to maintain microaerobic conditions could have on CFF in *C. jejuni* strains. Finally, to investigate the possible factors that could explain the differential morphology conversions between *C. jejuni* and *C. fetus*.

3.2. Results

3.2.1. The visualisation of *C. jejuni* morphologies under light and scanning electron microscopy under stationary phase stress & CFF of *C. fetus*

The *Campylobacter* Gram stained cells were visualised under 1000x magnification with light microscopy. Samples were compared across 4 time points on solid media – 1, 2, 3 and 4 days. Liquid culture samples were compared across the same 4 times points. On both solid and liquid media, samples of *C. jejuni* 11168H and 81116 both displayed a similar increase in the percentage of CF present over time (Figures 3.1, 3.2, 3.3 and 3.4). There was no significant difference in the accumulation of CF between the two *C. jejuni* strains on solid media (unpaired Student's *t*-test; 0.25, df = 22, P= 0.81) and in liquid cultures (unpaired Student's *t*-test; 0.311, df = 58, P = 0.76).

On solid media, *C. jejuni* samples had very few CF present on day 1 or day 2, with approximately 10% to 30% present. The majority of the population maintained the classical spiral rod morphology (Figure 3.1). From day 3 onwards there was a dramatic increase in the percentage CF within the population to approximately 90%, with almost no rod shaped bacteria present (Figure 3.1). The accumulation of CF can be increased on day 2 if the initial inoculums were larger, increasing the amount of cells and growth and hastening entrance into stationary phase thus, the accumulation of waste product (Figure 3.2). In a small proportion of samples, the results were not always consistent taken from solid media from areas of higher inoculums. Consistent results were obtained from single colony samples. A skew in the proportion of CF could be due to the biofilm-like nature of the larger and more mature growth. The larger amount of starting inoculum could lead the bacteria to create a protective structure to maintain an optimal environment for a proportion of cells, enabling maintenance of the rod morphology.

The homogenous nature of liquid culture was validated by the consistent gradual readings from all time points of each sample. The percentage of the CF in liquid media showed a slower progression of the accumulation, increasing steadily with the biggest jump in accumulation occurring at day 2, which could be a pivotal point of transition (Figure 3.3). The accumulation of CF on day 2 on solid media had the highest variance compared with all the other time points. Samples from liquid cultures were taken at the same times as the solid media and showed a gradual increase up to 40% CF by day 2, whilst on solid media there was only approximately 10% of CF cells present within the population on average.

The *C. jejuni* SEM samples were taken at 4 time points from solid media – days 1, 2, 3 and 4 and a Gram stain sample was taken from each of these samples for comparison as shown in Figure 3.4 and 3.5 respectively. The morphologies of either shape present within the populations were visualised by light microscopy and were also shown with SEM. The light microscopy resolution showed the CF cells from all samples appeared relatively uniform and the stain was retained. However, visualisation of CF of older samples (3 day and 4 day samples) under SEM showed a lack of uniformity in the membrane. The membrane showed ruffling and folding on the surface, suggesting the membrane is disrupted, though this could be due to the fixation technique or showing the cell membranes are compromised and possibly deteriorating (Figure 3.6).

In Figure 3.7 a 'doughnut' shaped intermediate structure (Ng *et al.*, 1985) was visualised in picture B but this structure has only been observed under SEM. The 'club' intermediate structure, which has been previously described in other studies (Thomas *et al.*, 1999) was not found. Neither of these morphologies were visualised under light microscopy. It has been suggested that the intermediate structure is very short lived or the intermediate structures are artefactual products of the fixation process for electron microscopy.

It has been found by Hudock *et al.* (2005) that *C. jejuni* incubated for extended periods of time whilst under nutrient deprivation and aerobic stress showed the increase in CF concurrent with DNA degradation within 3 days. *C. jejuni* samples from solid media from days 1 to 4 were taken and chromosomal DNA was isolated. The different aged samples were compared via agarose gel electrophoresis and the concentration and quality of DNA was measured using a NanoVue spectrophotometer (Table 3.1 and Figure 3.8). The samples with the highest percentage of CF (day 3 and 4 samples) displayed no visible degradation on the agarose gel in comparison with samples with almost no CF present (day 1 and 2 samples), nor were the concentrations or any of the 260/280 values skewed outside the normal range due to the age of the culture.

The progression of CFF within *C. jejuni* and *C. fetus* were compared using two strains from each species. *C. fetus* NCTC 10842 was used for comparison as this strain was observed by Amano & Shibata (1992) to not form the coccoid morphology. *C. fetus* 82-40 was used as this is the only commercially available *C. fetus* sequenced strain. The *C. fetus* strains were compared originally with the *C. jejuni* strains under stationary phase stress on solid media over a 4 day period. The main morphology observed within all the *C. fetus* strains and samples was the classical rod morphology (Figure 3.9). Samples were observed for longer incubation; at day 5-7, however there was still no change in the percentage of CF observed (data not shown). These findings are similar to those found with previous studies and the evidence presented here with a different strain that also lacks morphology change under stress conditions demonstrates that this is not due to strain variation in *C. fetus.*

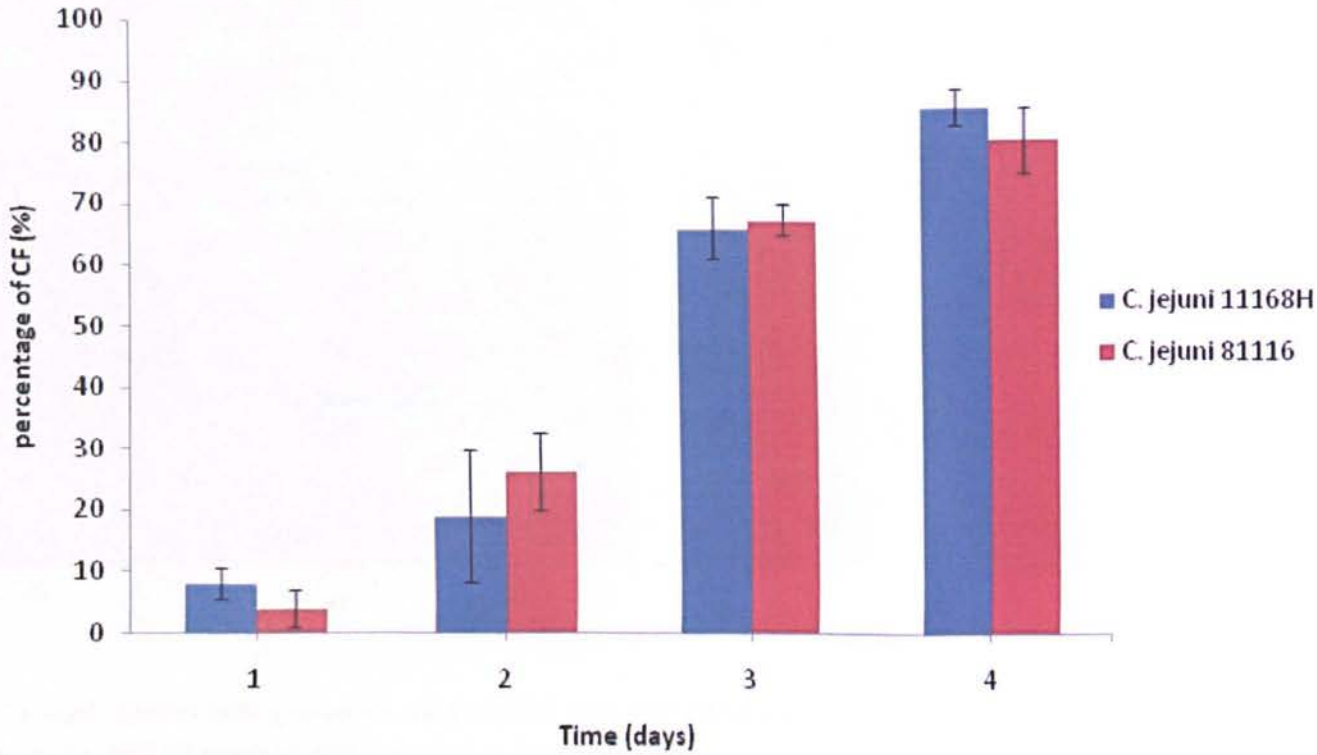

Figure 3.1. The mean percentage of CF in WT *C. jejuni* 11168H and 81116 solid media culture samples over a 4 day period.
The strains were grown microaerobically on CBA. Within each individual measurement 100 cells were counted. The samples were prepared and counted as described in section 2.1.2. These data are the mean of three individual experiments each done in triplicate. The error bars represent SD (N= 9).

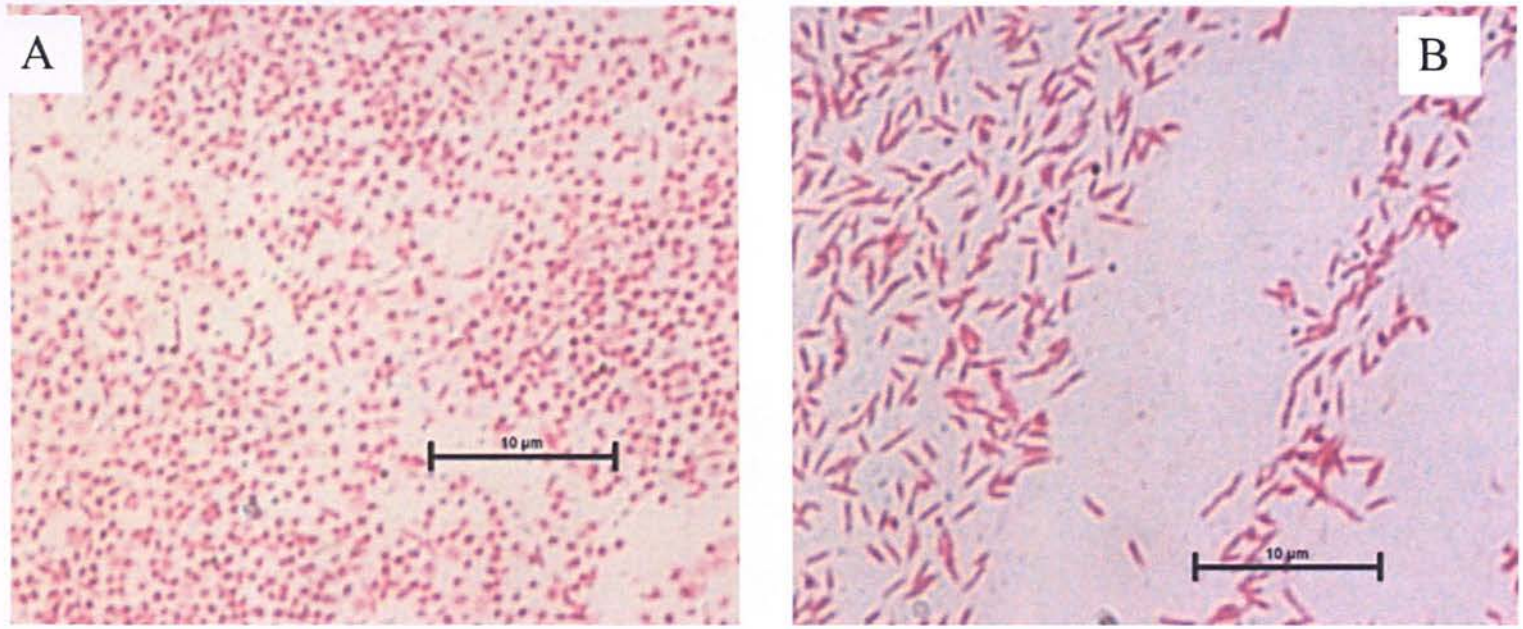

Figure 3.2. Image of *C. jejuni* 11168H cells grown on solid media visualised using light microscopy sampled at day 2 with A) large initial inoculum (several colonies/well growth) and B) smaller initial inoculum (single colony).

The strains were grown microaerobically on CBA media containing 5% defibrinated horse blood, and were prepared and visualised as described in section 2.1.2. The black bar in the bottom right hand corner of each image is representative of 10µm. The samples were all visualised under x1000 magnification and images were all taken with the Nikon 80i.

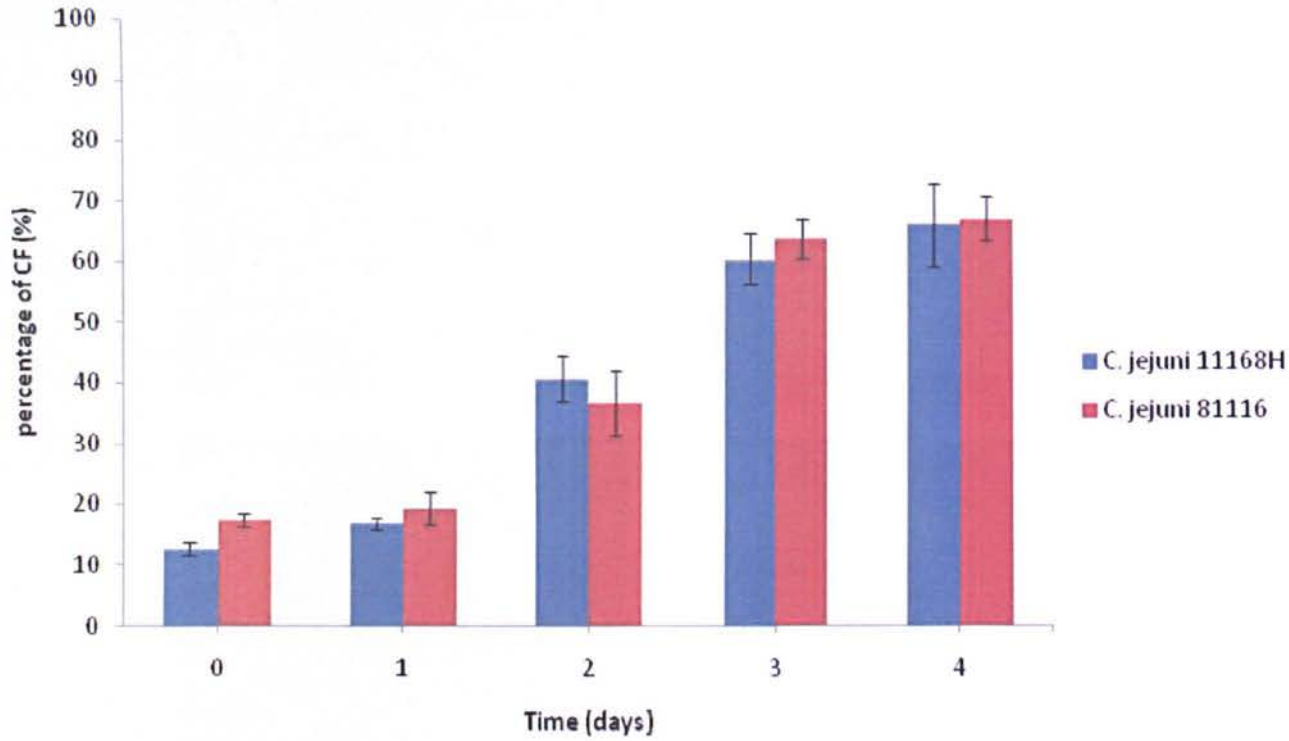

Figure 3.3. The mean percentage of CF in WT *C. jejuni* 11168H and 81116 liquid cultures over a 4 day period.
The liquid cultures were grown microaerobically with shaking (~200 rpm), starting at approximately 0.1 OD_{600nm} ml^{-1}. Within each individual measurement, 100 cells were counted. The samples were prepared and counted as described in section 2.1.2. These data are the mean of three individual experiments each done in triplicate. The error bars represent SD (N= 9).

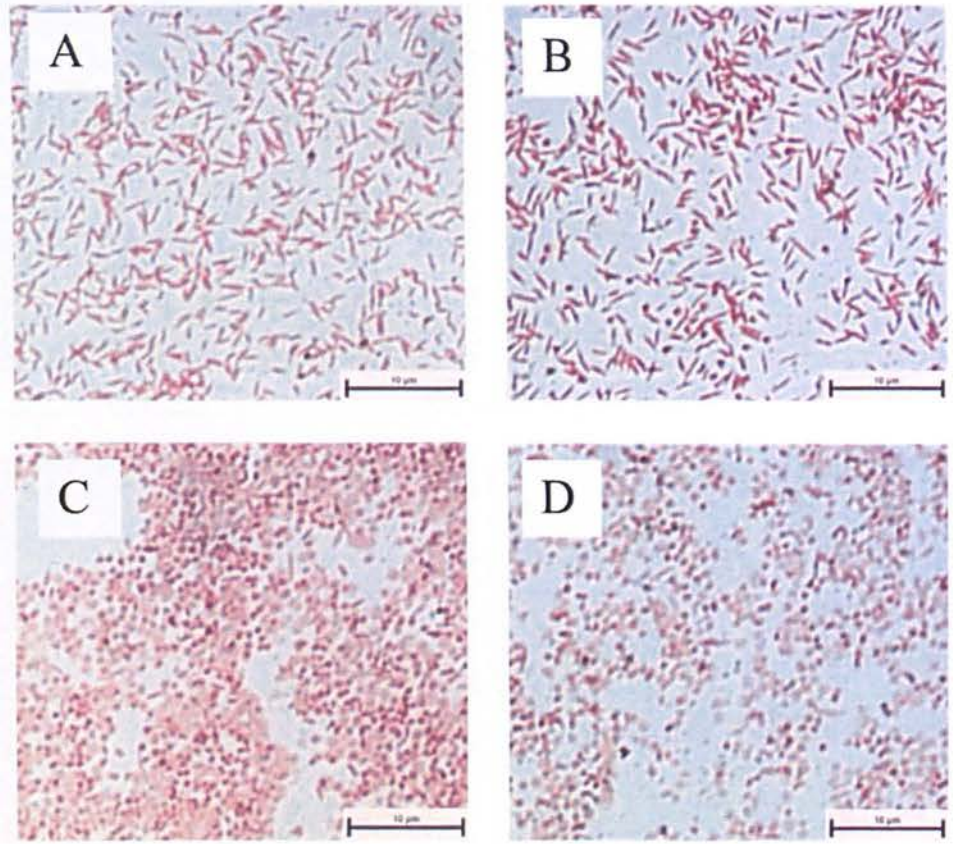

Figure 3.4. Images of *C. jejuni* 11168H cells grown on solid media visualised using light microscopy sampled at A) day 1 B) day 2 C) day 3 and D) day 4.

The strains were grown microaerobically on CBA media containing 5% defibrinated horse blood. The same samples were visualised using SEM for comparison in Figure 3.4. Samples were prepared and visualised as described in section 2.1.2. Sample A and B are predominately rod morphology whilst samples C and D are CF. The black bar in the bottom right hand corner of each image is representative of 10μm. The samples were all visualised under x1000 magnification and images were all taken with the Nikon 80i.

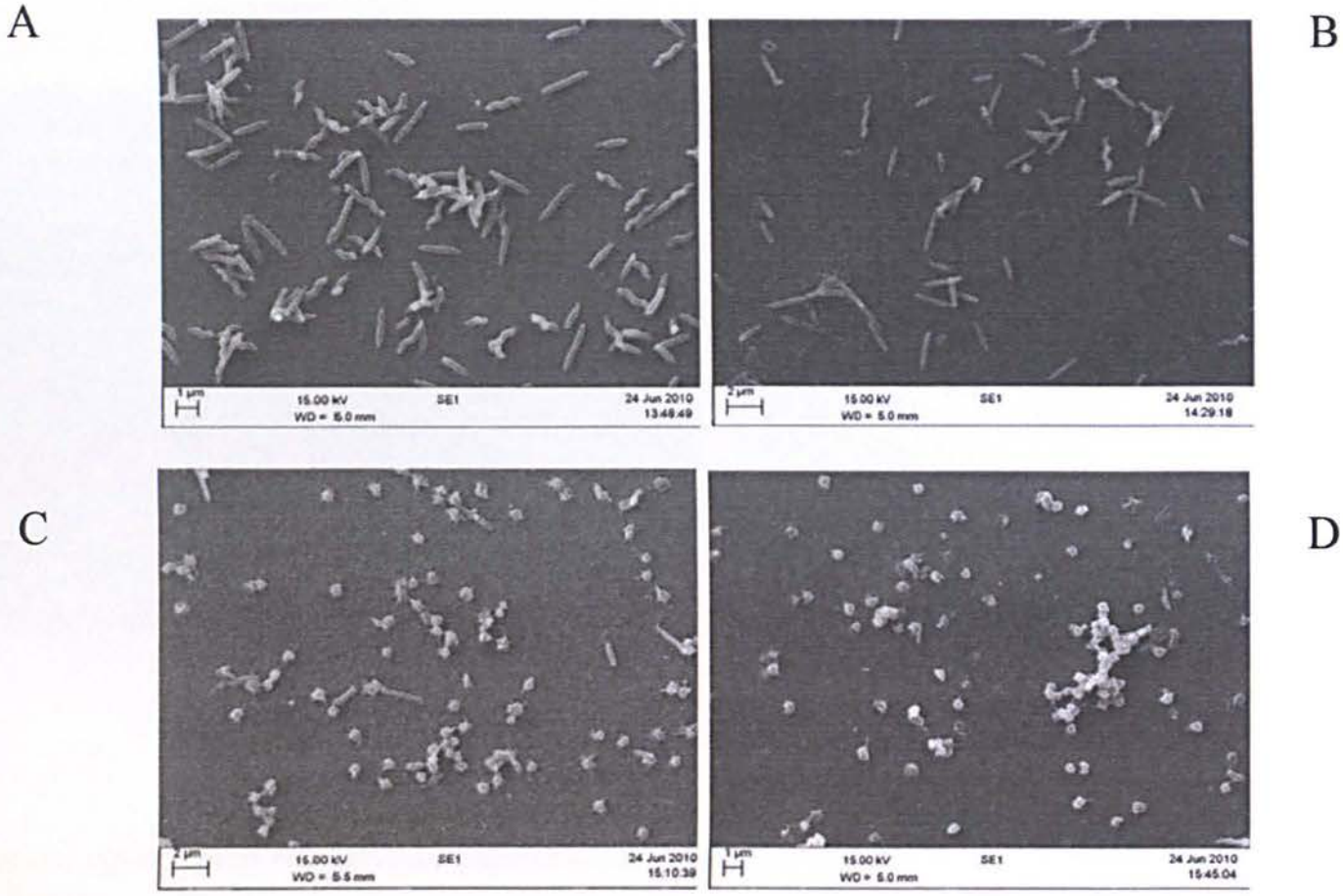

Figure 3.5. Images of *C. jejuni* 11168H cells grown on solid media visualised under scanning electron microscopy sampled at A) day 1 B) day 2 C) day 3 and D) day 4.

The strains were grown microaerobically on CBA media containing 5% defibrinated horse blood. The same samples were visualised with light microscopy for comparison in Figure 3.3. Samples were prepared and visualised as described in section 2.1.2. The respective scale bars for each image are shown in the bottom left hand corner. Images were taken using Zeiss EVO 50 Scanning electron microscope.

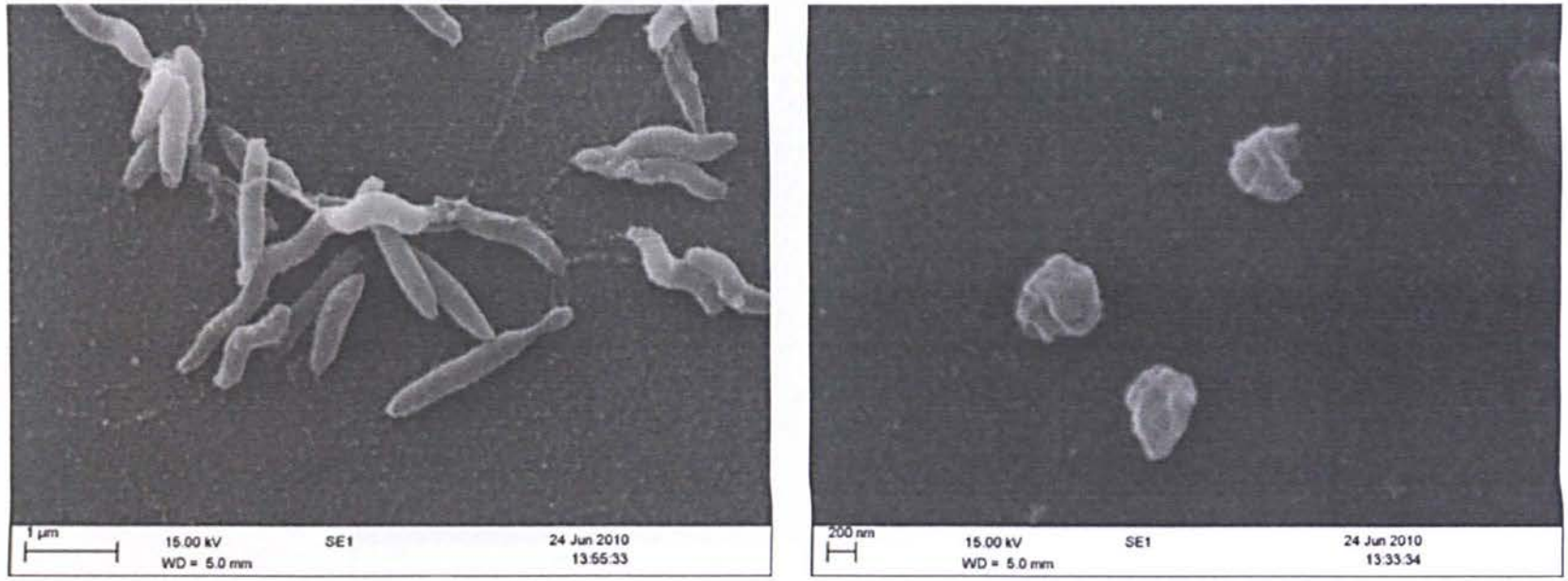

Figure 3.6. Images of *C. jejuni* 11168H rod and coccoid morphologies with higher magnification using scanning electron microscopy to show the lack of membrane uniformity.

The strains were grown microaerobically on CBA media containing 5% defibrinated horse blood. Samples were prepared and visualised as described in section 2.1.2. The respective scale bars for each image are shown in the bottom left hand corner. Images were taken using Zeiss EVO 50 Scanning electron microscope.

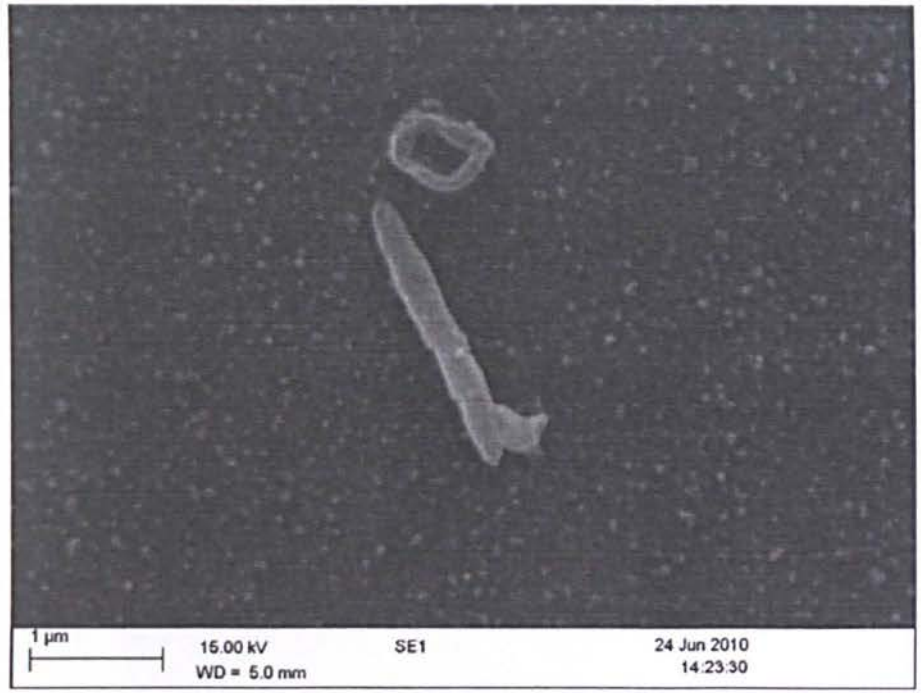

Figure 3.7. Image of *C. jejuni* 11168H intermediate 'doughnut' structure visualised under scanning electron microscopy.
The strains were grown microaerobically on CBA media containing 5% defibrinated horse blood. Samples were prepared and visualised as described in section 2.1.2. The scale bar is shown in the bottom left hand corner. Images were taken using Zeiss EVO 50 Scanning electron microscope.

Table 3.1. The concentration and absorbance ratios of *C. jejuni* 11168H chromosomal DNA isolated samples across a 4 day period.

Sample	Concentration (µg/ml)	A260/280	A260/230
Day 1	337	1.997	2.342
Day 2	268	1.98	2.188
Day 3	188.5	1.778	1.945
Day 4	237.5	1.779	1.973

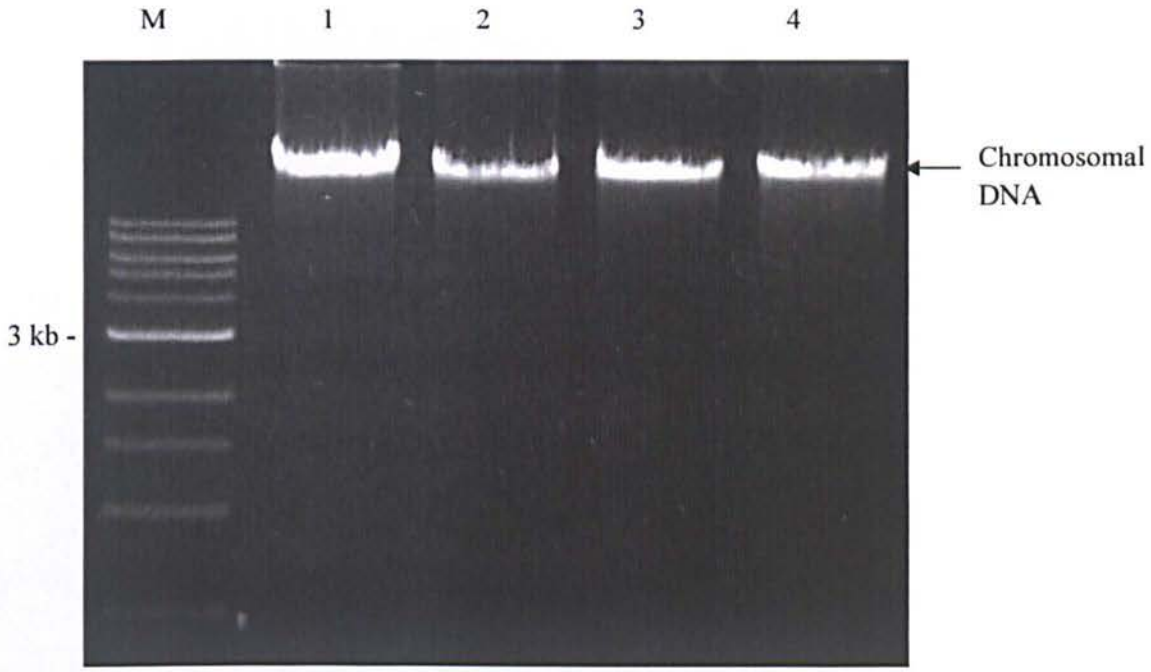

Figure 3.8. Agarose gel showing the integrity of intact *C. jejuni* 11168H chromosomal DNA isolated from samples across a 4 day period.

Equivalent amounts of DNA (500ng) were loaded into each lane. The chromosomal DNA degradation would be evident by smearing down the gel however all samples appear to be above the marker sizes, suggesting it is intact.

M - NEB 1 kb Ladder, 1- 1 day *C. jejuni* chromosomal DNA sample, 2- 2 day *C. jejuni* chromosomal DNA sample, 3- 3 day *C. jejuni* chromosomal DNA sample, 4- 4 day *C. jejuni* chromosomal DNA sample.

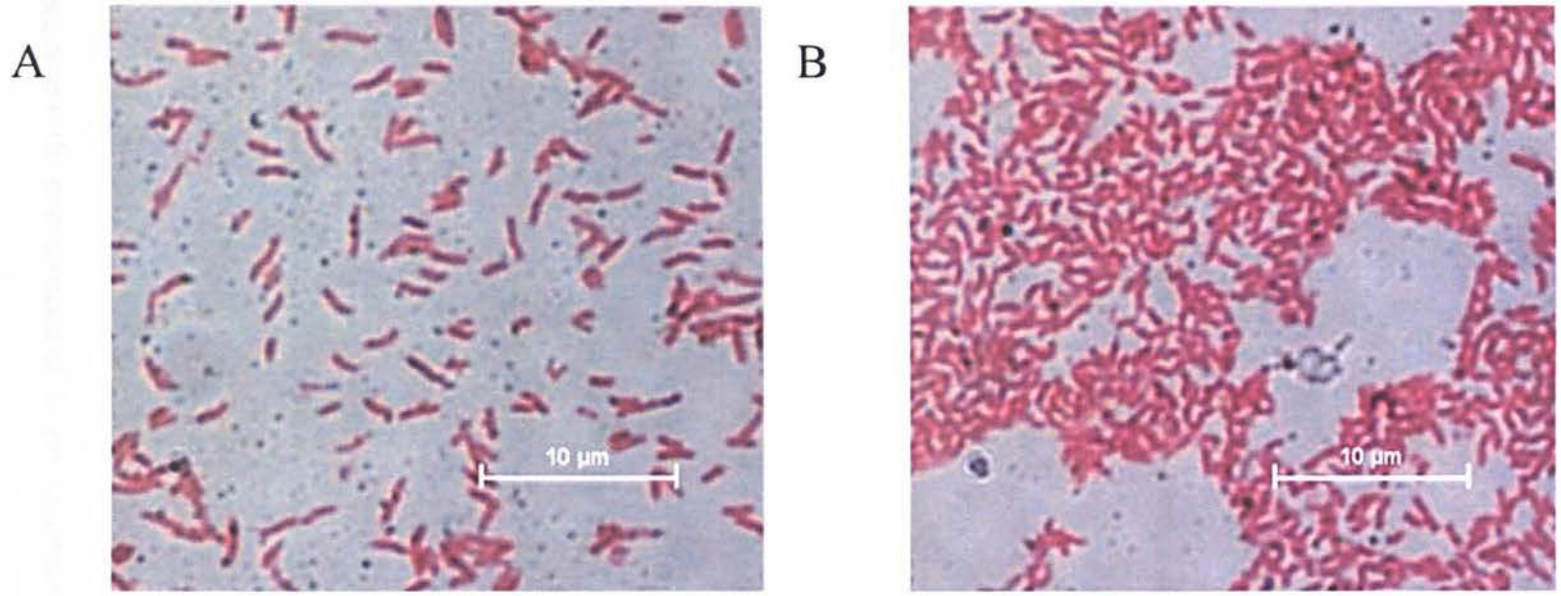

Figure 3.9. Images of *C. fetus* cells A) NCTC 10842 and B) 82-40 strains grown on solid media visualised under light microscopy and sampled on day 4.

The strains appear only to be in the rod morphology. The strains were grown microaerobically on CBA media containing 5% defibrinated horse blood. The white bar in the bottom right hand corner of each image is representative of 10µm. The samples were all visualised under 1000x magnification and images were captured with the Nikon 80i.

3.2.2. Comparison of *C. jejuni* CFF in jar and gas incubator systems and the accumulation of *C. jejuni* CF under ambient oxygen stress

The percentage of CF in the population was measured under microaerobic conditions across various time points showing an increase in CFF over time. The previous samples were incubated in a Don Whitley microaerophilic gas incubator system. However, this system was compared with Campygen atmosphere packs and jar system to determine whether the systems cause a fluctuation in accumulation of CF due to the variation in humidity. As seen in Figure 3.10., there are no differences in CFF between the two systems with either strain of 11168H (unpaired Student's *t*-test; 0.178, df = 15.793, $P = 0.86$) & 81116 (unpaired Student's *t*-test; 0.014, df = 15.994, $P = 0.99$).

The amount of CF present on solid media showed an increase under ambient oxygen levels over time compared to cultures under microaerobic conditions (Figure 3.11).

In comparison with control cultures grown in microaerobic conditions, oxygenic stress showed an increase in the percentage of CF at the initial time points on days 1 and 2, with the percentage of CF in the population on day 1 being approximately 30-50%. However, from day 3 onward the CFF of the strains cultured in microaerobic atmospheric conditions was similar to the strains cultured within ambient oxygenic levels. The rate of CF accumulation on solid media under ambient oxygen levels over time were shown to be similar with samples that were continuously subcultured from previous strains that were exposed to ambient oxygen levels (Figure 3.12).

The accumulation of CF within WT *C. jejuni* strains in liquid media was also measured to determine if the maintenance of the homogenous environment had different effects. There were no significant difference in optical density over time of *C. jejuni* strains in ambient

oxygenic and microaerobic conditions with either strain (strain 11168H - unpaired Student's *t*-test; 0.5233, df = 27, $P = 0.61$; strain 81116 - unpaired Student's *t*-test; 0.3578, df = 28, $P = 0.72$) (Figure 3.13). There was no dramatic change in CFF as found within the first time points on solid media, instead there was an overall increase in CF within the population at each time point compared to strains grown in microaerobic atmospheric conditions (Figure 3.14 and 3.15).

An overview of the effects of the various growth conditions (solid or liquid media cultures) and oxygenic environments (percentage of oxygen within the atmosphere) on the accumulation of CF in both *C. jejuni* 11168H and 81116 over time is shown in Table 3.2.

Table 3.2. The mean percentage of CF that accumulated under different growth conditions with varying percentages of oxygen across a 4 day period.

Growth Conditions	O_2 (%)	Time (days)	CF mean % to nearest percentile (SD)
Microaerobic conditions solid media (incubator) *C. jejuni* 11168H	5	1	4 (2.75)
		2	10 (5.52)
		3	47 (4.2)
		4	80 (3.02)
Microaerobic conditions solid media (gas jar) *C. jejuni* 11168H	5	1	7 (6.6)
		2	36 (2.33)
		4	87 (6.36)
Microaerobic conditions liquid cultures *C. jejuni* 11168H	5	0	13 (1.09)
		1	17 (0.96)
		2	41 (3.73)
		3	60 (4.15)
		4	66 (6.9)
Microaerobic conditions solid media (incubator) *C. jejuni* 81116	5	1	6 (1)
		2	26 (7)
		3	66 (6)
		4	77 (6)
Microaerobic conditions solid media (gas jar) *C. jejuni* 81116	5	1	2 (3.08)
		2	40 (3.89)
		4	74 (14)
Microaerobic conditions liquid cultures *C. jejuni* 81116	5	0	18 (1.03)
		1	19 (2.55)
		2	37 (5.32)
		3	64 (2.27)
		4	67 (2.62)
Ambient oxygenic conditions solid media *C. jejuni* 11168H	20	1	43 (1.75)
		2	50 (7.27)
		3	57 (2.62)
		4	57 (3.34)
Ambient oxygenic liquid cultures *C. jejuni* 11168H	20	0	19 (0.74)
		1	21 (2.22)
		2	43 (3.22)
		3	70 (5.86)
		4	75 (2.59)
Ambient oxygenic conditions solid media *C. jejuni* 81116	20	1	55 (5.93)
		2	49 (4.54)
		3	66 (5.46)
		4	78 (2.95)
Ambient oxygenic conditions liquid cultures *C. jejuni* 81116	20	0	21 (2.99)
		1	27 (1.9)
		2	45 (2.53)
		3	67 (2.7)
		4	68 (2.75)

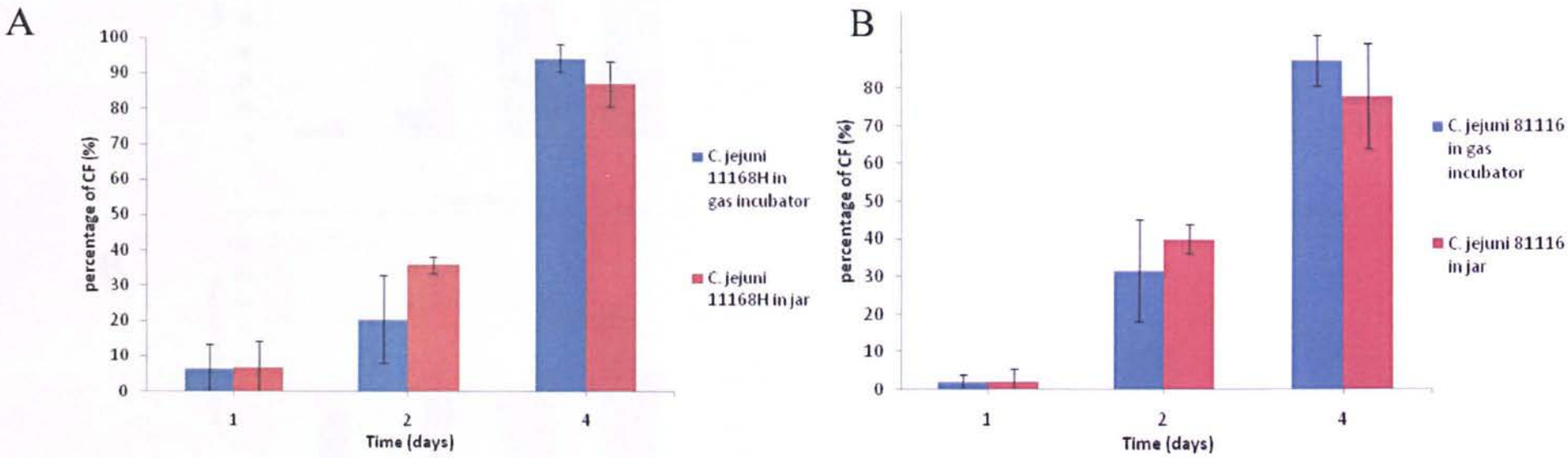

Figure 3.10. Effect of humidity and microaerobic growth on *C. jejuni* CFF over time.
Comparison of mean percentage of CF in A) *C. jejuni* 11168H and B) 81116 solid media culture samples over a 4 day period in microaerobic gas incubator *vs.* the gas jar system. The strains were grown microaerobically on CBA. Within each individual measurement, 100 cells were counted. The samples were prepared and counted as described in section 2.1.2. These data are the average of an individual experiment, which was done in triplicate with similar results each time. The error bars represent SD (N= 3).

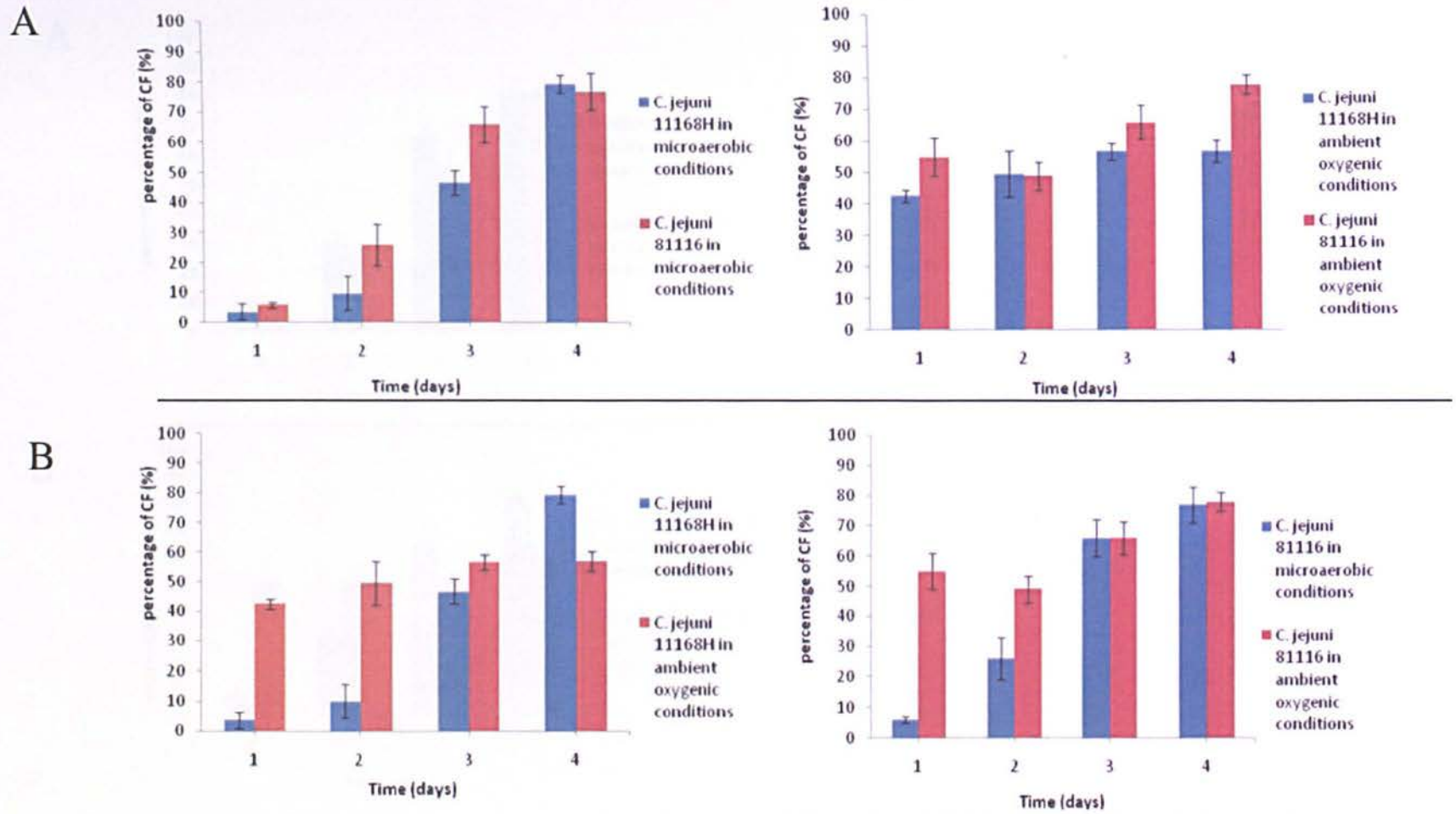

Figure 3.11. Effect of A) aerobic compared to microaerobic environments & B) strains of *C. jejuni* on CFF in cells that had been pre-exposed to a microaerobic environment.

The mean percentage of CF in WT *C. jejuni* 11168H and 81116 solid media culture samples over a 4 day period. The strains were grown microaerobically (O_2 = 5%) and in ambient oxygen levels (O_2 = 20%) on CBA. Within each individual measurement, 100 cells were counted. The samples were prepared and counted as described in section 2.1.2. These data are the mean of an individual experiment, which was done in triplicate with similar results each time. The error bars represent SD (N= 3).

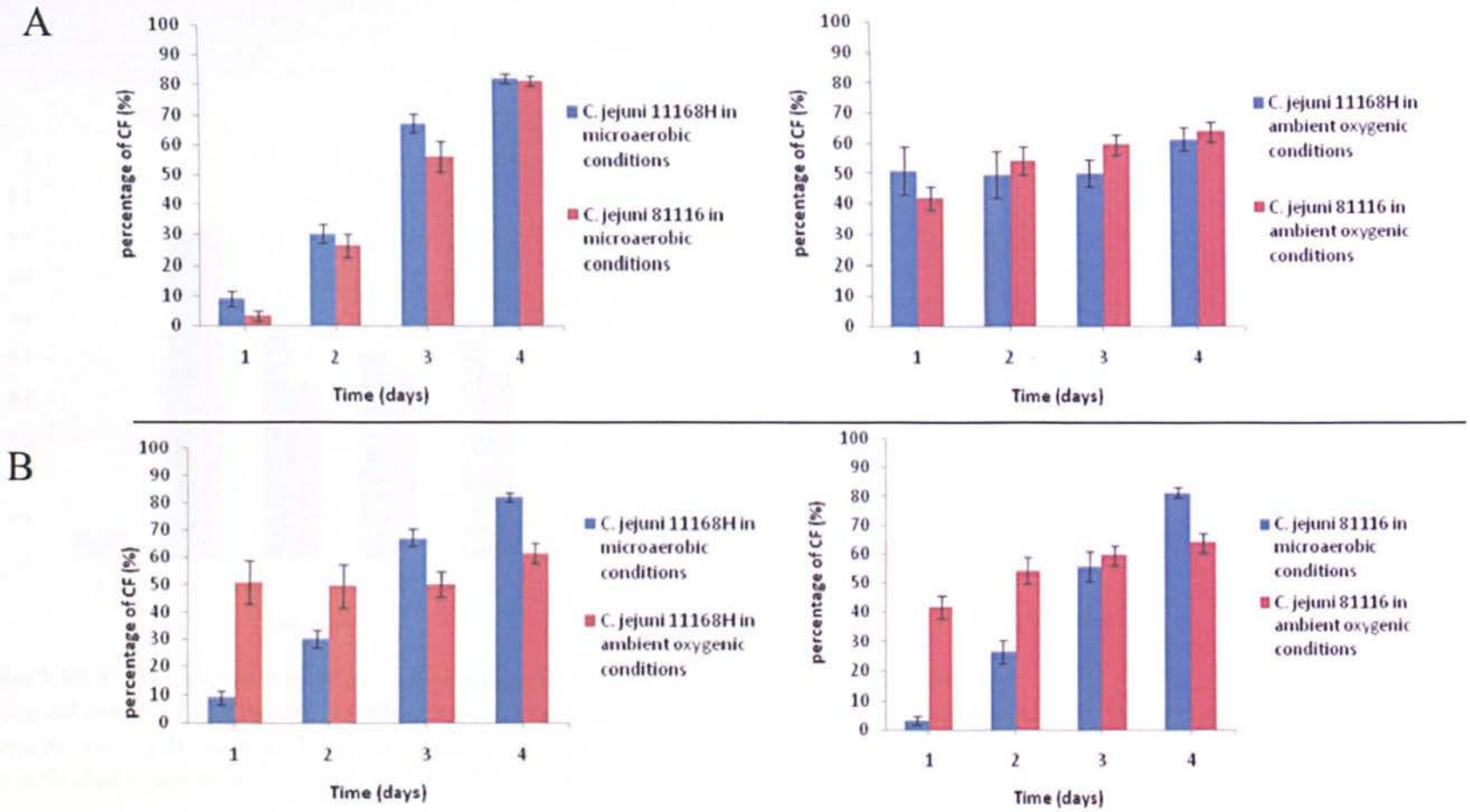

Figure 3.12. Effect of A) aerobic compared to microaerobic environments & B) strains of *C. jejuni* on CFF in cells pre-exposed to an aerobic environment.

The mean percentage of CF in WT *C. jejuni* 11168H and 81116 solid media culture samples over a 4 day period using strains that were subcultured from previous cultures exposed to ambient oxygen levels. The strains were grown microaerobically (O_2 = 5%) and in ambient oxygen levels (O_2 = 20%) on CBA. Within each individual measurement, 100 cells were counted. The samples were prepared and counted as described in section 2.1.2. These data are the mean of an individual experiment, which was done in triplicate with similar results each time. The error bars represent SD (N= 3).

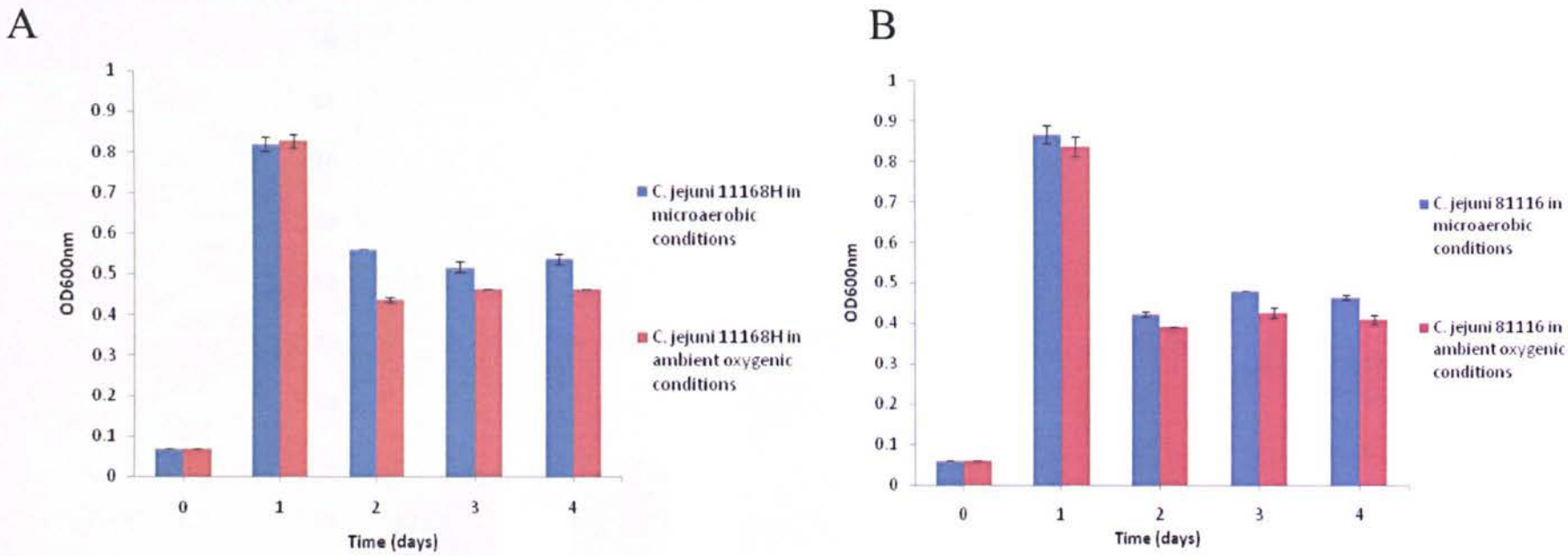

Figure 3.13. Effect on growth of two *C. jejuni* strains in an aerobic environment in liquid media.
The optical density of A) *C. jejuni* 11168H and B) 81116 in liquid media cultures grown in microaerobic (O_2 = 5%) and ambient oxygenic (O_2 = 20%) conditions over a 4 day period. The liquid cultures were grown with shaking (~200 rpm), starting at approximately 0.1 OD_{600nm} ml^{-1}. These data are the mean of an individual experiment, which was done in triplicate with similar results each time. The error bars represent SD (N= 3).

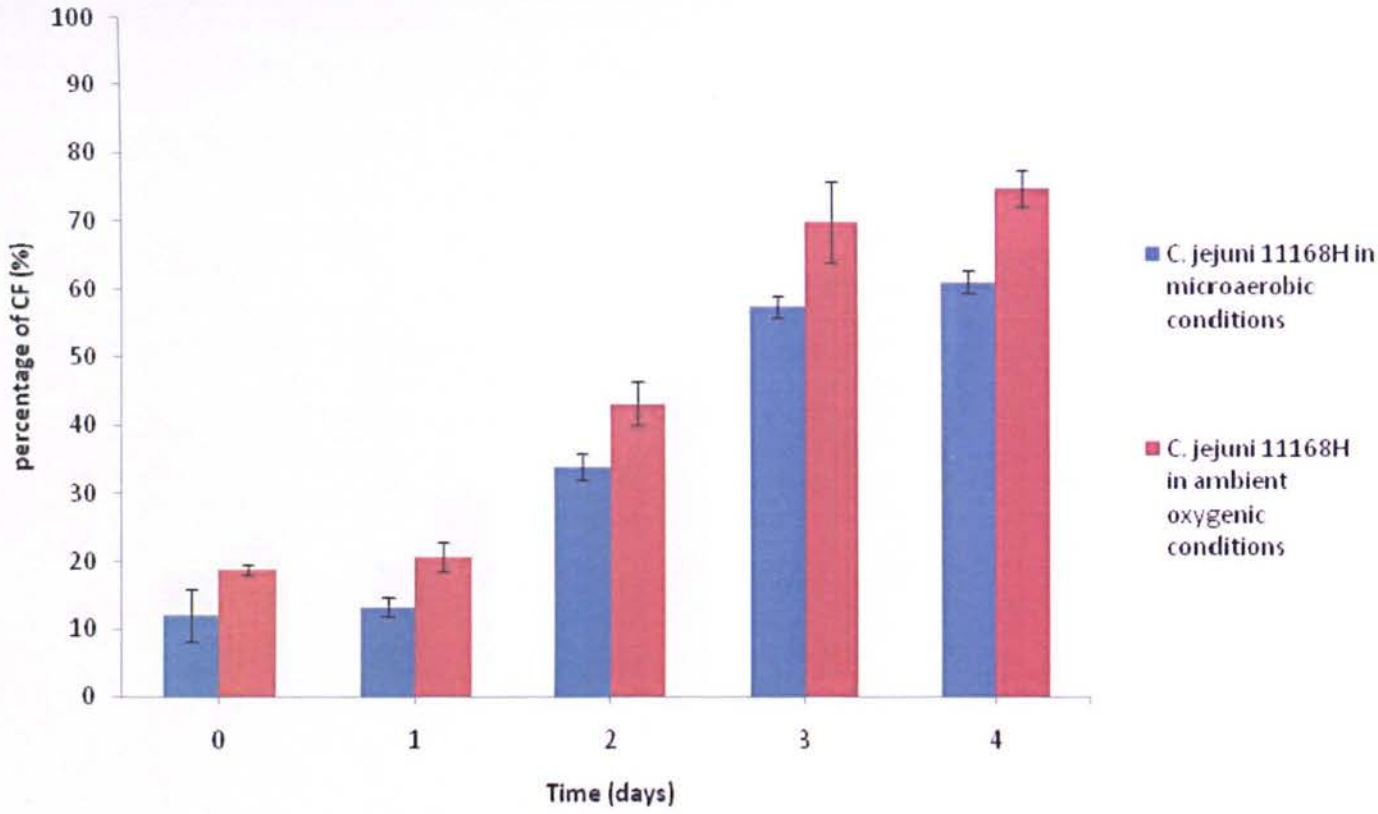

Figure 3.14. Effect on CFF of *C. jejuni* 11168H in aerobic environment in liquid media.
The mean percentage of CF in WT *C. jejuni* 11168H liquid cultures over a 4 day period, grown microaerobically (O_2 = 5%) and in ambient oxygenic conditions (O_2 = 20%) with shaking (~200 rpm), starting at approximately 0.1 OD_{600nm} ml^{-1}. Within each individual measurement, 100 cells were counted. The samples were prepared and counted as described in section 2.1.2. These data are the mean of an individual experiment, which was done in triplicate with similar results each time. The error bars represent SD (N= 3).

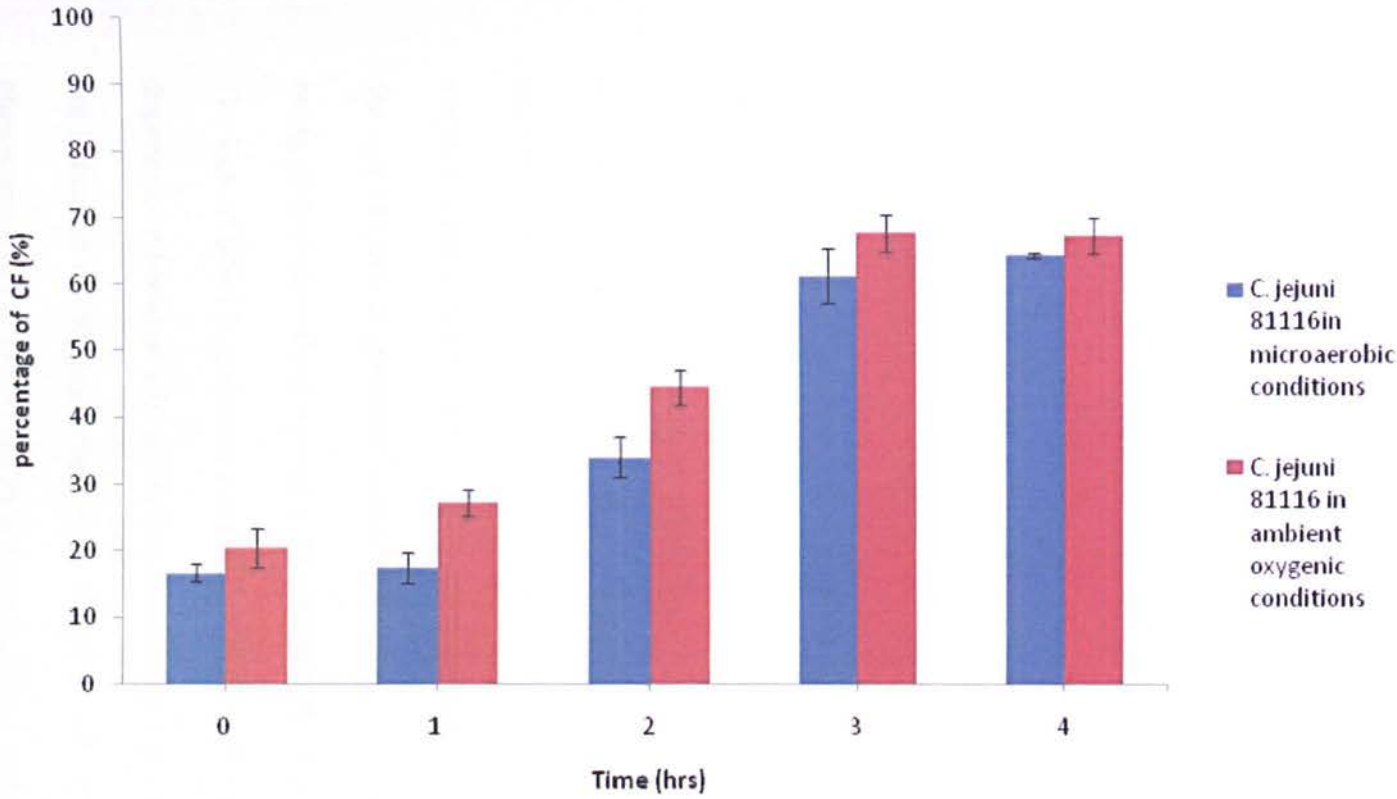

Figure 3.15. Effect on CFF of *C. jejuni* 81116 in aerobic environment in liquid media.
The mean percentage of CF in WT *C. jejuni* 81116 liquid cultures over a 4 day period, grown microaerobically (O_2 = 5%) and in ambient oxygenic conditions (O_2 = 20%) with shaking (~200 rpm), starting at approximately 0.1 OD_{600nm} ml^{-1}. Within each individual measurement, 100 cells were counted. The samples were prepared and counted as described in section 2.1.2. These data are the mean of an individual experiment, which was done in triplicate with similar results each time. The error bars represent SD (N= 3).

3.3. Discussion

As found in previous studies with *H. pylori*, no *C. jejuni* intermediate structures were visualised using light microscopy. However, the 'club' and 'doughnut' intermediate structures were previously visualised under scanning electron microscopy (Ng *et al.*, 1985, Thomas *et al.*, 1999, Moran & Upton, 1986). From the SEM images (Figure 4.4), the size of the intermediate structures do not differ greatly in comparison to the CF or the bacillary form and are therefore not too small to see under light microscopy. This furthers the speculation that intermediate structures are artefacts from the sample dehydration.

DNA degradation studies by Hudock *et al.* (2005) exhibited CF formed under three different environmental stress factors: nutrient deprivation; aerobic; and stationary phase stress. The cells exhibited high levels of DNA degradation and loss within 72 hrs of incubation in 1% peptone. However, within these experiments, degradation was not found in the day 3 and day 4 samples, which had a high percentage of CF within the population formed under stationary phase (Figure 3.5). The lack of DNA degradation could be due to the way the CF were formed. As previously stated, differential environmental stresses can vary the membrane integrity and the rate of accumulation of CF. An additional theory for the lack of DNA degradation found in these present studies was possibly due to the sample being taken from only solid media samples despite there being almost 90% CF present. The lack of DNA degradation found from the CF would suggest the cells are not degenerative forms at this age despite the morphology. The initial transition to the CF is not indicative of cell degeneration or cell death, and would further suggest that the phenomenon of CF would not be indicative of cell viability. The degenerative DNA study was adapted for the purification of chromosomal DNA from intact *C. jejuni* cells. Though no degeneration was found in the high coccoid population samples, it is still possible the

CF could be part of a protective role of *C. jejuni* survival as DNA has been found in the extracellular matrix of *C. jejuni* biofilms by DNase I digestion studies (Svensson *et al.*, 2009). Though the method of inserting DNA into the biofilm has been theorised to be *via* two routes, either *via* degenerative lysed cells releasing DNA into the surrounding matrix or living cells secreting DNA using vesicles. It was theorised in *P. aeruginosa*, that the mode of transmission of DNA into the matrix was *via* small vesicles due to the lack of evidence suggesting cell death or cell lysis (Kadurugamuwa, 1995; Whitchurch, 2002). In *C. jejuni* it is possible that the exogenous DNA for the biofilm matrix could be contributed by CF forms as opposed to vesicles. However to test this hypothesis would require further research.

The initial change in the CF accumulation within the *C. jejuni* population shows the effect of oxidative stress as a CF inducer (Figure 3.8). After several days of incubation, the amount of CFs formed reached similar levels to cultures that were grown under microaerobic conditions for the same period of time. It has been found in previous years that there are varying effects of oxygen dependent on other external factors, e.g. temperature, reactive oxygen species (ROS) quenchers and strain differences. Garenaux *et al.*, (2008) showed variable levels of sensitivity to oxidative stress at different temperatures, with the highest sensitivity at the optimal growth temperature of 42°C and the lowest sensitivity at 4°C. The high resistance against oxidative stress at low temperatures might be related to cross protection and the cold shock response as shown by the over-expression of several oxidative stress proteins at 4°C (Stintzi & Whitworth, 2003).

It is important to note whether the presence of the bacillary rod shape is due to selection of cells that are unable to form CF or whether it is a result of 'resuscitation' of CFs that were formed in the initial 24hrs of exposure to the aerobic environment. This was shown by the

strains that were continually sub-cultured whilst growing under aerobic conditions in comparison to the wild type strains in optimal conditions. However, the rate of CFF in both continuous subcultures and fresh cultures appeared to show similar results in conversion in ambient oxygenic and microaerobic environments (Figure 3.9). This shows adaptive mechanisms in ambient oxygenic environments did not affect the accumulation of CF over time.

The growth of cultures on solid media creates a microcosm biofilm-like environment. This was shown partly by the inconsistency and high variance in CF sampling from high inoculum growth from solid media (Figure 3.7). In a biofilm, bacteria form layers differentially exposed to oxygen, with the bacteria in the outer layer mostly affected and those in the inner layer protected from adverse effect of oxidative stress. The monospecies biofilms of *C. jejuni* have been shown to increase resistance to environmental stresses like oxidative/ aerobic stress (Joshua *et al.,* 2006). It was found by Gunther & Chen, (2009) that biofilms formed by *Campylobacter* are heterogeneous in morphology, with approximately equal ratio of coccoid and rod morphologies when grown under stressful conditions on plastic. It was suggested that CFs in biofilms of *C. jejuni* may have a supportive role by forming a layer of coccoid cells as a means of protecting the viable spiral rods from the hostile environment (Karlyshev *et al.*, 2005).

4.0. Investigation into the role of *spoT* in CFF

4.1. Introduction

spoT (Cj1272c) is a gene involved in the regulation of stringent response in *C. jejuni.* Stringent response is defined as a global stress response that promotes bacterial survival and adaptation under unfavourable environmental conditions and stresses, such as nutrient deprivation and aerobic shock (Gaynor *et al.,* 2005). The molecular signal or 'alarmone' of hyperphosphorylated guanosine nucleotide ((p)ppGpp) is the effector module of stringent response; when it is hydrolysed the signal molecule binds to the RNA polymerase holoenzyme to alter transcription and promoter specificity (Magnusson *et al.*, 2005). Within the model organism *E. coli,* the molecular signal is modulated by two genes, *relA* and *spoT*, which encode for mono-functional (p)ppGpp synthase and guanosine-3',5'-bis pyrophosphate 3'-pyrophosphohydrolase, respectively. These enzymes are involved in the maintenance of the hyperphosphorylated guanosine nucleotide. The lack of *relA* homologues in *Campylobacter* and *Helicobacter* originally led to the theory that these organisms lacked stringent response, however this has since been disproven with bioinformatics and experimentally derived data (Scoarughi *et al.,* 1999; Mouery *et al.*, 2006). A single *relA/spoT* gene that encodes a bifunctional synthetase-hydrolase has been identified in *Campylobacter* and *Helicobacter* (Alm *et al.,* 1999; Gaynor *et al.,* 2005,). Originally, this was thought to be a unique feature of Gram positive organisms but has since been found in Gram negative organisms such as alpha- and epsilonproteobacteria groups, including *Campylobacter* (Masuda & Bauer, 2004; Gaynor *et al.*, 2005).

Altering intracellular ppGpp levels has been previously shown to alter cell morphology in *C. jejuni* and other organisms. In *C. jejuni* strain 81-176 and the closely related bacterium *H. pylori,* deletion of *spoT* resulted in an accelerated rate of CFF and decreased resistance to aerobic shock and acid stress (Gaynor *et al.*, 2005; Mouery *et al.*, 2006). Increased

intracellular levels of ppGpp in *M. smegmatis* lead to spherical morphology compared to the typical elongated rod morphology (Ojha *et al.*, 2000). Mutation of *spoT* in *B. abortus* leads to branching and swelling of the bacterium, resulting in a rounder shape (Kim *et al.*, 2005).

In the *C. jejuni* strain NCTC 11168 genome, *spoT* is downstream of *amiA* and is considered to be in the same operon (Gaynor *et al.*, 2005). Several genes downstream of *spoT* have functions that could be considered essential, for example *rpoZ* (RNA polymerase omega subunit) and *pyrH* (uridylate kinase) (Gentry & Burgess, 1989). The other genes placed within this gene cluster could further implicate the importance of *spoT* in *C. jejuni.*

Due to this gene's connection to CFF in *C. jejuni* and *H. pylori,* it is important to see if the gene has a similar role in other strains of *C. jejuni*. Thus, the aim of this study is to determine the effect of the deletion of *spoT* in *C. jejuni* hypermotile derivative 11168H and 81116, and to compare these results with the previous results shown with *C. jejuni* 81-176 to verify if *C. jejuni spoT* can affect CFF.

4.2. Results

4.2.1. Construction and verification of *C. jejuni spoT::kan*^{r} mutants

Inactivation of *spoT* was achieved *via* SDM with the insertion of a *kan*^{r} cassette, preventing transcription of the full length gene and truncating the gene product. *spoT* was amplified by PCR from *C. jejuni* 11168H chromosomal DNA using primers spoT_for and spoT_rev. *spoT* was inserted into pGEM-T for further manipulation. The blunt ended *kan*^{r} cassette was inserted into *spoT via* the native *Bgl*II restriction site within the gene. The orientation of *kan*^{r} was determined by restriction digestion using *Sph*I, from which the size of the fragments demonstrated the orientation of the *kan*^{r} cassette. The *kan*^{r} cassette is in the correct orientation when it is read in the same direction as the target gene; the reverse could alter the expression. The restriction analysis was conducted to determine the orientation of the insert (Table 4.1, Figures 4.1 & 4.2). Figure 4.1 has a variation in the amino acid ORFs for segment 'd' due to an error from NEBCutter v2. Plasmids containing both orientations were obtained and the correct orientation clones were used for further experiments. The pGEM-T-*spoT*- *kan*^{r} plasmid was purified and used for transformation into *C. jejuni via* electroporation. Several stable *C. jejuni* mutant clones were isolated after transformation (Figure 4.3). The insertion of the *kan*^{r} cassette was verified by PCR using High Fidelity Phusion DNA Polymerase, which amplified *spoT* showing a 1.5 kb increase, the size of the *kan*^{r} cassette having inserted into the 2.2 kb gene (Figure 4.3).

Table 4.1. Restriction sites and the sizes of digested fragments from *Sph*I digest of pGEM-T-*spoT-kan*^{r}.

Dependent on the orientation of the *kan*^{r} cassette within *spoT*, *Sph*I restriction digestion leads to two different DNA fragment profiles. The native *Sph*I sites in pGEM-T-*spoT-kan*^{r} are located at the listed base numbers. The bands produced are the DNA fragment sizes after digestion, which were observed on agarose gel electrophoresis.

Correct orientation		**Reverse orientation**	
*Sph*I site	Bands produced (bp)	*Sph*I site	Bands produced (bp)
1657	5084	3108	3633
26	1631	26	3082

A

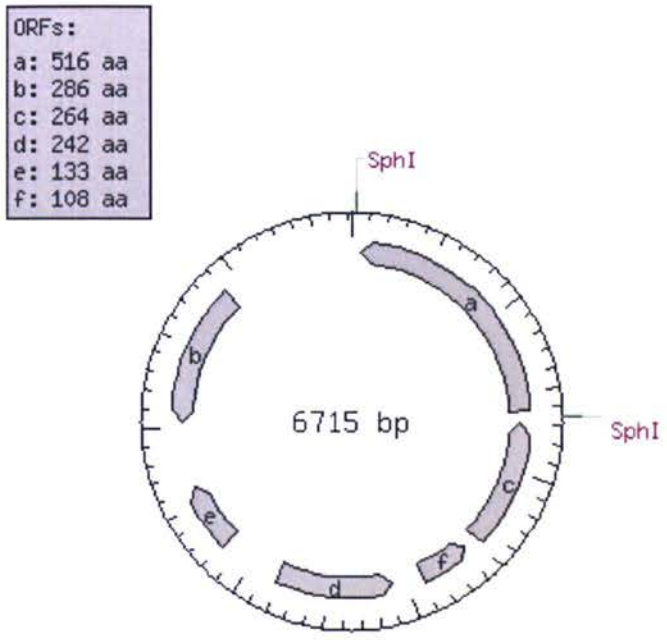

B

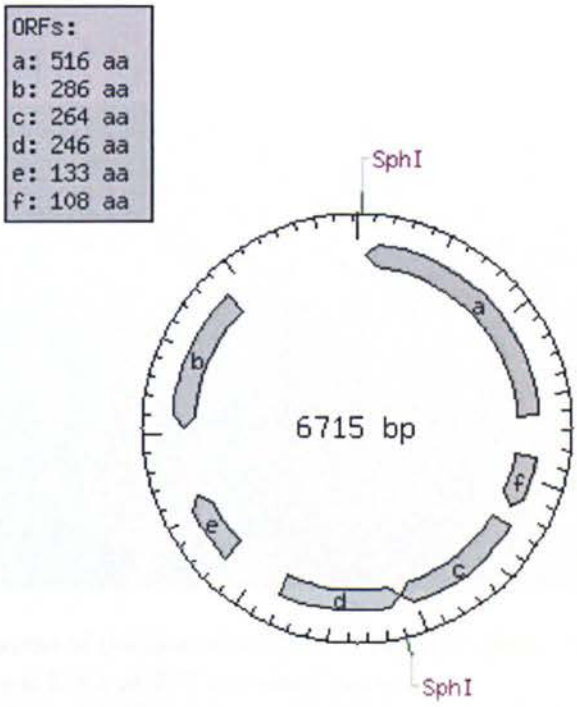

Figure 4.1. Illustration of the restriction sites of the *spoT-kan*^{r} plasmid showing A) correct and B) reverse of the insertion of *kan*^{r}.

*Sph*I restriction sites are also shown. Location of *spoT* is shown by a & c and the location of *kan*^{r} is shown by f respectively. Image produced by NEBCutter v2.

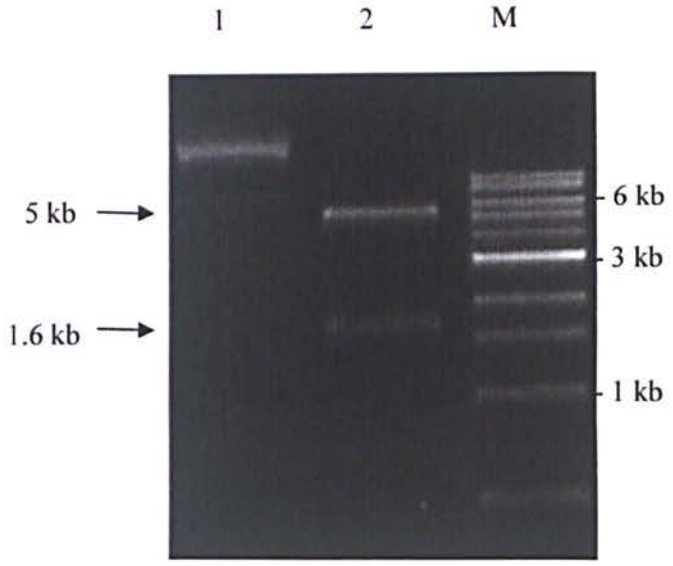

Figure 4.2. Restriction enzyme digest analysis of pGEM-T-*spoT-kan*^{r} plasmids.
The digested DNA fragments shown on 1% agarose gel to deduce the correct orientation of *kan*^{r} within the plasmid according to DNA fragment sizes. The approximate sizes of the bands were determined by comparison with the DNA ladder. Uncut plasmid appears larger in size on the agarose gel due to DNA coiling.
1- pGEM-T-*spoT-kan*^{r} uncut, 2- pGEM-T-*spoT-kan*^{r} digested with *Sph*I, M- NEB 1 kb Ladder.

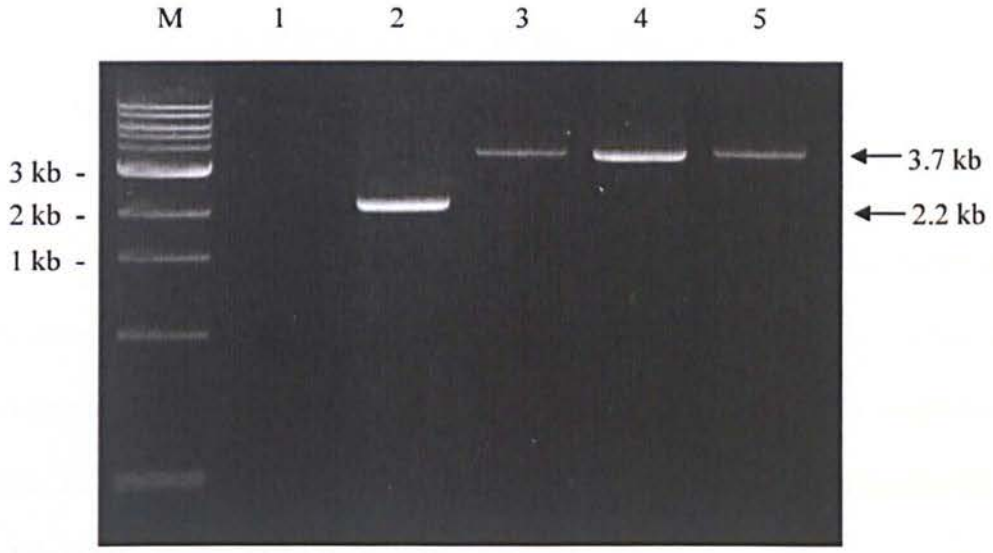

Figure 4.3. Verification of the insertion by PCR amplification of *spoT* gene using *C. jejuni* 11168H chromosomal DNA of WT and *spoT* mutants.
The presence of the *kan*^{r} leads to a 1.5 kb increase in size to the *spoT*. DNA was run on 1% agarose gel to determine the size of the *spoT* amplicons, which were determined by comparison with the DNA ladder. M- NEB 1 kb Ladder, 1- Negative control, 2- 11168H WT, 3- *spoT*::/kan^r clone 1, 4- *spoT*::/kan^r clone 2, 5- *spoT*::/kan^r clone 1.

4.2.2. Phenotypic effects of *C. jejuni spoT* knockout on growth and morphology

The difference in the OD_{600nm} of the *spoT*::*kan*^{r} mutant liquid media cultures and the WT *C. jejuni* strains over 48 hrs was recorded (Figure 4.4). The four time points were selected to show lag to early logarithmic (14 hrs), logarithmic to early stationary (24 hrs), stationary (38 hrs) and decline phase (48 hrs). The pattern of growth was the same for all strains, showing that the mutation did not hinder growth or induce premature death (strain 11168H - unpaired Student's *t*-test; - 1.1452, df = 28, $P = 0.26$), (strain 81116 - unpaired Student's *t*-test; - 1.5019 df = 28, $P = 0.14$).

However, the OD_{600} values for the *spoT*::*kan*^{r} in both strains were often higher at time points after 0 hr, as the culture grew, than the WT strains with the highest readings coming from 81116 *spoT*::*kan*^{r} (Figure 4.4)

Between the WT strains 11168H and 81116, the percentage of CF visualised and counted from Gram stain samples were very similar at each time point and replicate reading (unpaired Student's *t*-test; - 0.2701, df = 21, $P = 0.79$), (Figure 4.5). However, 11168H::*spoT/kan*^{r} and 81116::*spoT/kan*^{r} Gram stain samples displayed an approximate 10-20 % increase in CF in liquid cultures compared to WT strains (Figures 4.6 and 4.7). This increase in CF accumulation only became apparent and significant in samples after 24 hrs (strains 11168H unpaired Student's *t*-test; - 2.1683, df = 10, $P = 0.05$) (strains 81116 unpaired Student's *t*-test; - 2.4271, df = 10, $P = 0.04$).

Inactivation of *spoT* in *C. jejuni* 11168H and 81116 showed similar phenotypic responses with increased CF accumulation and optical density readings in tandem with growth, as in the previously experimentally tested strain *C. jejuni* 81-176 (Gaynor *et al.*, 2005).

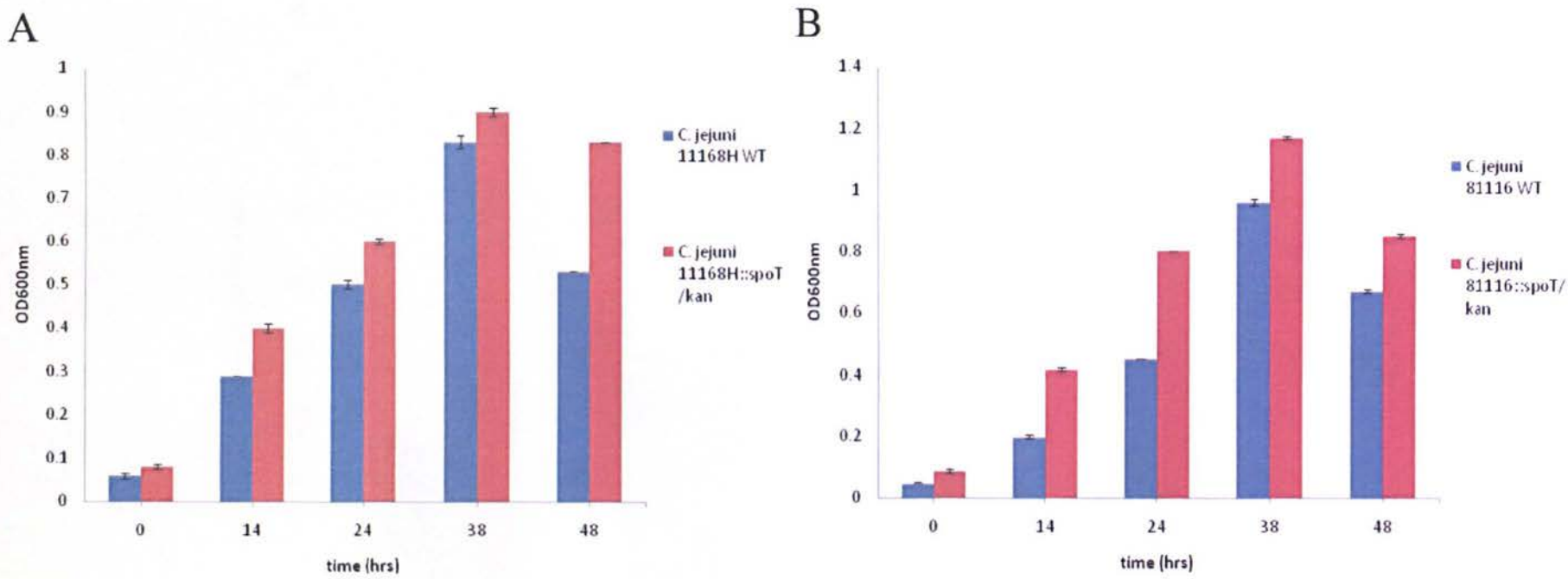

Figure 4.4. Effect of *spoT* knockout compared with WT on growth in liquid media.
The optical density of A) *C. jejuni* 11168H and B) 81116 WT and *spoT* mutants in liquid media cultures grown in microaerobic (O_2 = 5%) over a 48 hr period. The liquid cultures were grown with shaking (~200 rpm), starting at approximately 0.1 OD_{600nm} ml^{-1}. These data are the mean of an individual experiment, which was done in triplicate with similar results each time. The error bars represent SD (N= 3).

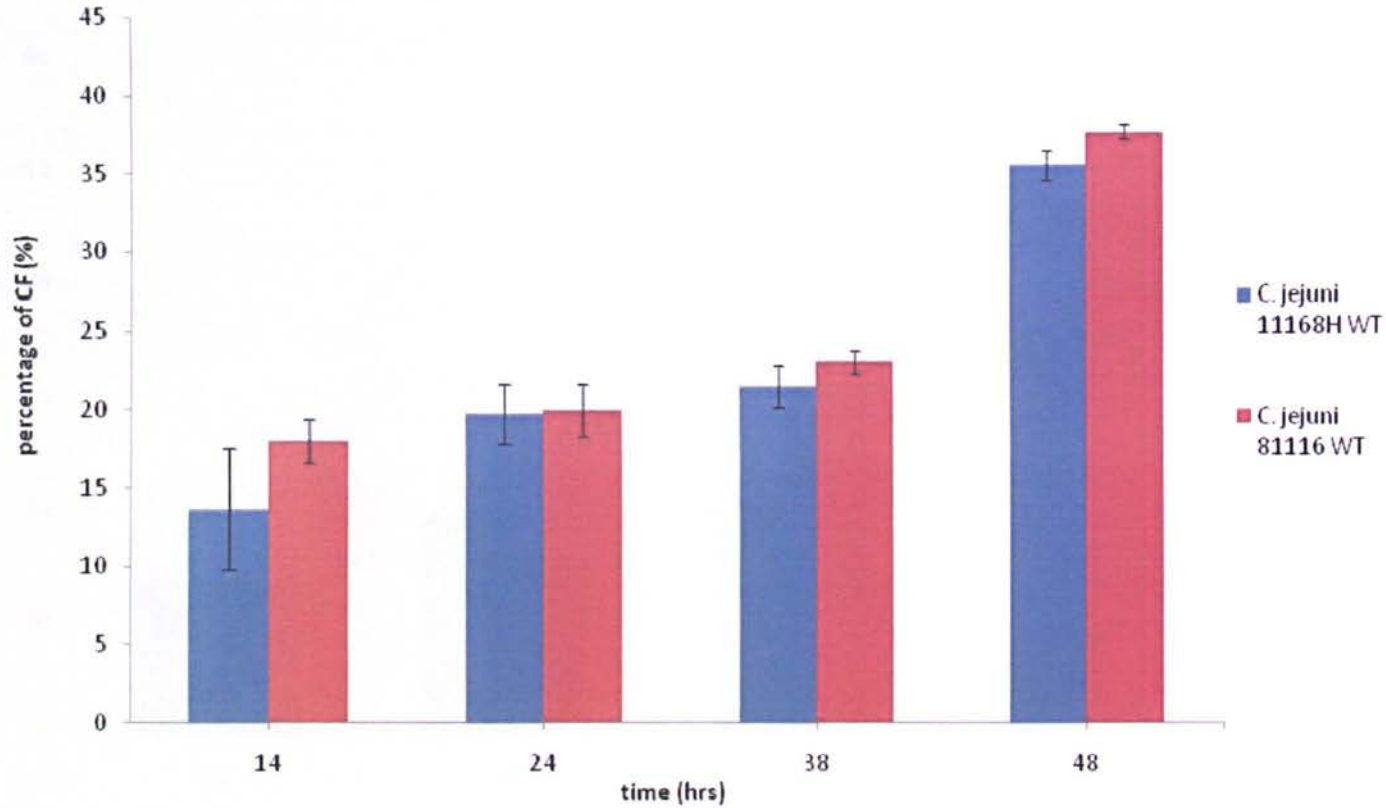

Figure 4.5. The mean percentage of CF in WT *C. jejuni* 11168H and 81116 liquid cultures over a 48 hr period.
The liquid cultures were grown microaerobically with shaking (~200 rpm), starting at approximately 0.1 OD_{600nm} ml^{-1}. Within each individual measurement, 100 cells were counted. The samples were prepared and counted as described in section 2.1.2. These data are the mean of an individual experiment, which was done in triplicate with similar results each time. The error bars represent SD (N= 3).

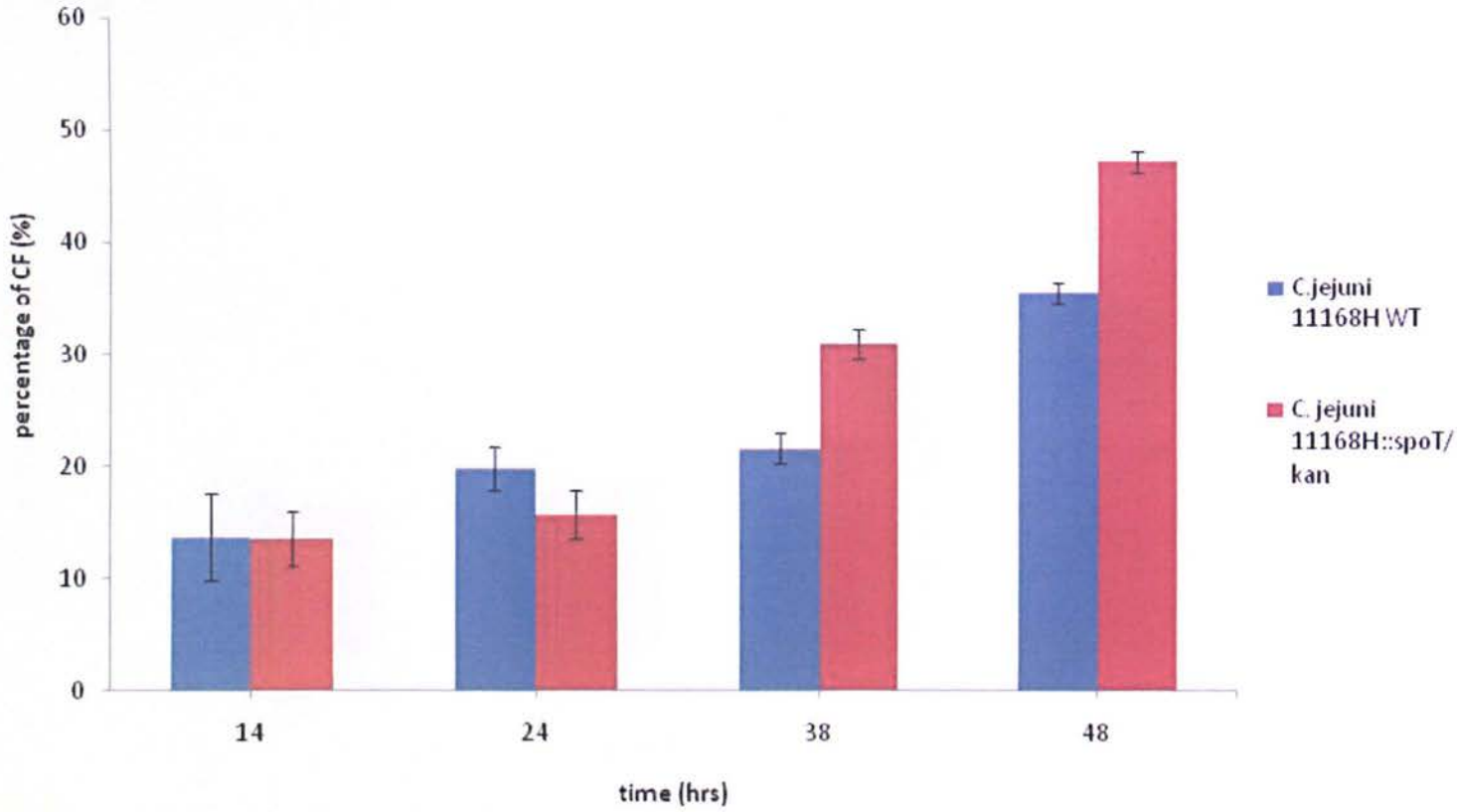

Figure 4.6. Effect on CFF of *spoT* mutation in *C. jejuni* 11168H compared to WT.
The liquid cultures were grown microaerobically with shaking (~200 rpm), starting at approximately 0.1 OD_{600nm} ml^{-1}. Within each individual measurement, 100 cells were counted. The samples were prepared and counted as described in section 2.1.2. These data are the mean of an individual experiment, which was done in triplicate with similar results each time. The error bars represent SD (N= 3).

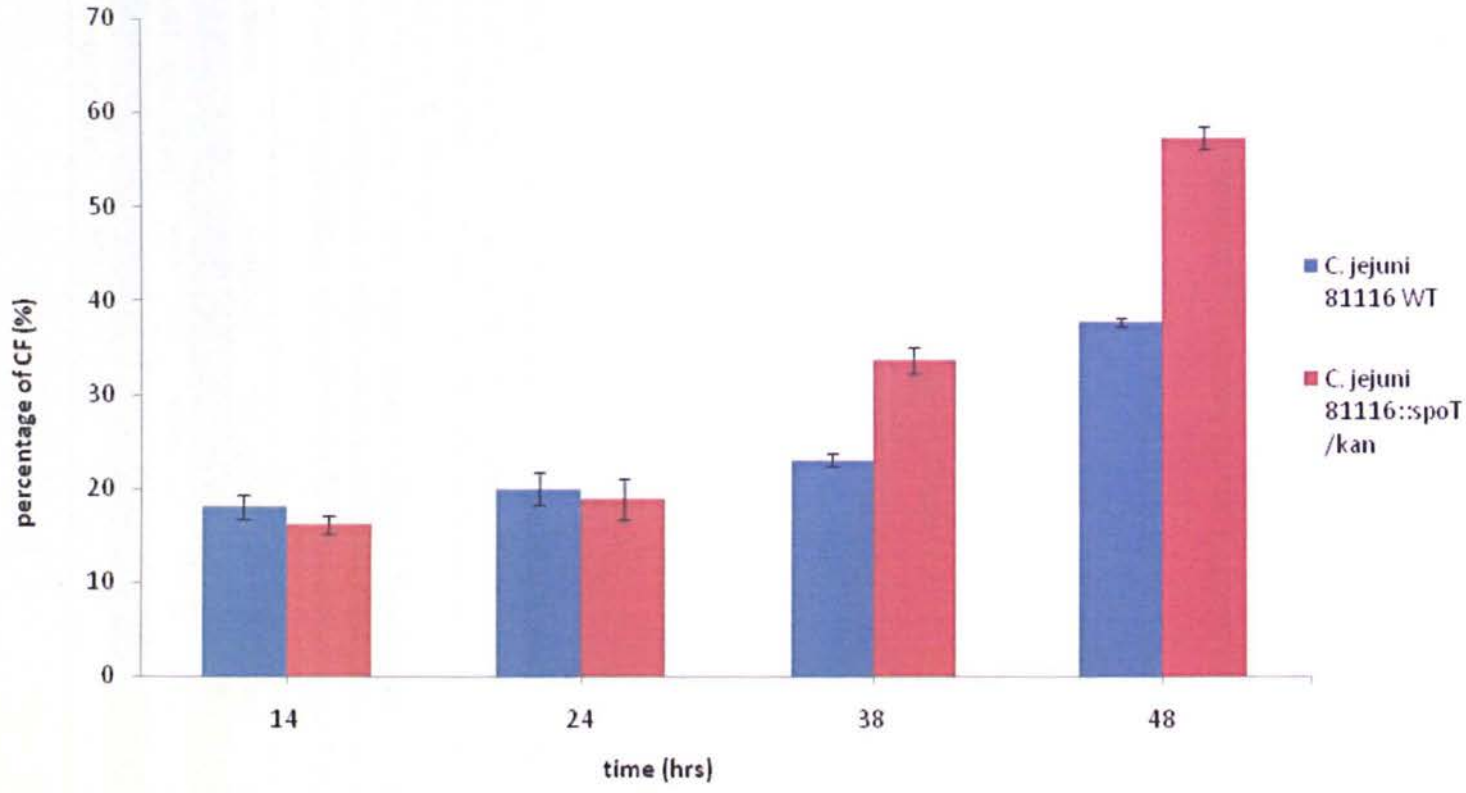

Figure 4.7. Effect on CFF of *spoT* mutation in *C. jejuni* 81116 compared to WT.
The liquid cultures were grown microaerobically with shaking (~200 rpm), starting at approximately 0.1 OD_{600nm} ml^{-1}. Within each individual measurement, 100 cells were counted. The samples were prepared and counted as described in section 2.1.2. These data are the mean of an individual experiment, which was done in triplicate with similar results each time. The error bars represent SD (N= 3).

4.2.3. Reduced rifampicin resistance in *C. jejuni* 11168H *spoT::kan*^{r} and 81116 *spoT::kan*^{r} mutants compared to WT

Previous studies with *C. jejuni* 81-176 *spoT* knockout strain experimentally showed a link between ppGpp and rifampicin binding to RNA polymerase β subunit (Gaynor *et al.*, 2005). The *spoT* knockout mutants showed a similar sensitivity to higher concentrations of rifampicin compared to WT strains, as with *C. jejuni* 81-176 (Gaynor *et al.*, 2005). WT *C. jejuni* 11168H presented a very high resistance to rifampicin, still forming single colonies at concentrations of 150 μg/ml and growth at 200 μg/ml, whilst *C. jejuni* 11168H::*spoT/kan*^{r} displayed sensitivity to 50 μg/ml and was unable to grow at concentrations higher than 100 μg/ml (Table 4.2). *C. jejuni* 81116 WT showed a higher sensitivity to rifampicin compared to *C. jejuni* strain 11168H and displayed attenuated growth at 50 μg/ml, whilst *C. jejuni* 81116::*spoT/kan*^{r} was unable to grow at all at 50 μg/ml.

Table 4.2. The rifampicin resistance of *C. jejuni* WT and *spoT* knockout mutants.
The strains from overnight plates were resuspended in BHI broth and streaked onto MH plates of various rifampicin concentrations. WT and *spot::kan*^{r} mutant strains were incubated on the MH plates at 37°C overnight.
Key: *** full growth/no effect to single colonies, ** weaker amount of growth with smaller single colonies,* no single colonies/growth only within the thick part of the streak, - no growth
This table is a combination of results from three experiments, conducted in replicate.

Organism	0 μg/ml	50 μg/ml	100 μg/ml	150 μg/ml	200 μg/ml
11168H WT	***	**	**	*/**	*
11168H::*spoT/kan*^{r}	***	*/**	-/*	-	-
81116 WT	***	*	-	-	-
81116::*spoT/kan*	***	-	-	-	-

4.4. Discussion

The aim of this study was investigate the effect of deleting the *spoT* gene in *C. jejuni* 11168H and 81116, to compare with previous experimentally shown *C. jejuni* strains and *H. pylori* strains. The results presented here demonstrate that there is little difference between the strains 11168H, 81-176, and 81116 in the role of *spoT* with regards to CFF; each *spoT::kan*^{r} strain displayed similar phenotypes. Although there was little difference between the strains investigated here and previously by Gaynor *et al.*, (2005), *spoT* could have a different relationship to CFF in other *Campylobacter* spp., for example *C. fetus* that does not form CF regardless of environmental stress.

In late growth stages, *C. jejuni* morphology transitions to the CF show the same trend found with *C. jejuni spoT::kan*^{r} strains despite the increased percentage of CF present.

The increase is only apparent after 24hrs incubation and is most likely due to the role of SpoT in stringent response, as after 24hrs the cultures would be entering early stationary phase.

The increase in OD_{600nm} readings of *spoT::kan*^{r} cultures compared to WT strains could be linked to the increase in CF accumulation and growth. The coccoid morphology of *spoT* mutant strains could also alter the absorbance readings. It is possible that an accumulation of proteins due to lack of *spoT* lead to the increase in the optical density and the higher CF percentage of the knockout mutants witnessed (Cashel *et al.*, 1996). It was demonstrated by Gaynor *et al.* (2005) that the *spoT* knockout mutant lead to an up-regulation in the expression of several heat shock proteins as the bacteria entered stationary phase, thus altering the growth and absorbance readings. Higher expression of proteins could divert

energy for protein translation, leading to a hindrance in growth, though the expressed proteins could still increase absorbance readings.

ppGpp is known to act on the transcription rates by binding to the β subunit of RNA polymerase. Rifampicin also binds to the β-subunit of RNA polymerase, only 27Å from the binding site of ppGpp (Zillig *et al.*, 1970; Reddy *et al.*, 1995). It was a suggested theory that RNA polymerase in the presence of ppGpp could block the binding of rifampicin physically or by the induction of an RNA polymerase conformational change (Gaynor *et al.*, 2005). A high level of resistance to rifampicin has been documented with several strains of *C. jejuni* and *Campylobacter* spp. with rifampicin at ≥100μg/ml being a common component to *Campylobacter* selective media (Aleksandrova *et al.*, 1990). The decrease in rifampicin resistance that was shown in *spoT::kan*^{r} 81116 and 11168H in comparison with WT strains indicated there is a decrease in (p)ppGpp.

Further experiments could have been conducted to show if the truncation of *spoT* was successful and phenotypic results were caused by the lack of a functional *spoT* and a depletion in (p)ppGpp. Complementation of the *spoT* mutant would help define the effects found in CFF and rifampicin resistance was due to the lack of a functional *spoT*. Western blotting is one method that could have been used to determine the lack of ppGpp bifunctional synthetase-hydrolase.

It was concluded by Gaynor *et al.* (2005) that *spoT* was pleiotropic due to the effects *spoT* deficient mutants had on adhesion, invasion, antibiotic resistance, survival through stationary phase and aerotolerance. Despite the connection the gene may have to cell shape, it cannot be considered a genetic determinant for the CF in *C. jejuni* due to its pleiotropic nature. The effect this gene may have on cell shape could be indirect, for

example due to involvement with another pathway or gene product. The lack of a functional *spoT* could allow other environmental stresses to have a greater effect on the organism, inducing the morphology change earlier. The transition to CF in *C. jejuni* has been shown to increase under various environmental stressors and without the ability to mount a stringent response could present a more sensitive bacterium.

SpoT may not be a genetic determinate of CF in *C. jejuni* due to its pleiotropic nature. However, it is possible that other genes within the same cluster could be directly involved with cell shape transition and/or maintenance, which led to a particular interest in *amiA*.

5.0. Investigation into the role of *amiA* in connection with CFF

5.1. Introduction

AmiA/ Cj1269c is annotated to encode for *C. jejuni N*-acetylmuramoyl-L-alanine amidase which cleaves peptidoglycan (Parkhill *et al.*, 2000; Gundogdu *et al.*, 2007). It has been demonstrated that the shape of bacteria can be influenced by the structure of peptidoglycan (Schwartz & Leutgeb, 1971; Stoker *et al.*, 1983; Begg & Donachie, 1985). Located within the same gene cluster as *amiA* is *spoT*, which has also been associated with cell shape transition in *C. jejuni*, albeit in an indirect manner (Gaynor *et al.*, 2005). Cell shape maintenance in other microorganisms is known to be genetically determined. *MreB* gene and gene products were shown by Doi *et al.* (1988) to have a possible determinative effect in cell morphology. Within the model organism *E. coli*, the role of *rodA* was shown to be necessary for the rod morphology (Stoker *et al.*, 1983; Begg & Donachie 1985). Chaput *et al.* (2005) considered *amiA* in *H. pylori* 26695 to be the first genetic determinant of CFF as the mutation of the gene function lead to a decrease in the formation of the coccoid morphology under normal growth conditions. It was theorised that AmiA cleaves sacculi leading to a 'looser' macromolecule to enable the morphology transition (Costa *et al.*, 1999; Chaput *et al.*, 2005). In these and other bacteria (Costa *et al.*, 1999), AmiA is known to be involved in peptidoglycan maintenance, suggesting a link between peptidoglycan biosynthesis and CFF.

Despite the promising research with *amiA* in *H. pylori*, there has been no research of the biological role or function of *amiA* within *C. jejuni*. Thus, as *C. jejuni* is closely related to *H. pylori*, the aim was to determine whether *amiA* had the same role in *C. jejuni*.

5.3. Results

5.3.1. The correlation between the expression of *amiA* with CF accumulation

The expression of *amiA* in *C. jejuni* 11168H was measured from samples cultured from solid media at 1 to 4 day intervals and in liquid media at 0.5, 1, 1.5 and 2 day intervals. The intervals used for measuring the expression of *amiA* on solid media were due to the dramatic increase of CF from day 2 to day 3 whilst the liquid culture samples represent the gradual increase of CF in correlation with age and the growth phases of the culture: lag; logarithmic; stationary; and decline phase. As previously shown in Chapter 3 (Figure 3.3), CF accumulation in liquid media over a 2 day period increased from ~15% CF at day 0.5 to ~40% by day 2. The quality of all mRNA samples were measured on a NanoVue system and Bioanalyser to check quantity and quality, respectively (Figure 5.1.).

Two different housekeeping genes were used to compare with *amiA* and determine the levels of expression. There is controversy regarding the use of 16S rRNA as an endogenous control in gene expression studies due to the relative levels of expression being approximately 100-fold higher for the rRNA locus than for protein encoding genes (Ritz *et al.*, 2009). Other housekeeping genes are preferred within *Campylobacter*. *rpoA* was shown to be the most stable housekeeping gene and thus considered the most suitable internal control in *C. jejuni* for RT-PCR (Ritz *et al.*, 2009). It is shown within these studies that the Ct levels of 16S rRNA were much higher than *amiA* and *rpoA*, with the average Ct value of 16S rRNA between 2 technical replicates of a biological sample being 5 values higher than *rpoA*. The dramatically high levels of 16S rRNA transcripts may not be indicative of the whole cell expression levels whilst under stress, hence why many consider 16S rRNA not to be a good endogenous control within *C. jejuni* and other

organisms despite the stable transcript levels (Eleaume & Jabbouri, 2004; Desroche *et al.*, 2005; Ritz *et al.*, 2009).

Expression studies using *C. jejuni* samples cultivated from solid media over 4 days showed no consistent significant change in *amiA* expression with either endogenous control (*rpoA* control -unpaired Student's *t*-test; 2.1521, df = 10, $P = 0.06$) (16S control -unpaired Student's *t*-test; 0.5526, df = 10, $P = 0.59$). As can be seen in Figure 5.2 the expression varied between samples and time points regardless of repetitions. The lack of significant results from biological replicates could be due to the heterogeneous nature of plate culture samples, leading to a mixture of various expression profiles.

Within liquid culture samples, the expression studies have shown that the expression of *amiA* does not change dramatically, with the highest recorded increase of 2.5 fold (Figure 5.3) (*rpoA* control -unpaired Student's *t*-test; 1.1273, df = 14, $P = 0.28$) (16S control - unpaired Student's *t*-test; 0.0178, df = 14, $P = 0.99$). Similarly, in solid media samples, there was no significant change in expression across the different time samples with either endogenous control gene. However, unlike the solid media samples, all the samples exhibited a similar basal level of expression. The liquid culture samples enable a higher amount of homogeneity in mRNA between the biological samples. It appeared that *amiA* expression is fixed or the amount of expression is not significant through the different phases of growth in liquid media (Figure 5.2 and 5.3).

The samples were analysed with all biological replicates combined at each time point. However, due to the results with the solid media culture samples showing such greater variance between biological samples, comparisons were made between each sample with its own endogenous control over time. This data was used to determine if there are

reoccurring expression profiles of *amiA* within each biological sample though no theme was found. This shows that the different expression on the solid media was not due to a mixture of different expression profiles being measured together.

Both on solid agar and in liquid media, there was no direct correlation between CFF and *amiA* expression in *C. jejuni* 11168H, however mRNA expression levels are not necessarily indicative of protein expression levels.

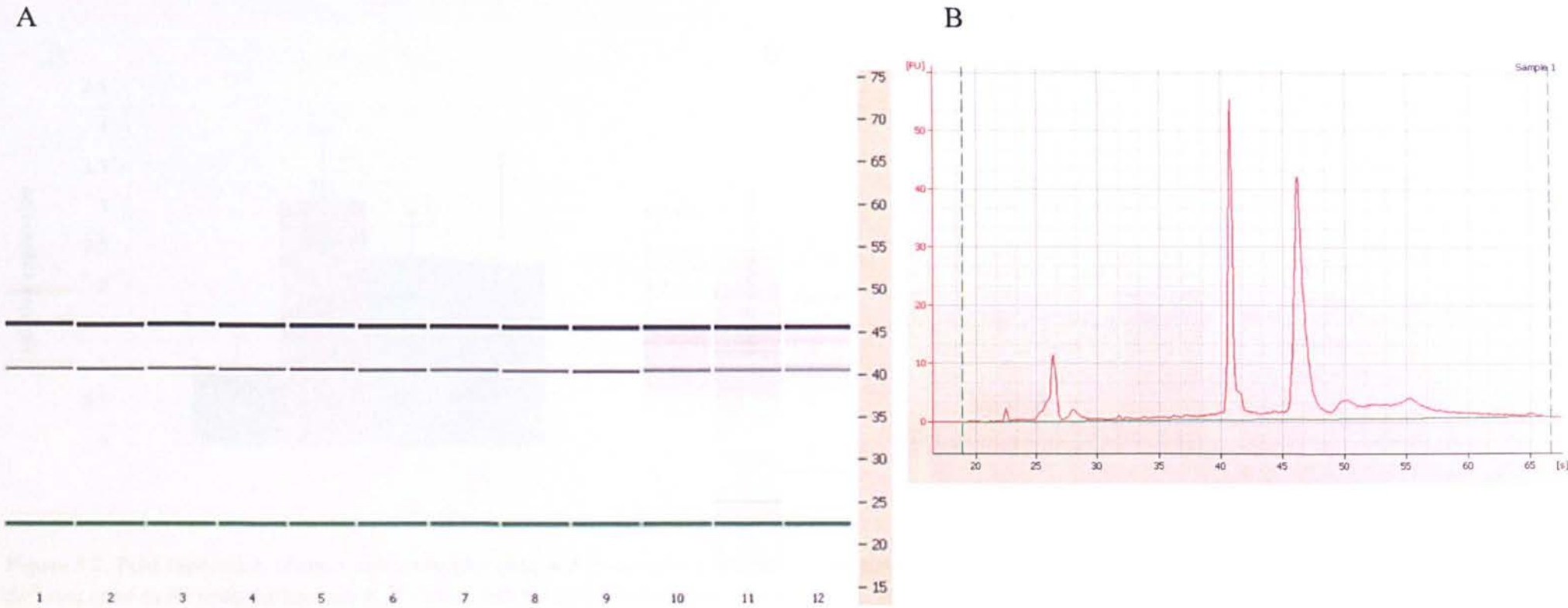

Figure 5.1. Analysis of total mRNA samples on the Agilent 2100 Bioanalyzer RNA 6000 Nano LabChip.
This is a representative set of results to demonstrate the quality of RNA used in all qPCR experiments.
A- Bioanalyser gel like image of the total mRNA samples showing no degradation. The distinct 16 and 23S bands are visible in all samples.
B- The fluorescence plot is the electropherogram for lane 1 with 16S and 23S peaks visible.
The clear visible bands with no smearing show there is no degradation.

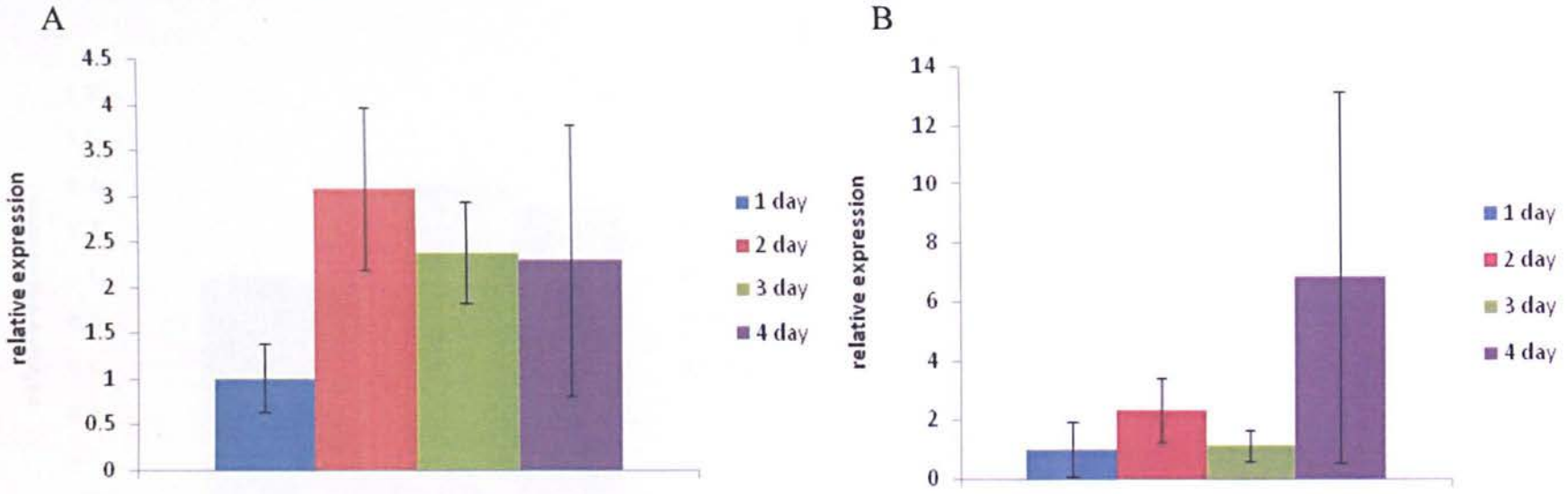

Figure 5.2. Fold expression of *amiA* using samples obtained from solid media at varying time points.
A- using *rpoA* as the endogenous control, B - using 16S rRNA as the endogenous control. This set of results is one experiment shown as an example of the varying expression between 3 biological replicates for each time point. The error bars represent SD.

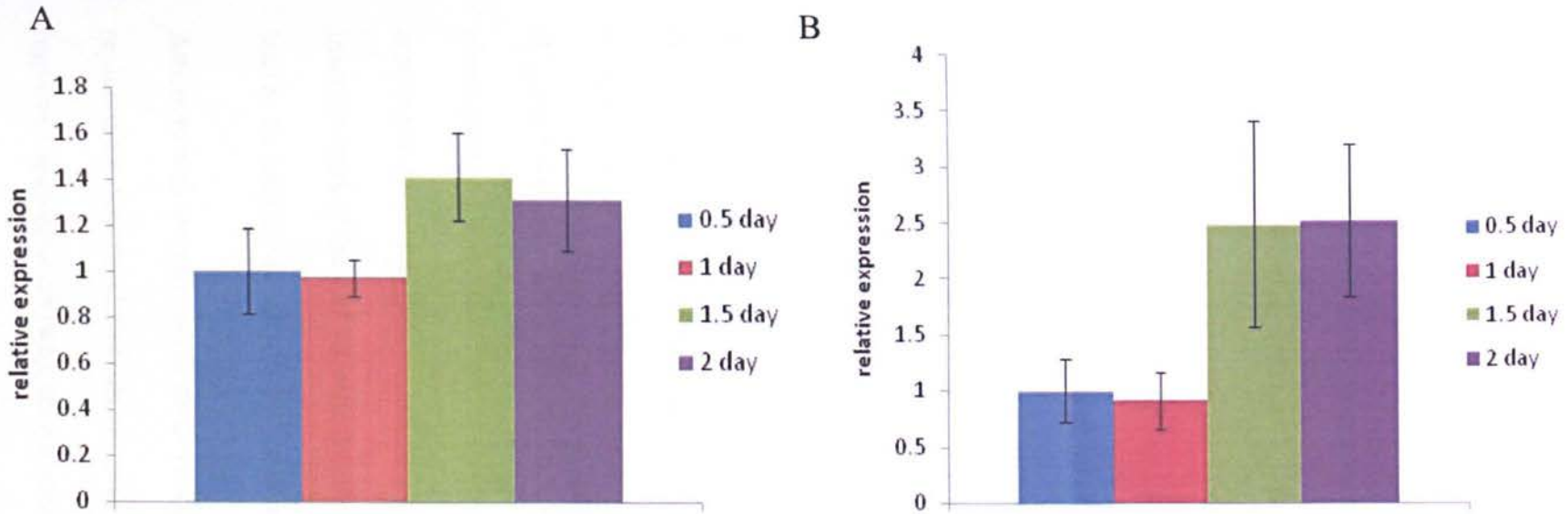

Figure 5.3. Fold expression profiles of *amiA* using samples obtained from liquid media at varying time points.
A- using *rpoA* as the endogenous control, B - using 16S rRNA as the endogenous control. This set of results is one experiment shown as an example of the expression between 3 biological replicates with 2 technical replicates for each time point. Similar results were found in other replicates of the experiment. The error bars represent SD.

5.3.2. Construction of *E. coli amiA::kan*^{r} and the non-viable *C. jejuni* knockout mutants

To further explore the function of *amiA*, the creation of a knockout mutant via SDM with the insertion of *kan*^{r}, to truncate the gene product was attempted. PCR amplification of *amiA* from *C. jejuni* 11168H chromosomal DNA used primers amiA_for and amiA_rev (sequences in Chapter 2, Table 2.8). The *amiA* PCR amplicon was then inserted into the pGEM-T cloning vector (Promega). The pGEM-T-*amiA* had *kan*^{r} gene inserted at two different sites to produce two different mutants: *amiA-kan*^{r}N (*N*-terminal insertion of *kan*^{r}) and *amiA-kan*^{r}C (*C*-terminal insertion of *kan*^{r}). The native *BsaB*I site within *amiA* was used for the insertion of *kan*^{r} in the *N*-terminal region. The native *Cla*I site in *amiA* was used for insertion in the *C*-terminal region. The same restriction sites were used for another version of *amiA-kan*^{r}N and *amiA-kan*^{r}C, which had a 0.5 kb extended flanking region at each terminal of *amiA*. This was to increase complementary regions, to improve horizontal gene replacement. These plasmids were called *amiAXF-kan*^{r}N and *amiAXF-kan*^{r}C. The reverse orientation of the *kan*^{r} cassette could alter gene expression, therefore the orientation of *kan*^{r} of all constructs was determined by restriction digestion using *Sph*I (Figures 5.4 to 5.10 and Tables 5.1 to 5.4) and verified by sequencing. Transformation via electroporation was conducted for chromosomal gene replacement of the *kan*^{r} derivatives conducted as previously described within Chapter 2 (2.3.5). The effect of different insertion sites of the *kan*^{r} cassette determined whether deletion of specific regions of *amiA* lead to the lack of viability in the mutants.

Attempts with the various plasmids yielded no successful viable transformants with allelic replacement. Several alterations to the transformation method were also attempted to improve transformation rates, such as changes in the DNA concentration used;

transformation via an alternative method using sepiolite (method described in Chapter 2 (2.3.5)); and changes to competent cell quality and quantity.

Due to the inability to create any *amiA* knockout mutants in *C. jejuni*, further investigation of *amiA* required the development of a system for regulated gene expression and construction of conditionally lethal mutants.

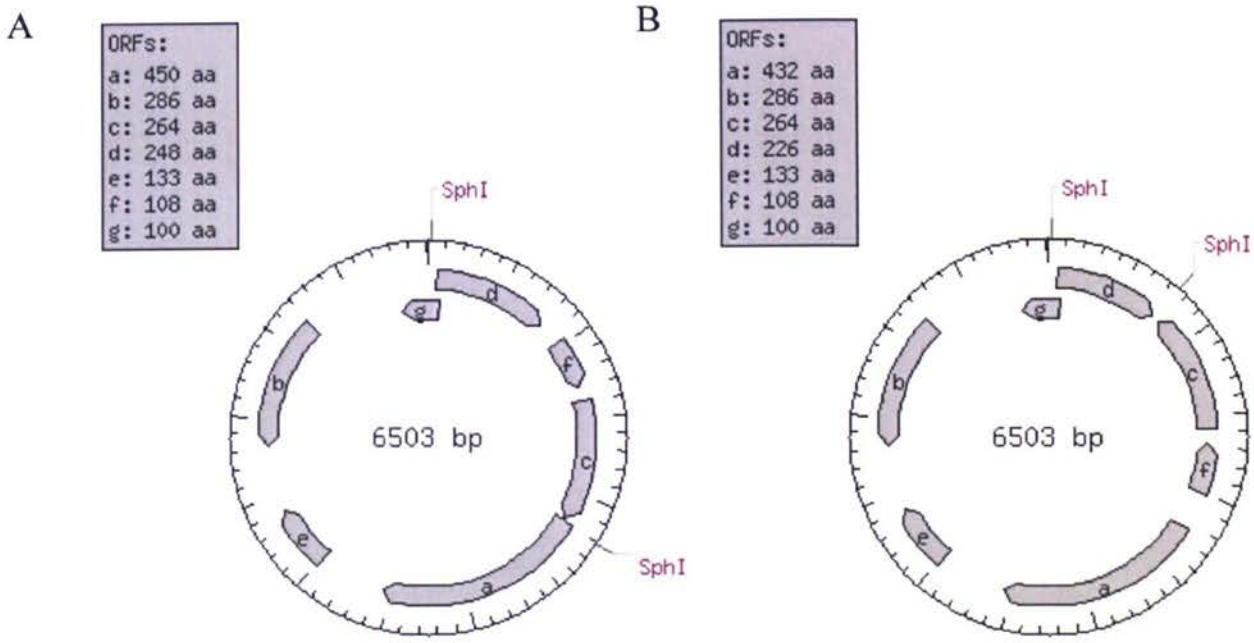

Figure 5.4. Illustration of *Sph*I restriction sites of the pGEM-T-*amiA*-*kan*^{r}N plasmid showing A) correct and B) reverse orientation of the insertion of *kan*^{r}.
Location of *amiA* is shown by a & d and the location of *kan*^{r} is shown by c respectively. Image produced by NEBCutter v2.

Table 5.1. Restriction sites and the sizes of digested fragments from *Sph*I digest of pGEM-T-*amiA*-*kan*^{r}N constructs with *kan*^{r} in the correct and reverse orientation.

Correct orientation of *kan*^{r}		Reverse orientation of *kan*^{r}	
*Sph*I site	Bands produced (bp)	*Sph*I site	Bands produced (bp)
2211	2185	760	734
26	4318	26	5769

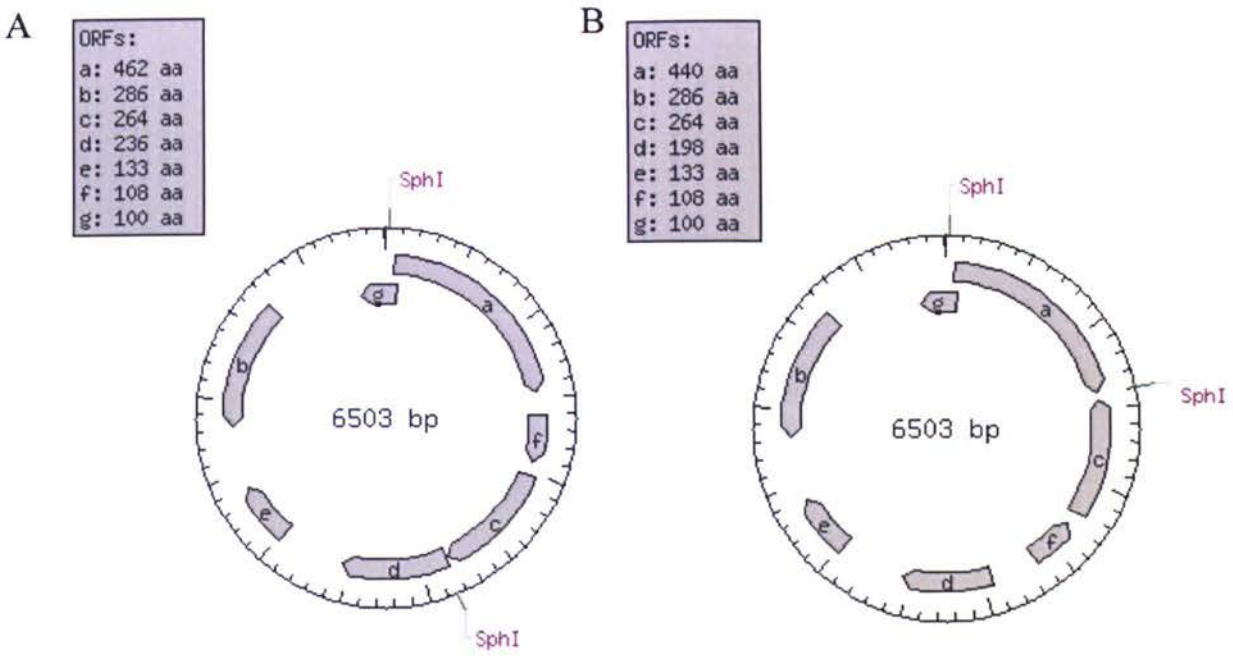

Figure 5.5. Illustration of *Sph*I restriction sites of the *amiA-kan*^{r}C plasmid showing A) correct and B) reverse of the insertion of *kan*^{r}.
Location of *amiA* is shown by d & a and the location of *kan*^{r} is shown by c & f respectively. Image produced by NEBCutter v2.

Table 5.2. Restriction sites and the sizes of digested fragments from *Sph*I digest of pGEM-T-*amiA-kan*^{r}C constructs with *kan*^{r} in the correct and reverse orientation.

Correct orientation of *kan*^{r}		Reverse orientation of *kan*^{r}	
*Sph*I site	Bands produced (bp)	*Sph*I site	Bands produced (bp)
2853	2827	1402	1376
26	3676	26	5130

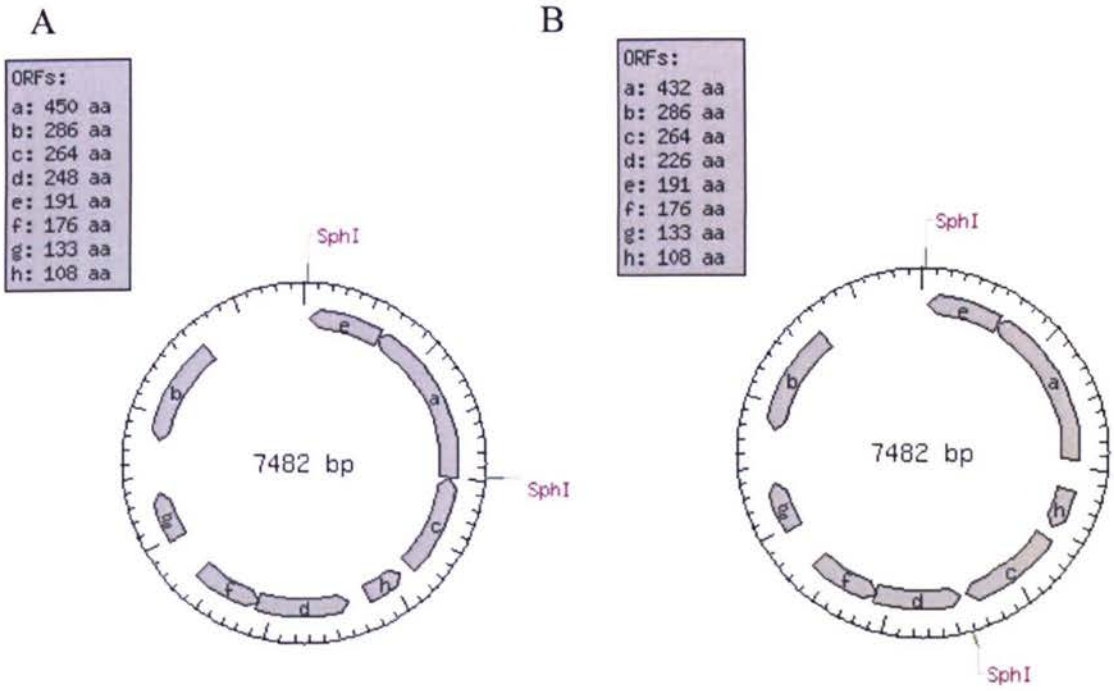

Figure 5.6. Illustration of *Sph*I restriction sites of the *amiAXF-kan*^{r}N plasmid showing A) correct and B) reverse of the insertion of *kan*^{r}.
Location of *amiA* is shown by a, d, e & f and the location of *kan*^{r} is shown by h & c respectively. Image produced by NEBCutter v2.

Table 5.3. Restriction sites and the sizes of digested fragments from *Sph*I digest of pGEM-T-*amiAXF-kan*^{r}N constructs with *kan*^{r} in the correct and reverse orientation.

Correct orientation of *kan*^{r}		Reverse orientation of *kan*^{r}	
*Sph*I site	Bands produced (bp)	*Sph*I site	Bands produced (bp)
1968	1942	3419	3388
26	5566	26	4120

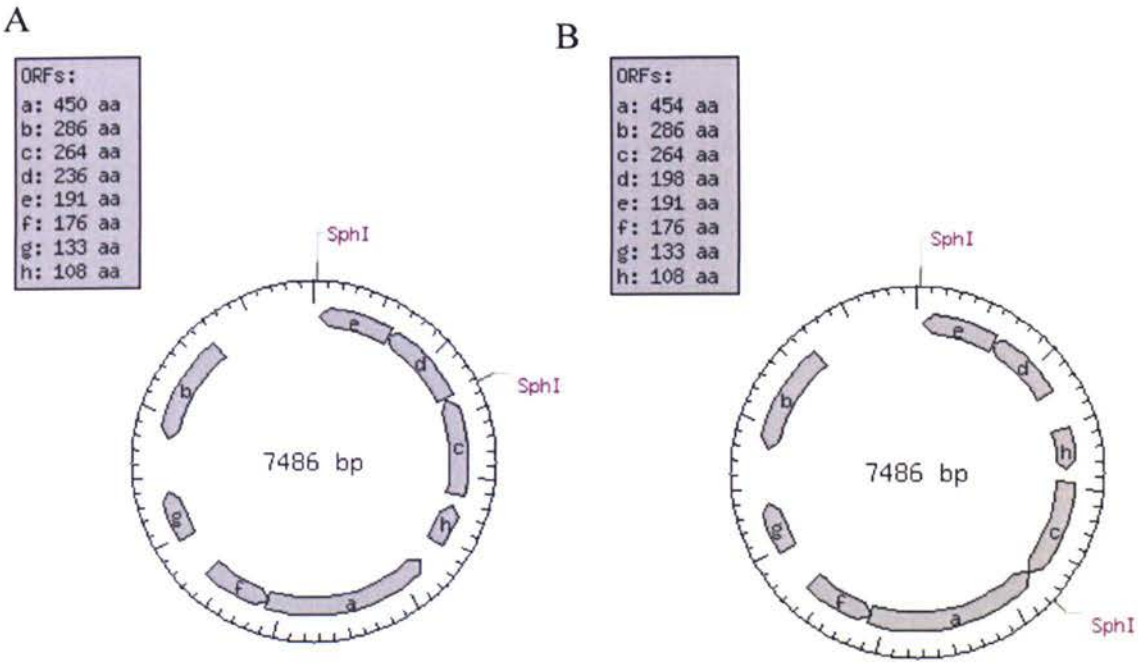

Figure 5.7. Illustration of *Sph*I restriction sites of the *amiAXF-kan*^{r}C plasmid showing A) correct and B) reverse of the insertion of *kan*^{r}.
Location of *amiA* is shown by a, d, e & f and the location of *kan*^{r} is shown by h & c respectively. Image produced by NEBCutter v2.

Table 5.4. Restriction sites and the sizes of digested fragments from *Sph*I digest of pGEM-T-*amiAXF-kan*^{r}C constructs with *kan*^{r} in the correct and reverse orientation.

Correct orientation of *kan*^{r}		Reverse orientation of *kan*^{r}	
*Sph*I site	Bands produced (bp)	*Sph*I site	Bands produced (bp)
1326	1300	2777	2751
26	6208	26	4757

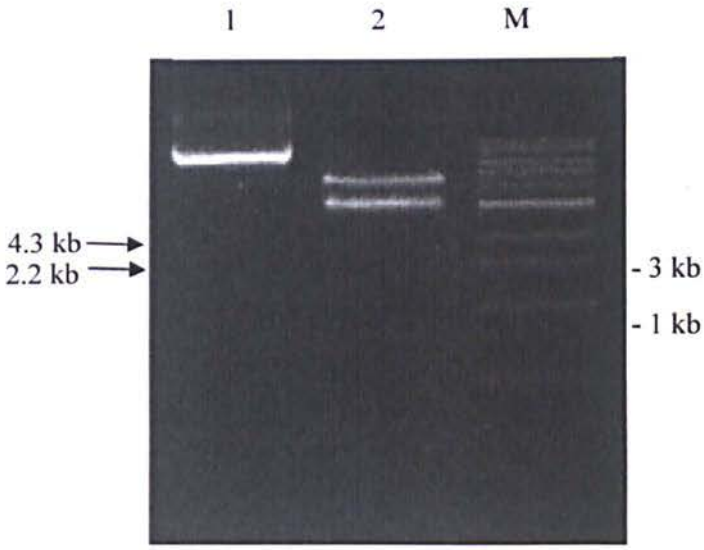

Figure 5.8. Restriction enzyme digest analysis of pGEM-T-*amiA-kan*^{r}N plasmids.
The digested DNA fragments shown on 1% agarose gel to deduce the correct orientation of *kan*^{r} within the plasmid according to DNA fragment sizes. The approximate sizes of the bands were determined by comparison with the DNA ladder. Uncut plasmid appears larger in size on the agarose gel due to DNA supercoiling.
1- pGEM-T-*amiA*-kan^{r}N uncut, 2- pGEM-T-*amiA-kan*^{r}N digested with *Sph*I, M- NEB 1 kb Ladder

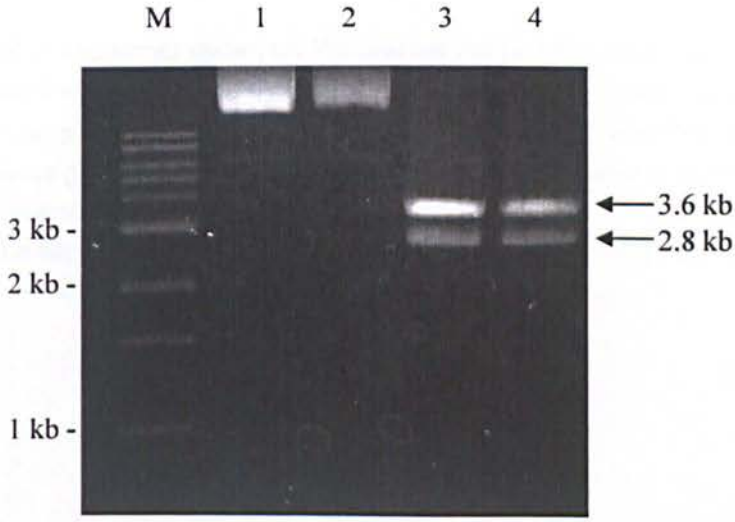

Figure 5.9. Restriction enzyme digest analysis of pGEM-T-*amiA-kan*^{r}C plasmids.
The digested DNA fragments shown on 1% agarose gel to deduce the correct orientation of *kan*^{r} within the plasmid according to DNA fragment sizes. The approximate sizes of the bands were determined by comparison with the DNA ladder. Uncut plasmid appears larger in size on the agarose gel due to DNA coiling. M- NEB 1 kb Ladder, 1- pGEM-T-*amiA*-kan^{r}C uncut, 2- pGEM-T-*amiA*-kan^{r}C clone 2 uncut, 3- pGEM-T-*amiA-kan*^{r}C digested with *Sph*I, 4 - pGEM-T-*amiA-kan*^{r}C clone 2 digested with *Sph*I.

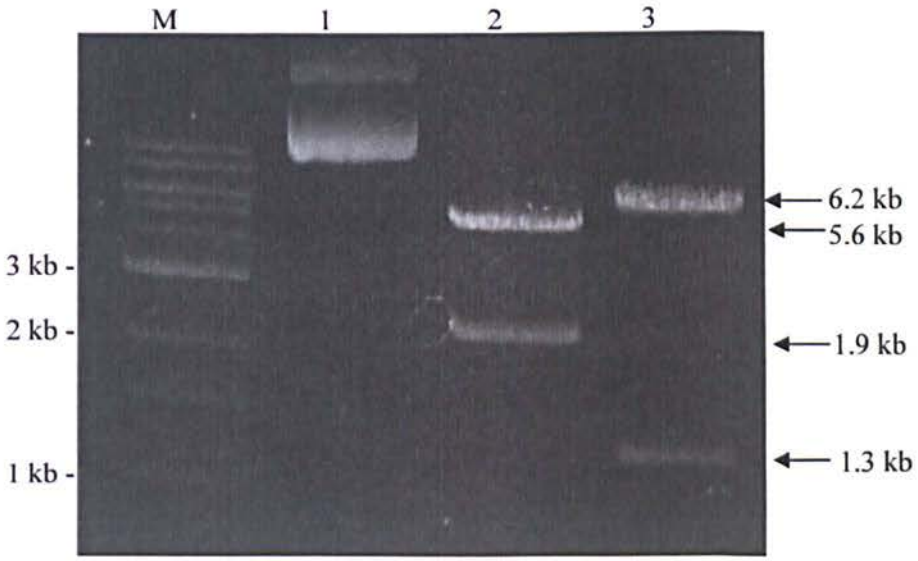

Figure 5.10. Restriction enzyme digest analysis of *amiAXF-kan*^{r}N and *amiAXF-kan*^{r}C plasmids.

The digested DNA fragments shown on 1% agarose gel to deduce the correct orientation of *kan*^{r} within the plasmid according to DNA fragment sizes. The approximate sizes of the bands were determined by comparison with the DNA ladder. Uncut *amiAXF-kan*^{r}N plasmid appears larger in size on the agarose gel due to DNA coiling. Only one uncut plasmid is shown, just to demonstrate that restriction digestion has occurred.

M- NEB 1 kb Ladder, 1- pGEM-T-*amiAXF*-kan^{r}N uncut, 2- pGEM-T- *amiAXF*-kan^{r}N digested with *Sph*I, 3 - *amiAXF*-kan^{r}C digested with *Sph*I.

5.3.3. Construction of a *C. jejuni* specific, arabinose inducible system – pRRBC

The pRRBC vector, derived from pRR plasmid, incorporates regulated expression of a gene of interest, regulated by an arabinose-inducible promoter from pBAD33. The pRR plasmid has complementary flanking regions of several highly conserved rRNA gene clusters in *Campylobacter,* allowing for the insertion of the construct into the chromosome by homologous recombination (Karlyshev & Wren, 2005). The native *Xba*I site in pRR was cut, the DNA fragments at the site blunt ended and the plasmid was dephosphorylated to prevent self ligation. The pBAD regulatory region and promoter from pBAD33 plasmid were isolated by restriction digestion with *Cla*I and *Sal*I. The DNA fragment from pBAD33 was blunt ended and isolated by agarose gel extraction. The pRR and the pBAD DNA were ligated to form an intermediate construct pRRB. The orientation of the pBAD33 fragment in pRR was determined by *Eco*RV digestion. The *cam*^{r} gene cassette was isolated from pAV35 by restriction digestion with *Kpn*I. This was subsequently blunt ended and extracted by agarose gel extraction. The extracted *cam*^{r} cassette was inserted into *Xba*I digested pRRB to form pRRBC, an arabinose-inducible vector specific for *Campylobacter.* The orientation of the *cam*^{r} was determined by digestion with *Sph*I and *Cla*I (Figures 5.11 & 5.12 and Table 5.5). The pRRBC construct was also verified by primer walking sequencing using primers camR1, pBADfor and pBAD-up to ensure that no point mutations were introduced during construction.

The native *Kpn*I site was used to insert either *amiA* or *egfp*. The *amiA* gene was amplified from *C. jejuni* 11168H chromosomal DNA using primers amiAexpr_for and amiAexpr_rev, which added flanking *Kpn*I restriction sites. The *egfp* gene was derived from pEGFP by *Xba*I digestion, blunt ended and agarose gel extraction. The orientation of *amiA* in pRRBC-amiA was determined by *Cla*I and *Pst*I restriction digest (Figure 5.13 &

5.14 and Table 5.6). The orientation of *egfp* in pRRBC-*egfp* was determined by *Sty*I (Figure 5.16 to 5.18 and Table 5.7). The sequence of the pRRBC derivatives were verified by primer walking sequencing using internal primers amiA1, amiA2 & amiA3 for pRRBC-*amiA* and gfp1 & gfp2 for pRRBC-*egfp* whilst the flanking regions were detected using pBAD-up and ak237. The pRRBC derivative constructs were transformed into *C. jejuni* by electroporation and chloramphenicol resistant clones were selected. However, due to the size of the construct (9000 bp), the efficacy of transformation was low, thus few transformants were obtained.

The presence of pRRBC derivatives allelic replacement within *C. jejuni* was verified using 2 set of primers. After transformation of pRRBC into the *C. jejuni* genome, there were three possible products of allelic replacement into three possible RNA clusters (Figure 5.20). The presence of pRRBC was determined by PCR using primers pBAD-up and ak237, which amplifies the region in the *cam*^{r} cassette through the gene of interest to the pBAD region. The location of the rRNA gene cluster that the system was inserted into was determined by PCR using primers ak233/234/235 and pBADfor for adjacent regions to RNA cluster I, II & III respectively, amplifying the region across part of *16S* and the pBAD region. Potentially, recombination can occur with any three rRNA clusters, singular or multiple. Two clones of each were isolated for each construct (Figure 5.15 & Figure 5.18). *C. jejuni* pRRBC-amiA derivative clones were created and both clones had the system located in rRNA cluster I (Figure 5.15). *C. jejuni* pRRBC-egfp derivative clones were created and were found to be located in rRNA cluster II (Figure 5.16 & 5.19). Analysis of *C. jejuni* pRRBC-egfp derivatives also showed low yield PCR products for the other primer pairs. This is due to a possible heterologous population with insertion into 2 different rRNA clusters or the occasional recombination of the system to the other rRNA

clusters, neither have shown to effect cell growth or function (Karlyshev & Wren, 2005). The presence of the insertion into 2 different rRNA clusters could be determined by other methods as well, such as whole genome sequencing or pulse field gel electrophoresis.

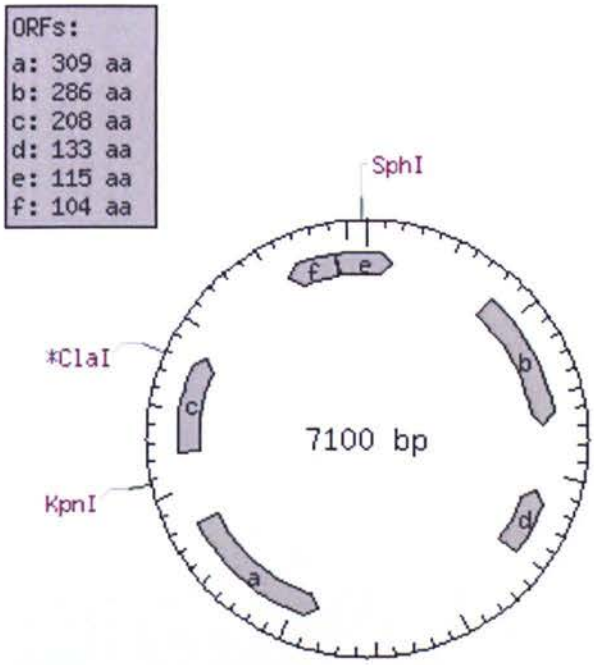

Figure 5.11. Diagram of pRRBC plasmid with individual *Kpn*I site for the insertion of gene of interest shown.

Verification restriction enzymes to determine the insertion of *cam*^{r} are shown. The location of the pBAD promoter and regulatory region is labelled a and *cam*^{r} is labelled as c. The blue star shows cleavage that can be affected by CpG methylation. Image produced by NEBCutter v2.

Table 5.5. Restriction sites and sizes of digested fragments of pRRBC with digestion *Sph*I and *Cla*I to verify the orientation of *cam*^{r} cassette and pRRB.

Correct orientation of *cam*^{r}		Reverse orientation of *cam*^{r}	
*Sph*I & *Cla*I site	Bands produced (bp)	*Sph*I & *Cla*I site	Bands produced (bp)
5783	1295	5245	1833
7078	5805	7078	5267

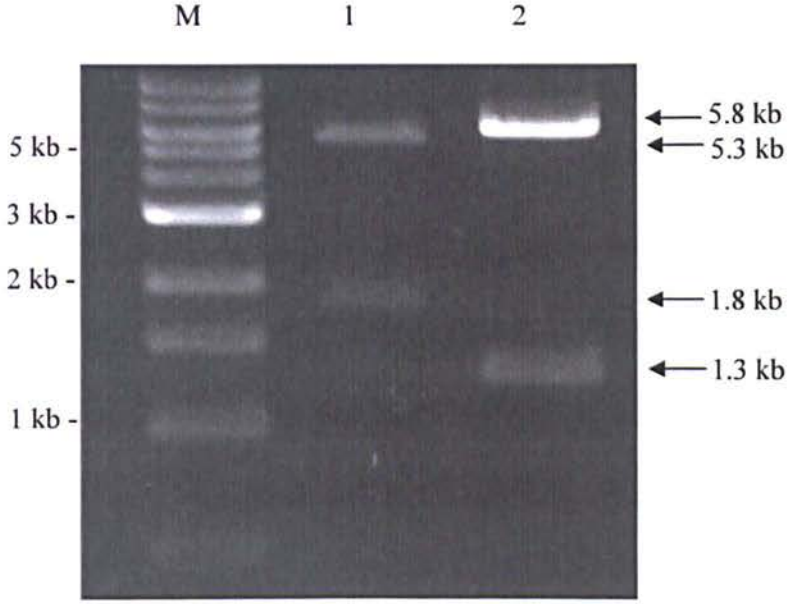

Figure 5.12. Restriction enzyme digest analysis of pRRBC plasmids.
The digested DNA fragments shown on 1% agarose gel to deduce the correct orientation of *kan*^{r} within the plasmid according to DNA fragment sizes. The approximate sizes of the bands were determined by comparison with the DNA ladder.
M- NEB 1 kb Ladder, 1-pRRBC reverse *cam*^{r} orientation, 2- pRRBC correct *cam*^{r} orientation.

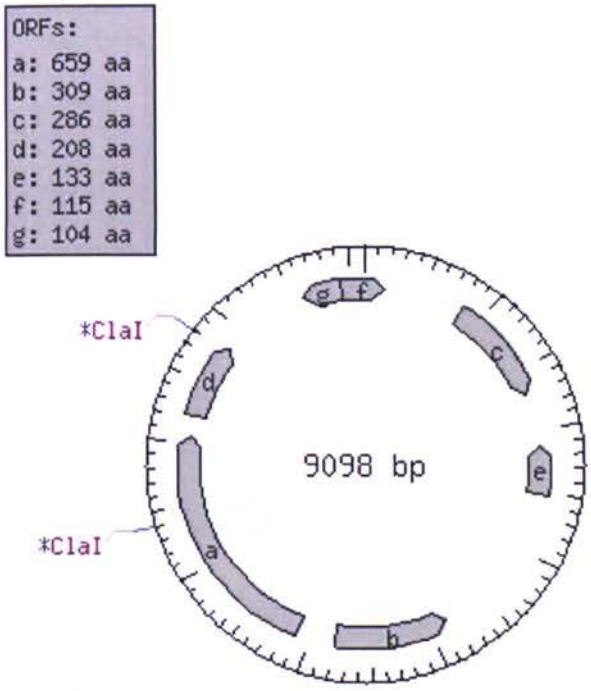

Figure 5.13. Diagram of pRRBC-amiA plasmid.
Verification restriction enzyme site *Cla*I to determine the presence of *amiA* are shown. The location of the pBAD promoter and regulatory region is labelled b, *cam*^{r} is labelled as d and *amiA* is labelled as a. The blue star shows cleavage that can be affected by CpG methylation. Image produced by NEBCutter v2.

Table 5.6. Restriction sites and sizes of digested fragments of pRRBC-amiA with digestion *Pst*I to verify the orientation of *amiA*.

Correct orientation of *amiA*		**Reverse orientation of *amiA***	
*Cla*I site	Bands produced (bp)	*Cla*I site	Bands produced (bp)
7781	1370	7781	1418
6411	7728	6363	7680

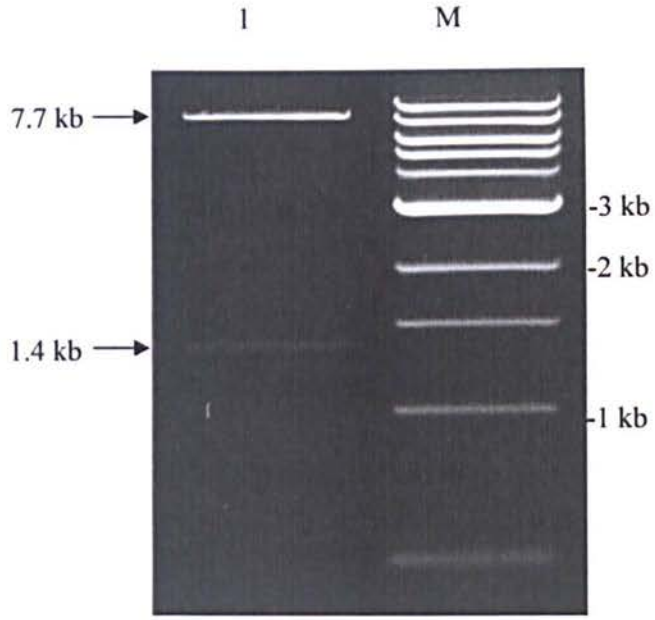

Figure 5.14. Restriction enzyme digest analysis of pRRBC-amiA plasmids.
The digested DNA fragments shown on 1% agarose gel show the correct orientation of *amiA* according to DNA fragment sizes after *Cla*I digestion. The approximate sizes of the bands were determined by comparison with the DNA ladder.
1-pRRBC-amiA digested with *Cla*I, M- NEB 1kb Ladder.

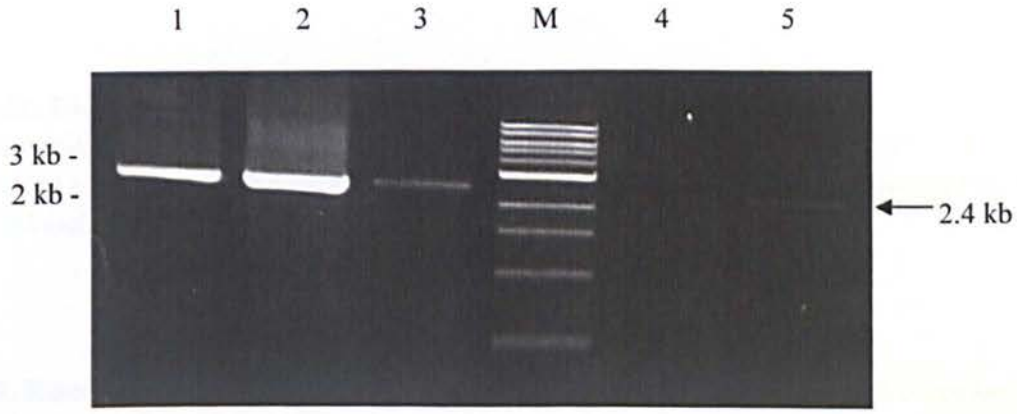

Figure 5.15. Verification of allelic replacement by PCR amplification of pRRBC-amiA using *C. jejuni* 11168H chromosomal DNA pRRBC-amiA derivatives.
The presence of pRRBC-amiA creates an amplicon length of 2.4 kb with pBAD-up/ak237 primers (left) and pBADfor/ak233 (right). There were no products from using primers pBADfor/ak234 & pBAD/ak235 (not shown). DNA with both primer sets, was run on a 1% agarose gel and the size of each amplicon was determined by comparison with the DNA ladder.
1- pRRBC-amiA plasmid , 2- pRRBC-amiA clone 1 with primers pBADup/ak237, 3- pRRBC-amiA clone 2 primers pBADup/ak237, M- NEB 1kb Ladder, 4- pRRBC-amiA clone 1 with primers pBADfor/ak233, 5 - pRRBC-amiA clone 2 with primers pBADfor/ak233.

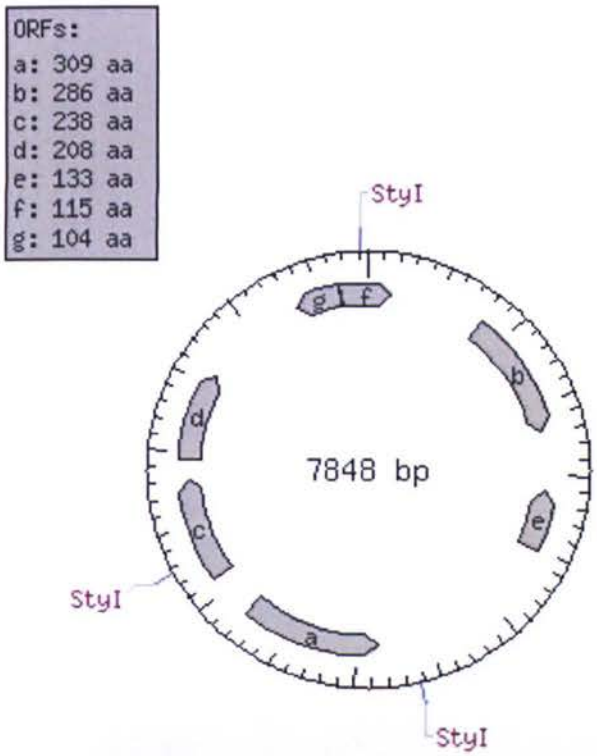

Figure 5.16. Diagram of pRRBC-egfp plasmid.
Verification restriction enzyme site *Sty*I to determine the orientation of *egfp* are shown. The location of the pBAD promoter and regulatory region is labelled a, *cam*^{r} cassette is labelled as d and *egfp* is labelled as c. Image produced by NEBCutter v2.

Table 5.7. Restriction sites and sizes of digested fragments of pRRBC-egfp with digestion *Sty*I to verify the orientation of *egfp*.

Correct orientation of *egfp*		**Reverse orientation of *egfp***	
*Sty*I site	Bands produced (bp)	*Sty*I site	Bands produced (bp)
7806	1635	7806	2006
5270	2535	5641	2209
3635	3635	3625	3635

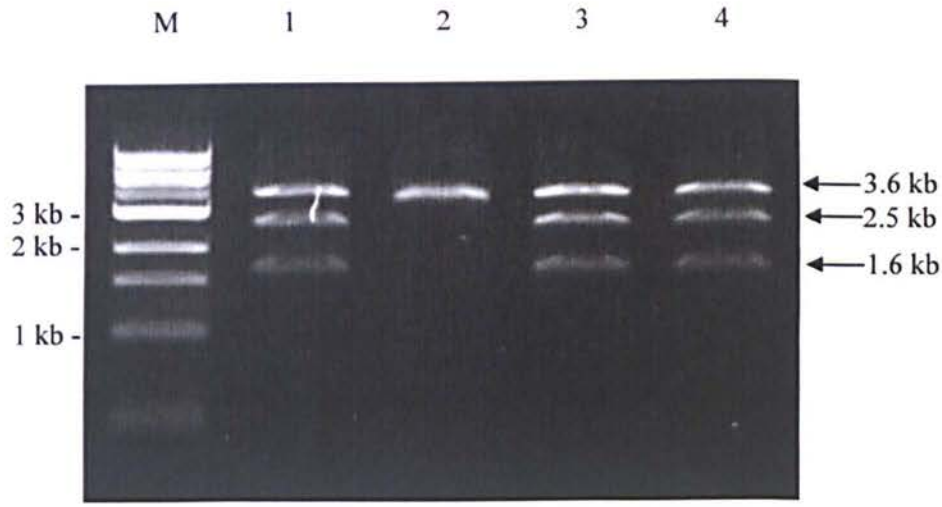

Figure 5.17. Restriction enzyme digest analysis of pRRBC-egfp plasmids.
The digested DNA fragments on 1% agarose gel show the correct orientation of *egfp* in pRRBC according to DNA fragment sizes after *Sty*I digestion. The approximate sizes of the bands were determined by comparison with the DNA ladder.
M- NEB 1kb Ladder, 1-pRRBC-egfp clone 1 digested with *Sty*I, 2- pRRBC digested with *Sty*I, 3-pRRBC-egfp clone 2 digested with *Sty*I, 4-pRRBC-egfp clone 3 digested with *Sty*I.

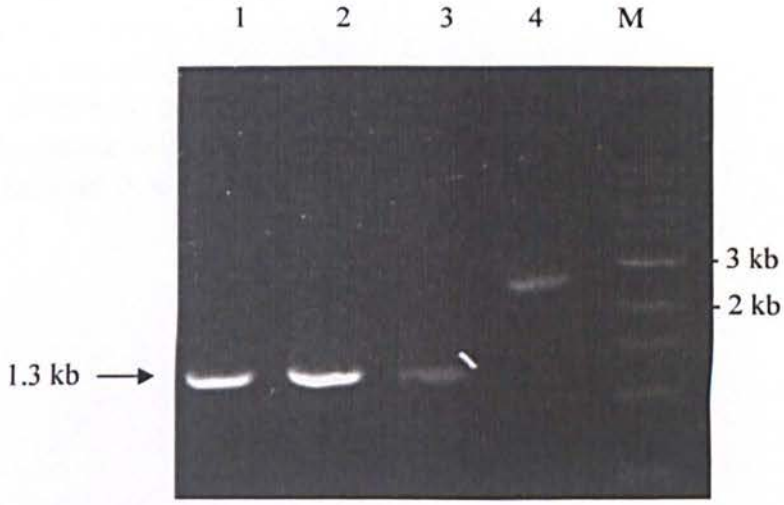

Figure 5.18. Verification of allelic replacement by PCR amplification of pRRBC-egfp using *C. jejuni* 11168H chromosomal DNA pRRBC-egfp derivatives pBAD-up/ak237.
PCR using the chromosomal DNA as template with pBADup/ak237 primer set, was run on a 1% agarose gel to and the size of product was determined by comparison with the DNA ladder. The presence of the system creates an amplicon length of 1.3 kb. pRRBC-amiA PCR sample with the same primer set was also run as a PCR control.1- pRRBC-egfp clone 1 with primers pBADup/ak237, 2- pRRBC-egfp clone 2 with primers pBADup/ak237, 3- pRRBC-egfp clone 3 with primers pBADup/ak237, 4- pRRBC-amiA clone 1 primers pBadup/ak237, M- NEB 1kb Ladder.

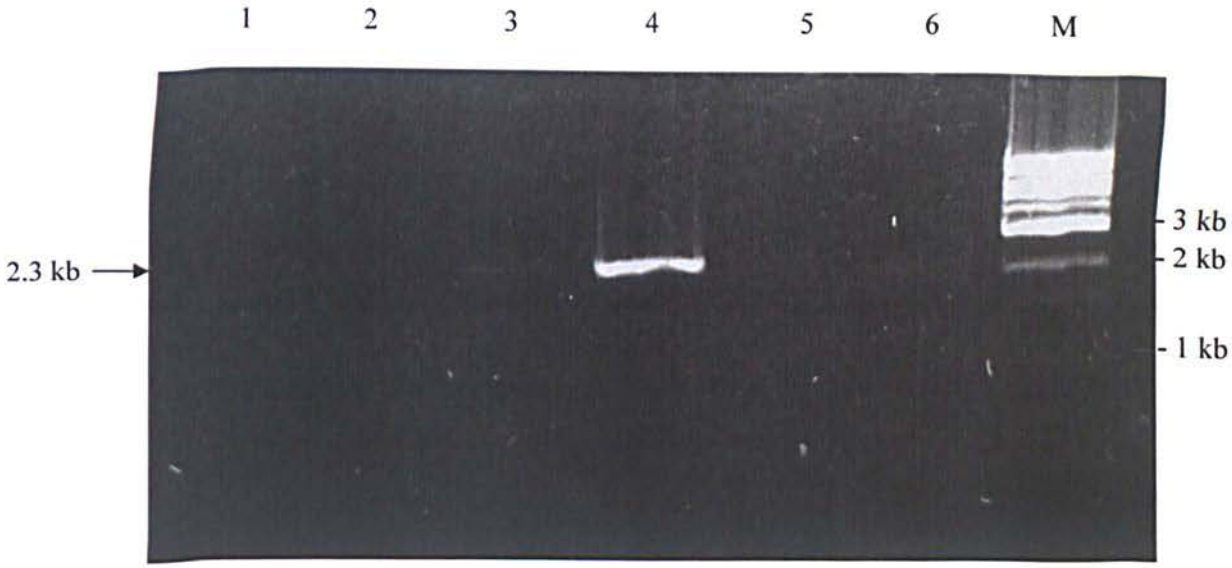

Figure 5.19. Verification of allelic replacement by PCR amplification of pRRBC-egfp using *C. jejuni* 11168H pRRBC-amiA derivatives chromosomal DNA with pBADfor/ak233/ak234/235. The presence of the system creates an amplicon length of 2.4 kb. PCR using the chromosomal DNA as template with the three primer sets, was run on a 1% agarose gel and the size of the product was determined by comparison with the DNA ladder.
1- pRRBC-egfp plasmid clone 1 with primer pBADfor/ak233, 2- pRRBC-egfp plasmid clone 2 with primer pBADfor/ak233, 3- pRRBC-egfp plasmid clone 1 with primer pBADfor/ak234, 4- pRRBC-egfp plasmid clone 2 with primer pBADfor/ak234, 5 - pRRBC-egfp plasmid clone 1 with primer pBADfor/ak235, 6 - pRRBC-egfp plasmid clone 2 with primer pBADfor/ak235, M- NEB 1 kb Ladder.

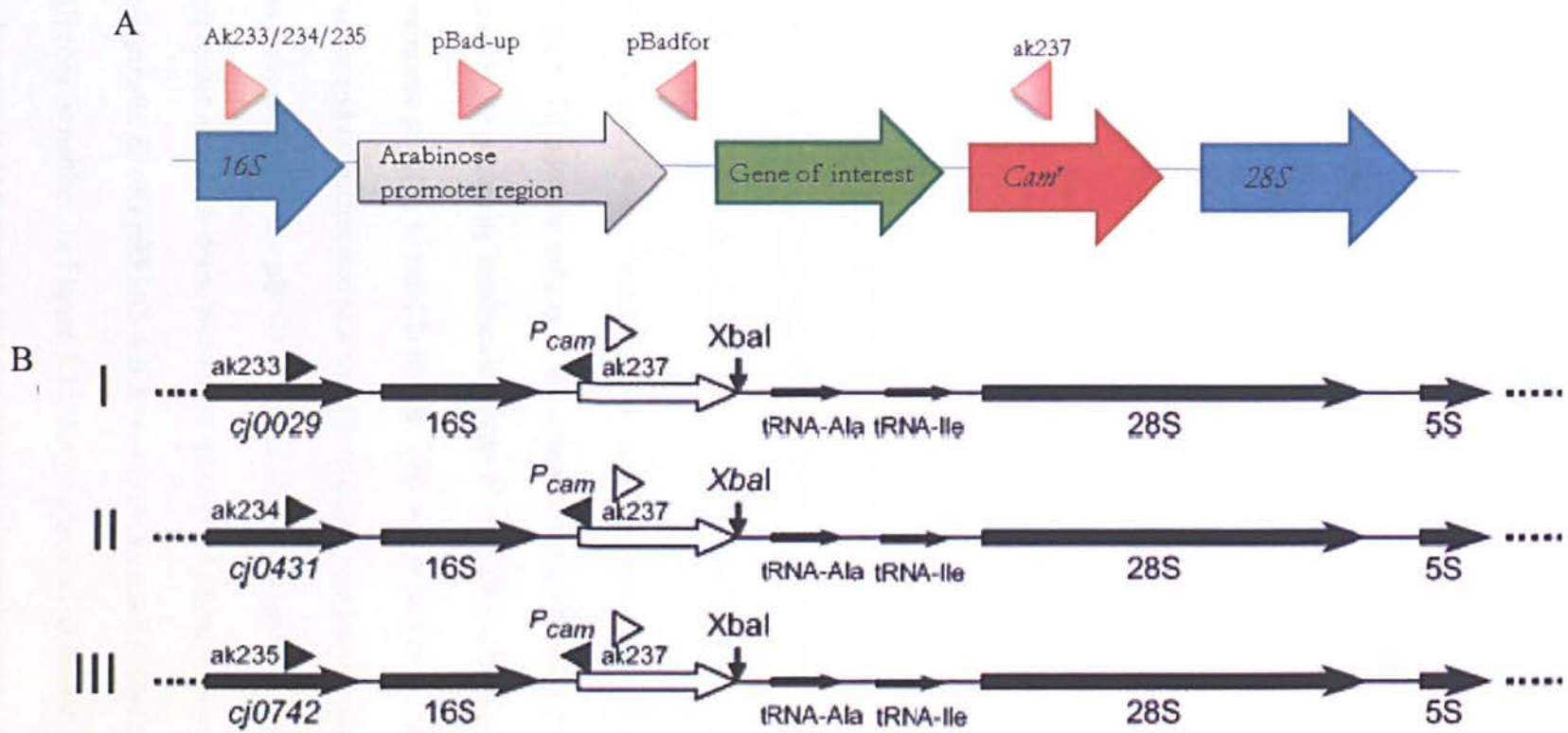

Figure 5.20. Diagrams of A) pRRBC with gene of interest with an rRNA cluster and B) the three possible products of allelic replacement from recombination of pRRC plasmid into the *C. jejuni* genome.

These are the same rRNA clusters that the pRRBC derivatives are located within after transformation. Both diagrams show the locations and the direction that the primers read from. Diagram B was taken from Karlyshev & Wren (2005).

5.3.4. Testing the inducible system with *egfp* derivative and phenotypic response of overexpression of *C. jejuni* AmiA in *E. coli*

Quantifying the expression of the pRRBC system was performed by using a visual quantifiable target gene, *egfp*. The *E. coli*-pRRBC-*egfp* system was used as a pilot system to ensure expression and that the level of expression was due to the presence of, and controlled by, variable concentrations of arabinose. As the concentration of arabinose present in the media increases, the amount of fluorescence from the colonies increased (Figures 5.21 to 5.24). The system was tightly controlled and not 'leaky' as no fluorescence was detected when the culture was not induced. No autofluorescence was detected, therefore fluorescence was only due to *egfp* expression. High level expression of *egfp* did not affect colony size or growth on solid media. This was verified in triplicate experiments with controls of the same culture grown concurrently with the induced culture for 1 day on the same media without arabinose present. Figures 5.21 to 5.24 showed the system worked within *E. coli* and the level of inducible expression could be regulated.

pRRBC-*amiA* was created to allow for a *Campylobacter* specific regulated expression system. To pilot the effects of the expression system, overexpression studies of *C. jejuni amiA* were primarily conducted within *E. coli.* Overexpression of the *amiA* was induced by arabinose at 0.1% within LB media. This was tested on solid LB media and in liquid LB media and no difference was shown. Glucose was used at the same concentration as it acts as a suppressor to the pBAD promoter and to compare with the culture with no inducer and repressor added, to demonstrate the robustness of the system. To show any visible effects on growth, *E. coli* pRRBC-AmiA was grown on solid media containing either arabinose, glucose or neither. In Figure 5.25, the presence of arabinose within the media demonstrated a decrease in colony size and the amount of growth when compared with a culture on

media with no arabinose added. The rate of growth was shown to decrease in the liquid cultures with arabinose compared to non-induced culture and repressed (with glucose at the same concentration) cultures. The optical density readings of induced cultures showed an immediate retardation in growth, whilst the control and repressed cultures continued to grow at a normal rate (Figure 5.26) (unpaired Student's *t*-test; 7.1207, df = 10, $P = 0.00$). As can be seen in Figure 5.26 the presence of glucose has no effect on the growth of the culture and grows at a similar rate as the non-induced culture. The CFU readings of all the cultures were measured at each time point that was measured for growth by optical density. As shown in Figure 5.27 the overexpression of AmiA produced 1 log fold decrease of CFU (unpaired Student's *t*-test; 3.2415, df = 22, $P = 0.00$) . The control and repressed culture exhibited no significant difference in CFU or retardation in growth, which ensured pRRBC-AmiA was a robust system and does not have a 'leaky' promoter.

To complement the results from the decrease in CFU concurrently with overexpression of AmiA, LIVE/DEAD viability stains were conducted. LIVE/DEAD staining used SYTO9 and propidium iodide (PI) for differential staining between fully intact cells and cells with damaged membranes. SYTO9 can bind to both types of cells whilst PI is only able to bind to DNA, which would only be available if the membrane was 'leaky'. Figure 5.28 demonstrates that as the expression of AmiA increased, more cells were stained with PI than just STYO9, showing the membrane integrity was compromised (unpaired Student's *t*-test; 14.2045, df = 10, $P = 0.00$).

The overexpression of *C. jejuni* AmiA led to no change in morphology (Figure 5.29) and all concentrations of arabinose tested all showed classical rod morphology in the *E. coli*. However, it was demonstrated from the pRRBC-amiA *E. coli* derivatives that the induction

of additional *C. jejuni* AmiA led to a decrease in viability, membrane integrity, CFU and colony size.

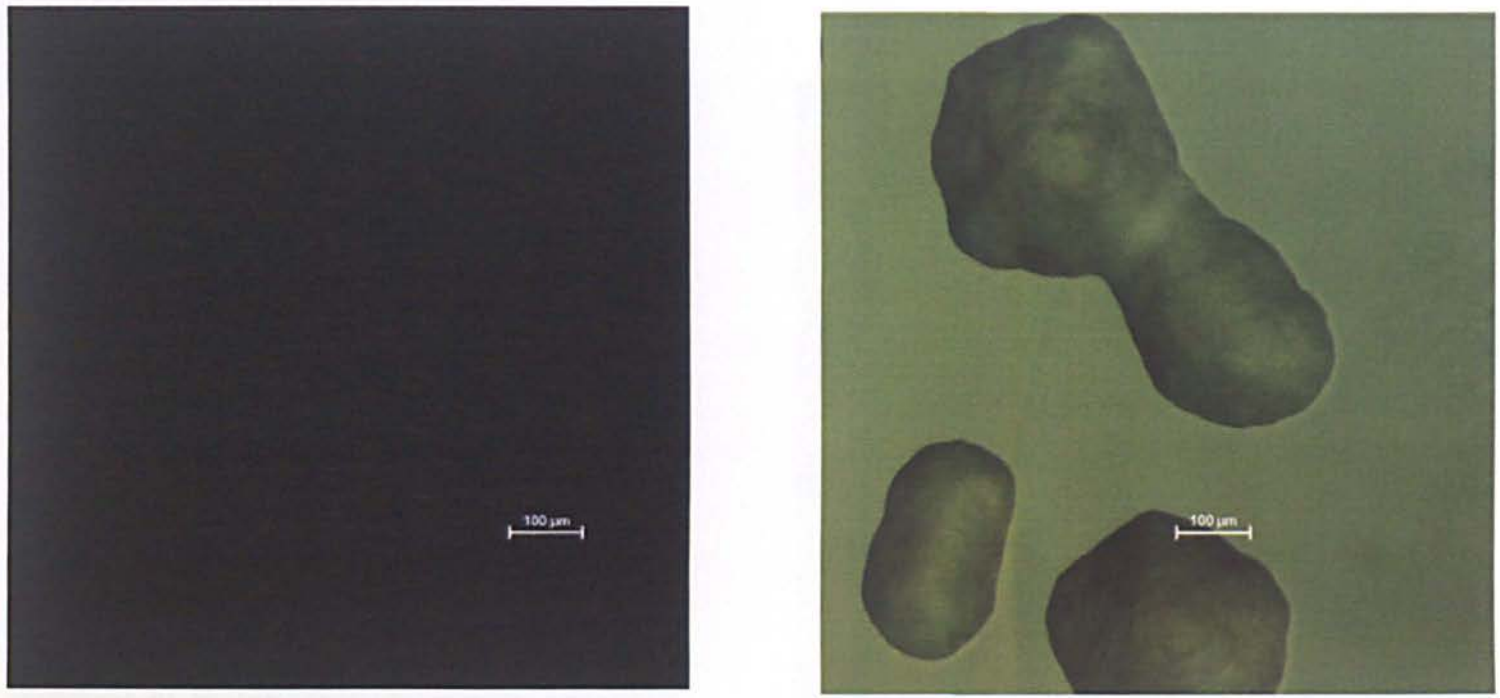

Figure 5.21. Effect of the no arabinose present within LB media on *E. coli*-pRRBC-egfp derivative.
The fluorescence and brightfield images are of bacterial colonies with no arabinose present within the media. One day cultures grown at 37°C are shown. The white scale bar represent 100µm.

Figure 5.22. Effect of 0.002% arabinose present within LB media on *E. coli*-pRRBC-egfp derivative.
The fluorescence and brightfield images are of bacterial colonies with 0.002% arabinose present within the media. One day cultures grown at 37°C are shown. The white scale bar represent 100µm.

Figure 5.23. Effect of 0.02% arabinose present within LB media on *E. coli*-pRRBC-egfp derivative.
The fluorescence and brightfield images are of bacterial colonies with 0.02% arabinose present within the media. One day cultures grown at 37°C are shown. The white scale bar represent 100µm.

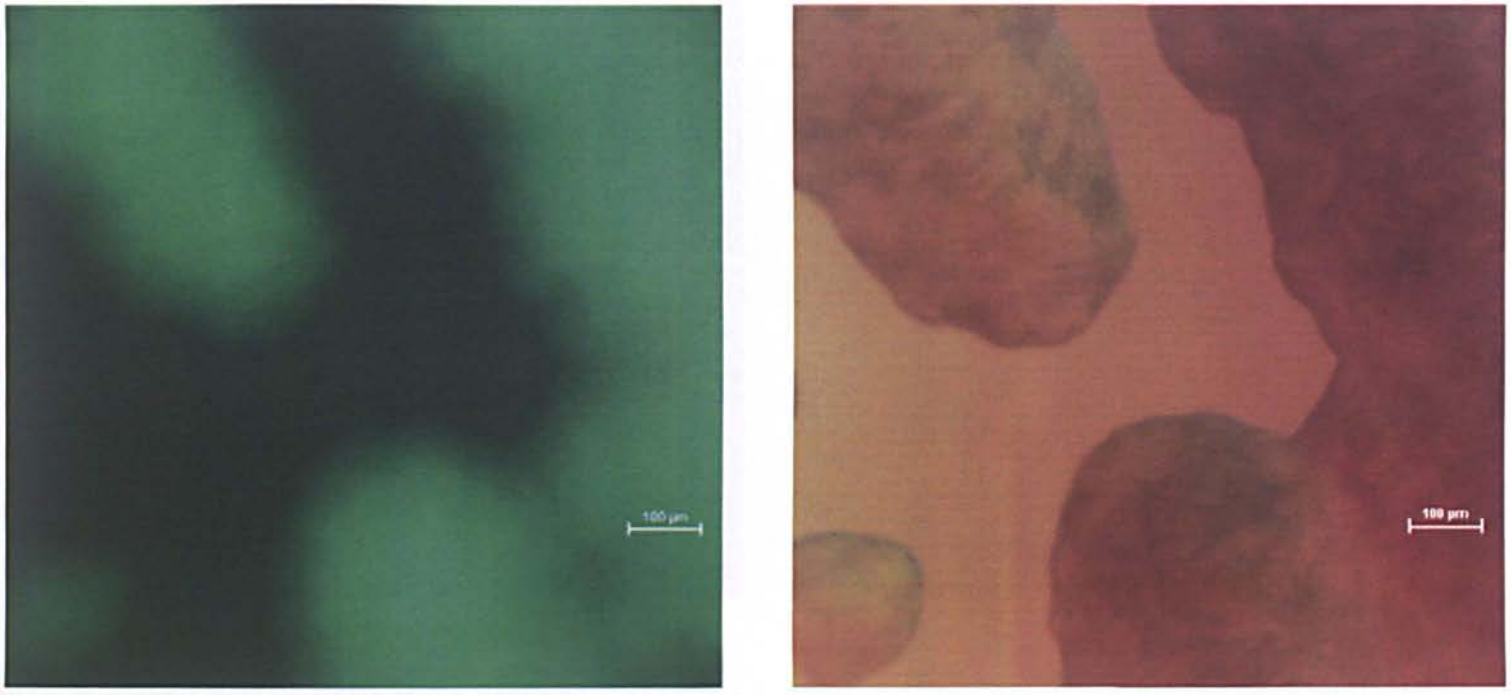

Figure 5.24. Effect of 0.2% arabinose present within LB media on *E. coli*-pRRBC-egfp derivative.
The fluorescence and brightfield images are of bacterial colonies with 0.2% arabinose present within the media. One day cultures grown at 37°C are shown. The white scale bar represent 100µm.

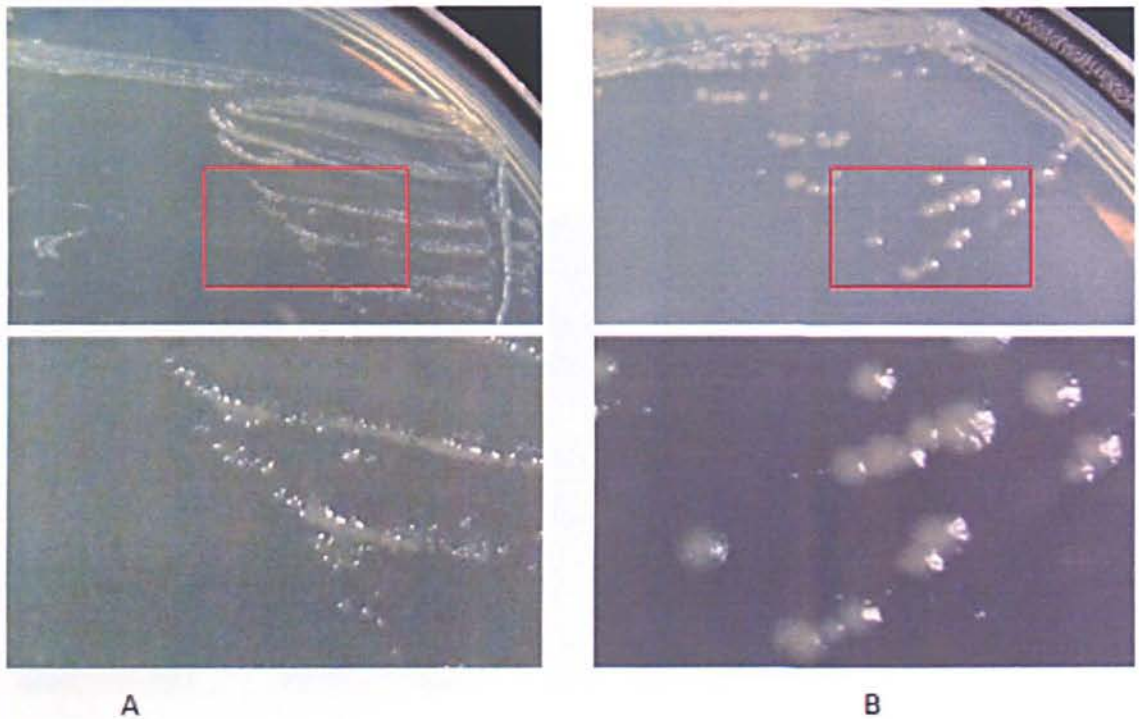

Figure 5.25. Effect of arabinose on growth of *E. coli*-pRRBC-amiA on LB agar plates supplemented with chloramphenicol.
One day cultures grown at 37°C are shown.
A) *E. coli*-pRRBC-amiA colonies grown on media containing arabinose at 0.2%
B) *E. coli*-pRRBC-amiA colonies grown on media with no arabinose.
The images in the lower row are amplified regions highlighted in the red boxes in the higher row.

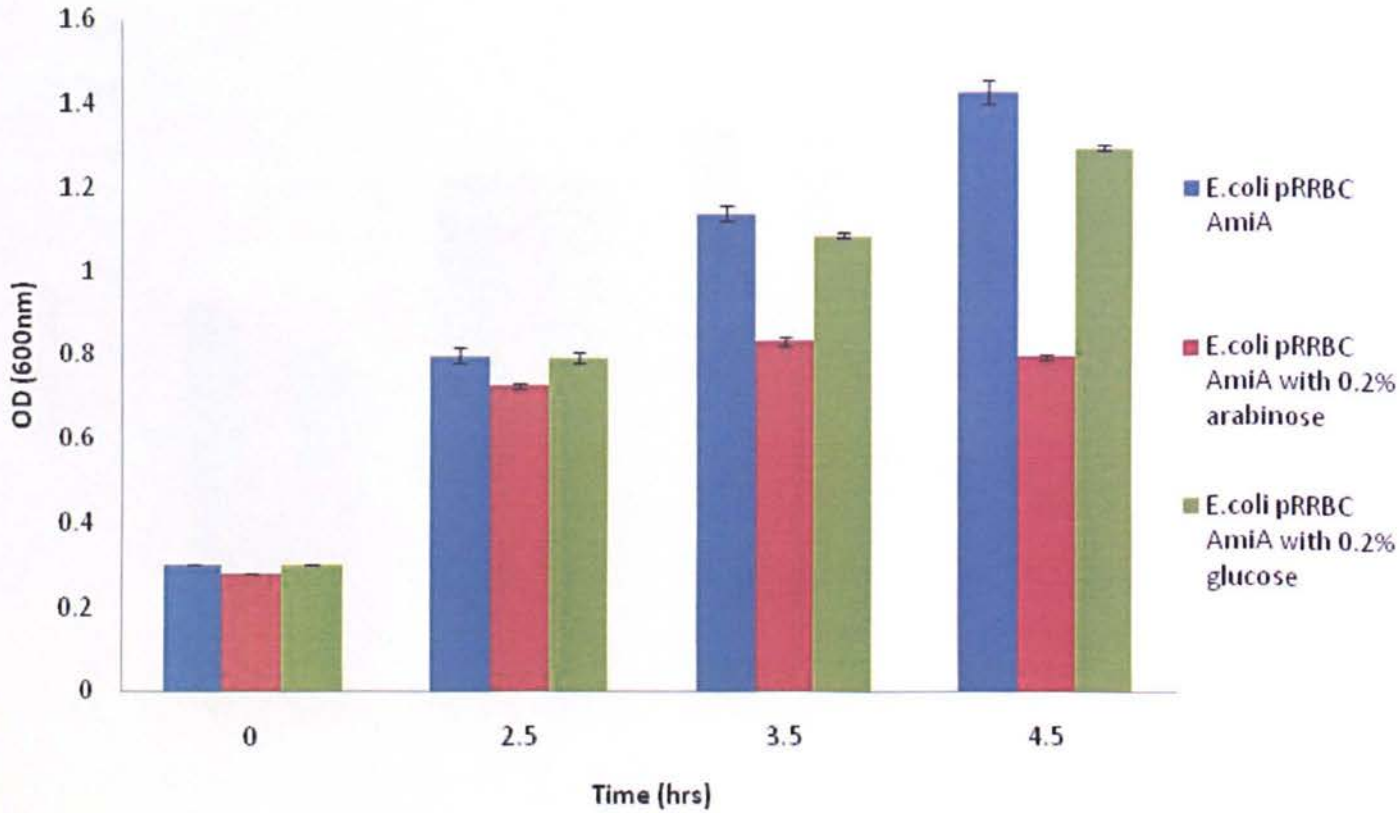

Figure 5.26. The effect of induction of AmiA on the growth of *E. coli*/pRRBC-*amiA* over time.
Each time point was measured in triplicates. The induced/repressed liquid cultures had arabinose or glucose added at 2.5hrs respectively. These data are the mean of an individual experiment, which was done in triplicate with similar results each time. The error bars represent SD (N= 3).

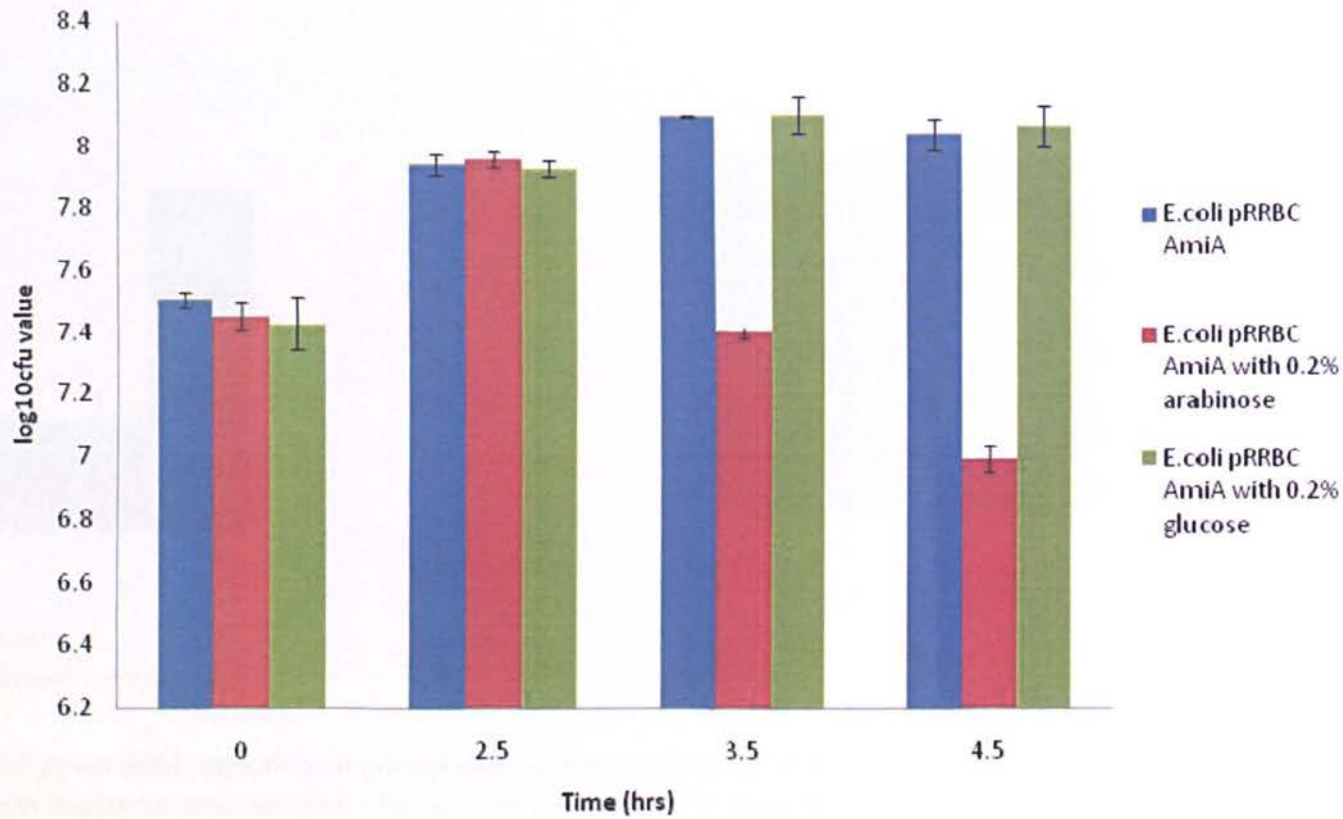

Figure 5.27. The effect of induction of *amiA* on the CFU counts and viability of *E. coli*/pRRBC-*amiA*.
The induced/repressed liquid cultures had arabinose or glucose added at 2.5hrs. These data are the mean of an individual experiment, which was done in triplicate with similar results each time. The error bars represent SD (N= 3).

A

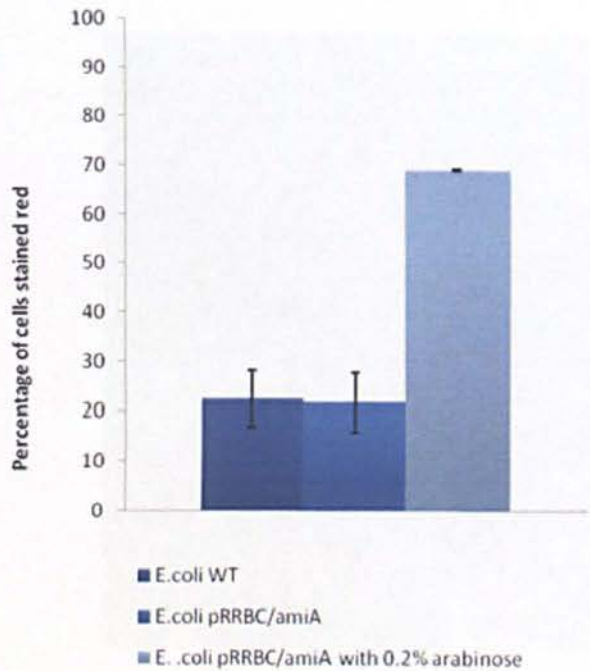

B

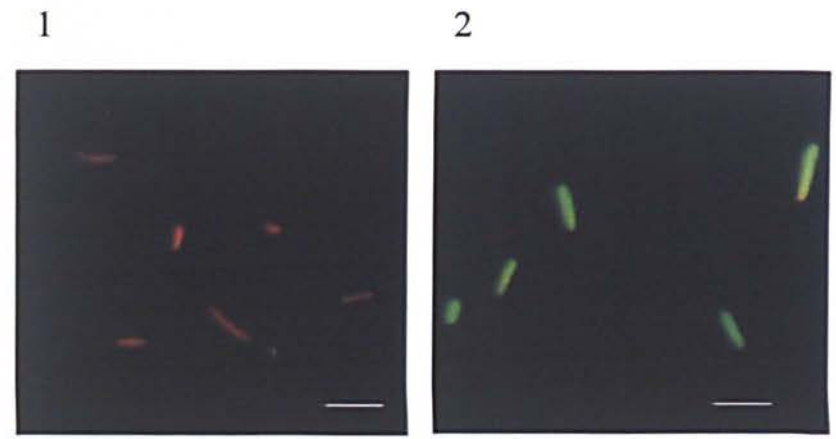

Figure 5.28. Effect of *C. jejuni amiA* induction on growth and membrane integrity of *E. coli* using BacLight LIVE/DEAD staining.
The graph and the images display the same samples. PI stains cells red and SYTO9 stains cells green.
A) the percentage of red cells in *E. coli*/pRRBC-*amiA* culture before and after induction compared with *E. coli* WT without the construct. Within each individual measurement, 50 cells were counted. These data are the mean of an individual experiment, which was done in replicate with similar results each time. The error bars represent SD (N= 3).
B) BacLight LIVE/Dead staining of *E. coli* pRRBC/*amiA* cells visualised using a confocal fluorescence microscope. 1- arabinose present at 0.2%, 2 – no arabinose. Scale bar represented in image corresponds to 1μm.

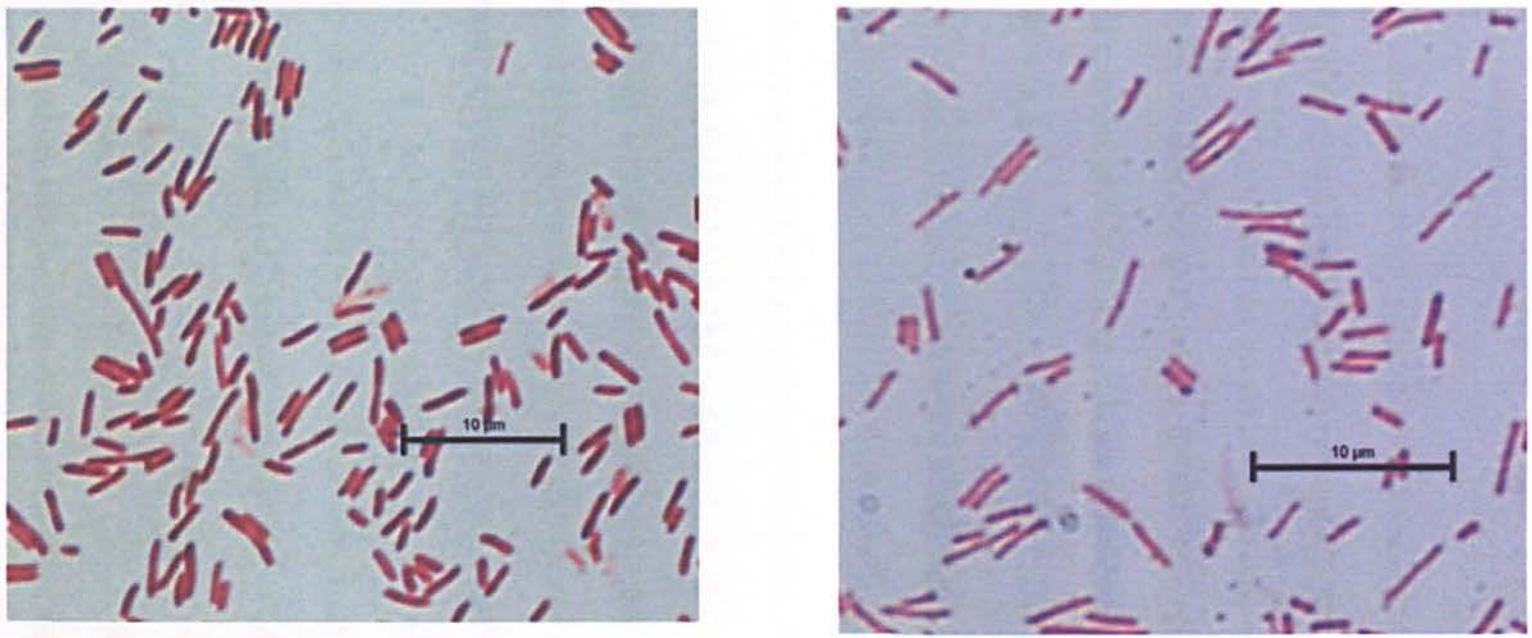

Figure 5.29. Effect of *C. jejuni amiA* induction on *E. coli* cell morphology.
One day cultures grown at 37°C are shown. Samples were prepared and visualised as described in section 2.1.2. The black bar in the bottom right hand corner of each image is representative of 10µm. The samples were all visualised under x1000 magnification and images were all taken with a Nikon 80i.

5.3.5. pRRBC in *C. jejuni*: troubleshooting and improvements

After integration of the pRRBC derivative constructs into *C. jejuni*, expression was tested. However, regardless of the concentrations of arabinose present in the media the systems would not activate in *C. jejuni*.

The transformation rates of pRRBC into *C. jejuni* were very low (no more than 4 colonies isolated in total) and it was hypothesized that this was possibly due to the large size of the plasmid (~7000bp without the presence of *egfp* or *amiA*). To increase the rates of successful insertion into the genome, pRRBC was reduced in size, eliminating redundant regions to create pRRBCD (Figure 5.30). The *egfp* gene was inserted into pRRBCD to pilot the system.

To remove redundant areas, pRRBC-*egfp* was digested with *Not*I producing two DNA fragments of 3 kb and 4.8 kb (Figure 5.31). Both products were blunt ended and each band was isolated separately using agarose gel extraction. The 3 kb band was subsequently digested with *Eco53*KI and *Ahd*I to produce two DNA fragments of 1.3 kb and 1.6 kb (Figure 5.31). The 1.6 kb band contains the redundant region of pRRBC-*egfp*. The 1.3 kb region was kept as it contained the origin of replication. This 1.3 kb fragment was subsequently blunt ended and isolated via agarose gel extraction and was ligated with the previously isolated 4.8 kb DNA fragment. The new reduced construct was verified by *Eco*RV digestion, which if correctly ligated would produce DNA fragments of the sizes 0.9 kb and 6.9kb (Figure 5.32) and the orientation was determined by primer walking sequencing of clones 1 and 3. This construct had the same efficiency to produce fluorescence upon induction and robustness with no 'leaky' promoters or auto-fluorescence in *E. coli* as the previous construct. However induction with the reduced pRRBC derivative showed no fluorescence like *C. jejuni* pRRBC-*egfp* derivative.

Although pRRBC-*egfp* and pRRBC-*amiA* were successfully inserted in the *C. jejuni* genome and the presence was verified by PCR, no phenotypic response was ever observed after induction. In particular, there was no fluorescence with cultures on both solid media and in liquid culture.

The lack of fluorescence with the pRRBC-*egfp* and pRRBCD-*egfp* derivatives was later thought to be due to the lack of sugar transporters within *C. jejuni*. The metabolism of *C. jejuni* is mainly dependent on amino acids such as aspartate, glutamate, proline and serine, unlike *E. coli* that is based on sugars (Guccione *et al.*, 2008; Stahl *et al.*, 2012). To allow the system to be induced, an *E. coli* sugar transporter gene was added to the reduced derivative. Previous reports on expression studies using the araBAD promoter in *E. coli* showed regulated expression by using a different concentration, it also demonstrated an 'all or nothing' or autocatalytic induction with individual cells within a culture. The presence of a mutant *lacY* (*lacY*A177C), a lactose permease gene from *E. coli* would allow diffusion of arabinose and for homogenous regulation of the araBAD promoter (Morgan-Kiss *et al.*, 2002).

The reduced pRRBCD-*egfp* derivative enabled for the insertion of *lacY*A117C into the system using a singular native *Sal*I site (Figure 5.30). *lacY* was amplified from *E. coli* K12 chromosomal DNA using primers lacY_for and lacY_rev by PCR. The *lacY* WT PCR product had *Sal*I flanking restriction sites introduced by the primers and was then inserted into the pGEM-T vector. Figure 5.34 shows the presence of the *lacY* gene in the vector determined using *Sal*I, which would cut out just the *lacY* gene. The vector was then used as a template for PCR with another set of primers, lacYA177C_for and lacYA177C_rev to introduce the point mutation, converting GCA to TGT at a reduced annealing temperature with High Fidelity DNA polymerase containing proof reading enzymes to prevent other

unintended point mutations. The new set of primers start at the point mutation although the primers have been designed with an altered sequence to change the base to create the amino acid change. The new PCR amplicon of pGEM-T-*lacY*A177C was linear and required phosphorylation to enable self-ligation to recreate the circular plasmid. The point mutation was confirmed by restriction enzyme digestion and primer walking sequencing. The amino acid mutation to convert alanine to cysteine created another *Bsm*AI restriction site for a specific restriction enzyme profile for clones with the point mutation (Figure 5.33 & 5.34 and Table 5.8). *lacY*A177C sequence was verified by primer walking sequencing using lacYA177C_for and lacYA177C_rev primers.

The singular native *Sal*I site in pRRBCD-*egfp* was used for the insertion of *lacY*A177C to create pRRBCD-*egfp*-*lacY*A177C. Due to the inability for directional insertion by using blunt ended *lacY*A177C, there was a possibility for reverse orientation of *lacY*A177C after ligation. This was verified by restriction digest using *Nde*I (Figure 5.35 & 5.36 and Table 5.9).

However, the insertion did not occur and no transformants were made with this construct. Within *E. coli,* pRRBCD-*egfp*-*lacY*A177C functioned in the same manner as pRRBC-*egfp* and pRRBCD-*egfp* upon induction, with still no additional effects on growth. The lack of expression of pRRBC and derivatives in *C. jejuni* could be due to faults within the flanking regions that were not visible by restriction digestion. Several restriction enzymes were used to determine if large portions of the rRNA flanking sequences were missing during construction of the mutant, however, to no avail.

The final attempt of enabling induction of the pRRBC system within *C. jejuni* was with an additional pRR based construct to occupy one other rRNA cluster, which contained

*lacY*A177C and an additional antibiotic selective marker to determine insertion of the new construct within *C. jejuni* pRRBC derivatives, that are already resistant to chloramphenicol.

pRRT is a plasmid derived from pRR containing the flanking regions of the *Campylobacter* rRNA gene clusters, with *tet*^{r} cassette present as the selective marker. pRRT is digested with *Xba*I, blunt ended and dephosphorylated using Antarctic phosphatase. The linear pRRT was ligated with blunt ended *lacY*A177C DNA fragment from pGEM-T-*lacY*A177C to form pRRT-*lacY*A177C. Verification of the insert and determination of the orientation of the insert was conducted by restriction enzyme analysis using *Nde*I (Figure 5.37 & 5.38 and Table 5.10). Two tetracycline and chloramphenicol resistance clones were isolated and exhibited the correct restriction digestion profile, however, only clone 1 was shown to be correct via primer walking sequencing using lacYA177C_for and lacYA177C_rev primers. The other clones were not correct due to a point mutation located in other parts of the sequence, which would alter the protein sequence as well. The pRRT-*lacY*A177C plasmid was purified and used for transformation into *C. jejuni* pRRBC-*amiA* derivative via electroporation. Six tetracycline and chloramphenicol resistance clones were isolated but were unable to be tested due to a lack of time.

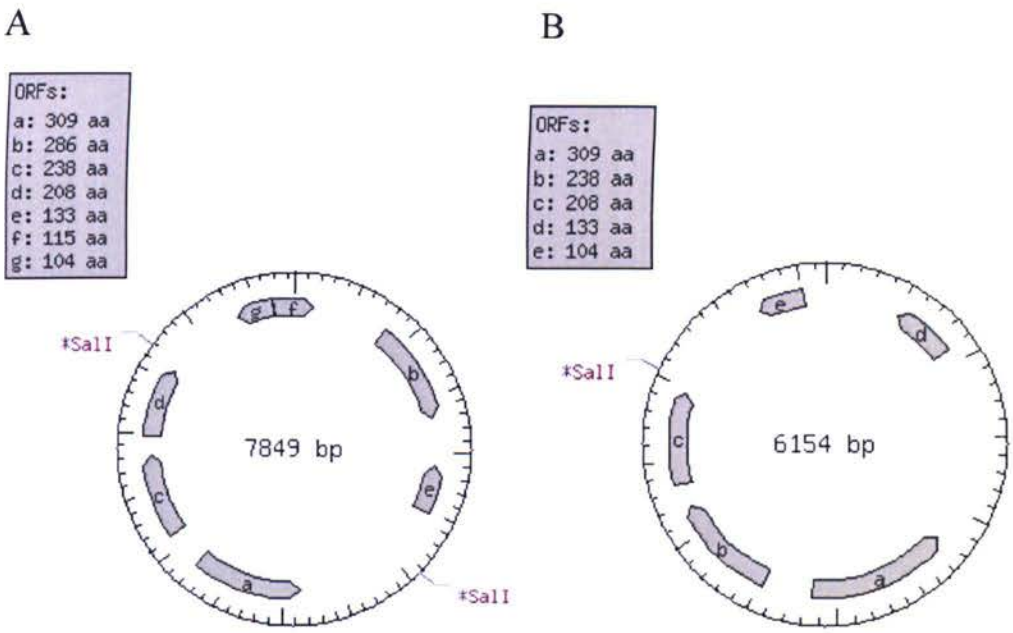

Figure 5.30. Diagram showing the difference between A- pRRBC-*egfp* and B- pRRBCD-*egfp*. The size of the plasmid was reduced by approximately 1.6 kb whilst maintaining all the genes and the origin of replication. pRRBC-*egfp* had two *Sal*I sites, which was reduced to a single site. The *Sal*I site was used for the insertion of *lacY*A117C. The star shows cleavage that could be affected by CpG methylation. Image produced by NEBCutter v2.

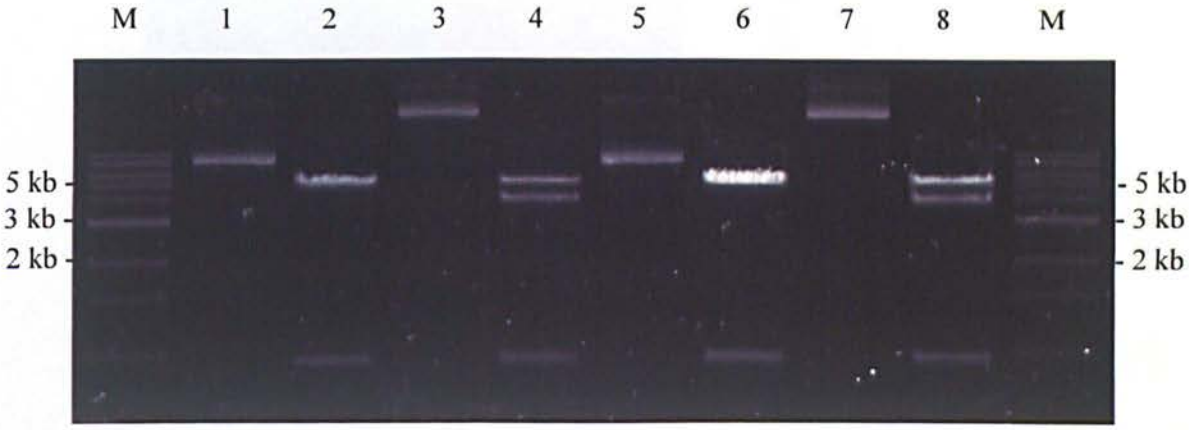

Figure 5.32. Verification of pRRBCD-*egfp* ligation using restriction enzyme digest analysis. pRRBCD-*egfp* after *Eco*RV digestion was run on a 1% agarose gel. pRRBCD-*egfp* clones 1 and 3 exhibited the correct restriction digestion profile. The approximate sizes of the bands were determined by comparison with the DNA ladder.
M- NEB 1 kb Ladder, 1- pRRBCD-*egfp* clone 1 uncut, 2- pRRBCD-*egfp* clone 1 cut with *EcoRV*, 3- pRRBCD-*egfp* clone 2 uncut, 4- pRRBCD-*egfp* clone 2 cut with *EcoRV*, 5- pRRBCD-*egfp* clone 3 uncut, 6- pRRBCD-*egfp* clone 3 cut with *Eco*RV, 7- pRRBCD-*egfp* clone 4 uncut, 8- pRRBCD-*egfp* clone 3 cut with *Eco*RV, M- NEB 1 kb Ladder.

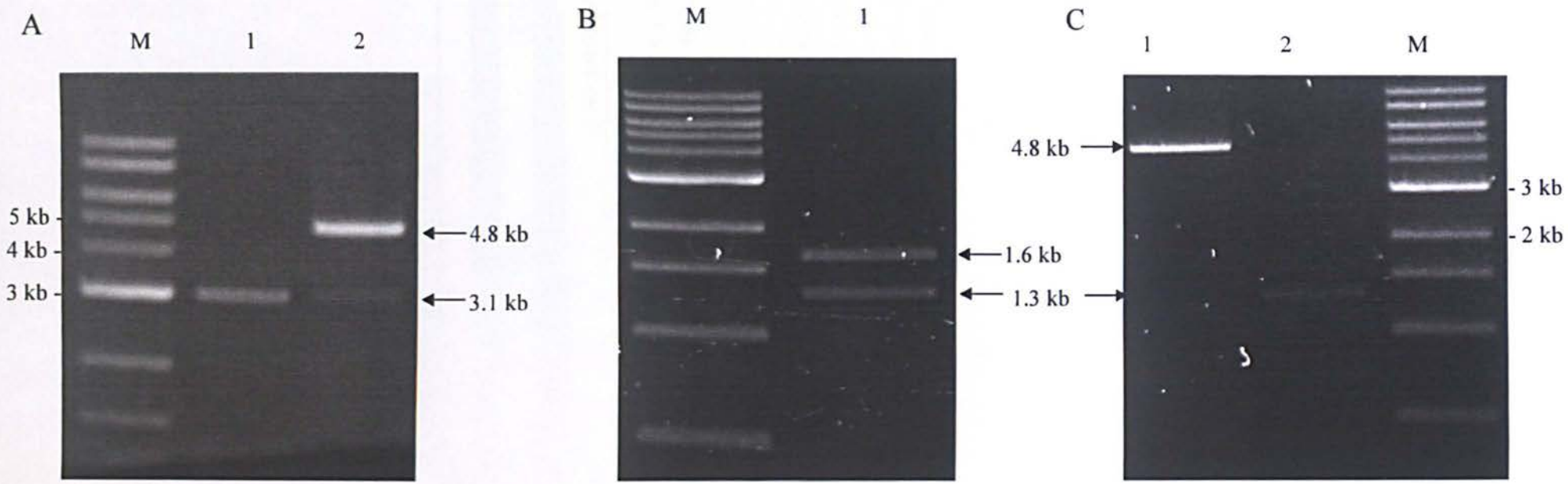

Figure 5.31. Agarose gel images showing the DNA fragments of pRRBC-*egfp* after various restriction enzyme digestions for the construction of pRRBCD-*egfp*.

The approximate sizes of the bands were determined by comparison with the DNA ladder.

A) M- NEB 1 kb Ladder, 1- 3.1 kb pRRBC-*egfp* DNA fragment after *Not*I digestion and agarose gel extraction, 2- 4.8 kb and 3.1 kb pRRBC-*egfp* DNA fragments after *Not*I digestion.

B) M- NEB 1 kb Ladder, 1- 3.1 kb DNA fragment after *Eco53*KI and *Ahd*I digestion producing two large fragments of 1.6 kb and 1.3 kb.

C) 1- 4.8 kb pRRBC-*egfp* DNA fragment after agarose gel extraction, 2- 1.3 kb pRRBC-*egfp* DNA fragment after agarose gel extraction, M- NEB 1 kb Ladder.

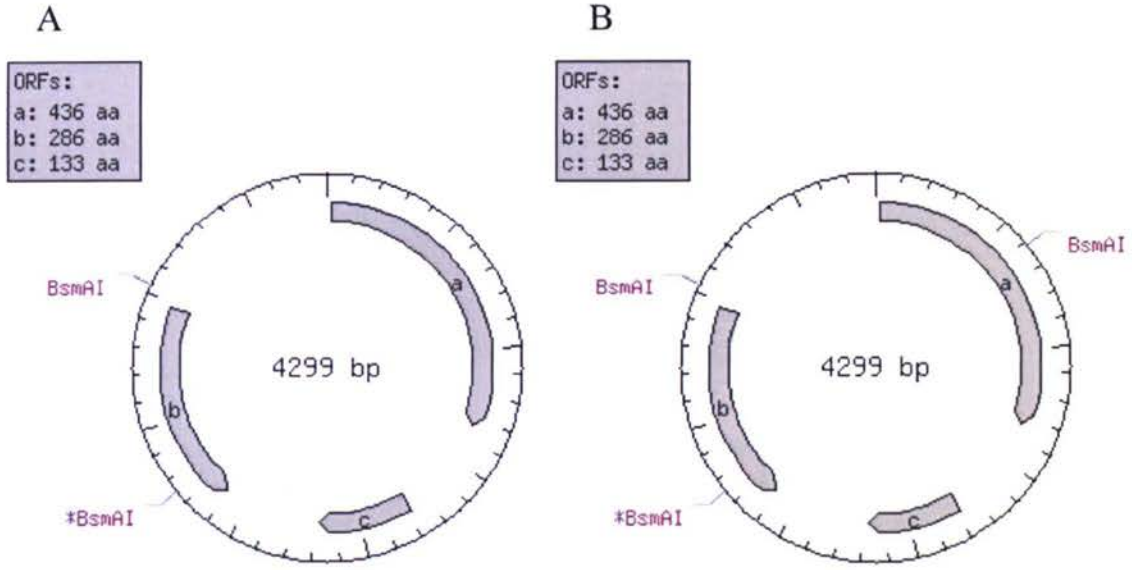

Figure 5.33. Diagram showing the difference the base point mutation has on the presence of *Bsm*AI restriction sites of A) pGEM-T-*lacY* and B) pGEM-T-l*acY*A177C plasmids.
lacY is labelled as a and the newly acquired restriction site from the point mutation is located in ORF labelled a. The stars show cleavage sites that could be affected by CpG methylation. Image produced by NEBCutter v2.

Table 5.8. Restriction sites and sizes of digested fragments of pGEM-T-*lacY* and p-GEM-T-l*acY*A177C with digestion *Bsm*AI to verify the point mutation.

pGEM-T-*lacY*		pGEM-T-*lacY*A177C	
*Bsm*AI site	Bands produced (b)	*Bsm*AI site	Bands produced (b)
2752	776	615	776
3528	3523	2752	1386
		3528	2137

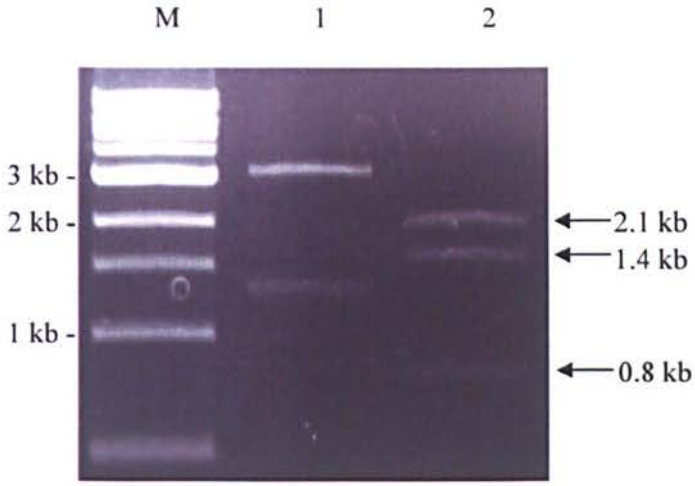

Figure 5.34. Restriction enzyme digest analysis showing the presence of the *lacY* in pGEM-T with *Sal*I, and the presence of the point mutation in pGEM-T-*lacY*A177C with *Bsm*AI.
The digested DNA fragments are shown on 1% agarose gel and the approximate sizes of the bands were determined by comparison with the DNA ladder.
M- NEB 1kb Ladder, 1- pGEM-T-*lacY*A177C digested with *Sal*I, 2- pGEM-T-*lacY*A177C digested with *Bsm*AI.

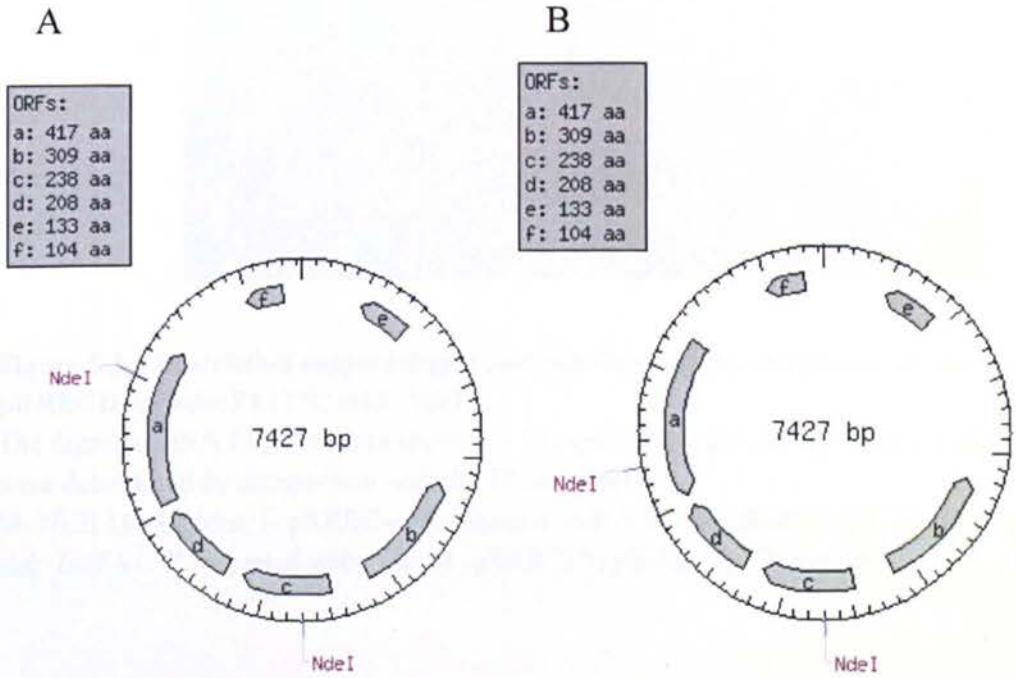

Figure 5.35. Diagram of pRRBCD-*egfp*-*lacY*A177C constructs with the verification restriction enzyme sites *Nde*I showing the A) correct and B) reverse orientation of *lacY*A177C.
Verification restriction sites *Nde*I are shown on image. The location of the pBAD promoter and regulatory region are labelled b, *cam*^{r} cassette is labelled as d, *lacY*A177C is labelled as a and *egfp* is labelled as c. Image produced by NEBCutter v2.

Table 5.9. Restriction sites and sizes of digested pRRBCD-egfp-lacYA177C after digestion with *Nde*I to verify the orientation of *lacY*A177C insert.

pRRBCD-*egfp-lacY*A177C in correct orientation		**pRRBCD-*egfp-lacY*A177C in reverse orientation**	
NdeI site	Bands produced (bp)	*NdeI* site	Bands produced (bp)
3699	2317	3699	1626
6016	5110	5325	5801

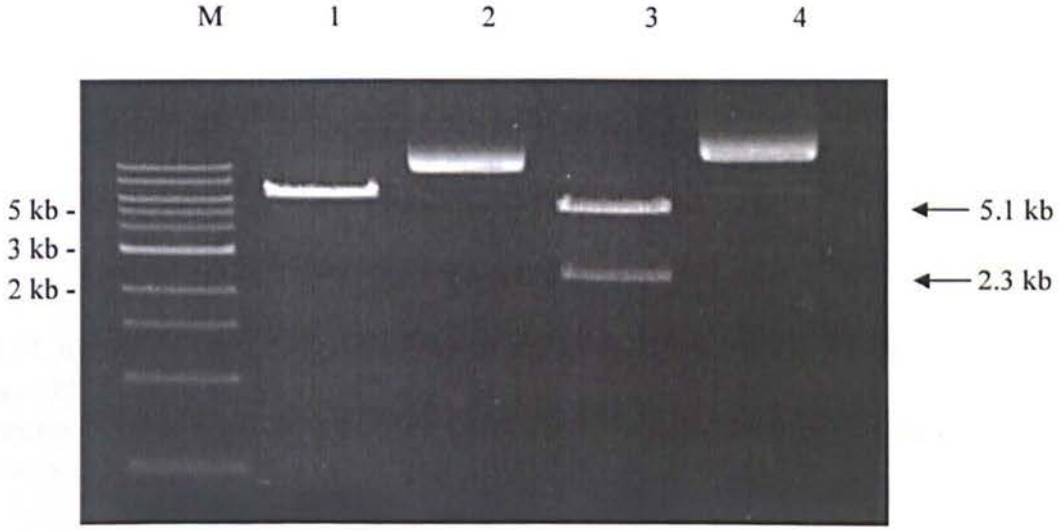

Figure 5.36. Restriction enzyme digest analysis showing the orientation of the *lacY* in pRRBCD-*egfp-lacY*A177C with *Nde*I.

The digested DNA fragments are shown on 1% agarose gel and the approximate sizes of the bands were determined by comparison with the DNA ladder.

M- NEB 1kb Ladder, 1- pRRBC-*egfp* digested with *Nde*I, 2 - pRRBC-*egfp* uncut, 3 - pRRBCD-*egfp-lacY*A177C digested with *Nde*I, 4 -pRRBCD-*egfp-lacY*A177C uncut.

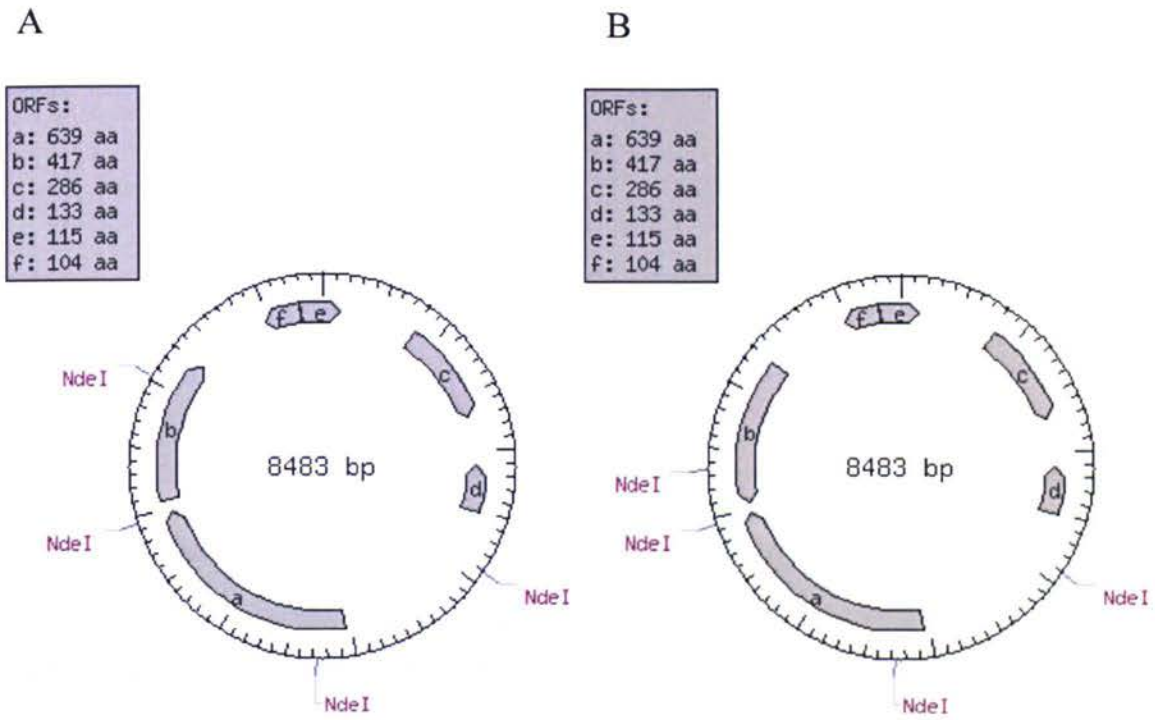

Figure 5.37. Illustration of the restriction sites of the pRRT-*lacY*A177C plasmid showing A) correct and B) reverse insertion of *lacY*A177C.
*Nde*I restriction sites are also shown. Location of *lacY*A177C is shown by a and the location of *tet*^{r} is shown by b. Image produced by NEBCutter v2.

Table 5.10. Restriction sites and the sizes of digested fragments from *Nde*I digest of pRRT-lacYA177C for the determination of the orientation of the *lacY*A177C.

Correct orientation		Reverse orientation	
*Nde*I site	Bands produced (bp)	*Nde*I site	Bands produced (bp)
2919	4373	2919	5064
4282	1665	4282	1665
5947	1363	5947	1363
7029	1082	6338	391

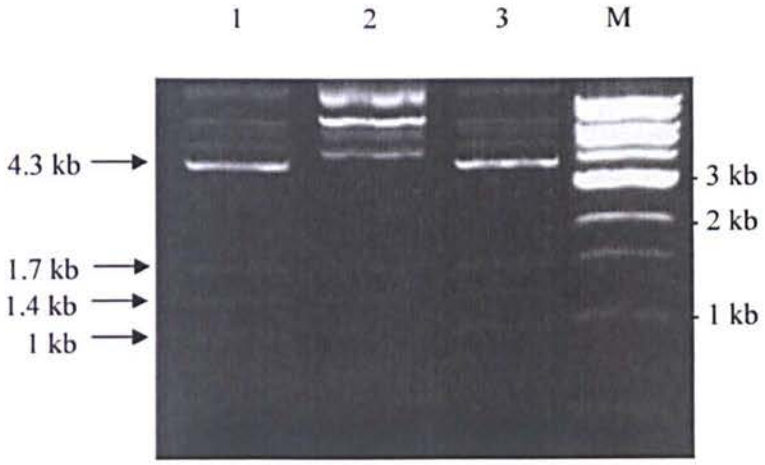

Figure 5.38. Restriction enzyme digest analysis of pRRT-*lacY*A177C.
The digested DNA fragments were run on a 1% agarose gel, showing the correct orientation of *lacY*A177C according to DNA fragment sizes. Unmarked bands that appear above 5 kb are due to incomplete digestion. pRRT-*lacY*A177C clone 1 and 3 show the correct orientation and insertion of *lacY*A177C.
1- pRRT-*lacY*A177C clone 1 digested with *Nde*I, 2- pRRT-*lacY*A177C clone 2 digested with *Nde*I, 3- pRRT-*lacY*A177C clone 3 digested with *Nde*I, M- NEB 1 kb Ladder.

5.4. Discussion

Expression studies using samples attained from solid media exhibited highly varying results with no correlation between biological samples. Compared with the expression studies using liquid culture samples, the results appear completely different where no marked change in expression was found across all of the time points. The biological samples were also compared with one another and each showed a different expression profile, with no reoccurring expression profiles found. The large difference in fold-change in the solid media culture samples could be due to two main factors: the various ages of the cells and the heterogeneous nature of solid media plate cultures. The solid media cultures that were older than the liquid culture samples e.g. 3 and 4 days have ~90% CFs. Some theories consider CF as degenerative forms with 'leaky' walls and the mRNA would have also degenerated prior to isolation thus the mRNA would not be representative of the CF present but just of the sub-population of stressed, more viable cells. However, this does not fully explain the inconsistent expression of samples with fewer CF and all mRNA samples were measured for integrity on the Bioanalyser prior to all expression studies.

Bacterial culture grown on a solid surface will have a heterogeneous population, creating a biofilm-like growth. By day 3 and 4 the cultures would be under a high level of stress due to depletion of nutrients and the build up of toxic products due to an increase in death of previous sub-populations. The culture would have cells at the surface interface exposed to different environmental stress compared to those underneath closer at the media apex. The heterogeneous environments would enable various sub-populations within the culture of stressed live and dead cells, which would skew the total mRNA collected and the expression of *amiA* and possibly other controls as well. Though solid media samples were not representative, the liquid media samples revealed interesting results. As stated

previously, no significant consistent change in the expression of *amiA* was shown between biological samples and maintained consistent expression, indicating there was no direct relationship between CFF and *amiA* expression.

Several attempts were made to knockout *amiA* using various different strains (11168H and 81116), constructs, different transformation methods, different insertion sites of the *kan*^{r} and the presence of extended flanking regions to encourage allelic replacement. However, all of these proved to be unsuccessful and led to the potential hypothesis that *amiA* in *C. jejuni* may be essential. According to Metris *et al.* (2011), *C. jejuni amiA* was labelled as 'non-essential', based on an *in silco* method that determined genes that were essential based on predictions of whether they coded for products that were necessary for generating energy or biomass. However, using two mapped transposon libraries, it was shown there were no successful inserts in *amiA*/Cj1269c (Metris *et al.*, 2011). The absence of an insert in the transposon libraries does not necessarily mean that the gene is essential and could be due to several reasons, e.g. sequence bias, transposon depletion, polar effects due to operon structure and chance. It is also considered that some areas are just resistant to accepting an insert.

The overexpression of AmiA in *E. coli* showed a dramatic effect on growth and membrane integrity, which was not previously expected whilst attempts at knocking out the *amiA* gene function showed a similar dramatic effect with no viability. Expression studies within *C. jejuni* showed that the expression of *amiA* did not increase dramatically in tandem with CFF. As it was shown previously within this chapter, the attempts to knockout *amiA* function in *C. jejuni* lead to no viable mutants, and the overexpression of the same gene in *E. coli* also leads to a drop in viability and a retardation of growth. In combination with the liquid culture expression studies in *C. jejuni*, a new possible theory is that the levels of

AmiA within the cell need to be maintained at a threshold level, where both over or under expression can be detrimental to the organism's viability and growth. The link of *amiA* with morphology change in *C. jejuni* has not been elucidated fully yet, though the LIVE/DEAD cell staining within *E. coli* pRRBC-*amiA* showed the decrease in membrane integrity during overexpression of *amiA*. This could be due to the change in peptidoglycan due to amidase activity, despite the lack of change in *amiA* expression. The lack of morphological change after *amiA* overexpression could be due to the differential structure of peptidoglycan in *E. coli* and *C. jejuni*. The model structure of peptidoglycan has been defined within *E. coli* and HPLC studies with *H. pylori* have demonstrated a high abundance of anhydro muropeptides and muropeptides with D-Ala- and Gly-terminated pentapeptide side chains suggesting alternative peptidoglycan structure models to *E. coli* (Costa *et al.*, 1999). *C. jejuni* has been shown to have a similar muropeptide profile to the closely related *H. pylori* (Frirdich *et al.*, 2012). Costa *et al.* (1999) demonstrated that an *amiA* mutation in *H. pylori* hindered the ability of the mutant to form CF, however the effects of overexpression were not investigated. The effects of high levels of AmiA on *C. jejuni* are still to be investigated.

pRRBC constructs used pRR as the basis for integration into *Campylobacter*. As stated by Karlyshev & Wren (2005) using the rRNA gene clusters in *C. jejuni* as the site for gene insertion has several advantages compared to other sites. The rRNA gene clusters in *Campylobacter* are redundant with multiple copies, reducing any effect the insertion may have on cell function and the highly conserved nature of these sites within the genome. Previous studies found that there was no effect on cell growth with insertion into the rRNA clusters (Karlyshev & Wren, 2005). Hence this was the reason for using the plasmid as the basis of the pRRBC.

The introduction of a sugar transporter into pRRBC was to enable expression with *C. jejuni.* The choice of sugar transporter was not limited to just mutated *lacY*. *lacY*A177C instead of *lacY*A177V was chosen as Morgan-Kiss *et al.* (2002) found a three fold increase in expression of their induced fluorescent protein in lacYA177C than lacYA177V. The relaxed specificity of the *lacY* mutant was shown to allow for homogenous regulation unlike the WT *E. coli* arabinose transporter *araE.*

The lack of difference between the non-induced culture and culture repressed expression with glucose in *E. coli* shows there was no 'leaking' within the construct and the overexpression results were due to induction and not due an external component within the media; the promoter was constitutively being expressed and the system was robust. The inability for pRRBCD-*egfp* or the *lacY* derivative to transform and function in *C. jejuni* was possibly due to a mutation that could not be determined by restriction enzyme analysis and primer walking sequencing, within the flanking regions or within another part of the construct as the mutation could be located in another area of the construct. The potential new biological role of *amiA* within *C. jejuni* requires further exploration hence further work into AmiA and the effects it has on peptidoglycan were carried out.

6.0. The elucidation of AmiA function and the effects on peptidoglycan

6.1. Introduction

Previous HPLC studies within *C. jejuni, H. pylori* and *E. coli* have shown the effects of several peptidoglycan enzymes on muropeptide compositions, which can alter cell morphology. HPLC studies have shown differing muropeptide compositions between *E. coli* and the epsilon proteobacteria, suggesting an alternative structural model of peptidoglycan within these organisms (Costa *et al.*, 1999; Frirdich *et al.*, 2012). Costa *et al.* (1999) showed a high abundance of anhydro muropeptides and muropeptides with D-Ala- and Gly-terminated pentapeptide side chains with *H. pylori* peptidoglycan.

The knockout mutant of AmiA function in *H. pylori* is unable to form a coccoid morphology. According to HPLC studies, the mutant showed an accumulation in the N-acetyl-D-glucosaminyl-β(1,4)-N-acetylmuramyl-L-Ala-D-Glu (GM-dipeptide), which may indicate an alternative AmiA function separate from amidase activity (Chaput *et al.*, 2006).

The aim of the study was to isolate *C. jejuni* AmiA protein and use enzymatic and proteolytic studies to determine the effect it has on *E. coli* peptidoglycan.

6.3. Results

6.3.1. Production and purification of AmiA x6His tagged protein

Due to the inability to knockout *amiA* within *C. jejuni*, the next step was to determine the function of AmiA. The *amiA* coding region was cloned into an arabinose-inducible system pBAD33 via PCR using a forward primer incorporating a *Xba*I restriction site, *C. jejuni* SD sequence, a start codon and a reverse primer incorporating a *Pst*I restriction site and hexa histidine-tag sequence. These restriction enzyme sites allowed directional cloning of the insert into the pBAD33 cloning vector multiple cloning site. The 2 kb *amiA*-x6His amplicon was produced via High Fidelity PCR at a low annealing temperature for the insertion of the various flanking regions with primers AmiAHis_for and AmiAHis_rev. Both pBAD33 and the *amiA*-x6His tagged products were digested with *Xba*I and *Pst*I. The vector was then dephosphorylated to reduce self-ligation of the plasmid and favour ligation of the insert. The insertion of *amiA*-x6His tag into pBAD33 was verified by restriction analysis using *Pst*I and *Xba*I, which cut out *amiA*-x6His tag sequence. If the insert was not present the plasmid would linearise (Figure 6.1 and 6.2). The sequence was verified by primer walking sequencing.

Several systems were used to try to purify the AmiA-x6His tagged protein. First, the pBAD33 –*amiA*His plasmid was transformed into XL2 *E. coli* competent cells, which yielded very little AmiA-His protein and high levels of contaminant proteins, despite various alterations to the salt, glycerol, and imidazole concentrations and to the pH. Two different methods of protein purification were performed: large scale protein purification using a Ni-NTA column and small scale protein purification using Ni^+ agarose magnetic beads. Neither method purified a higher concentration of AmiA-x6His tag protein

compared to WT *E. coli* cultures. WT *E. coli* does not produce *C. jejuni* AmiA or AmiA fusion protein and is used as a control. WT *E. coli* culture sample products purified from the purification methods were histidine rich contaminant proteins, one protein had a similar mass to AmiA-x6His tag protein. The protein samples were run on an SDS-PAGE gel and proteins were visualised using Coomassie staining or Western blotting. Coomassie staining showed similar protein bands in both the WT and the pBAD33-*amiA*His *E. coli* purified protein samples; both showed a band at ~75kDa, which is the size of AmiA-x6His tagged protein (Figure 6.3). The presence of the tagged fusion protein was shown through western blotting using antibodies specific to the epitope of the x6His tag (Figure 6.4). Figure 6.3 shows AmiA-x6His tag fusion protein eluted primarily within just the first eluate. Second, *C. jejuni* genomes are AT rich, therefore BL21-(DE3)-RIL codon plus competent *E. coli* cells were used to potentially increase the protein yield. The extra Codon Plus plasmid within the cell line coded for rarer *E. coli* tRNAs, enabling better translation from AT rich genomes and potentially increased heterologous protein yield. The resistance markers within this cell line were not compatible with previous constructs and so a new plasmid was required. The vector, pTrc99a, an IPTG-inducible system was used instead of pBAD33. An alternative set of primers, AmiAHis_foralt and *AmiAHis_revalt* were used to create *amiA*-x6His tag gene with an *E. coli* SD site for insertion into pTrc99a; to improve protein expression within *E. coli*. The pTrc99a plasmid has similar multiple cloning sites as pBAD33 and had single *Xba*I and *Pst*I sites enabling directional insertion as previously. The new plasmid was constructed and verified by restriction analysis using *Xba*I and *Pst*I (Figure 6.5 and 6.6). The restriction enzyme analysis for purified plasmid samples from the BL21-(DE3)-RIL cell line revealed the presence of the Codon Plus plasmid, which only had the *Pst*I restriction site. The full sequence of the Codon Plus plasmid was not disclosed

due to copyright regulations, however Agilent were able to disclose the restriction maps of the plasmid showing commonly used restriction enzymes.

However, after several alterations, the protein yield was still very low with the same contaminate bands present in the WT and purified extracts in the BL21-(DE3)-RIL and XL2 cell lines. Different purification methods were conducted including purification under native and denatured conditions, column and bead based purification with various amendments to the methodology. However, all variations produced low yields of protein. Though the yield from bacterial cultures was shown to be unsuccessful, they all showed the same effect on growth after induction. After induction the growth retarded dramatically and then plateaued with the pTrc99a-*amiA*His culture after induction in comparison with the non-induced culture, the culture not synthesising AmiA or the WT culture (unpaired Student's *t*-test; 2.3093, df = 16, $P = 0.03$). This was compared with WT cultures, containing pTrc99a without an insert and uninduced cultures to ensure the change in growth was due to the induction of AmiA (Figure 6.7)

Finally, the S30 High Yield T7 cell-free protein expression system was used. A possible reason for the lack of protein expression is that the protein is toxic to the cells in higher concentrations, therefore a cell-free system may allow purification of protein. This system required a plasmid or PCR DNA with a T7 promoter region, meaning that both the pBAD33 and pTrc99a vector constructs generated previously were not suitable and a new construct was made using the plasmid pGEM-T EASY (Promega). The *amiA* coding region was amplified using the primer sets AmiAHis_foralt and AmiAHis_revalt for insertion into pGEM-T EASY to make pGEM-T-*amiA*Hisalt. Another construct was made to compare the expression of AmiA without the His tag in the cell-free system because fusion proteins can have a decreased level of synthesis. The *amiA* PCR product using

primers AmiAHis_foralt and AmiA_rev was cloned into pGEM-T EASY to make pGEM-T-*amiA* (Figure 6.8). Insertion and orientation of construct was verified by *Xba*I and *Pst*I digestion (Figure 6.9). Figure 6.10 shows the S30 High yield T7 cell-free protein expression system produced AmiA-x6 His tagged protein and AmiA without the hexa histidine tag, which was confirmed with western blotting using unpurified samples. The cell-free system compared AmiA samples with a positive control; S30 T7 Control DNA encoding for Renilla luciferase and a negative control with no template DNA to measure the background protein levels. Even with this method, the yield was still not high enough for proteolytic studies; the background protein levels were very high and purification using the methods mentioned previously further decreased the yield. The protein synthesis in the cell-free system was not hindered by higher levels of AmiA, further suggesting the cause of low yield in the bacterial model was due to the detrimental effect on viability.

Further techniques could have been used to confirm the protein produced, such as mass spectrometry, creating a construct with the histidine tag on the N-terminal and western blotting using AmiA specific antibodies.

All the methods described to isolate AmiA proved inefficient for generating the higher yield necessary for further studies; for example proteolytic studies to fully elucidate the enzymatic function of AmiA. The proteolytic studies could be conducted by two methods; using a standardized proteolytic assay, which uses casein as the substrate and create another using peptidoglycan as the substrate. The peptidoglycan samples of *E. coli* and *C. jejuni* would be incubated with the purified *C. jejuni* AmiA protein. After incubation the samples would be compared using HPLC and mass spectrometry to determine the effects the enzyme would have on peptidoglycan subunits and structure.

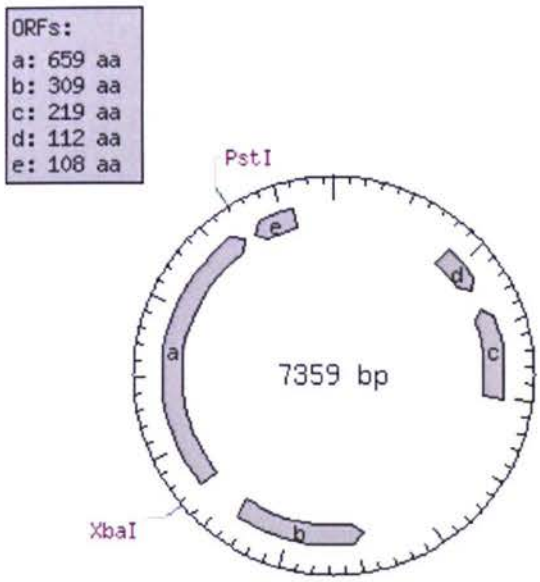

Figure 6.1. Diagram of pBAD33-*amiA*His construct.
Image displays the restriction sites, *Xba*I and *Pst*I flanking the x6 His tag gene. The location of pBAD promoter region and *amiA* is shown as b and a respectively. Image produced by NEBCutter v2.

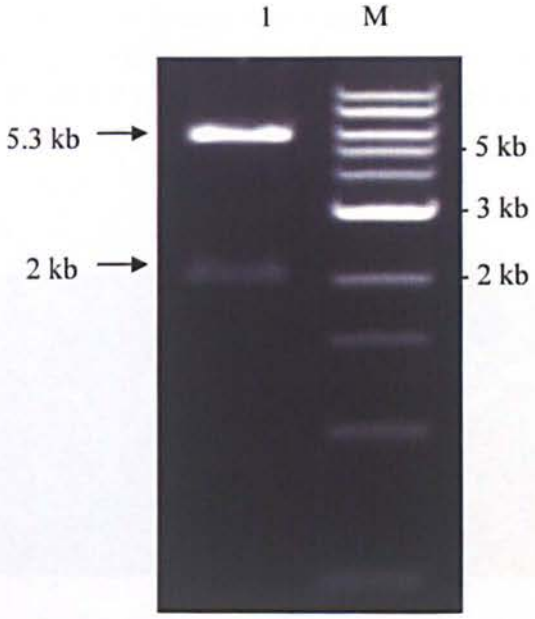

Figure 6.2. Restriction enzyme digest analysis for the verification of *amiA* insertion into pBAD33 using *Xba*I and *Pst*I.
1- pBAD33-*amiA*His digested with *Xba*I and *Pst*I, M- NEB 1 kb DNA Ladder.

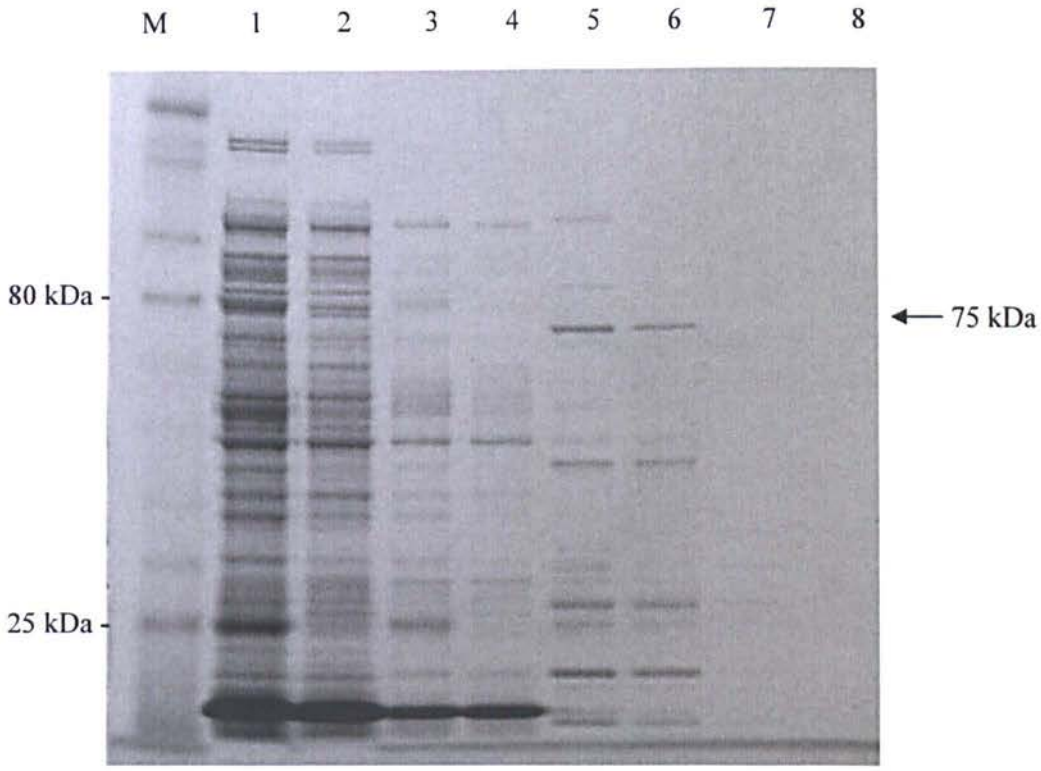

Figure 6.3. SDS gel image of *E. coli* XL2 pBAD33-AmiAHis and WT samples extracted from large scale protein purification.

The same samples were also used for western blotting. The fusion protein elutes mostly in eluate 1 with no visible levels of the protein present within eluate 2.

M- prestained protein ladder, 1- pBAD33-AmiAHis lysate, 2- WT lysate, 3- pBAD33-AmiAHis wash, 4- WT wash, 5- pBAD33-AmiAHis eluate I, 6- WT eluate I, 7- pBAD33-AmiAHis eluate II, 8- WT eluate II.

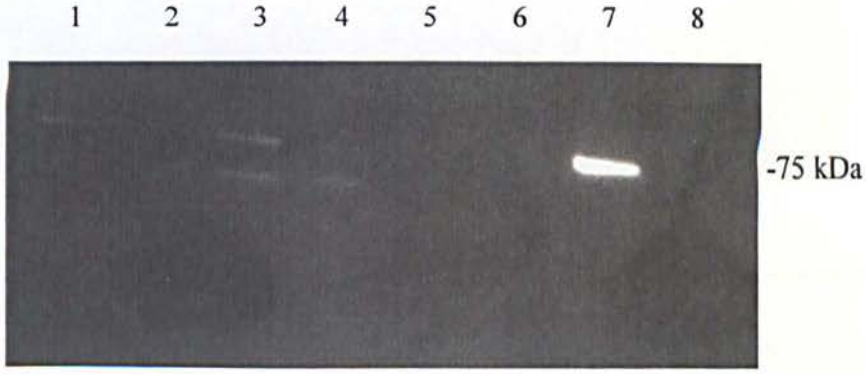

Figure 6.4. Western blotting SDS gel image of *E. coli* XL2 pBAD33-AmiAHis and WT samples extracted from large scale protein purification.

Antibodies used detect the epitope of x6 Histidine, The histidine tagged AmiA is detected.

1- pBAD33-AmiAHis lysate, 2- WT lysate, 3 - pBAD33-AmiAHis flow through, 4- WT flow through, 5- pBAD33-AmiAHis wash, 6- WT wash, 7- pBAD33-AmiAHis eluate I, 8- WT eluate I.

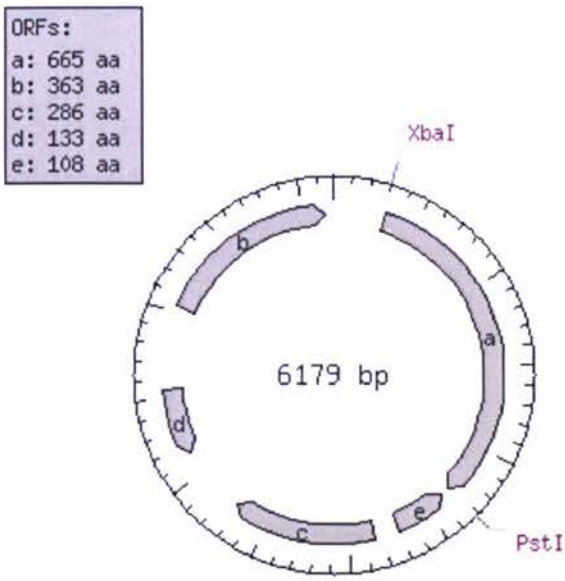

Figure 6.5. Diagram of pTrc99a-*amiA*His construct.
The image displays the restriction sites, *Xba*I and *Pst*I flanking the x6His tag sequence. The location of *amiA* is shown as a. Image produced by NEBCutter v2.

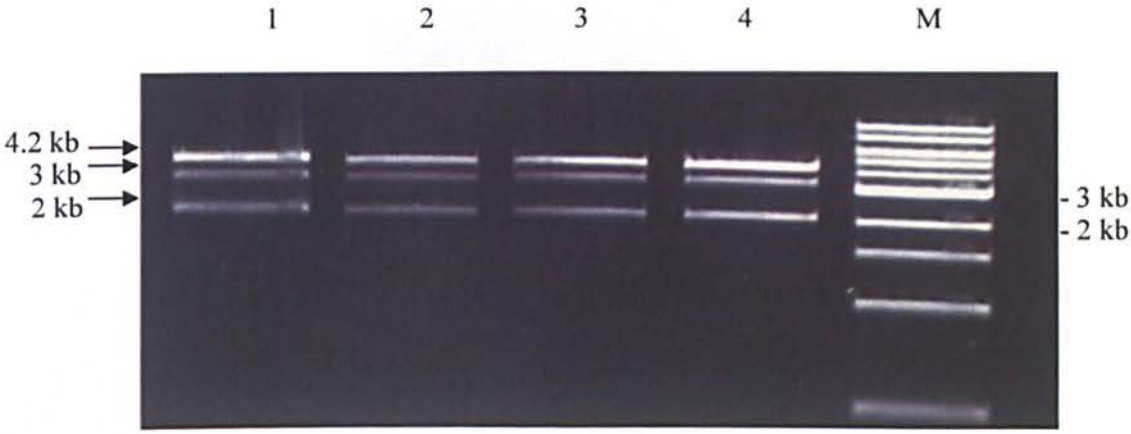

Figure 6.6. Verification of the presence of pTrc99a-*amiA*His plasmids in RIL codon plus *E. coli* after restriction enzyme digestion of *Xba*I and *Pst*I.
The 4.2 and 2 kb bands are the approximate sizes of pTrc99a and *amiA* respectively. The additional 3 Kb band is the size of the codon plus plasmid, which linearised due to the presence of a singular *Pst*I site.1- pTrc99a-*amiA*Hisalt clone 1 digested with *Xba*I and *Pst*I, 2- pTrc99a-*amiA*Hisalt clone 2 digested with *Xba*I and *Pst*I, 3- pTrc99a-*amiA*Hisalt clone 3 digested with *Xba*I and *Pst*I, 4- pTrc99a-*amiA*Hisalt clone 4 digested with *Xba*I and *Pst*I, M- NEB 1 kb DNA Ladder.

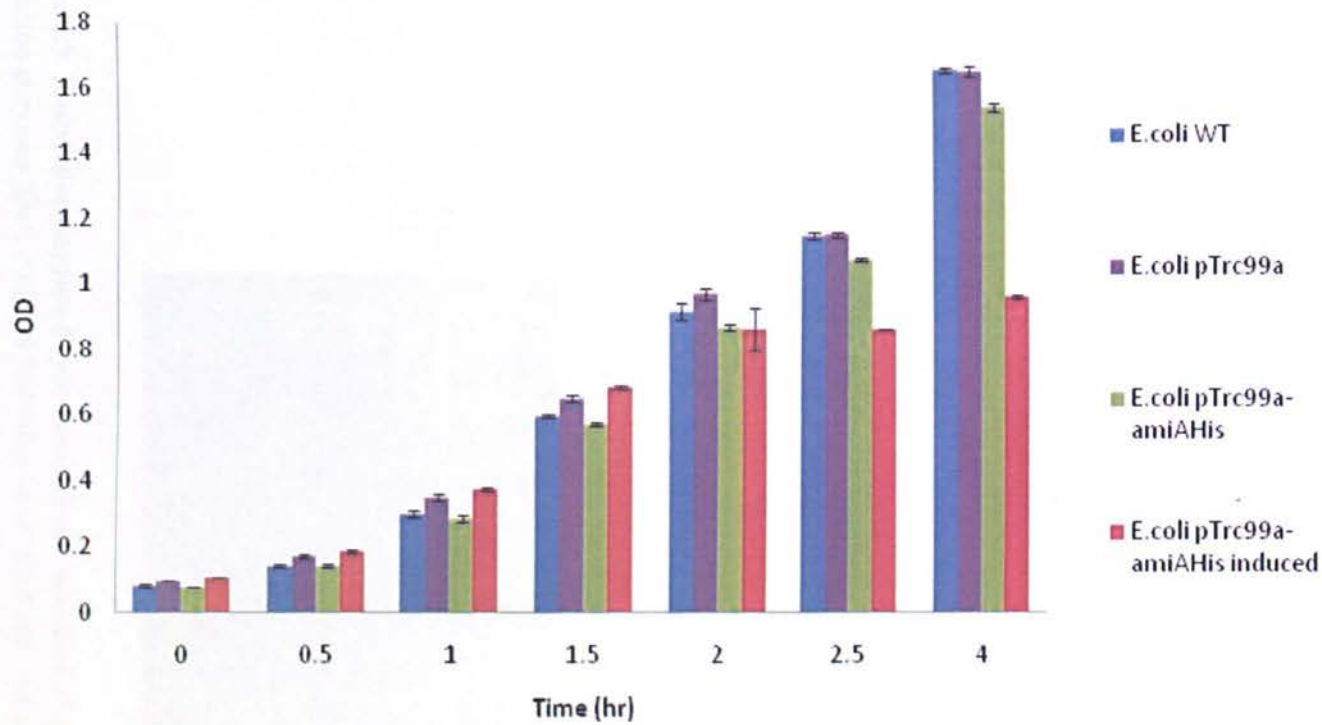

Figure 6.7. Effect on growth of *E. coli* with the overexpression of his tagged AmiA.
Growth was measured by optical density readings at OD_{600nm} over a 4 hr period. The induction of *E. coli* WT, pTrc99a and pTrc99a-*amiA*His(induced) occurred at 2 hrs with 100μM IPTG. The cultures were grown with shaking (~200 rpm), starting at approximately 0.1 OD_{600nm} ml^{-1}. These data are the mean of an individual experiment, which was done in triplicate with similar results each time. The error bars represent SD (N= 3).

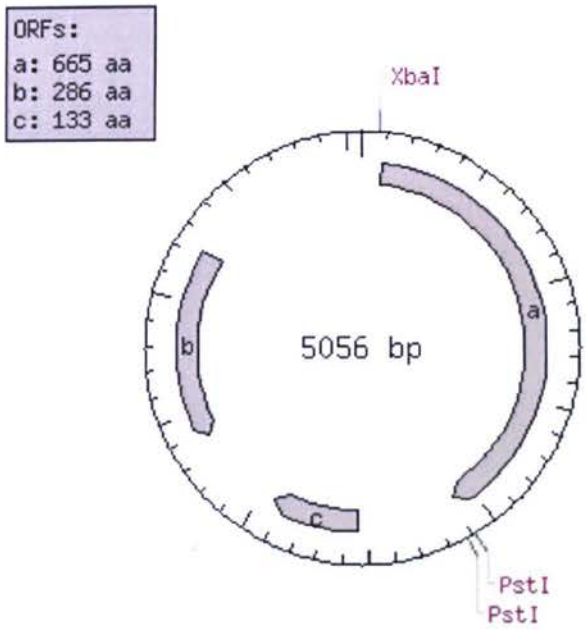

Figure 6.8. Diagram showing the insertion of *amiA* histidine tagged gene in pGEM-T.
This construct was used for fusion protein synthesis using the cell free system. Image shows the restriction enzyme sites of *Xba*I and *Pst*I flanking the *amiA* histidine tagged gene, labelled as a. Image produced by NEBCutter v2.

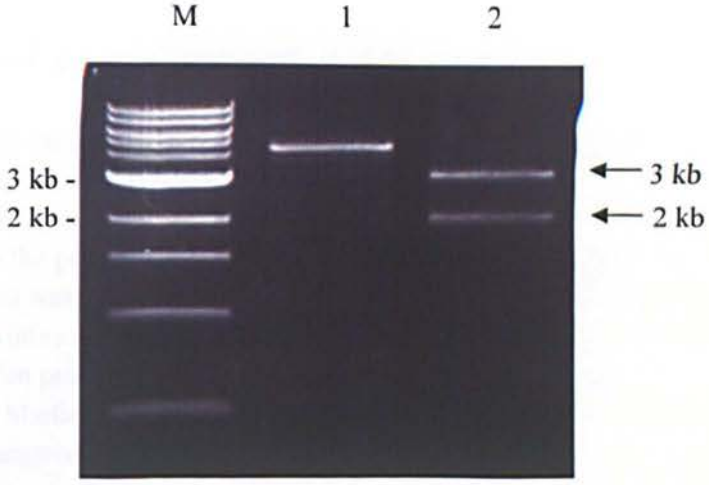

Figure 6.9. Restriction enzyme digest showing the insertion of *amiA*His in pGEM-T.
Restriction enzymes *Xba*I, *Pst*I and *Sty*I were used. *Xba*I and *Pst*I are flanking the *amiA* gene whilst *Sty*I digestion showed the orientation of the gene, which is in the forward orientation.
M- NEB 1kb DNA Ladder , 1- pGEM-T-*amiA*His digested with *Sty*I, 2- pGEM-T-*amiA*His digested with *Xba*I and *Pst*I,

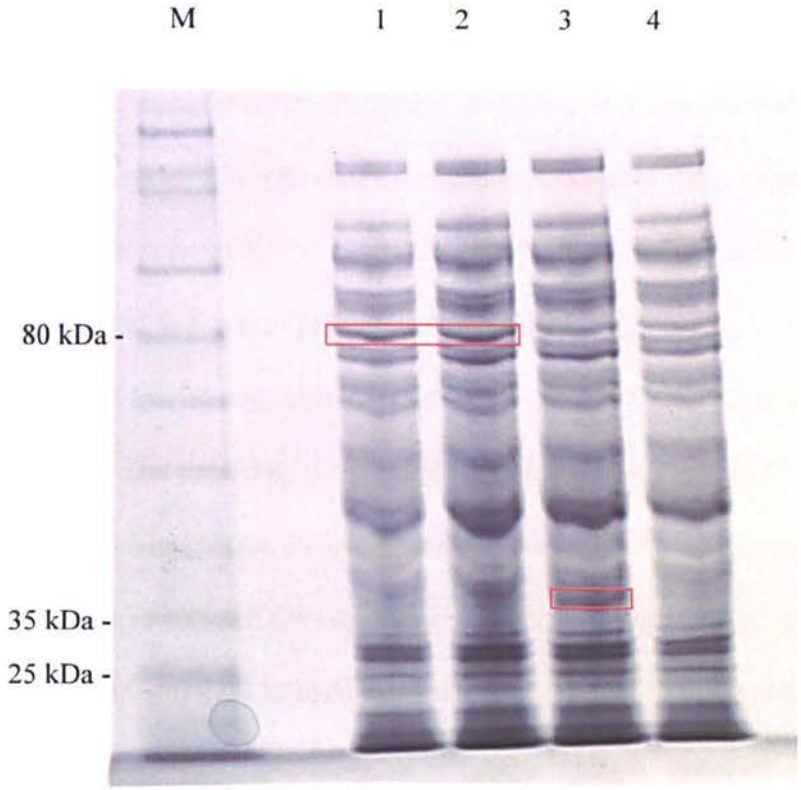

Figure 6.10. SDS PAGE gel showing AmiA production using S30 T7 high yield protein expression system.

AmiA with and without the presence of a histidine tag was synthesized for yield comparison with a positive and negative control. AmiA was visible at ~75kDa and the S30 control codon optimised DNA used as the positive control produced Renilla luciferase, which is visible at ~37kDa. The positive control shows the protein expression system is able to synthesize proteins. The presence of the synthesized proteins were shown by the comparison with the negative control, as the negative control is used to determine the protein expression background. The red boxes highlight the bands of the synthesized fusion proteins.

M- Prestained Protein Marker, 1- pGEM-T-*amiA*His, 2- pGEM-T-*amiA*, 3- positive control (S30 T7 control DNA), 4- negative control (no template DNA).

6.3.2. The isolation and analysis of peptidoglycan from *C. jejuni*, *E. coli* pRRBC-AmiA and WT *E. coli*

The effect of AmiA was studied to determine if the N-acetylmuramoyl-L-alanine amidase had the same effect on peptidoglycan as previously studied in other organisms. Four peptidoglycan samples from *E. coli* pRRBC-*amiA* (induced and non-induced sample), *E. coli* WT and *C. jejuni* WT were isolated and compared. Peptidoglycan was isolated from *E. coli* pRRBC-*amiA*, with and without induction with 0.1% arabinose whilst the liquid culture was grown. The peptidoglycan was also isolated from *C. jejuni* 11168H wild type culture grown to mid-log phase. A commercially available peptidoglycan isolated from *E. coli* K12 (Biosource) was used for comparison. The peptidoglycan samples were first compared with a TLC method as used by Barzilai *et al.* (1984) to determine if any changes to the structure were visible. The signal for the peptidoglycan was very faint, being only just visible, showing the system was unable to show the peptidoglycan (data not shown). Unfortunately, TLC lacked the resolution required to analyse the abundance of peptidoglycan, which could be due to the solvent system, and thus HPLC was used.

The HPLC method was similar to Glauner *et al.* (1988) for amidase treated peptidoglycan to analyse the muropeptide composition. Figure 6.11 shows very clear differences between the peptidoglycan samples. The *E. coli* pRRBC-AmiA without induction peptidoglycan sample and the commercially bought WT *E. coli* sample both have two peaks, a smaller peak at 2.8 mins and a larger peak at 3.2 mins. However, the overexpressed AmiA *E. coli* sample had just one peak at 2.9 mins. Likewise, the *C. jejuni* peptidoglycan had only one peak at 3.2 mins. There was a lack of the 3.2 mins peak in the *E. coli* peptidoglycan after induction of *C. jejuni* AmiA expression. The native *C. jejuni* peptidoglycan had only a 3.1 mins peak, close to the 3.2 mins peak naturally in *E. coli* WT and *E. coli*-pRRBC AmiA

without induction. This difference in peaks could be linked to AmiA on *C. jejuni* morphology change. However, more research is required on the action of AmiA. Further techniques like mass spectrometry to study the abundance of different muropeptide structures between the *C. jejuni* induced *E. coli* peptidoglycan and non-induced.

(on next page)

Figure 6.11. Muropeptide profiles from *E. coli* pRRBC-*amiA* and *C. jejuni* peptidoglycan samples.

HPLC chromatograms showing the different peaks between peptidoglycan samples extracted from *E. coli* pRRBC-*amiA* cultures A) induced for high level AmiA synthesis and B) without induction culture at native levels of AmiA and C) *C. jejuni*. The peaks of particular interest are highlighted within the red boxes.

A

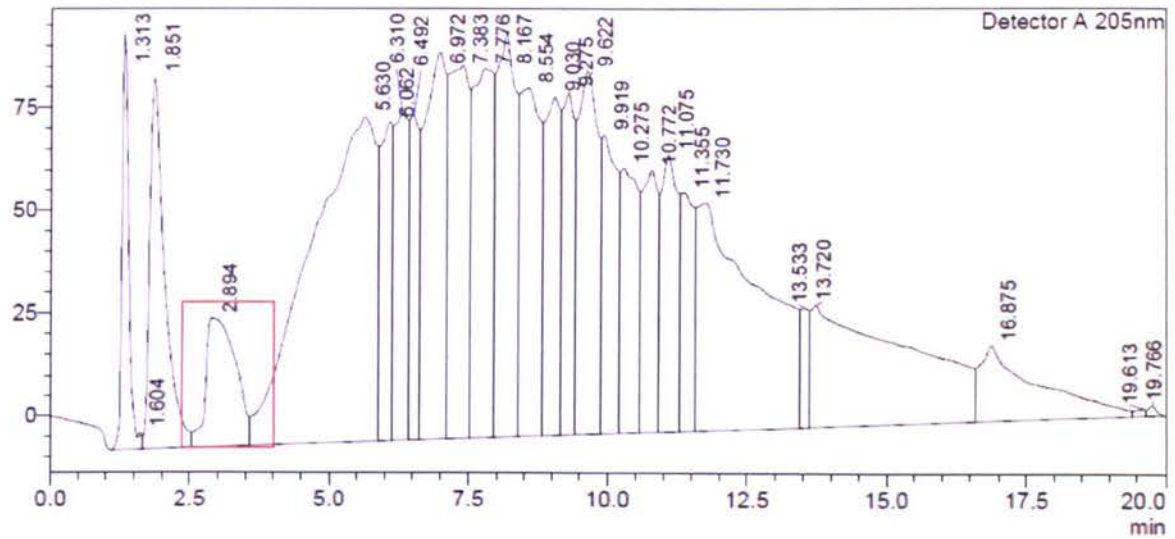
Detector A 205nm
1.313
1.851
1.604
2.894
5.630
6.062
6.310
6.492
6.972
7.383
7.776
8.167
8.554
9.030
9.275
9.622
9.919
10.275
10.772
11.075
11.355
11.730
13.533
13.720
16.875
19.613
19.766
min

B

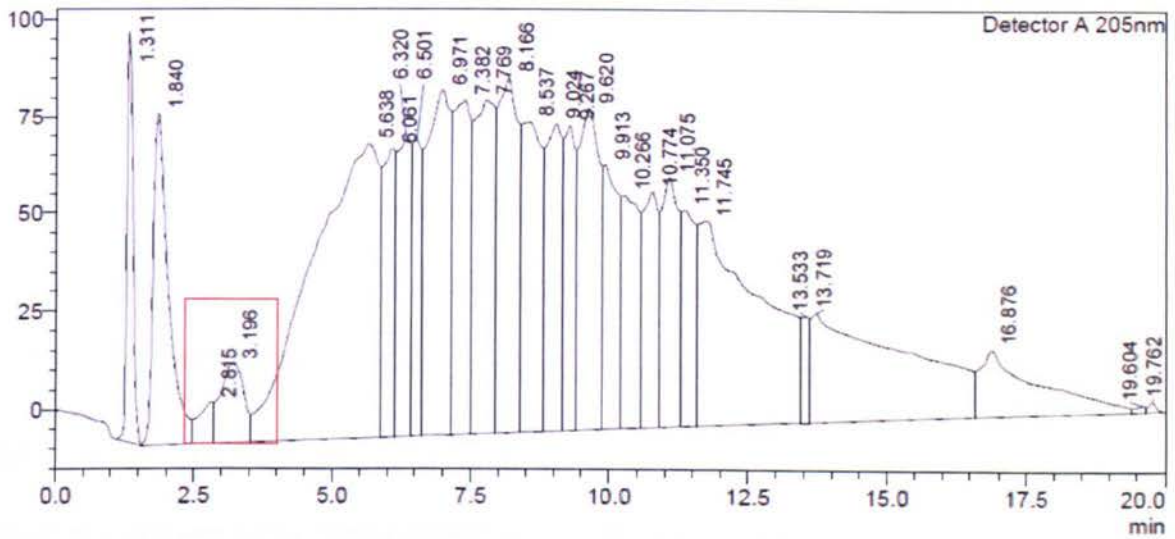
Detector A 205nm
1.311
1.840
2.915
3.196
5.638
6.061
6.320
6.501
6.971
7.382
7.769
8.166
8.537
9.024
9.267
9.620
9.913
10.266
10.774
11.075
11.350
11.745
13.533
13.719
16.876
19.604
19.762
min

C

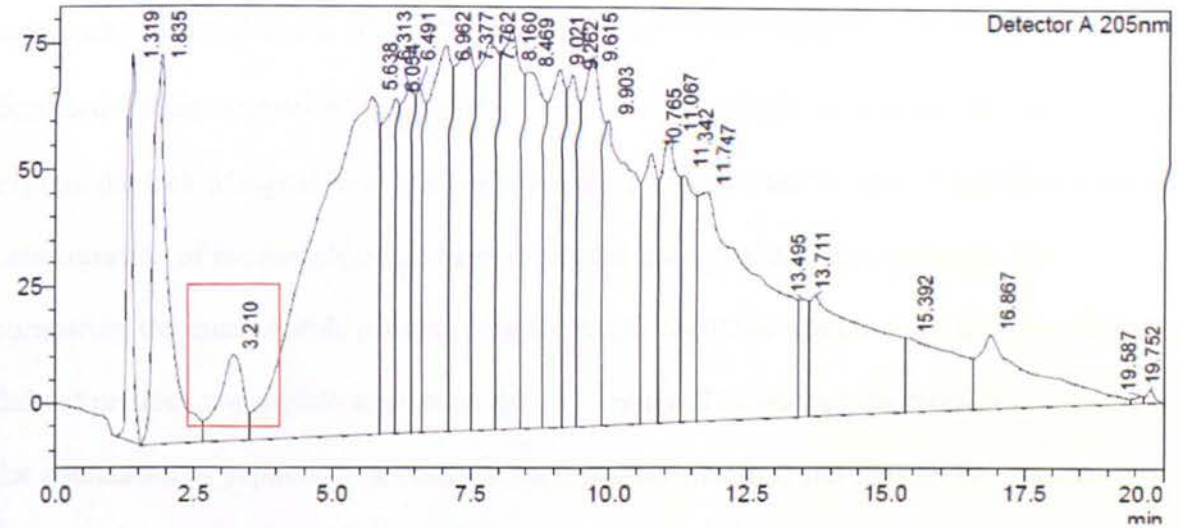
Detector A 205nm
1.319
1.835
3.210
5.638
6.054
6.313
6.491
6.962
7.377
7.762
8.160
8.469
9.021
9.262
9.615
9.903
10.765
11.067
11.342
11.747
13.495
13.711
15.392
16.867
19.587
19.752
min

6.4. Discussion

After induction there was a decrease in growth of *E. coli* cultures with pRRBC-AmiA construct according to OD_{600nm} and CFU, as shown in chapter 6 (Figure 6.26 & 6.27). This could be due to two possible reasons: firstly, the divergence of energy to the protein translation or secondly the protein has a toxic nature if overexpressed. Other protein constructs were used to verify the cell lines, plasmids, inducers and protein purification methods. As these all appeared valid and functioned as presumed, along with the previous results showing a hindrance in growth and an increase in membrane permeability after AmiA overexpression, it is more likely that the inability to purify large yields was due to the 'toxic' nature of high levels of *C. jejuni* that AmiA has upon *E. coli*.

The expression of the protein potentially requires a high level of regulation and/or maintenance, and the over or under expression of the protein could lead to a hindrance in growth and then cell death.

TLC was used to determine if there were dramatic changes to the muropeptide profile. However no signal was visible despite several attempts. Enzymatic treatments did not create an additional signal. The solvent system used by Barzilai *et al.* (1984) was originally designed for Gram-positive *Staphylococcus aureus* peptidoglycan samples and this could explain the lack of signal from the Gram-negative *C. jejuni* and *E. coli*. A higher amount or concentration of the sample could have improved the signal and the resolution for comparing the muropeptide profiles. Higher quantities of the sample were used but these did not produce any visible signals on the TLC either. TLC lacked the resolution to analyse the abundance of peptidoglycan and the muropeptide profiles, and thus HPLC was used.

The HPLC results have shown that higher levels of AmiA activity affect the muropeptide profile. The muropeptide profiles have shown a difference between the *E. coli* and *C. jejuni* peptidoglycan even with a method specialised for the muropeptides treated with amidases. This supports the previous studies that suggest an alternative peptidoglycan structure for *C. jejuni* and the potential different effects *C. jejuni* AmiA may have on *C. jejuni* peptidoglycan compared to *E. coli.*

Further work to elucidate each of the peaks using MALDI-MS and MS/MS analysis would be required. Additional further work to study the effect of AmiA on peptidoglycan is to use purified *C. jejuni* AmiA protein on isolated peptidoglycan from *C. jejuni* and *amiA* knockout *C. jejuni* and compare the muropeptide profiles using HPLC and mass spectrometry. It would also be of interest for further research on the effects of different growth conditions on the muropeptide profiles of *C. jejuni* peptidoglycan, especially conditions that induce CFF.

7.0. Discussion and Future Work

7.1. Summary and interpretation of the Results

The main aim of this study was to investigate the potential genetic determinants of CF, *amiA* and *spoT*, in *C. jejuni* 11168H, the hypermotile derivative of NCTC 11168 and 81116. No genes within *C. jejuni* are currently considered as genetic determinants for CFF, unlike in the closely related organism *H. pylori,* in which *amiA* was defined as the first genetic determinant for the CFF (Costa *et al.* 1999). *SpoT*, which is located downstream of *amiA*, has been previously linked to CFF in another strain of *C. jejuni* (Gaynor *et al.*, 2005).

Bioinformatic studies were conducted to compare the *amiA* and *spoT* gene and protein sequences from *C. jejuni, H. pylori* and *E. coli* to help determine functionality. Between the different organisms, *spoT* sequences (DNA and protein) showed high conservation and similarity, suggesting the biological role and function is similar. However, the main findings showed that between the different N-acetylmuramoyl-L-alanine amidases, the N-terminus showed high variability whist maintaining conservation of the 'amidase' C-terminal end. This conservation was found at both the DNA and the protein level and even within the same organism, as *E. coli* has five N-acetylmuramoyl-L-alanine amidases present within the genome, all of which were highly similar to one another. The redundancy within *E. coli* suggests the genes, despite having the same biological function, may play differential roles within the bacterial life cycle or that they may be activated as part of different regulatory networks. However, this was not investigated within these studies.

The classical structure of peptidoglycan was elucidated within *E. coli*, however the abundances of the various muropeptides was shown to differ within *H. pylori* and *C. jejuni*

(Costa *et al.*,1999; Frirdich *et al.*, 2012; Frirdich *et al.*, 2014). The high variation of the N-terminal end could be linked to the specificity to each organism and the N-terminus accounts for the variation. Studies with human serum amidases by Wang *et al.* (1999) were shown to have specificities for muropeptides with amino acid chains between the length of three and five. The variable N-terminus could alter the specificity dependent on the length of the amino acid chain to fit the enzyme site, possibly explaining an increase in muropeptide dipeptide motifs in an *amiA* knockout in *H. pylori* (Chaput *et al.*, 2005). The bioinformatics offered substantial possibilities for *amiA* as an annotated peptidoglycan hydrolase with a conserved 'amidase' region.

In Chapter 3, the progression of CFF within *C. jejuni* 11168H and 81116 was measured under different environmental stresses and different phases of growth in media. The progression of CF on solid and liquid media differed, as on solid media the percentage of coccoids ranged from 15% to 90% within a day while the progression in liquid media was slower and more gradual. The CFF of *C. fetus* samples were measured on solid and liquid media across a 4 day period, as with *C. jejuni.* The current findings regarding *C. fetus* NCTC 10842 and 82-40 agree with previous studies by Amano & Shibata (1992) that *C. fetus* is unable to form the coccoid morphology. DNA degradation was measured from *C. jejuni* samples of various ages with increasing amounts of CF to determine if the coccoid morphology is a degenerative state. Results in Chapter 3 showed that the CF was not indicative of DNA degeneration.

The presence of intermediate structures was observed under light and scanning electron microscopy in Chapter 3. The presence of these structures is controversial and within our studies, a possible intermediate doughnut structure was found under SEM. However, no intermediate structures were visible under light microscopy. There has been speculation

regarding the intermediate structure being either a transient state, existing for a very short period of time or an artefact of the fixation during the sample preparation, as the structure has only been visualised under SEM in previous studies (Ng *et al.*, 1985, Thomas *et al.*, 1999, Moran & Upton, 1986).

In Chapter 4, the phenotypic effects of *spoT* SDM were studied within *C. jejuni* 11168H and 81116. The knockout of SpoT function led to an increase in the accumulation of CFF on solid and liquid media over a 4 day period. The results from these two strains were compared with another previously studied strain *C. jejuni* 81-176, which was shown by Gaynor *et al.* (2005) in knockout studies to have similar effects. Though all the strains showed an increase in the accumulation of CF with age related stress, the effects of *spoT* knockout are pleiotropic, meaning the gene is not an exact determinant of cell morphology transitioning.

Chapter 5 studied the phenotypic effects of *amiA* knockout and overexpression. As shown previously, no viable knockout mutants of *amiA* were created within *C. jejuni.* The knockout of AmiA function within *C. jejuni* appeared to be lethal, which has not been shown within other organisms like *E. coli* and *H. pylori.* The knockout of *amiA* within the closely related organism *H. pylori* showed no defects to growth but an inability to form CF. This provoked possible theories of *C. jejuni amiA* being linked to viability. However, its connection with CFF has still to be investigated.

The inability to obtain large yields of AmiA within *E. coli* as shown in chapter 6 and the overexpression studies testing the pRRBC construct illustrated a potential role of *C. jejuni* AmiA, as both these experiments lead to the decrease in cell viability. The theory of *C. jejuni amiA* being linked to viability has not been shown before, and the differential

LIVE/DEAD staining helped show the possible reasoning was due to weakened cell membranes. The expression of *amiA* within *C. jejuni* was shown not to change in tandem with the accumulation of CFF, but interestingly remains at a similar level at all times on solid (*rpoA* control -unpaired Student's *t*-test; 2.1521, df = 10, $P = 0.06$) (16S control - unpaired Student's *t*-test; 0.5526, df = 10, $P = 0.59$) and liquid media (*rpoA* control - unpaired Student's *t*-test; 1.1273, df = 14, $P = 0.28$) (16S control -unpaired Student's *t*-test; 0.0178, df = 14, $P = 0.99$). The overexpression and the knockout of AmiA both have a dramatic effect on viability, suggesting that levels of *amiA* within *C. jejuni* require maintenance at a particular level.

In Chapter 6, HPLC studies showed a difference between the *E. coli* cultures with and without the expression of *C. jejuni amiA*. Pilot studies to verify the presence and compare the muropeptide profiles using TLC lacked the resolution required and hence required HPLC. These preliminary studies have shown that there is a difference with the overexpression of AmiA. This leads to a change in the muropeptide profile and, as previously mentioned within the chapter discussion, full elucidation of the change of muropeptides abundances requires MALDI-MS.

7.2. Discussion of the Results

The studies of coccoid morphology and the pathways for the shape change still have not been currently elucidated within the paradoxical organism *C. jejuni.* Despite our current attempts of finding genes that cause CFF, research within this field is still ongoing and requires further investigation into possible genes connected to the morphology change and the role of peptidoglycan within CFF.

The comparison of the *spoT* (DNA and protein) sequences showed very high similarity across *H. pylori* and *E. coli* sequences for *relA* and *spoT*, suggesting the role of the gene was similar across the various organisms.

SpoT in *C. jejuni* has been previously linked to being involved not only with morphology, but also to the adaptive abilities of the organism to aerobic stress (Gaynor *et al.*, 2005). Gaynor *et al.* (2005) showed the effects of an increased accumulation of CF with the knockout of *spoT* within *C. jejuni* strain 81-176. To compare strains and to determine whether the same effect was found within *C. jejuni* strains 81116 and 11168H, *spoT* was knocked out via SDM. The knockout of this gene was conducted in the other strains to compare if the effect was pleiotropic as found within *C. jejuni* strain 81-176. This showed that *spoT* was not a genetic determinant for CFF in *C. jejuni* however the gene is linked to morphology change. Due to the other genes that are located within the gene cluster, it is possible that the cluster is related to cell morphology and bacterial life cycle.

C. jejuni amiA has many similarities to the N-acetylmuramoyl-L-alanine amidases within *H. pylori* and *E. coli* as a peptidoglycan lytic enzyme, and thus could play a role within CFF. However, the current studies with *C. jejuni* AmiA have shown the enzyme may have a role not just within morphology but potentially within viability and bacterial life cycle.

H. pylori CF was considered a degenerative state and did not play a role within the life cycle of the organism (Kusters *et al.*, 1997). However, the role of the *C. jejuni* CF has been shown to be more complicated than just a degenerative state, as previous studies showed that different stressors lead to variation in viability and membrane permeability (Hazeleger *et al.*, 1995, Hazeleger *et al.*, 1998, He & Chen, 2010). The aim of this study was to demonstrate if *C. jejuni amiA* played the role as a genetic determinant of CFF, similar to *H. pylori amiA*. However, the unsuccessful SDM studies with *amiA* in chapter 5 showed the putative role of *C. jejuni amiA* was not linked just to bacterial morphology. This was also not the only reported unsuccessful knockout of *amiA*, as demonstrated by transposon libraries by Metris *et al.* (2011). Chapter 5 showed the expression of *amiA* within *C. jejuni* remained constant regardless of the percentage of CF present within the samples (*rpoA* control -unpaired Student's *t*-test; 1.1273, df = 14, $P = 0.28$) (16S control -unpaired Student's *t*-test; 0.0178, df = 14, $P = 0.99$). Also in chapter 5 and chapter 6, the knockout of *amiA* function and the overexpression of *C. jejuni* AmiA in *E. coli* showed similar results of decreased viability. This furthers the potential role of *amiA* in *C. jejuni* being linked to the bacterial life cycle and not just morphology, though these events are not independent of one another. However, to stipulate the role of *C. jejuni amiA* within bacterial viability, overexpression studies are required due to the lack of results from knockout studies. An alternative method for overexpression studies would be to insert another *amiA* gene within the *C. jejuni* rRNA cluster using pRRC plasmid with a constitutive expressed promoter to see the phenotypic effects of *amiA* overexpression. Although this would not be controllable as with the pRRBC system created, it could have revealed more regarding the effects of AmiA levels greater than native levels would have on morphology and viability.

Further studies for the elucidation of AmiA protein function within *C. jejuni* requires AmiA produced from a different production and purification system with fewer resultant impurities and contaminants, which were not obtainable within this study. The AmiA protein function could be determined by structural studies with the protein to determine specificity to specific products. Wang *et al.* (2003) showed human serum amidase was unable to cleave peptide chains with less than 3 amino acids and structural studies could show if such specificity exists within the *C. jejuni* and *H. pylori* AmiA protein. This could explain accumulation of dipeptide motifs in muropeptide profile of *H. pylori* CF. The theorised bifunctionality of *C. jejuni* AmiA could be elucidated by proteolytic assays and determining the effects the purified protein has on various peptidoglycan samples from *C. jejuni* and *C. fetus.* The purified protein could also be used to see the effects on *C. jejuni* peptidoglycan samples of various ages to determine if the protein does alter the muropeptide profile and explain the potential morphology change.

Currently there is no standard genetic model regarding CFF of *C. jejuni* despite extensive studies on the classical model of the maintenance and structure of peptidoglycan. However, it can be established from its close relation to *H. pylori* that *amiA* is not a genetic determinant for CFF in *C. jejuni*. Despite the fact that the role of *spoT* has been linked to CFF and that *amiA* has been shown to be connected to viability within these studies, a potential feedback loop within the gene cluster these genes are located within could lead to CFF or contain the gene which controls CFF. This would require further work into homology of other genes and gene products within the cluster that could be related to peptidoglycan maintenance.

7.3. Future work

There are several opportunities and avenues for further studies that could be taken based on the results obtained in this project.

Neither *amiA* nor *spoT* were shown to be genetic determinants for CFF in *C. jejuni.* Further research is needed into the other potential gene targets of the morphological transition from the rod to the coccoid morphology. A possible route for further research is to use microarray or RNA sequencing technology to search for more putative gene targets in *C. jejuni* which may be responsible for morphology change and/or are putative peptidoglycan hydrolases. Using several samples of *C. jejuni* from varying time points under differential stresses at transition points, (approximately 50% CFs) compared across the whole genome expression profile for specific genes, the changes in gene expression observed could be linked to the cell morphology change, by looking for genes that are highly expressed whilst the accumulation of CF is highest. However, this study would require a comparison between several strains of *C. jejuni* to ensure the change in morphology is not strain specific. In addition, this sort of experiment would require several biological replicates to reduce the likelihood of identifying genes involved in other processes. This study would produce lots of data on stress response and genes activated under various stress and so the data could also be used to compare gene expression in tandem with other stress responses, e.g. adhesins and surface proteins.

It was also shown by Amano & Shibata (1994) using peptidoglycan studies that *C. fetus* 82-40 was unable to form CF like *C. jejuni* and *C. coli.* In Chapter 4, a brief study of the CFF of the organism *C. fetus* was conducted and was shown not to produce CF under the same age related stress, which led to over 90% CF in *C. jejuni.* A possible avenue of

research is to demonstrate the phenotypic effects of *amiA* and *spoT* SDM within *C. fetus* strains to determine if these genes play a role in morphology change. Comparative genomics is another approach that could be used to investigate the possible genes that may play a role within CFF by the identification of all possible peptidoglycan lytic enzymes in *C. jejuni* and *C. coli* that are not present in *C. fetus.* Using the comparative genomics data, it would be possible to look for conserved DNA sequences, gene order or regulatory sequences that are related to peptidoglycan maintenance across various *Campylobacter* spp that form CF with species that cannot.

The construction of pRRBC system was shown to work. However, due to the inability to induce the system within *C. jejuni*, a possible avenue of further work is enabling the system to work efficiently. The pRRBC system could be used to test the regulated expression of other gene targets within *C. jejuni* or possibly other organisms and could be a benefit to several other studies as well. There are alternatives for the overexpression of genes within *Campylobacter* as used by Frirdich *et al.* (2012) utilized the pRRC plasmid, which could be used to demonstrate the effects of AmiA overexpression on *C. jejuni* morphology and muropeptide profile.

Initial HPLC studies, which were conducted in Chapter 6, have shown a difference in the muropeptide profiles between the high expression levels of AmiA and basal levels within *E. coli.* Additional research into the effects of AmiA overexpression on the muropeptide profiles within *C. jejuni* using HPLC and MALDI-MS to elucidate the abundances of each of the peaks is needed. As previously mentioned, *C. fetus* has been shown not to be able to form coccoids under stress, however, HPLC studies could elucidate the peptidoglycan structure of *C. fetus* (Amano & Shibata, 1992). If the structure of the peptidoglycan differs

from *C. jejuni*, *H. pylori* and *E. coli*, it could explain if the peptidoglycan is more 'rigid' and not able to alter morphology easily.

Further work on the purification of *C. jejuni* AmiA could be done by using mass spectrometry, purification of AmiA with histidine tag on the N-terminal and western blotting using amidase specific antibodies. If *C. jejuni* AmiA is isolated efficiently and in a high yield, it would be possible to do proteolytic studies, using a standardized proteolytic assay and another using isolated peptidoglycan as the substrate. The isolated peptidoglycan from *E. coli* and *C. jejuni* would be incubated with the purified *C. jejuni* AmiA protein and compared using HPLC and mass spectrometry. It would also be of interest to investigate the effects of the purified protein on the peptidoglycan of *C. jejuni amiA* knockout mutant and measure the effects using HPLC and mass spectrometry.

The role of *amiA* in *C. jejuni* and the genetic determinants of CFF have still not been elucidated. However a potential role of *amiA* in *C. jejuni* to viability has been hypothesized and *spoT* and *amiA* were linked to CFF. Nevertheless, further work is required to determine the role of the CFF within the *C. jejuni* life cycle and genetic determinants responsible for the morphology change.

8.0. References

Aizenman, E., Engelberg-Kulka, H.& Glaser, G., (1996), An *Escherichia coli* chromosomal "addiction module" regulated by guanosine-3'5'-bispyrophosphate: A model for programmed bacterial cell death, *Proc. Natl. Acad. Sci. USA*, **93**:6059-6063

Aleksandrova, N.Z., Minaev, V.I. & Gorelov A.A., (1990), Antibiotic resistance of Campylobacter and its epidemiologic significance, *Antibiot. Khimioter.*, **35**: 34-36

Alm, R.A., Ling, L.S., Moir, D.T., King, B.L., Brown, E.D., Doig, P.C., Smith, D.R., Noonan, B., Guild, B.C., deJonge, B.L., Carmel, G., Tummino, P.J., Caruso, A., Uria-Nickelsen, M., Mills, D.M., Ives, C., Gibson, R., Merberg, D., Mills, S.D., Jiang, Q., Taylor, D.E., Vovis, G.F., & Trust, T.J., (1999), Genomic sequence comparison of two unrelated isolates of the human gastric pathogen *Helicobacter pylori*, *Nature*, **397**:176-180

Amano, K.& Shibata, Y., (1992), Structural studies of peptidoglycans in *Campylobacter* species, *Microbiol. Immunol.*, **9**:961-967

Ausmees, N., Kuhn, J.R.& Jacobs-Wagner, C., (2003), The bacterial cytoskeleton: an intermediate filament-like function in cell shape, *Cell*, **115**: 705-713

Barzilai, A., Hyatt, A.C. & Hodes, D.S., (1984), Demonstration of differences between strains of *Staphylococcus aureus* by peptidoglycan fingerprinting, *J. Infect. Dis.*, **150**:583-588

Begg, K.J. & Donachie, W.D., (1985), Cell shape and division in *Escherichia coli*: experiments with shape and division mutants, *J. Bacteriol.*, **163**:615-622

Bernhardt, T.G. & de Boer, P., (2003), The *Escherichia coli* amidase AmiC is a periplasmic septal ring component exported via the twin arginine transport pathway, *Mol. Microbiol.*, **48**:1171-1182

Beumer, R.R., de Vries, J.& Rombouts, F.M., (1992), *Campylobacter jejuni* non-culturable coccoid cells, *Int. J. Food Microbiol.*, **15**:153-163

Boucher, S.N., Slater, E.R., Chamberlain, A.H.& Adams, M.R., *(1994), Production and* viability of coccoid forms of *Campylobacter jejuni*, *J. Appl. Bacteriol.*, **77**:303-307

Bovill, R.A.& Mackey, B.M., (1997), Resuscitation of 'non-culturable' cells from aged cultures of *Campylobacter jejuni*, *Microbiol.*, **143**:1575-1581

Branda, S.S., Vik,Å., Friedman, L.& Kolter, R., (2005), Biofilms: the matrix revisited, *Trends Microbiol.*, **13**:20-26

Buck, G.E., Parshall, K.A.& Davis, C.P., (1983), Electron Microscopy of the Coccoid Form of *Campylobacter jejuni*, *J. Clin. Microbiol.*, **18**: 420-421

Butzler, J.P. & Skirrow. M.B., (1979), *Campylobacter enteritis*, *Acta. Paediatr. Belg.*, **32**:89-94

Buzby, J., Allos, B.& Roberts, T., (1997), The Economic Burden of *Campylobacter* – Associated Gullian-Barré Syndrome, *J. Infect. Dis*, **176**:S192-197

Cabeen, M.T.& Jacobs-Wagner, C., (2007), Bacterial cell shape, *Nature*, **3**:601-610

Cabeen, M.T., Charbon, G., Vollmer, W., Born, P., Ausmees, N., Weibel, D.B.& Jacobs-Wagner, C., (2009), Bacterial cell curvature through mechanical control of cell growth, EMBO J, 28:1208-1219Cappelier, J.M., Rossero, A. & Federighi, M., (2000), Demonstration of a protein synthesis in starved *Campylobacter jejuni* cells, *Intl. J. Food. Microbiology*, **55**: 63-67

Cashel, M., Gentry, D.R., Hernandez, V.J. and Vinella, D., (1996), The stringent response. in *Escherichia coli* and *Salmonella*; *Cellular and Molecular Biology* . Washington, DC: American Society for Microbiology

Cellini, L., Robuffo, L., Maraldi, N.M. & Donelli, G., (2001), Searching the point of no return in *Helicobacter pylori* life: necrosis and/or programmed death?, *J Appl. Microbiol*, **90**:727-732

Chan, K.F., Tran, H.L., Kanenaka, R.Y.& Kathariou, S., (2001), Survival of Clinical and Poultry-Derived Isolates of *Campylobacter jejuni* at a Low Temperature (4°C), *Appl. Environ. Microbiol.*, **67**:4186-4191

Chaput, C., Ecobichon,C., Cayet, N., Girardin, S.E., Werts, C., Guadagini, S., Prevost, M.C., Megnin-Lecreulx, D., Labigne, A.& Boneca, I.G., (2006), Role of AmiA in the morphological transition of *Helicobacter pylori* and in immune escape, *PloS Pathog.*, **2**:e97

Chaveerach, P., ter Huurne, A.A.N.M., Lipamn, L.J.A., & van Knapen, F., (2003), Survival and Resuscitation of Ten Strains of *Campylobacter jejuni* and *Campylobacter coli* under acid conditions, *Appl. Environ. Microbiol.*, **69**: 711-714

Chou, S.P., Dular, R.& Kasatiya, S., (1983), Effect of ferrous sulphate, sodium metabisulfite and sodium pyruvate on survival of *Campylobacter jejuni*, *J. Clin. Microbiol.*, **23**:986-987

Chynoweth, R.W., Hudson, J.A.& Thom, K., (1998), Aerobic growth and survival of *Campylobacter jejuni* in food and stream, *Lett. Appl. Microbiol.*, **27**:341-344

Costa, K., Bacher, G., Allmaier, G., Dominguez-Bello, M.G., Engstrand, L., Falk, P., de Pedro, M.A.& Garcia-del Portillo, F., (1999) the morphological transition of *Helicobacter pylori* cells from spiral to coccoid is preceded by a substantial modification of the cell wall, *J. Bacteriol*, **181**: 3710-3715

Daniel, R.& Errington, J., (2003), Control of cell morphologies in bacteria: Two Distinct ways to make a rod-shaped cell, *Cell*, **113**:767-776

Debruyne, L., Gevers, D. &Vandamme, P., (2008): Taxonomy of the family *Campylobacteraceae*. In *Campylobacter* 3rdEdition, Nachamkin, I., Szymanski, C. M.&Blaser, M. J.eds,Washington DC: ASM Press, Chp 1:3-25

Desroche, N., Beltramo, C. & Guzzo, J., (2005), Determination of an internal control to apply reverse transcription quantitative PCR to study stress response in the lactic acid bacterium *Oenococcus oen*, *J. Microbiol. Methods.*, **60**: 325-333

Doi, M., Wachi, M., Ishino, F., Tomioka, S., Ito, M., Sakagami, Y., Suzuki, A. & Mastuhashi, M., (1988), Determinations of the DNA sequence of the *mreB* gene and of the gene products of the mre region that function in formation of the rod shape of *Escherichia coli* cells, *J. Bacteriol.*, **170**:4619-4624

Donelli, G., Matarrese, P., Fiorentini, C., Dainelli, B., Taraborelli, T., Di Campli, E., Di Bartolomeo, S.& Cellini, L., (1998), The effect of oxygen on the growth and cell morhphology of *Helicobacter pylori*, *FEMS Microbiol. Lett.*, **168**:9-15

Eleaume, H. & Jabbouri, S., (2004), Comparison of two standardisation methods in real-time quantitative RT-PCR to follow *Staphylococcus aureus* genes expression during *in vitro* growth, *J. Microbiol. Methods.*, **59**:363-370

Engelberg-Kulka, H., Amitai, S., Kolodkin, I.& Hazan, R., (2006), Bacterial programmed cell death and multicellular behavior in bacteria, *PLoS Genetics*, **2**:1518-1526

Federighi, M., Tholozan, J.L., Cappelier, J.M., Tissier, J.P.& Jouve, J.L., (1998), Evidence of non-coccoid viable but non-culturable *Campylobacter jejuni* cells in microcosm water by direct viable count, CTC-DAPI double staining and scanning electron microscopy, *Food Microbiol.*, **15**:539-550

Ferrero, R.L.& Lee, A., (1988), Motility of *Campylobacter jejuni* in a viscous environment: comparison with conventional rod-shaped bacteria, *J. Gen. Microbiol.*, **134**:53-59

Frirdich, E., Biboy, J., Adams, C., Lee, J., Ellermeier, J., Gielda, L.D., DiRita, V.J., Girardin, S.E., Vollmer, W. & Gaynor, E.C., (2012), Peptidoglycan-modifying enzyme Pgp1 is required for helical cell shape and pathogenicity traits in *Campylobacter jejuni*, *PLoS Pathog*, **8**(3): e1002602

Frirdich, E., Vermeulen, J., Biboy, J., Soares, F., Taveirne, M.E., Johnson, J.G., DiRita, V.J., Girardin, S.E., Vollmer, W. & Gaynor, E.C., (2014), Peptidoglycan LD-carboxypeptidase pgp2 influences *Campylobacter jejuni* helical cell shape and pathogenic properties, and provides the substrate for the DL-carboxypeptidase pgp1, *J. Biol. Chem.*, **287**: 8007-8018

Garénaux, A., Jugiau, F., Rama, F., de Jonge, R., Denis, M., Federighi, M. & Ritz, M., (2008), Survival of *Campylobacter jejuni* strains from different origins under oxidative stress conditions: effect of temperature, *Curr. Microbiol.*, **56**:293-297

Gaynor, E.C., Well, D.H., MacKichan, J.K.& Falkow, S., (2005) The *Campylobacter jejuni* stringent response controls specific stress survival and virulence-associated phenotypes, *Mol.Microbiol.*, **56**:8-27

Gentry, D.R., & Burgess, R.R., (1989), rpoZ, encoding the omega subunit of *Escherichia coli* RNA polymerase, is in the same operon as *spoT.*, *J. Bacteriol.*, **171**:1271-1277

Glauner, B., (1988), Seperation and quantification of muropeptides with high performance liquid chromatography, *Anal. Biochem.*, **172**:451-464

Graumann, P.L., (2007), Cytoskeletal elements in bacteria, *Annu. Rev. Microbiol.*, **61**:589-618

Griffiths, P.L., (1993), Morphological changes of *Campylobacter jejuni* growing in liquid cultures, *Lett. Appl. Microbiol.*, **17**:152-155

Gundogdu, O., Bentley, S.D., Holden, M.T., Parkhill, J., Dorrell, N. &Wren B.W., (2007), Re-annotation and re-analysis of the *Campylobacter jejuni* NCTC11168 genome sequence, *BMC Genomics*, **8**:162

Gunther, N.W. & Chen, C.Y., (2009), The biofilm forming potential of bacterial species in the genus *Campylobacter*, *Food Microbiol.*, **26**:44-51

Guzman, L.M., Belin, d., Carson, M.J. & Beckwith, J., (1995), Tight regulation, modulation, and high-level expression by vectors containing the arabinose PBAD promoter, *J. Bacteriol.*, **177**:4121-4130

Harvey, P.& Leach, S., (1998), Analysis of coccal cell formation by *Campylobacter jejuni* using continuous culture techniques, and the importance of oxidative stress, *J. Appl. Microbiol.*, **85**:398-404

Hazeleger, W.C., Arkesteijn, C., Toorop, A. & Beumer, R., (1994), Detection of the coccoid form of *Campylobacter jejuni* in chicken products with the use of the polymerase chain reaction, *Int. J. Food Microbiol.*, **24**:273-281

Hazeleger, W.C., Janse, J.D., Koenraad, P.M., Beumer, R.R., Rombouts, F.M. & Abee, T., (1995), Temperature dependent membrane fatty acid and cell physiology changes in coccoid forms of *Campylobacter jejuni*, *Appl. Environ. Microbiol.*, **61**:2713-2719

Hazeleger, W.C, Wouters, J.A., Rombouts, F.M. & Abee, T., (1998), Physiological activity of *Campylobacter jejuni* far below the minimal growth temperature, *Appl. Environ. Microbiol.*, **64**:3917-3922

He, Y.& Chen, C., (2010), Quantitative analysis of viable, stressed and dead cells of *Campylobacter jejuni* strain 81-176, *Food Microbiol.*, **27**:439-446

Heidrich, C., Templin, M.F., Ursinus, A., Merdanovic, M., Berger, J., Schwarz, H., de Pedro, M.A. & Holtje, J.V., (2001), Involvement of N-acetylmuramyl-L-alanine amidases in cell separation and antibiotic-induced autolysis of *Escherichia coli, Mol. Microbiol.*, **41**:167–178

Henriques, A.O., Glaser, P., Piggot, P.J.& Moran, C.P.Jr, (1998), Control of cell shape and elongation by the *rodA* gene in *Bacillus subtilis, Mol. Microbiol.*, **28**:235-247

Höller, C., Witthuhn, D. & Janzen-Blunck, B., (1998), Effect of low temperatures on growth, structure and metabolism on *Campylobacter coli* SP10, *Appl. Environ. Microbiol.*, **64**:581-587

Hudock, J.F., Borger, A.C. & Kaspar, C.W., (2005), Temperature-dependent genome degradation in the coccoid Form of *Campylobacter jejuni, Curr. Microbiol.*, **50**:110-113

Ikeda, N. & Karlyshev, A.V., (2012), Putative mechanisms and biological role of coccoid form formation in *Campylobacter jejuni, Eur. J. Microbiol. Immunol.*, **2**:41-49

Ishino, F., Park, W., Tomioka, S., Tamaki, S., Takase, I., Kunugita, K., Matsuzawa, H., Asoh, S., Ohta, T., Spratt, B.G. & Matsuhashi, M., (1986), Peptidoglycan synthetic ctivities in membranes of *Esherichia coli* caused by overproduction of penicillin-binding protein 2 and RodA protein, *J. Biol. Chem.*, **261**:7024-7031

Jacobs, C., Huang, L.J., Bartowsky, E., Normark, S. & Park, J.T., (1994), Bacterial cell wall recycling provides cytosolic muropeptides as effectors for beta-lactamase induction, *EMBO J.*, **13**:4684-4694

Jones, D.M., Sutcliffe, E.M. & Curry, A., (1991), Recovery of viable but nonculturable *Campylobacter jejuni, J. Gen. Microbiol.*, **137**:2447-2482

Jones, L.J., Carballido-Lopez, R. & Errington, J., (2001), Control of cell shape in bacteria: helical, actin like filaments in *Bacillus subtilis, Cell*, **104**:913-922

Joshua, G.W.P., Guterie-Irons, C., Karlyshev, A.V. & Wren, B.W., (2005), Biofilm formation in *Campylobacter jejuni, Microbiol.*, **152**:387-396

Justice, S.S., Hung, C., Theriot, J.A., Fletcher, D.A., Anderson, G.G., Footer, M.J. & Hultgren, S.J., (2003), Differentiation and developmental pathways of uropathogenic *Escherichia coli* in urinary tract pathogenesis, *PNAS*, **101**:1333-1338

Kadurugamuwa, J. & Beveridge, T. (1995), Virulence factors are released from *Pseudomonas aeruginosa* in association with membrane vesicles during normal growth and exposure to gentamicin: a novel mechaism of enzyme secretion, *J. Bacteriol.*, **177**:3998-4008

Karlyshev, A.K., Linton, D., Gregson, N. A. & Wren, B.W., (2002), A novel paralogous gene family involved in phase-variable flagella-mediated motility in *Campylobacter jejuni*, *Microbiol.*, **142**:473-480

Karlyshev, A.K.& Wren, B., (2005), Development and application of an insertional system for gene delivery and expression in *Campylobacter*, *Appl. Environ. Microbiol.*, **71**:4004-4013

Karmali, M.A., De Grandis, S. & Fleming, P.C., (1981), Antimicrobial susceptibility of *Campylobacter jejuni* with special reference to resistance patterns of Canadian isolates, *Antimicrob. Agents Chemother.*, **4**:593-597

Kelly, A.F., Park, S.F., Bovill, R.& Mackey, B.M., (2001), Survival of *Campylobacter jejuni* during stationary phase: evidence for the absence of a phenotypic stationary – phase response, *Appl. Environ. Microbiol.*, **67**: 2248-2254

Kerff, F., Petrella, S., Mercier, F., Sauvage, E., Herman, R., Pennartz, A., Zervosen, A., Luxen. A., Frere, J.M., Joris, B. & Charlier, P., (2010), Specific structural features of the N- acetylmuramoyl-L-alanine amidase AmiD from Escherichia coli and mechanistic implications for enzymes of this family, *J. Mol. Biol.*, **397**:249-259

Kim, S., Watanabe, K., Suzuki, H. &Watari H., (2005), Roles of *Brucella abortus* SpoT in morphological differentiation and intramacrophagic replication, *Microbiol.*, **151**:1607-*1617*

Klancik, A., Botteldoorn, N., Herman, L.& Mozina, S.S., *(2006), Survival and stress* induced of groEL and rpoD of *Campylobacter* from different growth phases, *Int. J. Food Microbiol.*, **112**:200-207

Klancik, A., Guzej, B., Jamnik, P., Vuckovic, D., Abram, M. & Mozina, S.S., (2009), Stress response and pathogenic potential of *Campylobacter jejuni* cells exposed to starvation, *Res Microbiol*, **160**(5):345-352

Koike, Y. & Shimazaki, Y., (1982), studies on the coccoid form of *Campylobacter* species:fluctuation in cellular morphology, *Bulletin of Nipon Veterinary and Zootechnical College*, **31**:136-142

Kolter, R.D., Siegele, D.A. & Tormo, A., (1993),The stationary phase of the bacterial life cycle, *Annu. Rev. Microbiol.*, **47**:855-874

Kusters, J.G., Gerrits, M.M., Van Strijp, J.A. & Vandenbrouke-Grauls, C.M., (1997), Coccoid forms are the morphological manifestation of cell death, *Infect. Immun.*, **66**: 3672-3679

Lai, C.J., Chen, S.Y., Lin, I.H., Chang, C.H.& Wong, H.C., (2009), Change of protein profiles in the induction of the viable but nonculturable state of *Vibrio parahaemolyticus*, *Intl. J. Food Microbiol.*, **135**: 118-124

Lazaro, B., Carcamo, J., Audicana, A., Perales, I.& Fernandez-Astorga, A., (1999), Viability and DNA maintenance in nonculturable spiral *Campylobacter jejuni* cells after long-term Exposure to low temperatures, *Appl. Environ. Microbiol.*, **65**: 4677-4681

Lee, Y.D., Moon, B.Y., Choi, J.P., Chang, H.G., Noh, B.S.& Park, J.H., (2005), Isolation, identification and characterization of aero-adaptive *Campylobacter jejuni*, *J. Microbiol. Biotechnol.*, **15**:992-1000

Livak, K.J. & Schmittgen, T.D., (2001), Analysis of relative gene expression data using real-time quantitative PCR and the $2^{(-\Delta\Delta CT)}$ method, *Methods*, **25**:402-408

Magnusson, L.U., Farewell A. & Nystrom, T., (2005).,ppGpp: a global regulator in *Escherichia coli, Trends Microbiol*, **13**: 236-242

Masuda, S. & Bauer, C.E., (2004), Null mutation of HvrA compensates for loss of an essential relA/spoT-like gene in *Rhodobacter capsulatus*, *J. Bacteriol.*, **186**: 235-239

Matsuzawa, H., Hayakawa, K., Sato, T. & Imahori, K., (1973), Characterization and genetic analysis of a mutant of *Esherichia coli* K-12 with rounded morphology, *J. Bacteriol.*, **115**:436-442

Medeema G.J., Schets, F.M., Van de Giessen, A.W. & Havelaar, A.H., (1992), Lack of colonisation of 1 day chicks by viable, non culturable *Campylobacter jejuni, J. Appl. Microbiol.*, **72**:512-516

Merrell, B.R., Walker, R.I. & Coolbaugh, J.C., (1981), *Campylobacter fetus ssp jejuni* a newly recognised enteric pathogen:morphology and intestinal colonization, *Scanning Electron Microsc.*, **41**:125-131

Metris, A., Reuter, M., Gaskin, D.J.H., Baranyi, J. & van Vliet, A.H.M., (2011), *In vivo* and *in silico* determination of essential genes of *Campylobacter jejuni*, *BMC Genomics.*, **12**:535

Metzger, S., Dror, I.B., Aizenman, E., Schreiber, G., Toone, M., Friesen, J.D., Cashel, M.& Glaser, G., (1988), The nucleotide sequence and characterization of the relA gene of Escherichia coli, *J BiolChem*, **263**:15699-15704

Moore, J.E., (2001), Bacterial dormancy in *Campylobacter*: abstract theory or cause for concern?,*Int. J.Food Sci. Technol*, **36**:593-600

Moran, A.P.& Upton, M.E., (1986), A comparative study of the rod and coccoid forms of *Campylobacter jejuni* ATCC 29428, *J. Appl. Bacteriol.*, **60**:103

Morgan-Kiss, R.M., Walder, C. & Cronan, J.E., (2002), Long-term and homogeneous regulation of the *Escherichia coli* araBAD promoter by use of a lactose transporter of relaxed specificity, *PNAS*, **99**:7373-7377

Mouery, K., Radar, B.A., Gaynor, E.C.& Guillemin, K., (2006), The stringent response is required for *Helicobacter pylori* survival of stationary phase, exposure to acid, and aerobic shock, *J. Bacteriol.*, **188**:5494-5500

Murphy, C., Carrol, C. & Jordan, K.N., (2006), Environmental survival mechanisms of the foodbourne pathogen *Campylobacter jejuni*, *J. Appl. Bacteriol.*, **100**:623-632

Ng, L.K., Sherburne, R., Taylor, D.E.& Stiles, M.E., (1985), Morphological forms and viability of *Campylobacter* species studied by electron microscopy.*J. Bacteriol.*, **164**:338-343

Ogg, J.E., (1962), Studies on the coccoid form of ovine *Vibrio fetus* I. Cultural and serologic investigations, *Am. J. Vet. Res.*, **23**:354-358

Ojha, A.K., Mukherjee, T.K. & Chatterji, D, (2000), High intracellular level of guanosine tetraphosphate in *Mycobacterium smegmatis* changes the morphology of the bacterium, *Infection Immun.*, **68**:4084-4091

Oliver, J.D., (2005), The viable but nonculturable state in bacteria, *J. Microbiol.*, **43**:93-100

Park, S.F., (2002), The physiology of *Campylobacter* species and its relevance to their role as foodborne pathogens, *In. J. Food Microbiol.*, **74**:177-188

Parkhill, J., Wren, B.W., Mungall, K., Ketley, J.M., Churcher, C., Basham, D., Chillingworth, T., Davies, R.M., Feltwell, T., Holroyd, S., Jagels, K., Karlyshev, A.K., Moule, S., Pallen, M.J., Penn, C.W., Quail, S.A., Rajandream, M.A., Rutherford, K.M., van Vliet, A.H., Whitehead, S. & Barrell, B.G., (2000), The genome sequence of the food-borne pathogen *Campylobacter jejuni* reveals hypervariable sequences, *Nature*, **403**:665-668

Pearson, A.D., Greenwood, M., Healing, T.D., Rollins, D.M., Shamat, M., Donaldson, J.& Colwell, R.R., (1993) Colonisation of broiler chickens by waterborne *Campylobacter jejuni*, *Appl. Environ. Microbiol.*, **59**:987-996

Pellgrini, O., Mathy, N., Gogos, A., Shapiro, L. & Condon, C., (2005), The *Bacilllus subtilis ydcDE* operon encodes an endoribonuclease of MazF/PemK family and its inhibitor, *Mol. Microbiol.*, **56**:1139-1148

Pennartz, A., Genereux, C., Parquet, C., Mengin-Lecreulx, D. & Joris, B., (2009), Substrate-induced inactivation of the *Escherichia coli* AmiD N-acetylmuramoyl-L-alanine

amidase highlights a new strategy to inhibit this class of enzyme, *Antimicrob. Agents Chemother.*, **53**:2991-2997

Popham, D.L.& Young, K.D., (2003), Role of penicillin-binding in bacterial cell morphogenesis, *Curr. Opin. Microbiol.*, **6**:594-599

Prescott, L.M., Harley, J.P. & Klein, D.A. (1996). Microbiology. Third Edition. Wm. C. Brown Publishers, Dubuque, IA. pp. 37-41

Reddy, P.S., Raghaven, A. & Chatterji, D., (1995), Evidence for a ppGpp-binding site on *Escherichia coli* RNA polymerase: proximity relationship with the rifampicin-binding domain, *Mol. Microbiol.*, **15**: 255-265

Rhodes, K.M. & Tattersfield, A.E., (1982), Guillian-Barre syndrome associated with *Campylobacter* infection, *Br. Med. J.*, **285**: 173-174

Ritz, M., Garénaux, A., Berge, M. & Federighi, M., (2009), Determination of *rpoA* as the most suitable internal control to study stress response in *C. jejuni* by RT-qPCR and application to oxidative stress, *J. Microbiol. Methods,* **76**:196-200

Robinson, D., (1981), Infective dose of *Campylobacter jejuni* in milk, *Br. Med. J. Clin. Res. Ed.,* **282**:1584

Rollins, D.M.& Colwell, R.R., (1986), Viable but nonculturable stage of *Campylobacter jejuni* and its role in survival in the natural aquatic environment, *Appl. Environ. Microbiol.*, **52**:531-538

Saha, S.K., Saha, S.& Sanyal, S.C., (1991), Recovery of injured *Campylobacter jejuni* cells after animal passage, *Appl. Environ. Microbiol.*, **57**: 3388-3389

Schraff, R.L., (2010), Health-related costs from foodbourne illness in the United States http://publichealth.lacounty.gov/eh/docs/ReportPublication/HlthRelatedCostsFromFoodborneIllinessUS.pdf

Schwarz, U. & W. Leutgeb., (1971), Morphogenetic aspects of murein structure and biosynthesis, *J. Bacteriol.*, **106**:588-595

Scoarughi G.L., Cimmino, C. & Donini, P., (1999), *Helicobacter pylori*: a eubacterium lacking the stringent response, *J. Bacteriol.*, **181**:552-555

Shimomura, H., Hayashi, S., Yokota, K., Oguma, K.& Hirai, Y., (2004), Alteration in the composition of cholesterylglucosides and other lipids in *Helicobacter pylori* undergoing morphological change from spiral to coccoid form, *FEMS Microbiol. Lett.*, **237**: 407-413

Singh, S.K., SaiSree, L., Ravi, A.N., & Reddy, M., (2012) Three redundant murein endopeptidases catalyze an essential cleavage step in peptidoglycan synthesis of *Escherichia coli* K12, *Mol. Microbiol.,* **86**:1036–1051.

Stahl, M., Butcher, J. & Stinzi, A., (2012), Nutrient acquisition and metabolism by *Campylobacter jejuni, Front Cell Infect. Microbiol.*, **2**:5

Stintzi, A. & Whitworth, L., (2003), Investigation of the *Campylobacter jejuni* cold shock response by global transcript profiling, *Genome Lett.*, **2**:24-33.

Stoker, N.G., Pratt, J.M. & Spratt, B.G., (1983), Identification of the rodA gene product of *Escherichia coli, J. Bacteriol.*, **155**:854-859

Sutherland, I.W., (2001), The biofilm matrix – an immobilized but dynamic microbial environment, *Trends Microbiol.*, **9**: 222-227

Svensson, S.L., Frirdich, E.& Gaynor, E.C., (2008), Survival strategies of *Campylobacter jejuni*: stress responses, the viable but nonculturable state, and biofilms, In Nachamkin, I., Szymanski, C.M.&Blaser, M.J.eds, *Campylobacter* 3rdEdition, Washington DC: ASM Press, Chp 32:571-590

Swulius, M.T. & Jensen G.J., (2012), The helical MreB cytoskeleton in *Esherichia coli* MC1000/pLE7 is an artifact of the N-terminal yellow fluorescent protein tag, *J. Bacteriol.*, **194**:6382-6386

Sycuro, L.K., Pincus, Z., Gutierrez, K.D., Biboy J., Stern, C.A., Vollmer ,W. & Salama, N., (2010), Peptidoglycan crosslinking relaxation promotes *Helicobacter pylori*'s helical shape and stomach colonization, *Cell*, **141**:822-833

Takamiya, M., Ozen, A., Rasmussen, M., Alter, T., Gilbert, T., Ussery, D.W. & Knøchel S., (2011), Genome Sequence of *Campylobacter jejuni* strain 327, a strain isolated from a turkey slaughterhouse., *Stand Genomic Sci.*, **4**:113-22

Tam, C., Rodrigues, L.& O'Brien, S., (2003), Guillian-Barré syndrome associated with *Campylobacter jejuni* infection in England, 2000-2001, *Clin. Infect. Dis.*, **37**:307-310

Tamames, J., Gonzales-Moreno, M., Mingorance, J., Valencia, A. & Vicente, M., (2001), Bringing gene order into bacterial shape, *Trends Genet.*, **17**: 124-126

Tangwatcharin, P., Chanthachum, S., Khopaibool, P. & Griffiths, M.W., (2006), Morphological and physiological responses of *Campylobacter jejuni* to stress, *J. Food Prot.*, **69**:2747-2753

Tholozan, J.L., Cappelier, J.M., Tissier, J.P., Delattre, J.P. & Federighi, M., (1999), Physiological characterisation of viable-but-nonculturable *Campylobacter jejuni* cells, *Appl. Environ. Microbiol.*, **65**:1110-1116

Thomas, C., Hill, D.J. & Mabey, M., (1999a), Evaluation of the effect of temperature and nutrients on the survival of *Campylobacter* spp. In water microcosms, *J. Appl. Microbiol.*, **86**:1024-1032

Thomas, C., Hill, D.J. & Mabey, M., (1999b), Morphological changes of synchronized *Campylobacter jejuni* populations during growth in single phase liquid culture, *Lett. Appl. Microbiol.*, **28**:194-198

Trieu-Cuot, P., Gerbaud, G., Lambert, T. & Courvalin, P., (1985), *In vivo* transfer of genetic information between Gram-positive and Gram-negative bacteria, *EMBO J.*, **4**:3583-3587

Uehara, T. & Park, J.T., (2007) An anhydro-N-acetylmuramyl-L-alanine amidase with broad specificity tethered to the outer membrane of *Escherichia coli*, *J. Bacteriol.*, **189**:5634–5641

Ursing, J.B., Lior, H. & Owen, R.J., (1994), Proposal of minimal standards for describing new species of the family *Campylobacteraceae*, *Int. J. Syst. Bacteriol.*, **44**:842-845

Vandamme, P. & de Ley J., (1991), Proposal for a new family, *Campylobacteraceae, Int. J. Syst. Bacteriol.*, **41**:451-455

Verhoeff-Bakkenes, L., Hazeleger, W.C., Zwietering, M.H. & De Jonge R., (2007), Lack of response of INT-407 cells to the presence of non-culturable *Campylobacter jejuni*, *Epiemiol. Infect.*, **136**:1401-1406

Verhoeff-Bakkenes, L., Hazeleger, W.C., De Jonge, R. & Zwietering, M.H., (2008), *Campylobacter jejuni*: a study on environmental conditions affecting culturability and *in vitro* adhesion/invasion, *J. Appl. Microbiol.*, **106**:924-993

Vinella, D., Joseleau-Petit, D., Thévenet, D., Bouloc, P. & D'Ari, R., (1993), Penicillin-binding protein 2 inactivation in *Escherichia coli* results in cell division inhibition, which is relieved by FtsZ overexpression, *J. Bacteriol.*, **175**:6704-6710

Vollmer, W., Joris, B., Charlier, P. & Foster S., (2008), Bacterial peptidoglycan (murein) hydrolases, *FEMS Microbiol. Rev.*, **32**:259-286

Wang, Z.M., Li, X., Cocklin, R.R., Wang, M., Wang, M., Fukase, K., Inamura, S., Kusumoto, S., Gupta, & Dziarski, R., (2003), Human peptidoglycan recognition protein-L is an N-acetylmuramoyl-L-alanine amidase, *J. Biol.Chem.*, **278**:49044-49052

Wassenaar, T.M., Fry, B.N. & van der Zeijst, B.A., (1993), Genetic manipulation of *Campylobacter*: Evaluation of natural transformation and electro-transformation,*Gene*, **132**:131-135

Whitchurch, C.B., Tolker-Nielsen, T., Ragas, P.C. & Mattick, J.S., (2002), Extracellular DNA required for Bacterial Biofilm Formation, *Science*, **295**:1487

Wilharm, G., Lepka, D., Faber, F., Hofmann, J., Kerrinnes, J. & Skiebe, E, (2010), A simple and rapid method of bacterial transformation, *J. Microbiol. Meths.*, **80**:215-216

Young, K.D., (2001), Approaching the physiological functions of penicillin-binding proteins in *Esherichia coli*, *Biochimie*, **83**:99-102

Young, K.D., (2006), The selective value of bacterial shape, *Microbiol. Mol. Biol. Rev.*, **70**(3):660-703

Zillig, W., Zechel, K., Rabussay, D., Schachner, M., Sethi, V.S., Palm, P., Heil, A. & Seifert W., (1970), On the role of different subunits of DNA-dependent RNA polymerase from *E. coli* in the transcription process, *Cold Spring Harb.Symp. Quant. Biol.*, **35**: 47-58